NEW CHEMICAL AND BIOSYNTHETIC METHODOLOGIES FOR THE STUDY OF LANTHIPEPTIDES

BY

NOAH A. BINDMAN

DISSERTATION

Submitted in partial fulfillment of the requirements
for the degree of Doctor of Philosophy in Chemistry
in the Graduate College of the
University of Illinois at Urbana-Champaign, 2014

Urbana, Illinois

Doctoral Committee:

Professor Wilfred A. van der Donk, Chair
Professor Paul J. Hergenrother
Professor John A. Katzenellenbogen
Professor Douglas A. Mitchell

Abstract

Recent genome sequencing efforts have revealed that a common biosynthetic route to peptide natural products involves ribosomally synthesized and posttranslationally modified peptides (RiPPs). One of the largest classes of RiPPs is the lanthionine-containing peptides (lanthipeptides), which are characterized by intramolecular thioether crosslinks dubbed lanthionine (Lan) and methyllanthionine (MeLan). The evolvability and brevity of lanthipeptide biosynthetic pathways as well as the substrate tolerance of the biosynthetic machinery facilitates the heterologous expression of lanthipeptides and renders the ribosome-derived compounds attractive for bioengineering efforts. A major drawback to the production of lanthipeptides, either in *E. coli* or in vitro, is the removal of the leader peptide after posttranslational modification to generate the mature natural product. In this thesis, Chapter 2 will discuss a method to introduce a photolabile linker between lanthipeptide leader and core regions. Posttranslational modification of the lanthipeptide by its cognate synthetase in vitro, followed by UV-light mediated removal of the leader peptide, yielded the mature lanthipeptide. Chapter 3 will spotlight a novel way to engineer the ribosomal machinery to incorporate a hydroxy acid into the peptide thus generating an ester linkage directly between the lanthipeptide leader and core regions, which is selectively hydrolyzed under mild alkaline conditions.

Labeling of natural products with biophysical probes has greatly contributed to investigations of their modes of action and has provided tools for visualization of their targets. However, the mode of action of only a few lantibiotics has been determined thus far. A general challenge is the availability of a suitable functional group for chemoselective modification. Chapter 4 will discuss novel methodology to introduce an N-terminal ketone into various lanthipeptides by the generation of a cryptic N-terminal dehydro amino acid by the cognate

biosynthetic enzymes. Spontaneous hydrolysis of the N-terminal enamines after leader peptide removal results in α-ketoamides that site-specifically react with an aminooxy-derivatized alkyne or fluorophore. The fluorescently-modified lantibiotics were added to bacteria, and their cellular localization was visualized by confocal fluorescence microscopy as a means to determine their modes of action.

To my parents for their love and support

Acknowledgements

First and foremost, I want to thank my advisor Professor Wilfred van der Donk. Your unique combination of intelligence and kindness has made you an absolute pleasure to work with. Especially during my early years of graduate school, when I was figuring out how to become a scientist, your endless supply of knowledge was integral to the success of my projects. I will also always appreciate the value you place on teaching, both in the laboratory and the classroom. Most important to me, however, is your ability to run a successful laboratory while treating us graduate students with the utmost respect and for that I give you my deepest thanks. I would also like to thank the rest of my committee, Professor Paul Hergenrother, Professor John Katzenellenbogen, and Professor Doug Mitchell, for your guidance and encouragement, especially during my literature seminar, preliminary examination, original research proposal, and final defense.

I have been fortunate these past five years to work with fantastic colleagues. Firstly, thank you to Patrick Knerr and John Hung. Your friendship has meant the world to me and I could not imagine graduate school without either of you. Next, to Neha Garg, Nancy Shi, Ayse Ökesli, and Min Zeng, the rest of the class of 2013/14, or as Pat has dubbed us, 'The Magnificent Seven'. Your helpful advice, support, and most importantly your friendship, has been integral to my success. I also want to sincerely apologize to everyone who has had the privilege(?) distinction(?) of sitting next to me throughout the years. Thank you first to Kevin Clark for putting up with the inane babbling (I honestly thought they were intelligent questions) of a very young graduate student. Also, thank you to Rebecca Splain for being the exact kind of bay-mate any fifth year student would ever want – a very competent post-doc. In all seriousness though, it was an absolute pleasure working with both of you. Thank you to all of the past and current

members of the van der Donk lab, but especially Spencer Peck, Chantal Garcia de Gonzalo, Manuel Ortega, Gabrielle and Christopher Thibodeaux, Xiling Zhao, Isabel Neacato, and Subha Mukherjee for being great resources and making the lab an enjoyable place to work. Finally, I sincerely appreciate all of the hard work put in by my undergraduate researchers Robert Koehler, Nicholas Herrman, and Tia Harper. I hope you gained as much from the experience as I did.

A good support system is necessary for any graduate student and I was very lucky to make many wonderful friends here in Champaign. First, my most sincere appreciation goes to 'lab mom' Martha Freeland. Your support helped me stay sane throughout my early years in graduate school. The lab has not been the same since you left. Paul Gormisky, Jill Horne, Mike and Jess Evans, Jeremy and Debbie Kemmerer, Claire Knezevic, Rahula Strohl, Amy Thornsen, and Callie Croushore thank you for all the laughs and good times, especially during our late night trips to Crane Alley. I will miss all of you dearly. Also, thank you to all the past and present members of the Speed Marvels (softball) and Prion (Ultimate Frisbee) for helping me manage my stress in the most enjoyable ways possible.

Finally, I want to thank my parents, my brothers, and my wonderful wife Sam. Your love and support throughout my entire life has made my graduate studies possible. I could speak at length about what each of you has meant to me, but instead I'll simply say that I could not have done any of this without you.

Table of Contents

LIST OF FIGURES, SCHEMES, AND TABLES

Chapter 1: Introduction

Taken in part from Bindman and van der Donk.[1]

1.1. NATURAL PRODUCTS AS ANTIBIOTICS AGAINST DRUG-RESISTANT PATHOGENS

The emergence of antibiotic-resistant pathogens, such as methicillin-resistant *Staphylococcus aureus* (MRSA) and vancomycin-resistant *Enterococcus* (VRE), has amplified the need for new classes of antimicrobial compounds. In 2007, MRSA was responsible for over 100,000 infections and 20,000 deaths in the U.S., more deaths than caused by HIV/AIDS.[2] One reason for the increase of antibiotic-resistant pathogens is the quick spread of resistance genes. In 1980, less than five percent of *S. aureus* isolated from hospitals had a resistance marker for methicillin whereas in 2007 that number had jumped to almost sixty percent.[2] Alarmingly, with the increase of drug-resistant bacteria, very few new classes of antibiotics have been developed since the 1960s. Several challenges have contributed to the decline in discovery of novel antibiotics. One factor is that pharmaceutical companies are spending less on research and development towards new antibiotics, which if administered correctly are used for only a short period by a patient, unlike drugs for chronic diseases, which must be taken every day of the patients' life. Furthermore, it is easier and less expensive to modify the structure of a known antibiotic than to search for an antibiotic with a novel mode of action.[3] Therefore, an immense need exists for the discovery and study of novel antibiotics.

One potential route for the discovery of new antibiotics is to study the natural defensive arsenal of bacteria, which has been developed as a consequence of the evolutionary pressure of living in nutrient starved conditions. This route has been largely successful in developing

clinically useful antibiotics; over two-thirds of all antibiotics on the market are, or are derived from, natural products.[4] Peptide natural products have been important players in the search for novel antibiotics because their unique three-dimensional structures (with many sp^3 hybridized carbons) allow tight binding and a high degree of specificity and potency to their targets. Indeed, the glycopeptide vancomycin, isolated in the 1950s from the soil bacterium *Amycolatopsis orientalis*, has been used as a last line of defense drug against MRSA for over 50 years. More recently, peptide natural product based compounds such as telavancin[5] and teicoplanin,[6] as well as the lipopeptide daptomycin,[7] were marketed in the U.S. and/or Europe for their ability to kill Gram-positive drug resistant bacteria. Many other peptide-based natural products are currently under development and some are in clinical trials and may soon assist in the fight against drug-resistant bacteria.[8,9]

1.2. RIBOSOMALLY SYNTHESIZED AND POSTTRANSLATIONALLY MODIFIED PEPTIDES

Many peptide natural products, including the antimicrobial compounds vancomycin and daptomycin, are non-ribosomal peptides (NRPs) that are biosynthesized by a modular assembly line of proteins encoded by relatively large gene clusters (~40-60 kb).[10] The recent genome sequencing efforts have revealed that another very common biosynthetic route to peptide natural products involves ribosomally synthesized and posttranslationally modified peptides (RiPPs) (Figure 1.1). These compounds are produced in all domains of life but are most prevalent, or at least best studied, in bacteria, serving as natural bio-warfare agents. In retrospect it is not surprising that RiPPs are widespread given the potential benefits these biosynthetic pathways have for the producing organisms, including evolvability. Evolution of new NRPs requires rare

mutations in the biosynthetic enzymes that change the outcome of an enzymatic reaction somewhere along the assembly line and requires that all downstream enzymes tolerate this change. By contrast, RiPPs can evolve more readily because of a direct link between gene sequence and natural product. In addition, the relative brevity of RiPP biosynthetic pathways, as well as the substrate tolerance of the biosynthetic machinery, favors molecular evolution. These same attributes also facilitate their heterologous expression and render the ribosome-derived compounds attractive for bioengineering efforts and for genome-mining strategies to discover new compounds.[11]

The majority of peptides synthesized on the ribosome are produced as linear precursor peptides of about 20-110 amino acids with an N-terminal leader peptide and C-terminal core peptide. Modification of the core peptide by the biosynthetic machinery followed by leader peptide removal yields the mature natural product (Figure 1.1, bottom). The leader peptide is thought to play several roles in the biosynthesis of mature RiPPs, including serving as a secretion signal for export, a recognition motif for the posttranslational modification (PTM) enzymes, and a mechanism of self resistance by keeping the biosynthetic intermediates inactive in the native producing organism.[12] Many different classes of RiPPs are produced by bacteria, each characterized by their unique PTMs and gene clusters. Most of these RiPPs are macrocyclic, which reduces their proteolytic susceptibility and preorganizes them for target recognition. This thesis will focus on the production and maturation of one class of RiPPs, the lanthipeptides; for an extensive review of the biosynthesis and bioengineering of other RiPP classes I refer the reader to recent reviews.[1,13]

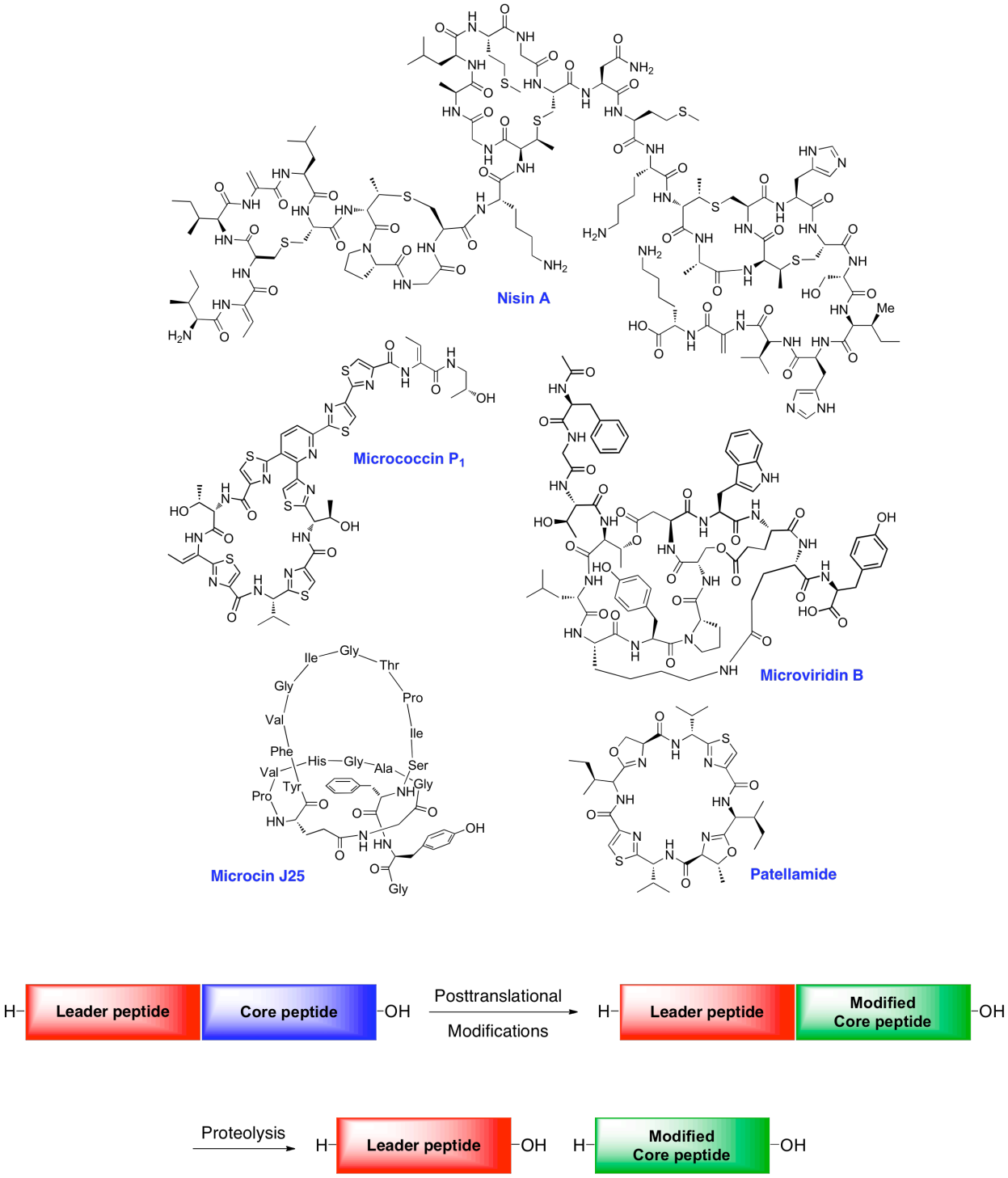

Figure 1.1. RiPP biosynthesis and structures. Top, Representative structures of RiPPs. Bottom, General scheme of leader peptide guided synthesis of RiPPs. Figure adapted from Bindman and van der Donk.[1]

1.3. LANTHIPEPTIDE BIOACTIVITIES AND MODES OF ACTION

Lanthionine-containing peptides (lanthipeptides) represent the longest known class of RiPPs. Nisin (Figure 1.1), the first discovered and most studied lantibiotic (antimicrobial lanthipeptide), has been utilized worldwide in the food industry for over 50 years as a preservative added to cheese, beer, wine, salad dressing, and many other food items.[14] Interestingly, despite this extensive period of use, no widespread bacterial resistance has developed, presumably because of its dual mode of action: binding to lipid II, thereby inhibiting transglycosylation during cell wall biosynthesis, and subsequent formation of pores in the cell membrane.[15,16] Many other lantibiotics, including mersacidin, lacticin 481, lacticin 3147, plantaricin C, and haloduracin α, also bind to lipid II but they do not form pores.[17-20] Still others have the ability to form pores but do not recognize lipid II,[21] and may have a range of other modes of action.

Lantibiotics possess potent activities against a wide range of gram-positive bacteria, including clinically relevant strains such as MRSA and VRE.[22] Indeed, two lantibiotics are already in clinical development for their abilities to treat *Clostridium difficile* (actagardine derivative) and Gram-positive infections (mutacin 1140).[23,24] Lanthipeptides in clinical development for indications that are not infectious diseases include duramycin, which aids in the treatment of cystic fibrosis.[25] Finally, the lantibiotic geobacillin was discovered to be active against *Streptococcus dysgalactiae*, one of the causative agents of bovine mastitis.[26] Despite the success of these peptides, many lantibiotics readily degrade or are insoluble at neutral pH and thus cannot be used in the clinic. Current efforts are aimed at bioengineering techniques to generate lantibiotic analogues with improved pharmacokinetic properties.

1.4. LANTHIPEPTIDE BIOSYNTHESIS

The bioactivities of lanthipeptides are the result of their extensive posttranslational modifications. At present, four compound classes have been reported that differ in the enzymes that introduce the characteristic thioether crosslinks. After ribosomal synthesis of the precursor peptide LanA (e.g. LctA for lacticin 481, Figure 1.2A), a series of serine and threonine residues in the C-terminal core region of LanA are dehydrated to form dehydroalanines and dehydrobutyrines, respectively. For class I lanthipeptides, the dehydratase LanB carries out the dehydrations. Alternatively, the N-terminal regions of the bifunctional enzymes LanM (class II), LanKC (class III), or LanL (class IV) catalyze the dehydration reactions.[27-30] The mechanism of dehydration has been thoroughly characterized in class II lanthipeptides.[31,32] The LanM enzyme catalyzes an ATP-dependent phosphorylation event on the side chain hydroxyl of Ser or Thr.[31] This phosphoryl intermediate is then eliminated, producing a dehydro amino acid (Figure 1.2B). More recently, the dehydration mechanism of NisB, the dehydratase of the class I lantibiotic nisin, was studied and shown to occur via glutamylation of the Ser or Thr residue, rather than phosphorylation, followed by glutamate elimination.[33] The subsequent Michael-type additions of cysteine residues onto the dehydro amino acids are catalyzed by the enzyme LanC (class I) or the C-terminal regions of LanM (class II), LanKC (class III), and LanL (class IV) (Figure 1.2B). The resulting thioether structures are called lanthionine and methyllanthionine when formed from Ser and Thr, respectively. Some class III LanKC synthetases do not protonate the enolate generated during the Michael-type addition, but instead catalyze addition of this enolate to another dehydroalanine forming a carbon-carbon bond.[29] The structures thus formed have been termed labionin.

In all known examples, an N-terminal leader peptide on the LanA substrate peptide guides at least part of these posttranslational modifications, but the leader peptide must be removed from the core peptide in the final step of maturation to produce the natural product (Figure 1.2A).[12,34] In the native organism, this step is catalyzed by the protease LanP (class I) or the protease domain of an ATP-binding cassette transmembrane transporter termed LanT (class II), which removes the leader peptide through proteolysis after residue –1 (amino acids in the leader peptide are indicated with negative residue numbers counting backwards from the natural protease cleavage site and amino acids in the core peptide are indicated with positive residue numbers counting forwards from the natural protease cleavage site) (Figure 1.2A).[35,36] The proteases responsible for leader peptide cleavage in class III and class IV lanthipeptides are currently unknown. A host of other, less common posttranslational modifications found in individual lanthipeptides will not be covered here but have been described elsewhere.[23]

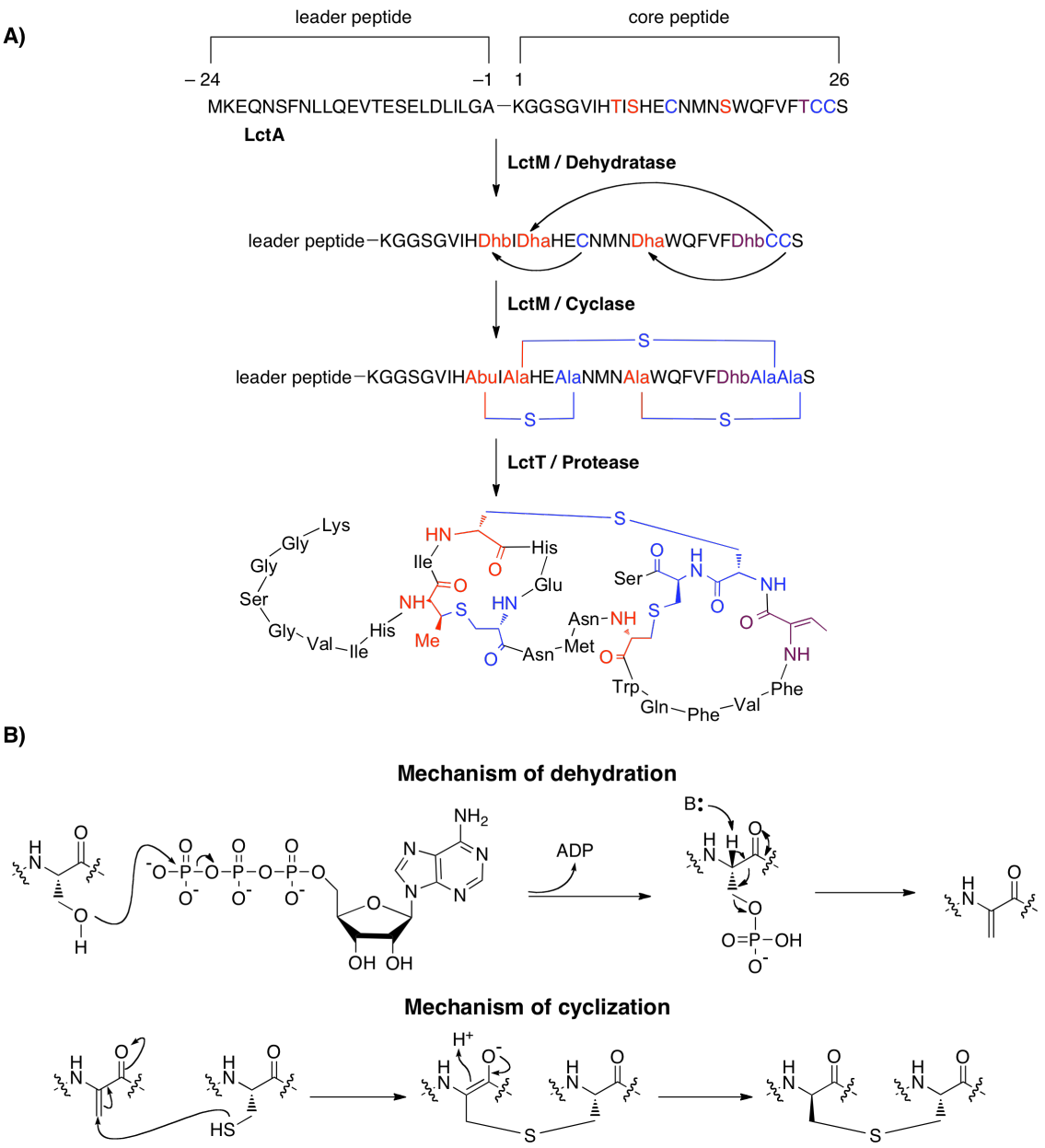

Figure 1.2. Biosynthesis and proposed mechanisms for dehydration and cyclization of lacticin 481. A) Biosynthesis of lacticin 481. The synthetase LctM transforms a linear precursor peptide LctA into a polycyclic structure. The transporter LctT then removes the leader peptide and secretes the product lacticin 481. B) Proposed mechanisms of class II lanthipeptide dehydration and cyclization. Figure adapted from Bindman and van der Donk.[1]

1.5. BIOENGINEERING OF LANTHIPEPTIDES

The biosynthesis of about a dozen lanthipeptides has been thoroughly characterized and bioengineering efforts have thus far focused on those peptides. Efforts to construct mutants with improved pharmacokinetic properties or biological activities have focused on three approaches: 1) engineering of lanthipeptides in producing strains and heterologous hosts, 2) engineering of lanthipeptides in *Escherichia coli*, and 3) *in vitro* engineering of lanthipeptides.[23]

1.5.1. Bioengineering studies in producing strains and heterologous hosts.

The generation of lantibiotic analogues in producing strains or in heterologous bacterial hosts has been achieved utilizing two methods; *in cis*, where the wild type (wt) *lanA* is modified by site-directed mutagenesis or gene replacement, or *in trans*, where a separate *lanA* gene is added, usually in a plasmid, with concomitant disruption of the endogenous *lanA*.[37] These techniques have lead to the discovery of nisin and lacticin 3147 analogues with improved bioactivity from large libraries of analogues.[38-40] Similarly, the structure-function relationships of nukacin ISK-1 and actagardine have been analyzed by site-saturation mutagenesis.[41,42] Although the production of lantibiotic mutants in producing strains has led to the discovery of peptides with improved antibacterial properties, one potential drawback is that particularly active products could overwhelm or circumvent the native immunity mechanisms of the producer organism,[39] killing the bacteria before the desired product is expressed or leading to shut-down of expression. One means to overcome potential toxicity is to prevent leader peptide removal within the producer,[43-45] but this strategy then requires subsequent removal of the leader peptide, which is often non-trivial and will be discussed throughout this thesis.

1.5.2. In vivo engineering of lanthipeptides in *E. coli*

Because of the fast generation time, well-studied fermentation behavior, and ease of genetic manipulation, several laboratories, including our own, have developed heterologous expression of lanthipeptides in *E. coli*. The first report in 2005 demonstrated that nukacin ISK-1 could be successfully produced in *E. coli* by coexpression of the substrate and its NukM modifying enzyme, although in vitro leader peptide removal using a commercial protease resulted in a truncated analogue.[46] This work was expanded in 2011 as four prochlorosins, both components of the two-component lantibiotic haloduracin, and nisin were produced in *E. coli* using a similar strategy of coexpression of substrates with the modification enzymes.[43] In this study, the leader peptides were also removed in vitro with commercial proteases at engineered cleavage sites. Subsequently, several other lanthipeptides have been produced in *E. coli* using the same strategy including lacticin 481 and cinnamycin.[47-49] The relatively high titers of modified lanthipeptides produced in *E. coli* by co-expression from pRSFDuet plasmids has also enabled the structural characterization of products of silent clusters as well as compounds that are produced in very small quantities in the native producers.[26,49] A different strategy was used for the two-component lantibiotic lichenicidin, which was successfully expressed in *E. coli* from a fosmid carrying the native cluster including the bifunctional protease/transporter. This approach resulted in secretion of the mature product without the need of in vitro removal of the leader peptide.[50,51] Both methods have also allowed incorporation of non-proteinogenic amino acids, either by using stop-codon suppression methodology with orthogonal tRNA/tRNA synthetases[43] or by using the natural promiscuity of some of the native tRNA/tRNA synthetase pairs (e.g. Met).[51]

1.5.3. In vitro engineering of lanthipeptides.

The construction of lanthipeptides and analogues via in vitro reconstitution of the activities of the biosynthetic enzymes has been exploited as an alternative to isolation of lanthipeptides from bacterial production systems.[27] Facilitated by the relative ease of heterologous production of the precursor peptides, LanA, and the biosynthetic enzymes, LanM, in *E. coli*, the in vitro route allows for the incorporation of amino acid substitutions into the peptide substrates via site-directed mutagenesis (mainly native amino acids), or solid phase peptide synthesis (native or non-proteinogenic amino acids),[52] providing access to a much larger pool of structures than with in vivo methods. The first successful in vitro reconstitution of the lanthionine-forming machinery[27] allowed studies on the high substrate tolerance and mechanism of the posttranslational modification enzymes.[18,31,35,53-55] Incorporation of nonproteinogenic amino acids into lanthipeptides has been achieved for lacticin 481 by ligation of synthetic lacticin 481 core peptides with the leader peptide using either 1,3 dipolar cycloaddition (Figure 1.3) or native chemical ligation.[52,56] Modification by LctM and subsequent leader peptide removal with the commercial protease LysC yielded a panel of lacticin 481 analogues, including two variants with improved bioactivity. The ability to produce non-native lantibiotic analogues is valuable for mode of action and bioactivity studies as well as for understanding the specificities and mechanistic details of the posttranslational modification enzymes.

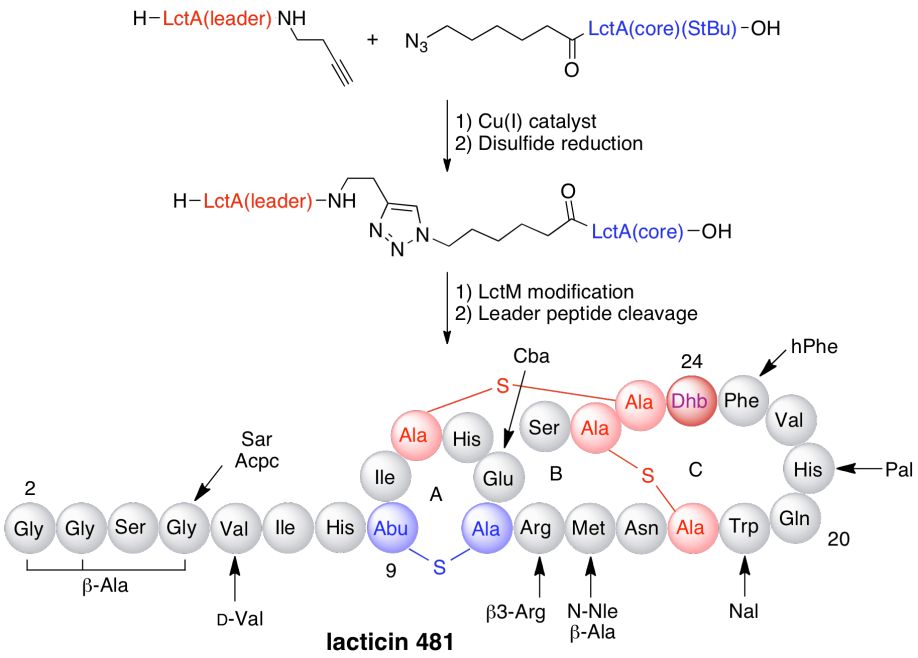

Figure 1.3. In vitro engineering of lacticin 481. Copper-catalyzed alkyne/azide cycloaddition followed by LctM modification of the core peptide and leader peptide removal allowed the incorporation of non-proteinogenic amino acids into lacticin 481 analogues. Sar, sarcosine; Acpc, aminocyclopropanoic acid; Cba, 4-cyanoaminobutyric acid; *N*-Nle, *N*-butyl glycine; Nal, naphthyl alanine; Pal, pyridynyl alanine; hPhe, homophenylalanine. Figure adapted from Bindman and van der Donk.[1]

1.6. SUMMARY AND OUTLOOK

A major drawback to the production of lanthipeptides, either in vivo in *E. coli* or in vitro, is the removal of the leader peptide to generate the mature natural product. This step is often achieved by engineering a proteolytic cleavage site (Glu, Lys, Ile-Glu-Gly-Arg) at the –1 position and using a commercial endoprotease (GluC, LysC or trypsin, Factor Xa) to remove the entire leader peptide, a process that will be described in more detail in Chapter 4. Although this strategy has been effective in several cases, it can be unproductive if the core region contains the

same cleavage site. Also, in lacticin 481, the leader peptide has been removed utilizing the endoprotease LysC, which cleaves off the N-terminal lysine, yielding Δ1-lacticin 481, a mutant with decreased bioactivity.[52] Thus, it would be beneficial to develop new strategies to remove the leader peptide that are independent of the amino acid sequence of the core region. In this thesis, Chapter 2 will discuss a method to introduce a photolabile linker between lanthipeptide leader and core regions. Posttranslational modification of the lanthipeptide by its cognate synthetase in vitro, followed by UV-light mediated removal of the leader peptide, yielded the mature lanthipeptide. This method will also allow the facile incorporation of non-proteinogenic amino acids into lanthipeptides as the core peptide is synthesized on the solid phase. Chapter 3 will spotlight a novel way to engineer the ribosomal machinery to incorporate a hydroxy acid into the peptide thus generating an ester linkage directly between the lanthipeptide leader and core regions utilizing the relaxed substrate specificity of pyrrolysyl tRNA synthetase. By incubating the peptide under mild alkaline conditions, the subsequent ester bond was selectively hydrolyzed, yielding the core region with an N-terminal hydroxyl group.

Labeling of natural products with biophysical probes has greatly contributed to investigations of their modes of action and has provided tools for visualization of their targets. However, the mode of action of only a few lantibiotics has been determined thus far. A general challenge is the availability of a suitable functional group for chemoselective modification. Chapter 4 will discuss novel methodology to introduce an N-terminal ketone into various lanthipeptides by the generation of a cryptic N-terminal dehydro amino acid by the cognate biosynthetic enzymes. Spontaneous hydrolysis of the N-terminal enamines after leader peptide removal results in α-ketoamides that site-specifically react with an aminooxy-derivatized alkyne or fluorophore. The fluorescently-modified lantibiotics were added to bacteria, and their cellular

localization was visualized by confocal fluorescence microscopy as a means to determine their modes of action.

1.7. REFERENCES

(1) Bindman, N.; van der Donk, W. A., RiPPs: Ribosomally Synthesized and Posttranslationally Modified Peptides; *Natural Products: Discourse, Diversity & Design*, **2014**, *Ch. 24*, in press.

(2) Taubes, G., The bacteria fight back, *Science* **2008**, *321*, 356.

(3) Fischbach, M. A.; Walsh, C. T., Antibiotics for emerging pathogens, *Science* **2009**, *325*, 1089.

(4) Clardy, J.; Fischbach, M. A.; Walsh, C. T., New antibiotics from bacterial natural products, *Nat. Biotechnol.* **2006**, *24*, 1541.

(5) Higgins, D. L.; Chang, R.; Debabov, D. V.; Leung, J.; Wu, T.; Krause, K. M.; Sandvik, E.; Hubbard, J. M.; Kaniga, K.; Schmidt, D. E., Jr.; Gao, Q.; Cass, R. T.; Karr, D. E.; Benton, B. M.; Humphrey, P. P., Telavancin, a multifunctional lipoglycopeptide, disrupts both cell wall synthesis and cell membrane integrity in methicillin-resistant Staphylococcus aureus, *Antimicrob. Agents Chemother.* **2005**, *49*, 1127.

(6) Greenwood, D., Microbiological properties of teicoplanin, *J. Antimicrob. Chemother.* **1988**, *21 Suppl A*, 1.

(7) Miao, V.; Coeffet-Legal, M. F.; Brian, P.; Brost, R.; Penn, J.; Whiting, A.; Martin, S.; Ford, R.; Parr, I.; Bouchard, M.; Silva, C. J.; Wrigley, S. K.; Baltz, R. H., Daptomycin biosynthesis in Streptomyces roseosporus: cloning and analysis of the gene cluster and revision of peptide stereochemistry, *Microbiology* **2005**, *151*, 1507.

(8) Reddy, K. V.; Yedery, R. D.; Aranha, C., Antimicrobial peptides: premises and promises, *Int. J. Antimicrob. Agents* **2004**, *24*, 536.

(9) Oyston, P. C.; Fox, M. A.; Richards, S. J.; Clark, G. C., Novel peptide therapeutics for treatment of infections, *J. Med. Microbiol.* **2009**, *58*, 977.

(10) Walsh, C. T., Polyketide and nonribosomal peptide antibiotics: modularity and versatility, *Science* **2004**, *303*, 1805.

(11) Velásquez, J. E.; van der Donk, W. A., Genome mining for ribosomally synthesized natural products, *Curr. Opin. Chem. Biol.* **2011**, *15*, 11.

(12) Oman, T. J.; van der Donk, W. A., Follow the leader: the use of leader peptides to guide natural product biosynthesis, *Nat. Chem. Biol.* **2010**, *6*, 9.

(13) Arnison, P. G. B., M. J.; Bierbaum, G.; Bowers, A. A.; Bulaj, G.; Camarero, J. A.; Campopiano, D. J.; Clardy, J.; Cotter, P. D.; Craik, D. J.; Dawson, M.; Dittmann, E.; Donadio, S.; Dorrestein, P. C.; Entian, K.-D.; Fischbach, M. A.; Garavelli, J. S.; Göransson, U.; Gruber, C. W.; Haft, D. H.; Hemscheidt, T. K.; Hertweck, C.; Hill, C.; Horswill, A. R.; Jaspars, M.; Kelly, W. L.; Klinman, J. P.; Kuipers, O. P.; Link, A. J.; Liu, W.; Marahiel, M. A.; Mitchell, D. A.; Moll, G. N.; Moore, B. S.; Nair, S. K.; Nes, I. F.; Norris, G. E.; Olivera, B. M.; Onaka, H.; Patchett, M. L.; Reaney, M. J. T.; Rebuffat, S.; Ross, R. P.; Sahl, H.-G.; Saris, P.; Schmidt, E. W.; Selsted, M. E.; Severinov, K.; Shen, B.; Sivonen, K.; Smith, L.; Stein, T.; Süssmuth, R. E.; Tagg, J. R.; Tang, G.-L.; Vederas, J. C.; Walsh, C. T.; Walton, J. D.; Willey, J. M.; van der Donk, W. A., Ribosomally synthesized and post-translationally modified peptide natural products: Overview and recommendations for a universal nomenclature., *Nat. Prod. Rep.* **2013**, *30*, 108.

(14) Delves-Broughton, J.; Blackburn, P.; Evans, R. J.; Hugenholtz, J., Applications of the bacteriocin, nisin, *Antonie van Leeuwenhoek* **1996**, *69*, 193.

(15) Breukink, E.; de Kruijff, B., Lipid II as a target for antibiotics, *Nat. Rev. Drug Discov.* **2006**, *5*, 321.

(16) Schneider, T.; Sahl, H. G., Lipid II and other bactoprenol-bound cell wall precursors as drug targets, *Curr. Opin. Investig. Drugs* **2010**, *11*, 157.

(17) Brötz, H.; Bierbaum, G.; Leopold, K.; Reynolds, P. E.; Sahl, H. G., The lantibiotic mersacidin inhibits peptidoglycan synthesis by targeting lipid II, *Antimicrob. Agents Chemother.* **1998**, *42*, 154.

(18) Oman, T. J.; Lupoli, T. J.; Wang, T. S.; Kahne, D.; Walker, S.; van der Donk, W. A., Haloduracin alpha binds the peptidoglycan precursor lipid II with 2:1 stoichiometry, *J. Am. Chem. Soc.* **2011**, *133*, 17544.

(19) Wiedemann, I.; Bottiger, T.; Bonelli, R. R.; Wiese, A.; Hagge, S. O.; Gutsmann, T.; Seydel, U.; Deegan, L.; Hill, C.; Ross, P.; Sahl, H. G., The mode of action of the lantibiotic lacticin 3147--a complex mechanism involving specific interaction of two peptides and the cell wall precursor lipid II, *Mol. Microbiol.* **2006**, *61*, 285.

(20) Wiedemann, I.; Bottiger, T.; Bonelli, R. R.; Schneider, T.; Sahl, H. G.; Martinez, B., Lipid II-based antimicrobial activity of the lantibiotic plantaricin C, *Appl. Environ. Microbiol.* **2006**, *72*, 2809.

(21) Brötz, H.; Josten, M.; Wiedemann, I.; Schneider, U.; Gotz, F.; Bierbaum, G.; Sahl, H. G., Role of lipid-bound peptidoglycan precursors in the formation of pores by nisin, epidermin and other lantibiotics, *Mol. Microbiol.* **1998**, *30*, 317.

(22) Piper, C.; Cotter, P. D.; Ross, R. P.; Hill, C., Discovery of medically significant lantibiotics, *Curr. Drug. Discov. Technol.* **2009**, *6*, 1.

(23) Knerr, P. J.; van der Donk, W. A., Discovery, biosynthesis, and engineering of lantipeptides, *Annu. Rev. Biochem.* **2012**, *81*, 479.

(24) Ghobrial, O.; Derendorf, H.; Hillman, J. D., Pharmacokinetic and pharmacodynamic evaluation of the lantibiotic MU1140, *J. Pharm. Sci.* **2010**, *99*, 2521.

(25) Zhao, M.; Li, Z.; Bugenhagen, S., 99mTc-labeled duramycin as a novel phosphatidylethanolamine-binding molecular probe, *J. Nucl. Med.* **2008**, *49*, 1345.

(26) Garg, N.; Tang, W.; Goto, Y.; van der Donk, W. A., Geobacillins: lantibiotics from *Geobacillus thermodenitrificans*, *Proc. Natl. Acad. Sci. U. S. A.* **2012**, *109*, 5241.

(27) Xie, L.; Miller, L. M.; Chatterjee, C.; Averin, O.; Kelleher, N. L.; van der Donk, W. A., Lacticin 481: In vitro reconstitution of lantibiotic synthetase activity, *Science* **2004**, *303*, 679.

(28) Goto, Y.; Li, B.; Claesen, J.; Shi, Y.; Bibb, M. J.; van der Donk, W. A., Discovery of unique lanthionine synthetases reveals new mechanistic and evolutionary insights, *PLoS Biol.* **2010**, *8*, e1000339.

(29) Meindl, K.; Schmiederer, T.; Schneider, K.; Reicke, A.; Butz, D.; Keller, S.; Guhring, H.; Vertesy, L.; Wink, J.; Hoffmann, H.; Bronstrup, M.; Sheldrick, G. M.; Süssmuth, R. D., Labyrinthopeptins: a new class of carbacyclic lantibiotics, *Angew. Chem. Int. Ed.* **2010**, *49*, 1151.

(30) Kodani, S.; Hudson, M. E.; Durrant, M. C.; Buttner, M. J.; Nodwell, J. R.; Willey, J. M., The SapB morphogen is a lantibiotic-like peptide derived from the product of the developmental gene *ramS* in *Streptomyces coelicolor*, *Proc. Natl. Acad. Sci. U.S.A.* **2004**, *101*, 11448.

(31) Chatterjee, C.; Miller, L. M.; Leung, Y. L.; Xie, L.; Yi, M.; Kelleher, N. L.; van der Donk, W. A., Lacticin 481 synthetase phosphorylates its substrate during lantibiotic production, *J. Am. Chem. Soc.* **2005**, *127*, 15332.

(32) You, Y. O.; van der Donk, W. A., Mechanistic investigations of the dehydration reaction of lacticin 481 synthetase using site-directed mutagenesis, *Biochemistry* **2007**, *46*, 5991.

(33) Garg, N.; Salazar-Ocampo, L. M.; van der Donk, W. A., In vitro activity of the nisin dehydratase NisB, *Proc. Natl. Acad. Sci. U. S. A.* **2013**, *110*, 7258.

(34) van der Meer, J. R.; Polman, J.; Beerthuyzen, M. M.; Siezen, R. J.; Kuipers, O. P.; de Vos, W. M., Characterization of the *Lactococcus lactis* nisin A operon genes *nisP*, encoding a subtilisin-like serine protease involved in precursor processing, and *nisR*, encoding a regulatory protein involved in nisin biosynthesis, *J. Bacteriol.* **1993**, *175*, 2578.

(35) Furgerson Ihnken, L. A.; Chatterjee, C.; van der Donk, W. A., In vitro reconstitution and substrate specificity of a lantibiotic protease, *Biochemistry* **2008**, *47*, 7352.

(36) Håvarstein, L. S.; Diep, D. B.; Nes, I. F., A family of bacteriocin ABC transporters carry out proteolytic processing of their substrates concomitant with export, *Mol. Microbiol.* **1995**, *16*, 229.

(37) Cortés, J.; Appleyard, A. N.; Dawson, M. J., Chapter 22. Whole-cell generation of lantibiotic variants, *Methods Enzymol.* **2009**, *458*, 559.

(38) Field, D.; Connor, P. M.; Cotter, P. D.; Hill, C.; Ross, R. P., The generation of nisin variants with enhanced activity against specific gram-positive pathogens, *Mol. Microbiol.* **2008**, *69*, 218.

(39) Rink, R.; Wierenga, J.; Kuipers, A.; Kluskens, L. D.; Driessen, A. J.; Kuipers, O. P.; Moll, G. N., Dissection and modulation of the four distinct activities of nisin by mutagenesis of rings A and B and by C-terminal truncation, *Appl. Environ. Microbiol.* **2007**, *73*, 5809.

(40) Cotter, P. D.; Deegan, L. H.; Lawton, E. M.; Draper, L. A.; O'Connor, P. M.; Hill, C.; Ross, R. P., Complete alanine scanning of the two-component lantibiotic lacticin 3147: generating a blueprint for rational drug design, *Mol. Microbiol.* **2006**, *62*, 735.

(41) Islam, M. R.; Shioya, K.; Nagao, J.; Nishie, M.; Jikuya, H.; Zendo, T.; Nakayama, J.; Sonomoto, K., Evaluation of essential and variable residues of nukacin ISK-1 by NNK scanning, *Mol. Microbiol.* **2009**, *72*, 1438.

(42) Boakes, S.; Ayala, T.; Herman, M.; Appleyard, A. N.; Dawson, M. J.; Cortes, J., Generation of an actagardine A variant library through saturation mutagenesis, *Appl. Microbiol. Biotechnol.* **2012**, *95*, 1509.

(43) Shi, Y.; Yang, X.; Garg, N.; van der Donk, W. A., Production of lantipeptides in *Escherichia coli*, *J. Am. Chem. Soc.* **2011**, *133*, 2338.

(44) Lin, Y.; Teng, K.; Huan, L.; Zhong, J., Dissection of the bridging pattern of bovicin HJ50, a lantibiotic containing a characteristic disulfide bridge, *Microbiol. Res.* **2011**, *166*, 146.

(45) Valsesia, G.; Medaglia, G.; Held, M.; Minas, W.; Panke, S., Circumventing the effect of product toxicity: Development of a novel two-stage production process for the lantibiotic gallidermin, *Appl. Environ. Microbiol.* **2007**, *73*, 1635.

(46) Nagao, J.; Harada, Y.; Shioya, K.; Aso, Y.; Zendo, T.; Nakayama, J.; Sonomoto, K., Lanthionine introduction into nukacin ISK-1 prepeptide by co-expression with modification enzyme NukM in *Escherichia coli*, *Biochem. Biophys. Res. Commun.* **2005**, *336*, 507.

(47) Ökesli, A.; Cooper, L. E.; Fogle, E. J.; van der Donk, W. A., Nine post-translational modifications during the biosynthesis of cinnamycin, *J. Am. Chem. Soc.* **2011**, *133*, 13753.

(48) Oman, T. J.; Knerr, P. J.; Bindman, N. A.; Velasquez, J. E.; van der Donk, W. A., An engineered lantibiotic synthetase that does not require a leader peptide on its substrate, *J. Am. Chem. Soc.* **2012**, *134*, 6952.

(49) Tang, W.; van der Donk, W. A., Structural characterization of four prochlorosins: a novel class of lantipeptides produced by planktonic marine cyanobacteria, *Biochemistry* **2012**, *51*, 4271.

(50) Caetano, T.; Krawczyk, J. M.; Mosker, E.; Süssmuth, R. D.; Mendo, S., Heterologous expression, biosynthesis, and mutagenesis of type II lantibiotics from *Bacillus licheniformis* in *Escherichia coli*, *Chem. Biol.* **2011**, *18*, 90.

(51) Oldach, F.; Al Toma, R.; Kuthning, A.; Caetano, T.; Mendo, S.; Budisa, N.; Süssmuth, R. D., Congeneric lantibiotics from ribosomal in vivo peptide synthesis with noncanonical amino acids, *Angew. Chem. Int. Ed.* **2012**, *51*, 415.

(52) Levengood, M. R.; Knerr, P. J.; Oman, T. J.; van der Donk, W. A., In vitro mutasynthesis of lantibiotic analogues containing nonproteinogenic amino acids, *J. Am. Chem. Soc.* **2009**, *131*, 12024.

(53) Chatterjee, C.; Patton, G. C.; Cooper, L.; Paul, M.; van der Donk, W. A., Engineering dehydro amino acids and thioethers into peptides using lacticin 481 synthetase, *Chem. Biol.* **2006**, *13*, 1109.

(54) Levengood, M. R.; van der Donk, W. A., Use of lantibiotic synthetases for the preparation of bioactive constrained peptides, *Bioorg. Med. Chem. Lett.* **2008**, *18*, 3025.

(55) Oman, T. J.; van der Donk, W. A., Insights into the mode of action of the two-peptide lantibiotic haloduracin, *ACS Chem. Biol.* **2009**, *4*, 865.

(56) Zhang, X.; van der Donk, W. A., On the substrate specificity of dehydration by lacticin 481 synthetase, *J. Am. Chem. Soc.* **2007**, *129*, 2212.

Chapter 2: Photochemical Cleavage of Leader Peptides

Taken in part from Bindman and van der Donk., Photochemical Cleavage of Leader Peptides, *Chem. Commun.*, **2010**, 46, 8935-8937.[1] Reproduced with permission of The Royal Society of Chemistry.

2.1 INTRODUCTION

The ability to produce non-native lanthipeptide analogues is valuable for lanthipeptide mode of action and bioactivity studies, as well as for investigation of the specificities and mechanistic details of the post-translational modification enzymes. Indeed, mutation of a conserved Glu or Asp residue to Ala in several lantibiotics either lowered the compounds activity or rendered the compound completely inactive, signifying the importance of the residue to the lantibiotic mode of action.[2-7] Unfortunately, despite the success of these examples, the removal of the leader peptide usually presents a major technical hurdle. The native proteases that cleave the modified substrates endogenously are often membrane associated as part of ATP-binding cassette transporters,[8] with soluble domains having low in vitro activity.[9,10] Hence, although a few successful examples have been reported,[11-13] the cognate proteases are not a general solution for removal of leader peptides. To address these limitations, various other methods for in vitro removal of the leader peptides have been reported.[1] The most common strategy has been incorporation of Lys or Glu at the –1 position for subsequent treatment with endoproteinases LysC or GluC, respectively.[14-17] Whereas these approaches have worked in select cases, use of GluC and LysC typically does not work if the core peptide contains a Lys or Glu, unless that residue is "deactivated" for proteolysis by adjacent posttranslationally modified amino acids. Also, the activity of the commercial protease on the –1 position can be sluggish or nonexistent

when the cleavage site is proximal to a posttranslationally modified amino acid.[7,17-19] Therefore, an alternative, general method for the removal of the leader peptides would be valuable.

The incorporation of 2-nitrophenyl or 2-nitroveratrole groups at appropriate sites in peptides and proteins has allowed the site-specific light-mediated cleavage of the polyamide backbone. For instance, introduction of phenylglycine derivative **2.1** (Scheme 2.1) in ion channels allowed their temporal photo-activation.[20] Other examples of linkers that allow photolytic scission of peptide chains are the commercially available β-amino acid **2.2** and a series of linkers incorporating a nitrophenyl group in the peptide chain, exemplified by **2.3**.[21] These linkers are effective, but they are less attractive for leader peptide removal as their use would result in core peptides carrying non-natural nitrosoaryl groups (e.g. **2.7-2.9**, Scheme 2.1). Therefore, we designed linker **2.4**, which was envisioned to generate the native core peptide **2.10** upon photolysis.

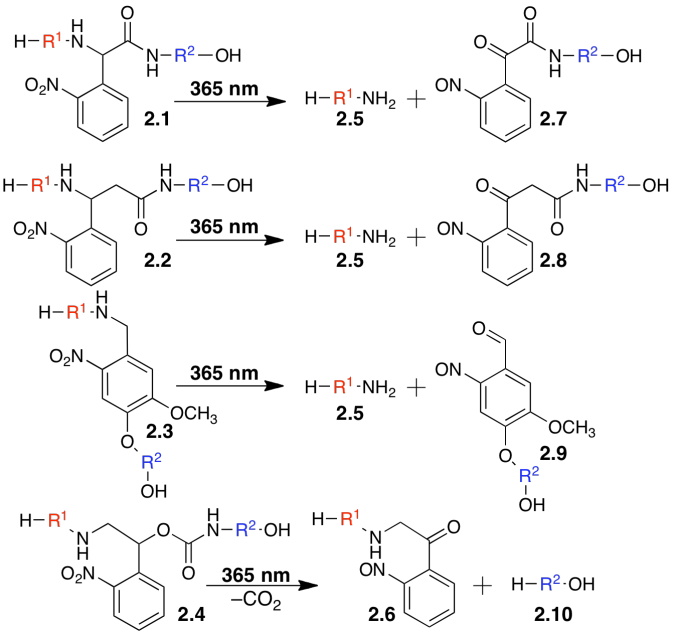

Scheme 2.1. Photochemical cleavage of 2-nitrophenyl derivatives (**2.1-2.4**) linking N- and C-terminal peptide fragments. For the purpose of this work, R^1 would represent the leader peptide and R^2 the core peptide. Scheme adapted from Bindman and van der Donk.[1]

2.2. RESULTS AND DISCUSSION

2.2.1. Design and synthesis of photocleavable linker 2.17.

We considered two major criteria in our design of a reagent that could introduce linker **2.4** into peptides. First, compatibility with fluorenylmethyloxycarbonyl-SPPS (Fmoc-SPPS) was desired in order to take advantage of the ease of this approach for the synthesis of peptides and to facilitate incorporation of non-canonical amino acids. Second, the linker had to be amenable to our previously developed segment coupling strategy that links the leader peptide with the core peptide using a Cu(I)-catalyzed alkyne azide cycloaddition (CuAAC)[22] between a leader peptide with a C-terminal alkyne and a core peptide with an N-terminal azide.[23] In this previous work, the enzyme LctM was able to process substrate analogues of the precursor peptide LctA in which the core and leader peptides had been fused via a triazole.[23] Linkers **2.15-2.17** (Scheme 2.2) were designed to fulfill both criteria and linker **2.18**, a related photolabile compound that required a more lengthy synthesis and was not used for SPPS, was reported during the course of this study.[24] Each linker contained two distinct functionalities; an electrophilic region to trap an N-terminal amine on a growing peptide chain and an azide, which could be reduced to an amine to facilitate peptide elongation by SPPS or coupled to an alkyne-labeled peptide via a CuAAC bioconjugation.

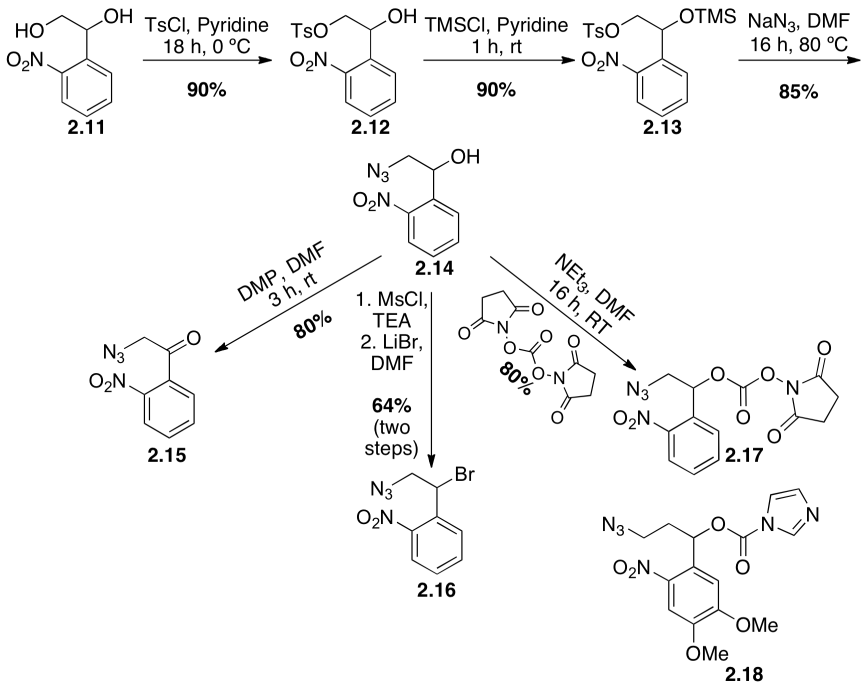

Scheme 2.2. Synthesis of photolabile linkers **2.15**, **2.16**, and **2.17**. Photolabile linker **2.18** was previously synthesized.[24] Scheme adapted from Bindman and van der Donk.[1]

Photolabile linkers **2.15-2.17** were synthesized starting from commercial diol **2.11** (Scheme 2.2). Activation of the primary alcohol of **2.11** with *p*-toluenesulfonyl chloride (TsCl) was followed by protection of the secondary alcohol as the trimethylsilyl (TMS) ether to yield **2.13**. The *p*-toluenesulfonate group of **2.13** was then displaced with sodium azide. TMS protection of the primary alcohol of **2.13** was required to prevent epoxide formation and subsequent azide addition to the benzylic carbon. Fortuitously, under the displacement reaction conditions, the TMS protecting group also was removed, affording secondary alcohol **2.14**. Compound **2.14** was oxidized to the ketone by Dess-Martin periodinane to generate linker **2.15**. We postulated that this linker could be incorporated into a resin-bound peptide via a reductive alkylation reaction. However, reductive alkylation of primary amines at the N-terminus of peptides with linker **2.15**, whether on- or off-resin, never produced product. The reductive

alkylation strategy was therefore abandoned in favor of a nucleophilic substitution reaction. We hypothesized that the secondary bromide of linker **2.16** might be more amenable to reaction with the terminal amine of a resin-bound peptide. Thus, linker **2.16** was synthesized by converting the secondary alcohol of compound **2.14** to the methylsulfonate followed by displacement with lithium bromide. This linker was successfully reacted with the resin-bound pentamer H-GASSA-O-Wang in the presence of diisopropylethylamine (DIPEA), as determined by electrospray ionization mass spectrometry (ESI-MS) (Figure 2.1A,C). However, the nucleophilic substitution reaction was only efficient if glycine was the N-terminal amino acid; the reaction with the peptide H-AASSA-O-Wang proceeded in low yields (Figure 2.1B), presumably because of a steric clash between linker **2.16** and the more bulky amino acid. Therefore, the substitution strategy was abandoned for one in which a peptide could be incorporated into the photocleavable linker via a carbonyl addition-elimination reaction. Thus, photocleavable linker **2.17** was synthesized by reacting the secondary alcohol of **2.14** with disuccinimidyl carbonate. We suspected linker **2.17** would be more versatile than linkers **2.15** or **2.16** given the extensive use of carbonates in chemical biology.

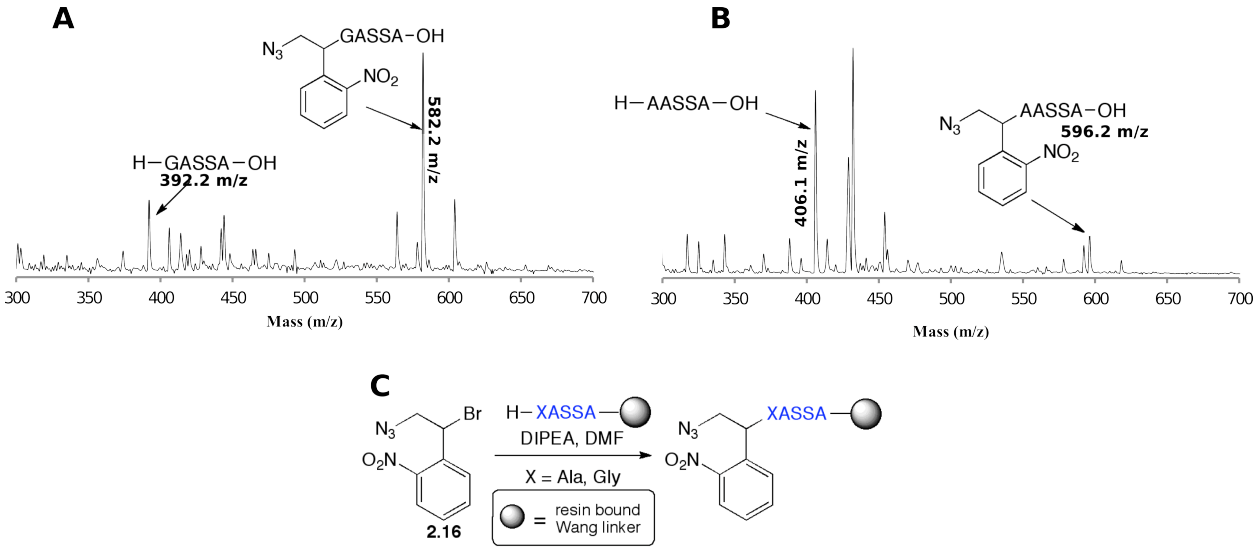

Figure 2.1. ESI-MS spectra of alkylation reactions of linker **2.16** and pentapeptides A) H-GASSA-O-Wang and B) H-AASSA-O-Wang (H-GASSA-OH $[M+H]^+$ calc'd = 392.2 Da.; N_3-GASSA-OH $[M+H]^+$ calc'd = 582.4 Da.; H-AASSA-OH $[M+H]^+$ calc'd = 406.2 Da.; N_3-AASSA-OH $[M+H]^+$ calc'd = 596.4 Da.) C) Schematic representation of the reaction between linker **2.16** and pentapeptides with an N-terminal Ala or Gly.

2.2.2. Differential scanning calorimetry measurements of compounds 2.12-2.14 and 2.17.

Because of their large ratio of oxygen and nitrogen atoms to carbon atoms, compounds **2.12-2.14** and **2.17** were analyzed by differential scanning calorimetry (DSC) to ensure their safety under the conditions used (Figure 2.2). The determined heat of decomposition of each compound was compared to benzoyl peroxide (BPO) as standard reference material.[25] Briefly, if the heat quantities of the decomposition reactions of compounds **2.12-2.14** and **2.17** were lower than the heat quantity of decomposition of BPO the compound was judged not to be a Class 5 explosive and thus safe to utilize in the temperature range tested.

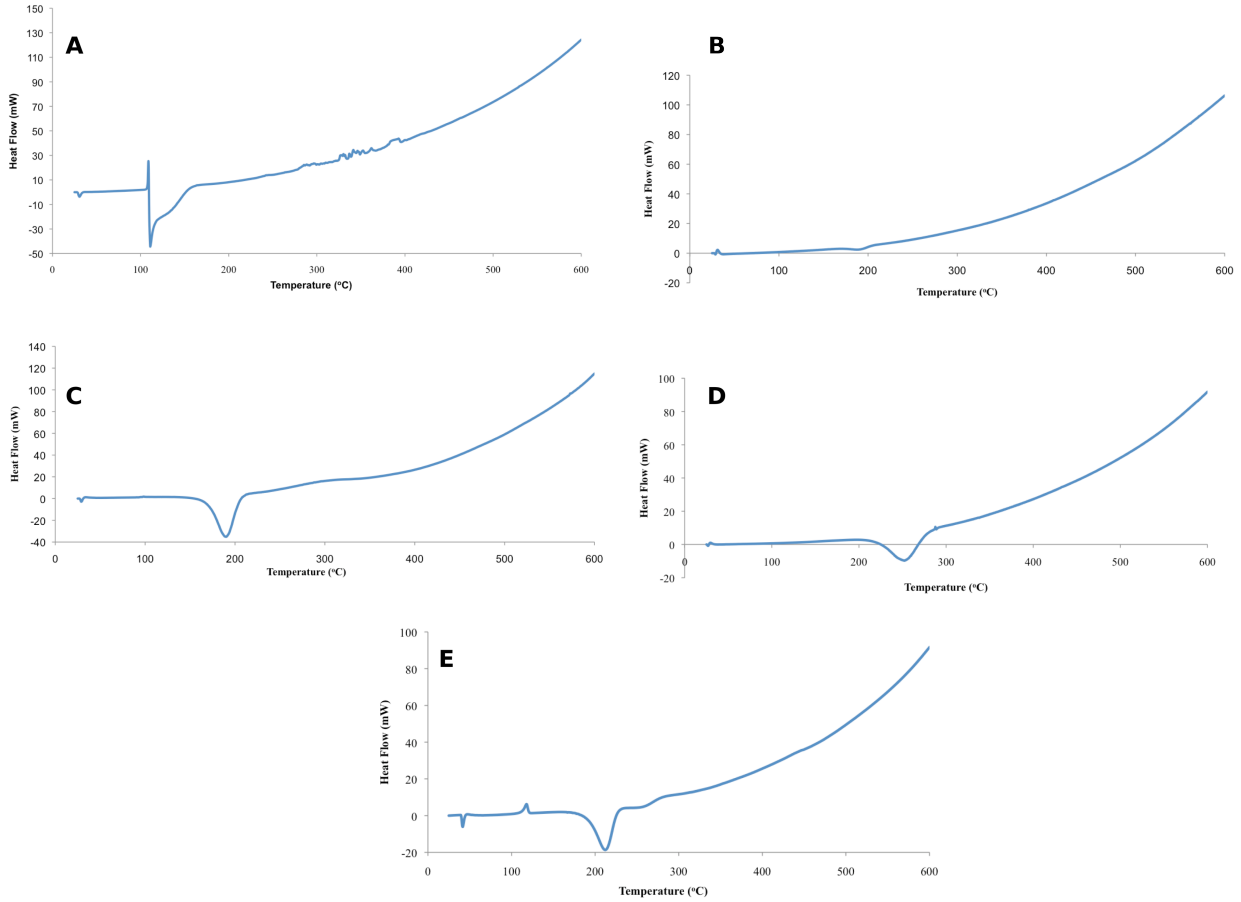

Figure 2.2. DSC data of **2.12**-**2.14**, **2.17**, and BPO. A) Standard reference compound BPO. Peak onset = 109 ºC, peak = 110 ºC, exotherm = -2350 J/g. B) Compound **2.12**. Peak onset = 170 ºC, peak = 191 ºC, exotherm = -1220 J/g. C) Compound **2.13**. Peak onset = 170 ºC, peak = 190 ºC, exotherm = -860 J/g. D) Compound **2.14**. Peak onset = 225 ºC, peak = 252 ºC, exotherm = -1595 J/g. E) Compound **2.17**. Peak onset = 190 ºC, peak = 212 ºC, exotherm = -1220 J/g.

Each of the compounds tested had heat quantities of decomposition less than that of benzoyl peroxide. However, the baseline of each of the spectra increased dramatically after 250 ºC. Therefore, we cannot rule out exotherms at high temperatures that could have been obscured by the baseline. Therefore, care should still be taken before using these compounds at higher

temperatures than employed in this study and DSC analysis that is accurate at higher temperatures should be utilized prior to use at high temperatures.

2.2.3. Compatibility of linker 2.17 with SPPS.

To investigate the compatibility of linker **2.17** with Fmoc-SPPS, a model peptide with the sequence AGLSA was assembled on pre-loaded Wang resin using standard Fmoc methodology with O-(1H-6-chlorobenzotriazol-1-yl)-N,N,N',N'-tetramethyluronium hexafluorophosphate (HCTU) and N-methyl morpholine (NMM) as coupling reagents. The peptide was reacted with linker **2.17** in the presence of DIPEA and the resulting product was analyzed by ESI-MS (Figure 2.3). Unlike the nucleophilic substitution reaction with linker **2.16**, linker **2.17** was successfully incorporated at room temperature onto a pentapeptide with an N-terminal Ala, yielding **2.19**.

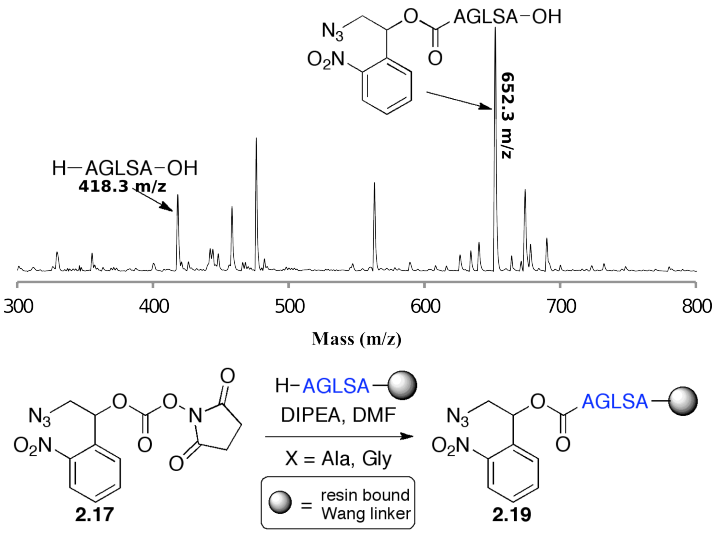

Figure 2.3. Reaction between photolabile linker **2.17** and pentapeptide H-AGLSA-O-Wang. ESI-MS spectrum (top) and schematic representation (bottom) of the reaction between the pentapeptide H-AGLSA-O-Wang and photolabile linker **2.17** yielding azidopeptide **2.19** (H-AGLSA-OH $[M+H]^+$ calc'd = 418.2 Da.; N3-AGLSA-OH $[M+H]^+$ calc'd = 652.4 Da.).

After successful coupling of a C-terminal peptide fragment to the linker, the compatibility of the linker with the reactions employed for the installment of an N-terminal peptide was evaluated. The azide functionality of **2.19** was reduced *in situ* with tri-*n*-butylphosphine, followed by coupling with Fmoc-Ala-OH to generate peptide **2.20** (Scheme 2.3). Standard peptide elongation was performed followed by peptide cleavage from resin using 95% trifluoroacetic acid, and reversed-phase high performance liquid chromatography (RP-HPLC) purification, producing peptide **2.21**. To test the photolability of linker **2.17** the purified peptide was irradiated at 365 nm and the N- and C-terminal peptide fragments **2.22** and **2.23** were obtained successfully as determined by ESI-MS and RP-HPLC (Figure 2.4).

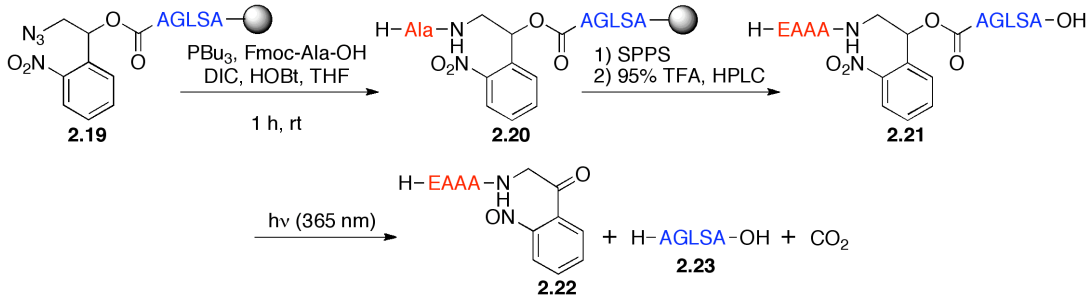

2.19 **2.20** **2.21** **2.22** **2.23**

Scheme 2.3. Synthesis of decapeptide **2.21** followed by photolysis to generate peptides **2.22** and **2.23**.

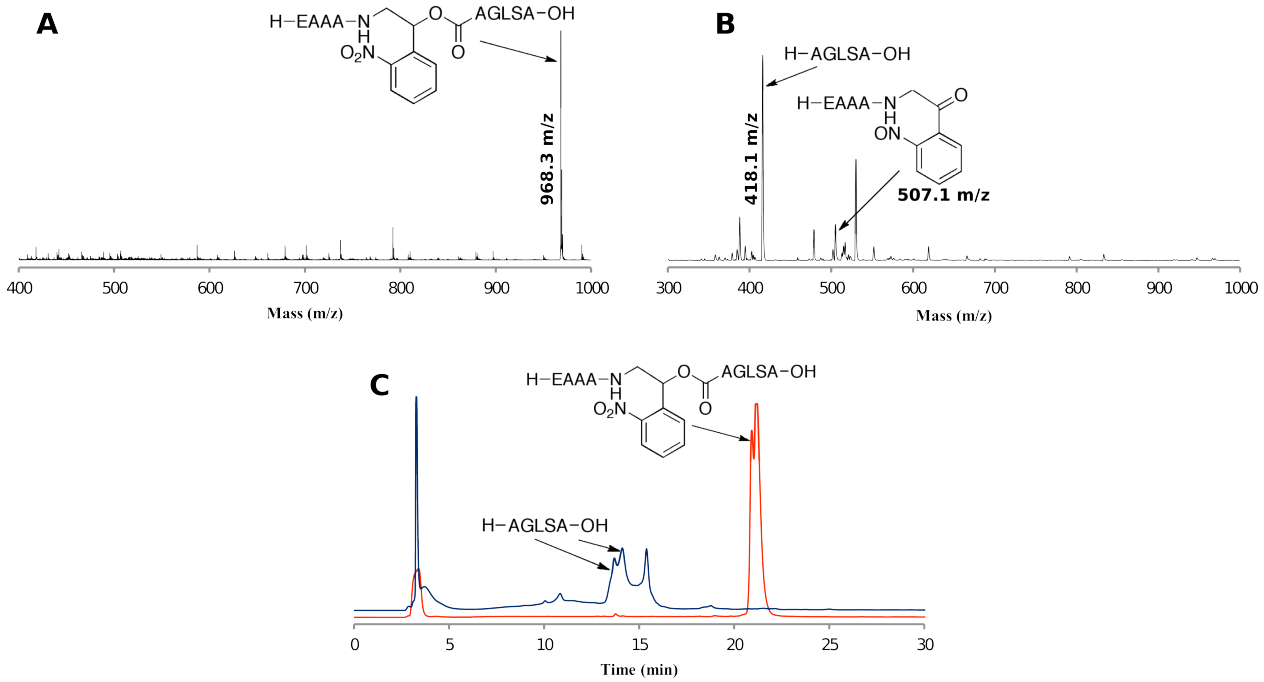

Figure 2.4. Analysis of the photolysis of decapeptide **2.21**. ESI-MS spectra of decapeptide **2.21** before (A) and after (B) photolysis. C) Analytical RP-HPLC spectrum of decapeptide **2.21** before (red) and after (blue) photolysis; two diastereomers of H-AGLSA-OH were formed presumably as a result of epimerization of the C-terminal alanine as described in section 2.2.4 (full length decapeptide $[M+H]^+$ calc'd = 968.6 Da; H-AGLSA-OH $[M+H]^+$ calc'd = 418.2 Da.; H-EAAA-(2-nitrosophenyl) $[M+H]^+$ calc'd = 506.3 Da.).

In order to show that the incorporation of photolabile linker **2.17** into peptides synthesized by SPPS was general, the amino acids directly preceding and following the linker were varied. Thus, a series of short resin-bound pentamers (**2.24a-i**) (Scheme 2.4) with differing N-terminal amino acids (Table 2.1) were synthesized and reacted with linker **2.17**. Our results showed that the linker was successfully incorporated at room temperature onto all N-terminal amino acids tested, including branched amino acids and amino acids containing functionalized side chains, to produce **2.25a-i** (Table 2.1). The azide functionality of **2.25a-i** was then reduced

as described above, followed by coupling with Fmoc-Xxx^2-OH to yield peptides **2.26a-i**. Once more, a wide variety of amino acids, including branched amino acids and amino acids containing functionalized side chains, were successfully incorporated onto the N-terminal portion of the linker. Standard peptide elongation followed by peptide cleavage from resin produced peptides **2.27a-i** in good yields (Table 2.1). The purified peptides were then irradiated at 365 nm and the desired C-terminal peptides were obtained successfully and in high yields and purities in all cases (Table 2.1; Figures 2.5, 2.6, 2.7). In this and other studies,[26-28] photolysis was accompanied by the formation of various strongly absorbing decomposition products arising from the nitrosoaryl group (Figure 2.5B, Figure 2.6). In the current design, however, these side products are not part of the desired C-terminal peptide fragment **2.29** as confirmed by mass spectrometry. The ease of the synthesis and high yields of peptides **2.29a-i** illustrate the compatibility of linker **2.17** with SPPS.

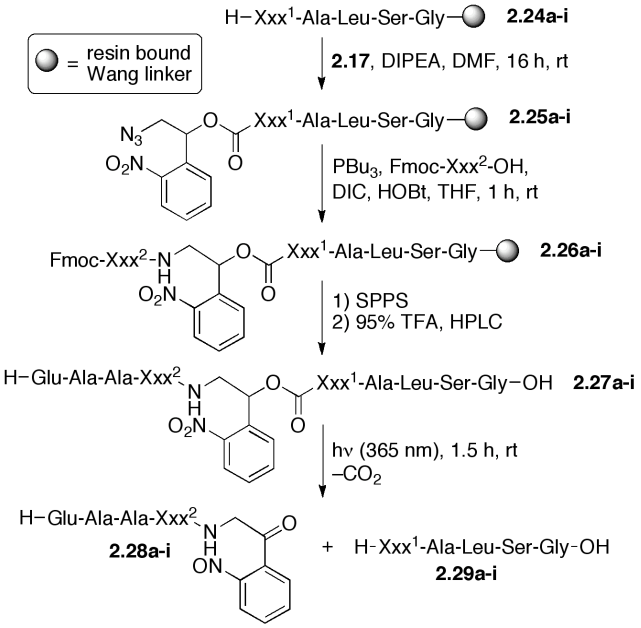

Scheme 2.4. Synthesis of decapeptides **2.27a-i** followed by photolysis to produce peptides **2.28a-i** and **2.29a-i**. Amino acids representing Xxx^1 and Xxx^2 are described in Table 2.1. Scheme adapted from Bindman and van der Donk.[1]

			Yield (%)		
2.24-2.29	**Xxx[1]**	**Xxx[2]**	**2.27[a]**	**2.29[b]**	**Per step[c]**
a	Thr	Ala	43	70	94
b	Val	Ala	21	72	90
c	Lys	Ala	27	87	93
d	Gly	Gly	39	83	94
e	Leu	Leu	44	61	93
f	Tyr	Tyr	16	83	90
g	Pro	Pro	17	81	90
h	Trp	Trp	14	70	83
i	Glu	Glu	21	91	92

Table 2.1. Synthesis and photolysis of decapeptides **2.27a-i** using a variety of amino acids flanking the photolabile linker. [a]Isolated yields based on resin loading. [b]Isolated yields after photolysis and RP-HPLC based on **2.27**. [c]Yields based on resin loading. Table adapted from Bindman and van der Donk.[1]

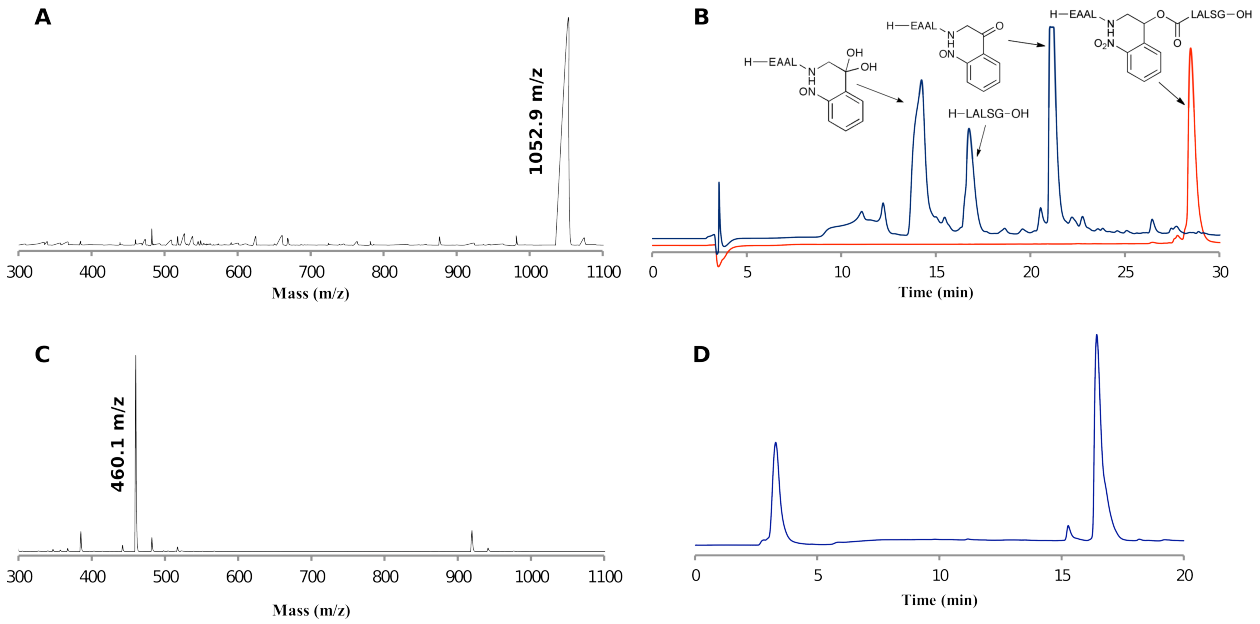

Figure 2.5. ESI-MS spectra and RP-HPLC traces of **2.27e** and photolysis products. A) ESI-MS spectrum of **2.27e** $[M+H]^+$ calc'd = 1052.5 Da. B) RP-HPLC spectrum of **2.27e** before (red) and after (blue) the photolysis reaction. C) ESI-MS spectrum of RP-HPLC peak at 16.2 min corresponding to purified **2.29e** $[M+H]^+$ calc'd = 460.3 Da. D) RP-HPLC spectrum of **2.29e** after purification. The peak at 3-4 min is associated with salts.

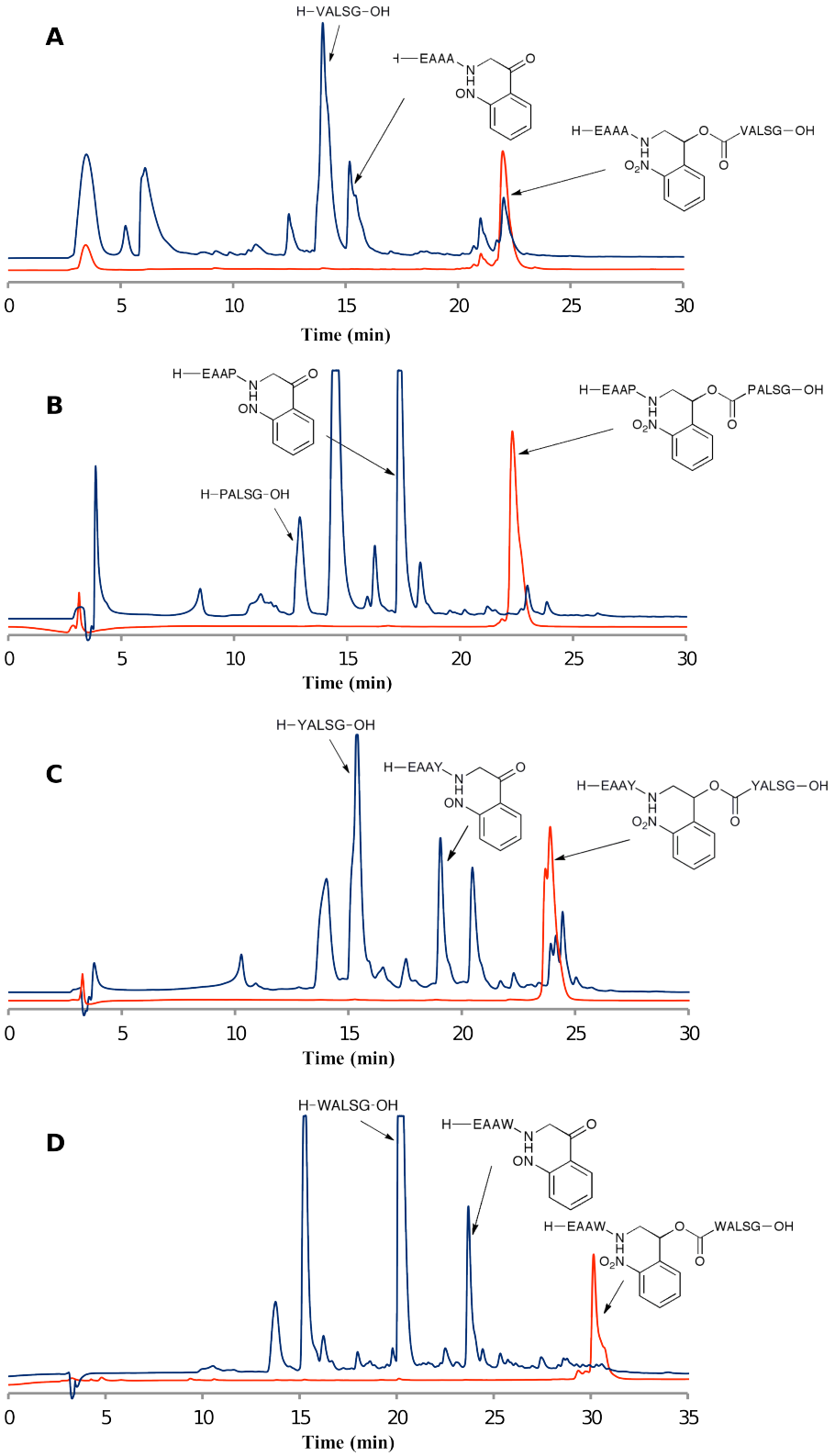

Figure 2.6. RP-HPLC spectra of **2.27** before (red) and after (blue) photolysis. A) **2.27b**, B) **2.27f**, C) **2.27g**, and D) **2.27h**. Photolysis reaction generates **2.28** and **2.29**.

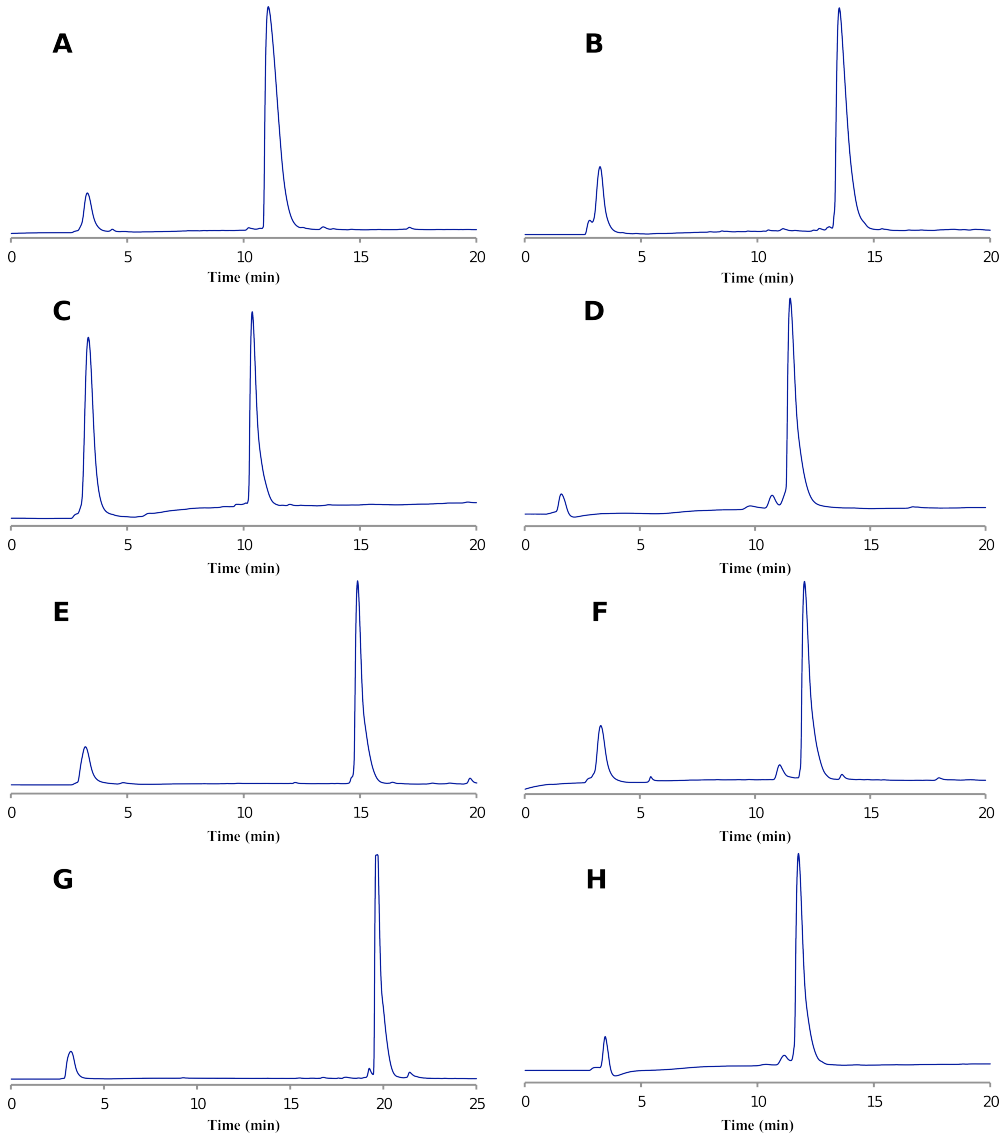

Figure 2.7. RP-HPLC spectra of **2.29** after RP-HPLC purification. A) 2.29a, B) 2.29b, C) 2.29c, D) 2.29d, E) 2.29f, F) 2.29g, G) 2.29h, H) 2.29i.

2.2.4. Azide reduction with tri-*n*-butylphosphine causes racemization at the peptides most C-terminal amino acid.

After the synthesis of decapeptide **2.21**, only peptides with a C-terminal glycine were employed in this study because the C-terminal Ala of the pentapeptide AGLSA underwent epimerization when subjected to the conditions used to synthesize peptide **2.20** (Figure 2.4C).

Epimerization was presumably the result of deprotonation of the α-proton of the C-terminal alanine by the strong phosphazene base created by reaction of tri-*n*-butylphosphine and azide. This problem was minimized either by using Gly as the C-terminal residue, instead of Ala, or by using 2-chlorotrityl resin preloaded with alanine, which did not result in epimerization, presumably due to the steric bulk of the trityl group.

2.2.5. Incorporation of linker 2.17 into LctA to prepare lacticin 481.

We next sought to apply the photocleavable linker methodology to the preparation of the class II lantibiotic lacticin 481 (see Figure 1.2A). To evaluate whether the light-mediated leader peptide removal could yield full length, mature lacticin 481, a mutant of the LctA substrate peptide was generated. First, a mutant of the LctA core peptide, LctA(1-27)N15R/F21H(Cys-S*t*Bu) (hereafter referred to as LctA(core)(Cys-S*t*Bu), **2.30**; for amino acid sequence see legend of Scheme 2.5), was synthesized on pre-loaded Wang resin by SPPS. The mutations at positions 15 and 21 result in an active, and more soluble mutant of lacticin 481.[29] Also, the side chain thiol functionality of the cysteines were protected as *tert*-butyl disulfides because the triazole cycloaddition reaction with peptides containing free sulfhydryl groups does not proceed.[23] Azidopeptide **2.31** was synthesized by the addition of linker **2.17** to peptide **2.30** in the presence of DIPEA, followed by peptide cleavage from resin and RP-HPLC purification (Scheme 2.5). The LctA(core)(Cys-S*t*Bu) substrate was then cleaved from the resin for use in a CuAAC bioconjugation.

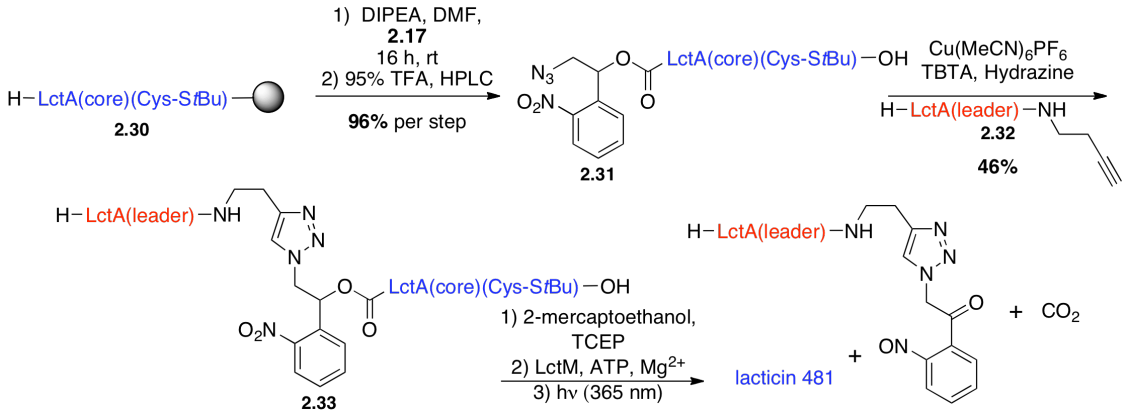

Scheme 2.5. CuAAC reaction between LctA(leader) and LctA(core)(Cys-S*t*Bu) followed by enzymatic modification by LctM and photolysis to afford lacticin 481. The amino acid sequence of LctA(leader) is KEQNSFNLLQEVTESELDLILGG. Amino acid sequence of LctA(core)(Cys-S*t*Bu) is KGGSGVIHTISHEC(S*t*Bu)RMNSWQHVFTC(S*t*Bu)C(S*t*Bu)S. Scheme adapted from Bindman and van der Donk.[1]

The second substrate in the cycloaddition reaction, the alkyne-linked leader peptide (**2.32**), was synthesized as follows. The leader peptide analogue Fmoc-LctA(–23 - –1)A–1G (LctA(leader); for amino acid sequence see legend of Scheme 2.5), lacking the N-terminal Met, was synthesized on preloaded 2-chlorotrityl resin. This Met deletion does not interfere with the processing of LctA by LctM. After SPPS, the peptide was cleaved from solid support with a 10% acetic acid solution. This strategy retains the amino acid side chain protecting groups so that the C-terminal carboxylate of the peptide could be coupled to but-3-yn-1-amine. The A–1G mutation prevented any possible epimerization of the C-terminal amino acid of the leader peptide during activation by HOBt and DIC during the alkyne addition step. With the alkyne functionality in place, removal of the N-terminal Fmoc group with 20% piperidine, deprotection of the amino acid side chain protecting groups with 95% TFA, and RP-HPLC purification yielded peptide

2.32. Substrates **2.31** and **2.32** were conjugated in a CuAAC reaction and analyzed by matrix assisted laser desorption ionization-time of flight mass spectrometry (MALDI-TOF MS) (Figure 2.8, top). Along with the product peak (6131 Da), a peak with molecular weight 3269 Da was present, which was generated by the photocleavage of **2.33** by the 337 nm laser on the MALDI-TOF instrument. The photolysis peak disappeared when the cycloaddition reaction mixture was analyzed by ESI-MS, confirming that the cleavage was specific to the MALDI conditions (Figure 2.8, bottom). After deprotection of the S*t*Bu groups of **2.33** with β-mercaptoethanol and TCEP, the resulting substrate analogue was incubated with LctM, resulting in the anticipated four dehydrations (Figure 2.9). Subsequent photolysis afforded mature, biologically active lacticin 481 (Figure 2.10).

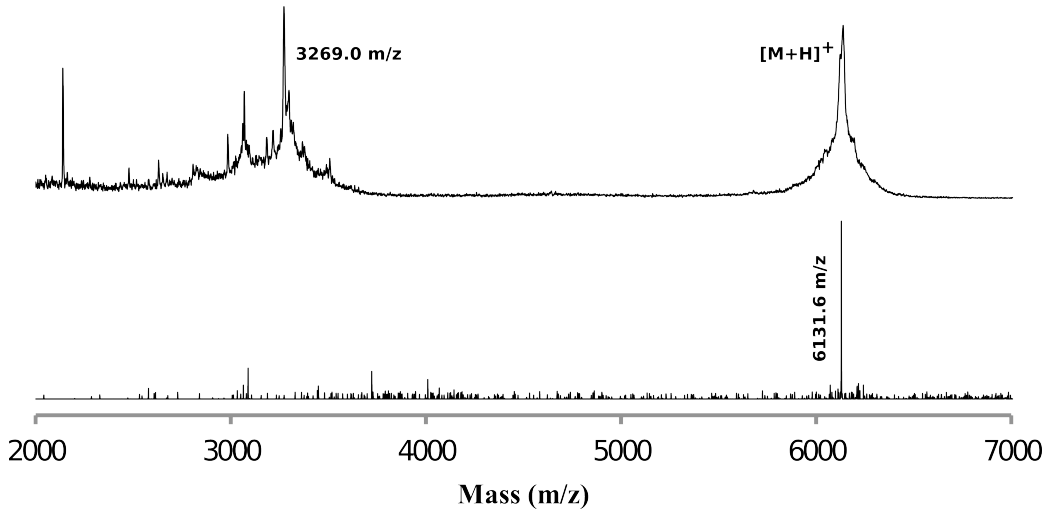

Figure 2.8. Formation of triazole-linked LctA. MALDI-TOF (top) and ESI (bottom) MS spectra of cycloaddition product **2.33**. $[M+H]^+$ calc'd = 6131.9 Da. Peak at 3269.0 Da in MALDI-TOF MS spectrum represents the photocleavage product generated by the 337 nm nitrogen laser.

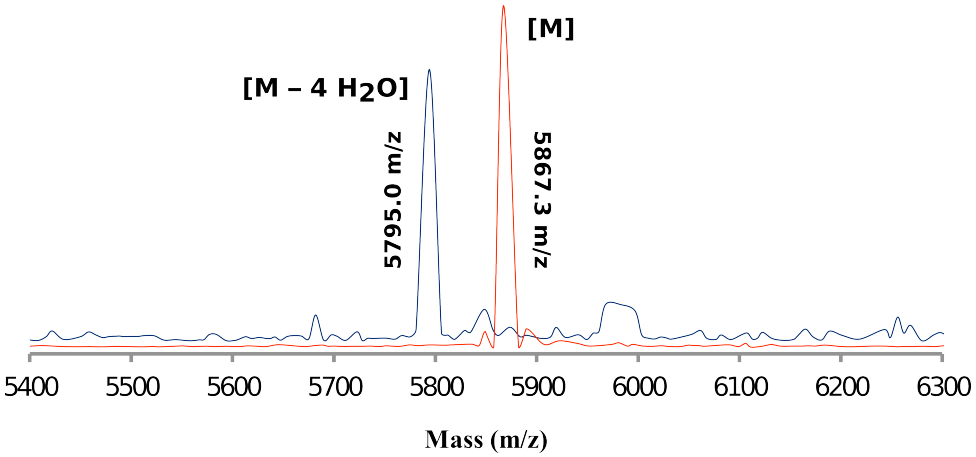

Figure 2.9. Modification of triazole-linked LctA by LctM. MALDI-TOF MS spectrum of triazole-linked LctA(leader)-LctA(core) before (red) and after (blue) incubation with LctM. $[M+H]^+_{before}$ calc'd = 5867.8 Da, $[M+H]^+_{after}$ calc'd = 5795.7 Da. Figure adapted from Bindman and van der Donk.[1]

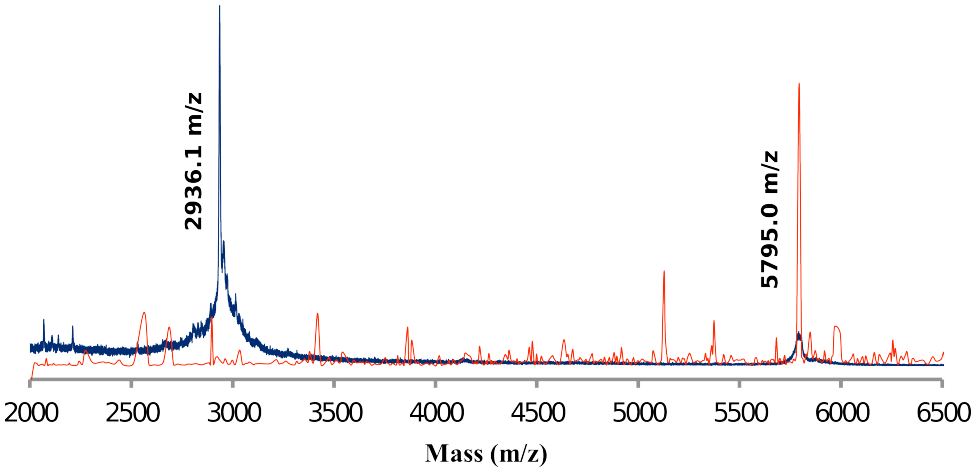

Figure 2.10. Photolysis of triazole-linked LctA modified by LctM. MALDI-TOF MS spectrum of LctM modified-triazole-linked LctA(leader)-LctA(core) before (red) and after (blue) the photocleavage reaction. $[M+H]^+_{before}$ calc'd = 5795.7 Da, $[M+H]^+_{after}$ calc'd = 2934.3 Da.

2.3 SUMMARY AND OUTLOOK

The successful in vitro reconstitution of the activities of many of the posttranslational modification enzymes involved in lanthipeptide biosynthesis has helped researchers study the mode of action, bioactivity, and enzyme specificity for a number of the lanthipeptides. Indeed, incorporation by SPPS of the non-proteinogenic amino acids naphthylalanine, 4-pyridynylalanine, and homophenylalanine into the core region of lacticin 481-RH (incorporating the N15R/F21H mutations) produced analogues with increased biological activity compared to that of wild type lacticin 481-RH.[23] However, in that study the commercial protease Lys-C was utilized to remove the leader peptide, producing lacticin 481 mutants lacking the N-terminal Lys. This N-terminal amino acid deletion decreased the bioactivity of lacticin 481 by 2.5-3-fold.[23] Therefore, a more general method for the removal of the leader peptide, involving the incorporation of photolabile linker **2.17** into peptides, was developed.

My studies show that photolabile linker **2.17** was appended successfully to several resin-bound peptides followed by reduction of the azide functionality and the stepwise addition of amino acids to the N-terminus. The decapeptides were cleaved from the resin and RP-HPLC purified, followed by photolysis at 365 nm to yield the C-terminal peptides. Importantly, the identity of the amino acids directly preceding and following linker **2.17** had minimal effect on the yield of linker incorporation and peptide elongation, demonstrating the compatibility of linker **2.17** with a wide variety of peptides synthesized by SPPS.

These studies also demonstrated linker compatibility with a CuAAC reaction because the bioorthogonality of the ‘click’ reaction allows the attachment of the core and leader regions of lanthipeptides with only the sulfhydryl group of the cysteine side chains needing to be protected. My results illustrated that linker **2.17** was successfully incorporated between leader and core

regions of the lantibiotic lacticin 481, and that after S*t*Bu deprotection, the activity of LctM was successfully reconstituted. Photolysis of the modified product afforded mature lacticin 481.

This methodology can be utilized for the preparation of native lacticin 481 and can be extended to the preparation of lacticin 481 analogues using previously published procedures.[23] This methodology adds one linear step (the addition of linker **2.17**) compared to our previous approach using a commercial protease to remove the leader peptide. However, unlike use of proteases such as Lys-C, light-mediated removal of the leader peptide is not sequence dependent and can provide the full-length natural product. It is anticipated that this general methodology may also find use for other lanthipeptides and other classes of ribosomally synthesized and posttranslationally modified peptides.

2.4. EXPERIMENTAL

2.4.1. Materials.

Fmoc amino acids and resins were purchased from Advanced ChemTech, Novabiochem, or Chem-Impex. *N*,*N'*-diisopropylcarbodiimide (DIC) and O-(1H-6-Chlorobenzotriazole-1-yl)-1,1,3,3-tetramethyluronium hexafluorophosphate (HCTU) were purchased from Advanced ChemTech and 1-hydroxybenzotriazole (HOBt) was purchased from Chem-Impex. Solvents commonly used in peptide synthesis and purification, including dimethylformamide (DMF), dichloromethane (DCM), trifluoroacetic acid (TFA), and acetonitrile (MeCN) were obtained in RP-HPLC grade or better and used directly without further purification. Tri-*n*-butylphosphine, piperidine, and *N*-methyl morpholine (NMM) were purchased from Acros whereas pyridine, *N*,*N*-diisopropylethylamine (DIPEA), and β-mercaptoethanol were purchased from Sigma Aldrich. Tris-(2-carboxyethyl)phosphine (TCEP) was obtained from Molecular Probes as the

TCEP-HCl salt. The ligand *tris*-(benzyltriazolylmethyl)amine (TBTA), tetrakis(MeCN)copper(I) hexafluorophosphate, and hydrazine were purchased from Sigma Aldrich and 3-butyn-1-amine hydrochloride was purchased from AB Chem Inc. For the synthesis of the photocleavable linker, *p*-toluenesulfonyl chloride, methanesulfonyl chloride, trimethylsilyl chloride, sodium azide, lithium bromide, and *N*-hydroxysuccinimidyl carbonate were purchased from Sigma Aldrich. The irradiation used for photochemical reactions was generated using a UVP Blak-Ray lamp (Ultraviolet Products, San Gabriel, CA) with a 365 nm filter.

2.4.2. Synthesis of photolabile linkers 2.15-2.17.

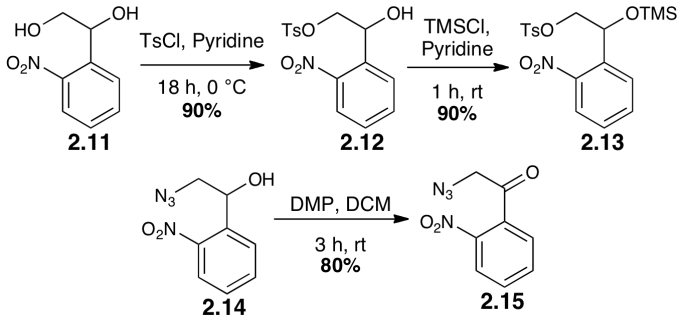

Synthetic design of photolabile linker 2.15.

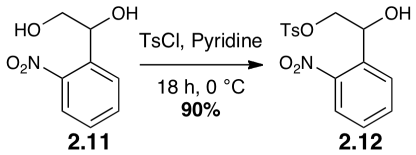

2-Hydroxy-2-(2-nitrophenyl)ethyl 4-methylbenzenesulfonate (2.12).

Into a 50 mL round-bottomed flask was placed *p*-toluenesulfonyl chloride (1.46 g, 7.64 mmol, 1.4 equiv) and 1-(2-nitrophenyl)-1,2-ethanediol (**2.11**, 1.0 g, 5.46 mmol, 1 equiv). The flask was sparged with a nitrogen stream for 5 min. Distilled pyridine (25 mL) was added and the

reaction flask was placed in a 0 ºC icebath. The mixture was stirred for 18 h at 0 ºC, allowed to warm to room temperature, and quenched with H_2O (80 mL). Crude product was extracted with Et_2O (2 × 50 mL) and combined extracts were washed successively with 1 M $KHSO_4$ (3 × 30 mL), sat. aqueous $NaHCO_3$ (3 × 30 mL), and sat. aqueous NaCl (2 × 50 mL). The organic layer was dried over $MgSO_4$, concentrated by rotary evaporation, and purified by SiO_2 gel column chromatography (eluted with hexanes/EtOAc (4:1); Rf = 0.065) yielding compound **2.12** (1.65 g, 90%) as an orange oil. *See also Notebook II, page 73*.

^{1}H NMR: (399.947 MHz, $CDCl_3$) δ=2.43 (s, 3H, CH_3), 3.95 (bs, 1H, OH) 4.14 (dd, J = 7.3, 3.2 Hz, 1H, CH_2), 4.36 (dd, J = 2.7, 7.8 Hz, 1H, CH_2), 5.51 (dd, J = 2.7, 4.7 Hz, 1H, CH), 7.31 (d, J = 8.1 Hz, 2H, CH_{tosyl}), 7.44 (t, J = 7.8 Hz, 1H, CH_{phenyl}), 7.65 (t, J = 7.3 Hz, 1H, CH_{phenyl}), 7.75 (d, J = 8.3 Hz, 2H, CH_{tosyl}), 7.85 (d, J = 7.8 Hz, 1H, CH_{phenyl}), 7.95 (d, J = 8.1 Hz, 1H, CH_{phenyl}).

^{13}C NMR: (100.527 MHz, $CDCl_3$) δ=21.9, 67.9, 73.5, 124.9, 128.2, 129.4, 130.3, 132.5, 134.1, 134.4, 145.4, 147.7.

HRMS $[M+H]^+$ $C_{15}H_{16}NO_6S$ calcd = 338.0698, found = 338.0704.

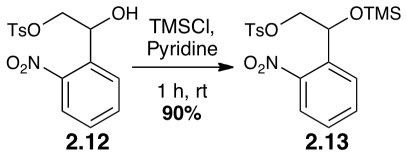

2-(2-Nitrophenyl)-2-((trimethylsilyl)oxy)ethyl 4-methylbenzenesulfonate (2.13).

Into a 50 mL round-bottomed flask was placed tosyl derivative **2.12** (1.69 g, 5.0 mmol, 1 equiv). The flask was purged with a nitrogen stream for 5 min followed by the addition of distilled pyridine (25 mL). To this flask was added TMSCl (2.17 g, 20 mmol, 4 equiv) dropwise and the solution was stirred for 1 h at room temperature. At this time the reaction was quenched

with H_2O (80 mL), crude product was extracted with Et_2O (2 × 50 mL), and the combined extracts were washed successively with 1 M $KHSO_4$ (3 × 30 mL), sat. aqueous $NaHCO_3$ (3 × 30 mL), and sat. aqueous NaCl (2 × 50 mL). The organic layer was dried over $MgSO_4$ and concentrated by rotary evaporation, yielding compound **2.13** (1.84 g, 90%) as a tan solid. *See also Notebook II, page 74*.

^{1}H NMR: (399.746 MHz, $CDCl_3$) δ=0.01 (s, 9H, CH_3), 2.41 (s, 3H, CH_3), 4.05 (dd, J = 6.6, 4.4 Hz, 1H, CH_2), 4.16 (dd, J = 2.9, 6.8 Hz, 1H, CH_2), 5.47 (dd, J = 6.6, 6.6 Hz, 1H, CH), 7.27 (d, J = 8.1 Hz, 2H, CH_{tosyl}), 7.43 (t, J = 7.8 Hz, 1H, CH_{phenyl}), 7.61 (t, J = 7.7 Hz, 1H, CH_{phenyl}), 7.70 (d, J = 8.3 Hz, 2H, CH_{tosyl}), 7.79 (d, J = 7.9 Hz, 1H, CH_{phenyl}), 7.89 (d, J = 8.3 Hz, 1H, CH_{phenyl}).

^{13}C NMR: (100.527 MHz, $CDCl_3$) δ=-0.02, 21.8, 68.4, 73.7, 124.6, 128.1, 129.1, 129.8, 130.0, 133.1, 133.7, 135.6, 144.9, 147.8.

HRMS $[M+Na]^+$ $C_{18}H_{23}N_6NaSSi$ calcd = 432.0913, found = 432.0917.

M.P. = 83-87 °C.

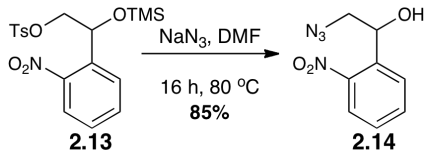

2-Azido-1-(2-nitrophenyl) ethanol (2.14).

Into a 25 mL round-bottomed flask was placed sodium azide (0.52 g, 2.52 mmol, 2 equiv). The flask was purged with a nitrogen stream for 5 min. To this flask was added trimethylsilyl ether derivative **2.13** (0.52 g, 1.26 mmol, 1 equiv) in DMF (9 mL) and the reaction was stirred at 80 ºC for 16 h. At this time the reaction was quenched with H_2O (80 mL), crude product was extracted with Et_2O (2 × 50 mL), and the combined extracts were washed with sat.

aqueous NaCl (2 × 50 mL). The organic layer was dried with $MgSO_4$, concentrated by rotary evaporation, and purified by SiO_2 gel column chromatography (eluted with hexanes/EtOAc (4:1); Rf = 0.29) yielding **2.14** (0.23 g, 85%) as a red oil. *See also Notebook IV, page 41*.

^{1}H NMR: (399.947 MHz, $CDCl_3$) δ=2.64 (d, J = 3.7 Hz, 1H, OH), 3.44 (dd, J = 7.6, 4.9 Hz, 1H, CH_2), 3.74 (dd, J = 3.0, 9.5 Hz, 1H, CH_2), 5.49 (m, 1H, CH), 7.47 (t, J = 7.8 Hz, 1H, CH_{phenyl}), 7.69 (t, J = 8.0 Hz, 1H, CH_{phenyl}), 7.90 (d, J = 7.8 Hz, 1H, CH_{phenyl}), 8.00 (d, J = 8.3 Hz, 1H, CH_{phenyl}).

^{13}C NMR: (100.527 MHz, $CDCl_3$) δ=57.4, 69.2, 125.0, 128.8, 129.2, 134.1, 136.3, 147.9.

HRMS $[M + Na]^+$ $C_8H_8N_4O_3Na$ calcd = 231.0494, found = 231.0483.

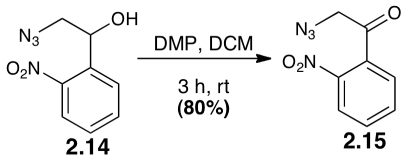

2.14 **2.15**

2-Azido-1-(2-nitrophenyl)ethanone (2.15).

Into a 50 mL round-bottomed flask was added **2.14** (50 mg, 0.24 mmol, 1 equiv) in CH_2Cl_2 (10 mL) followed by Dess-Martin periodinane (119 mg, 0.28 mmol, 1.2 equiv) and the reaction was stirred for 3 h at room temperature. At this time the solution was concentrated by rotary evaporation, crude product was passed over a short SiO_2 plug and eluted with CH_2Cl_2 (200 mL). The eluent was then concentrated by rotary evaporation yielding **2.15** as a light yellow solid (80% yield). *See also Notebook I, Page 61*.

^{1}H NMR: (399.947 MHz, $CDCl_3$) δ=4.29 (s, 2H, CH_2), 7.40 (d, J = 8.0 Hz, 1H, CH_{phenyl}), 7.67 (t, J = 8.0 Hz, 1H, CH_{phenyl}), 7.78 (t, J = 7.8 Hz, 1H, CH_{phenyl}), 8.21 (d, J = 8.3 Hz, 1H, CH_{phenyl}).

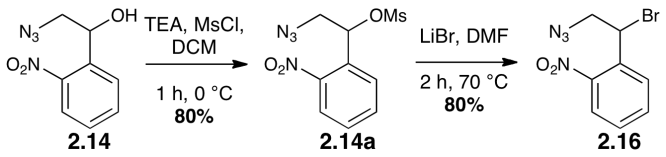

Synthetic design of photolabile linker 2.16 from intermediate 2.14.

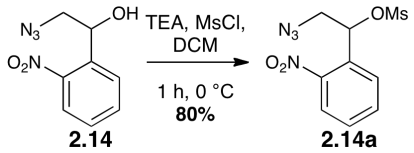

2-Azido-1-(2-nitrophenyl)ethyl methanesulfonate (2.14a).

Into a 10 mL round-bottomed flask was placed azide derivative **2.14** (93.7 mg, 0.45 mmol, 1 equiv). The flask was purged with a nitrogen stream for 5 min followed by the addition of DCM (3 mL). Triethylamine (68.8 mg, 94.8 µL, 0.68 mmol, 1.5 equiv) was then added and the solution was cooled to 0 ºC. MsCl (57.3 mg, 38.7 µL, 0.50 mmol, 1.1 equiv), dissolved in dry DCM (1 mL), was added dropwise via a syringe pump over 5 min. The reaction was stirred at 0 ºC for 1 h. At this time, solvent was evaporated under reduced pressure and the solid residue was dissolved in ethyl acetate (45 mL). The solution was washed with 5% aqueous $NaHCO_3$ (w/v) (2 × 40 mL) and sat. aqueous NaCl (2 × 40 mL), dried with $MgSO_4$, and concentrated by rotary evaporation yielding **2.14a** (103 mg, 80%) as a light green oil. *See also Notebook I, Page 99*.

^{1}H NMR: (399.947MHz, $CDCl_3$) δ=3.09(s, 3H, CH_3), 3.64 (dd, 1H, CH_2), 3.82 (dd, 1H, CH_2), 6.29 (dd, 1H, CH), 7.57 (t, 1H, CH_{phenyl}), 7.73 (t, 1H, CH_{phenyl}), 7.82 (d, 1H, CH_{phenyl}), 8.09 (d, 1H, CH_{phenyl}).

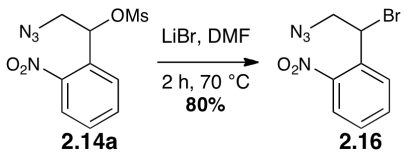

2.14a **2.16**

1-(2-Azido-1-bromoethyl)-2-nitrobenzene (2.16).

Into a 10 mL round-bottomed flask was placed LiBr (94.7 mg, 1.09 mmol, 5.8 equiv). The flask was sparged with a nitrogen stream for 5 min followed by the addition of mesylate derivative **2.14a** (54.3 mg, 0.19 mmol, 1 equiv) dissolved in DMF (2 mL). The reaction was stirred at 70 ºC for 2 h. At this time the reaction was quenched with H_2O (40 mL), crude product was extracted with Et_2O (2 × 50 mL), and combined extracts were washed with H_2O (3 × 30 mL) and sat. aqueous NaCl (40 mL). The organic layer was dried with $MgSO_4$ and concentrated by rotary evaporation yielding **2.16** (41.0 mg, 80%) as an orange oil. *See also Notebook II, Page 20*.

^{1}H NMR: (399.947MHz, $CDCl_3$) d=3.43 (dd, 1H, CH_2), 3.90 (dd, 1H, CH_2), 5.73 (t, 1H, CH), 7.47 (t, 1H, CH_{phenyl}), 7.64 (t, 1H, CH_{phenyl}), 7.84 (d, 1H, CH_{phenyl}), 7.87 (d, 1H, CH_{phenyl}).

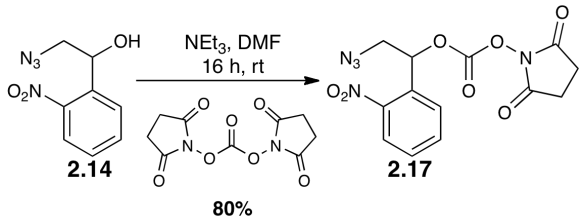

2.14 **2.17**

80%

Synthetic design of photolabile linker 2.17 from intermediate 2.14.

2-Azido-1-(2-nitrophenyl)ethyl (2,5-dioxopyrrolidin-1-yl) carbonate (2.17).

Into a 10 mL round-bottomed flask was added a solution of azide derivative **2.14** (41.6 mg, 0.2 mmol, 1 equiv) in DMF (1.0 mL). *N*-hydroxysuccinimidyl carbonate (85.0 mg, 0.33

mmol, 1.65 equiv) was then added followed by NEt_3 (83.6 μL, 0.60 mmol, 3 equiv). The reaction was stirred at room temperature for 16 h. At this time solvent was removed by rotary evaporation and crude product was purified by SiO_2 gel column chromatography (eluted with hexanes/EtOAc (1:1); Rf = 0.45). Fractions were collected and concentrated by rotary evaporation yielding **2.17** (55.9 mg, 80% yield) as a yellow oil. *See also Notebook III, Page 26*.

^{1}H NMR: (499.947 MHz, $CDCl_3$) δ=2.80 (s, 4H, CH_2), 3.76 (dd, J = 6.4, 7.1 Hz, 1H, CH_2), 3.93 (dd, J = 3.0, 10.7 Hz, 1H, CH_2), 6.46 (dd, J = 3.0, 3.7 Hz, 1H, CH), 7.57 (m, J = 4.3 Hz, 1H, CH_{phenyl}), 7.77 (d, J = 4.1 Hz, 2H, CH_{phenyl}) 8.11 (d, J = 8.3 Hz, 1H, CH_{phenyl}).

^{13}C NMR: (100.578 MHz, $CDCl_3$) δ=25.6, 54.5, 77.8, 125.5, 128.3, 130.4, 131.2, 134.7, 147.5, 150.9, 168.4.

HRMS $[M+H]^+$ $C_{13}H_{12}N_5O_7$ calcd = 350.0737, found = 350.0727.

M.P. = 110-115 ^oC.

2.4.3. Peptide synthesis and subsequent reactions to determine the compatibility of linker 2.17 with SPPS.

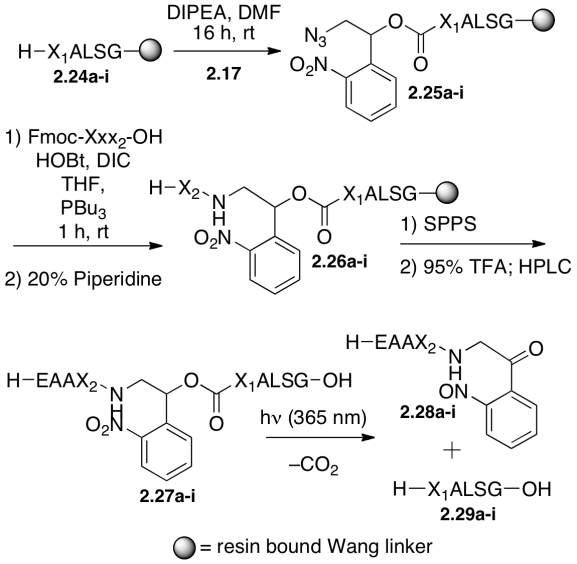

Synthetic design of decapeptides 2.27a-i followed by photocleavage resulting in peptides 2.28a-i and 2.29a-i.

General procedure for solid-phase peptide synthesis.

C-terminal peptides (**2.24a-i**) were synthesized using standard Fmoc based SPPS techniques using an automated peptide synthesizer (either Aapptec 396 or Rainin PS3 synthesizers). Preloaded Wang resin (0.1 mmol) was first swollen in dimethylformamide (DMF) (3 × 5 mL × 10 min). Fmoc-amino acids (0.4 mmol, 4 equiv) were coupled to resin-bound peptide using HCTU (165 mg, 0.4 mmol, 4 equiv) as coupling reagent and 0.4 M NMM (2 mL) as activating reagent (45 min per coupling step). Fmoc deprotection was performed with piperidine (20% in DMF; 3 × 5 mL × 3 min). After completion of the coupling of the final amino acid, the Fmoc group was removed to produce the free amino group. *See also Notebook IV, Page 18*.

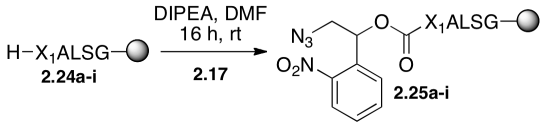

Peptide attachment to photocleavable linker (2.25a-i).

For the synthesis of azidopeptides **2.25a-i**, into a 5 mL round-bottomed flask was added pre-swelled resin containing a five-mer peptide (**2.24a-i**, 0.1 mmol, 1 equiv). The flask was sparged with a nitrogen stream for five min followed by the addition of photocleavable linker **2.17** (70 mg, 0.2 mmol, 2 equiv) dissolved in DMF (3 mL). DIPEA (64.5 mg, 87 μL, 0.5 mmol, 5 equiv) was then added and the solution was stirred at room temperature with a non-ridged silica coated stir bar for 12-16 h. A non-ridged stir bar was used to assure no resin damage would occur while stirring. At this time, the resin was filtered and washed with DMF (3 × 5 mL). *See also Notebook IV, Page 21*.

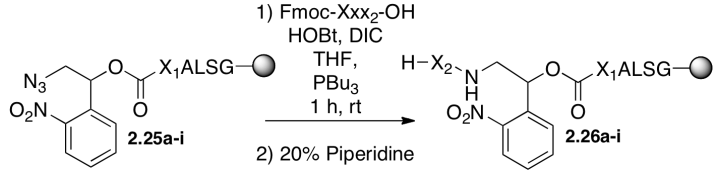

One pot azide reduction and amino acid coupling (2.26a-i).

Pre-swelled resin containing the azidopeptides **2.25a-i** (0.1 mmol, 1 equiv) was added to a 5 mL round-bottomed flask. To this flask was added a solution of various Fmoc protected amino acids (Fmoc-Xxx-OH, 0.4 mmol, 4 equiv), and HOBt (54 mg, 0.4 mmol, 4 equiv) in THF (3 mL). DIC (50.2 mg, 62 μL, 0.4 mmol, 4 equiv) was then added followed by the addition of tri-*n*-butylphosphine (101.2 mg, 125 μL, 0.5 mmol, 5 equiv). The reaction was stirred at room temperature with a non-ridged silica coated stir bar for 1 h. At this time the resin was filtered and washed with DMF (3 × 5 mL). *See also Notebook IV, Page 22*.

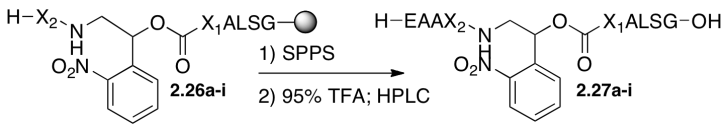

Extension of the peptide chain.

The final amino acids were added by standard Fmoc based SPPS techniques as described above starting and ending with an Fmoc deprotection. *See also Notebook IV, Page 23*.

General procedure for peptide cleavage from resin and purification.

Peptides prepared on Wang resin were cleaved from the resin by adding a solution of trifluoroacetic acid (TFA) (5 mL), triisopropylsilane (TIPS) (100 μL), and H_2O (100 μL) to the resin (0.1 mmol) and stirring the solution for 2 h at room temperature. The solution was concentrated by purging with a nitrogen stream and peptide was precipitated with cold diethyl ether and pelleted by centrifugation (5 min, 22,789 ×*g*). The crude peptides were dissolved in an aqueous 0.1% TFA solution, lyophilized, and purified by preparative RP-HPLC on a Waters Delta-Pak^{TM} C18 column (2.5 cm × 10.0 cm) employing a water-acetonitrile solvent system. A linear gradient was used from 2% to 80% solvent B over 45 min (solvent A = 0.1% TFA in H_2O; solvent B = 80% acetonitrile in H_2O, 0.086% TFA). Peptides were monitored by their absorbance at 220 nm. Fractions containing product **2.27a-i** as analyzed by MALDI-TOF or ESI-MS were collected, lyophilized, and weighed to determine yield. *See also Notebook IV, Page 23*. Note: The linker contains a stereogenic center and was prepared in racemic form, resulting in two diastereomers of peptides **2.27a-i** (as seen in Figure 2.6A,B).

Characterization of peptides 2.27a-i.

H—EAAA—Linker—TALSG—OH (**2.27a**). RP-HPLC; R_t = 20.2-21.4 min. LRMS (ESI): calcd $C_{41}H_{63}N_{11}O_{18}$, $[M+H]^+$ 998.4, observed 998.1.

H—EAAA—Linker—VALSG—OH (**2.27b**). RP-HPLC; R_t = 23.0-24.0 min. LRMS (ESI): calcd $C_{42}H_{65}N_{11}O_{17}$, $[M+H]^+$ 996.4, observed 996.1.

H—EAAA—Linker—KALSG—OH (**2.27c**). RP-HPLC; R_t = 19.2-20.6 min. LRMS (MALDI): calcd $C_{43}H_{68}N_{12}O_{17}$, $[M+H]^+$ 1025.5, observed 1027.3.

H—EAAG—Linker—GALSG—OH (**2.27d**). RP-HPLC; R_t = 19.7-21.0 min. LRMS (ESI): calcd $C_{38}H_{57}N_{11}O_{17}$, $[M+H]^+$ 940.4, observed 940.1.

H—EAAL—Linker—LALSG—OH (**2.27e**). RP-HPLC; R_t = 28.0-29.2 min. LRMS (MALDI): calcd $C_{46}H_{73}N_{11}O_{17}$, $[M+H]^+$ 1052.5, observed 1052.9.

H—EAAY—Linker—YALSG—OH (**2.27f**). RP-HPLC; R_t = 23.6-25.0 min. LRMS (MALDI): calcd $C_{52}H_{69}N_{11}O_{19}$, $[M+H]^+$ 1152.5, observed 1152.9.

H—EAAP—Linker—PALSG—OH (**2.27g**). RP-HPLC; R_t = 22.0-23.9 min. LRMS (MALDI): calcd $C_{44}H_{65}N_{11}O_{17}$, $[M+H]^+$ 1020.5, observed 1021.2.

H—EAAW—Linker—WALSG—OH (**2.27h**). RP-HPLC; R_t = 29.9-31.2 min. LRMS (MALDI): calcd $C_{56}H_{71}N_{13}O_{17}$, $[M+H]^+$ 1198.5, observed 1199.4.

H—EAAE—Linker—EALSG—OH (**2.27i**). RP-HPLC; R_t = 19.0-20.2 min. LRMS (MALDI): calcd $C_{44}H_{65}N_{11}O_{21}$, $[M+H]^+$ 1084.4, observed 1085.7.

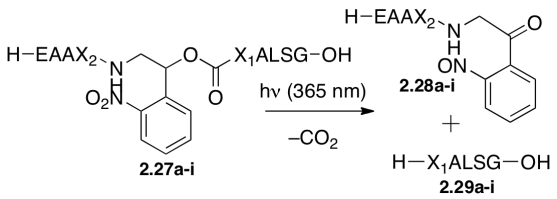

General procedure for photocleavage of the polypeptide backbone.

Into a 5 mL round-bottomed flask was added a solution of peptide **2.27a-i** (4-20 mg) dissolved in 0.1% TFA (1.0-2.0 mL). The solution was irradiated at 365 nm for 1-2 h (until starting material had disappeared as shown by MALDI-TOF MS); the UV irradiation from the MALDI-TOF did not cleave the linker in peptides **2.27a-i**. The crude material was then purified by preparative RP-HPLC on a C18 column employing a water-acetonitrile solvent system. Peptides were monitored by their absorbance at 220 nm. Fractions containing product **2.29a-i** (as analyzed by ESI-MS) were collected, lyophilized, and weighed to determine the yield. Purity was assessed by analytical RP-HPLC (Figure 2.7) (Grace Vydac® C18 column (4.6 x 250 mm); a linear gradient was used from 2% to 80% solvent B over 45 min (solvent A = 0.1% TFA in H_2O; solvent B = 80% acetonitrile in H_2O, 0.086% TFA)). *See also Notebook IV, Page 86*.

Characterization of peptides 2.29a-i.

H—TALSG—OH (**2.29a**). Analytical RP-HPLC; R_t = 10.8-12.0 min. LRMS (ESI): calcd $C_{18}H_{33}N_5O_8$, $[M+H]^+$ 448.2, observed 448.0.

H—VALSG—OH (**2.29b**). Analytical RP-HPLC; R_t = 13.2-14.4 min. LRMS (ESI): calcd $C_{19}H_{35}N_5O_7$, $[M+H]^+$ 446.3, observed 446.1.

H—KALSG—OH (**2.29c**). Analytical RP-HPLC; R_t = 10.1-11.0 min. LRMS (ESI): calcd $C_{20}H_{38}N_6O_7$, $[M+H]^+$ 475.3, observed 475.1.

H—GALSG—OH (**2.29d**). Analytical RP-HPLC R_t = 11.2-12.2 min. LRMS (ESI): calcd $C_{16}H_{29}N_5O_7$, $[M+H]^+$ 404.2, observed 404.0.

H—LALSG—OH (**2.29e**). Analytical RP-HPLC R_t = 16.2-17.1 min. LRMS (ESI): calcd $C_{20}H_{37}N_5O_7$, $[M+H]^+$ 460.3, observed 460.1.

H—YALSG—OH (**2.29f**). Analytical RP-HPLC R_t = 14.7-15.8 min. LRMS (ESI): calcd $C_{23}H_{35}N_5O_8$, $[M+H]^+$ 510.3, observed 510.1.

H—PALSG—OH (**2.29g**). Analytical RP-HPLC R_t = 11.9-13.0 min. LRMS (ESI): calcd $C_{19}H_{33}N_5O_7$, $[M+H]^+$ 444.2, observed 444.0.

H—WALSG—OH (**2.29h**). Analytical RP-HPLC R_t = 19.4-20.4 min. LRMS (ESI): calcd $C_{25}H_{36}N_6O_7$, $[M+H]^+$ 533.3, observed 533.1.

H—EALSG—OH (**2.29i**). Analytical RP-HPLC R_t = 11.5-12.5 min. LRMS (ESI): calcd $C_{19}H_{33}N_5O_9$, $[M+H]^+$ 476.3, observed 476.1.

2.4.4. Incorporation of linker 2.17 into LctA.

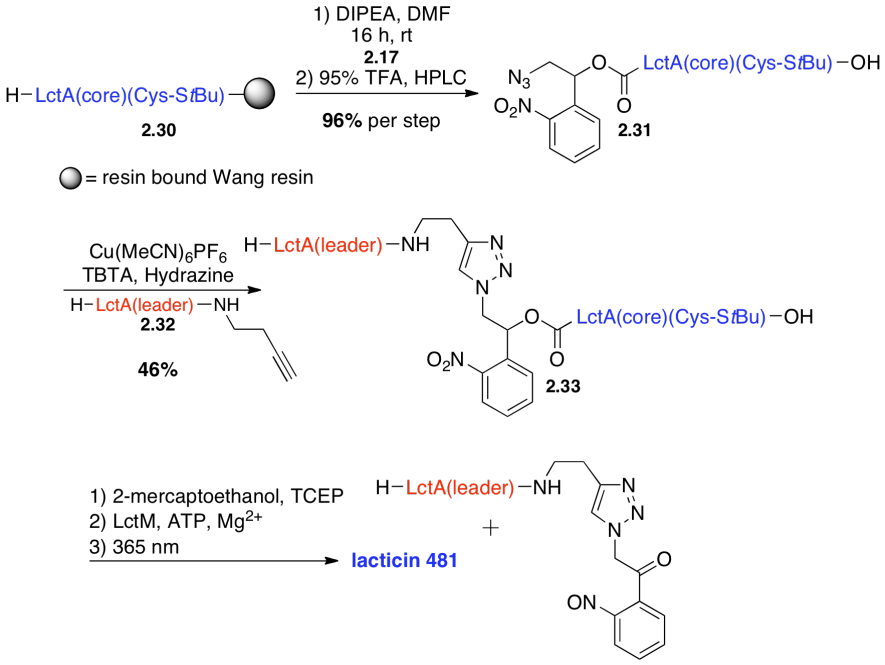

CuAAC bioconjugation between alkyne-linked LctA(leader) and azide-linked LctA(core)(Cys-S*t*Bu) followed by photolysis to afford lacticin 481.

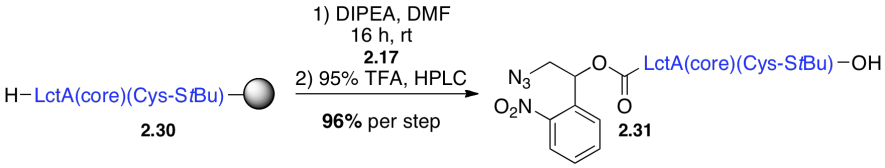

Synthesis of linker modified LctA(core)(Cys-S*t*Bu) (2.31).

The core peptide of LctA with its Cys residues protected as S*t*Bu disulfides (LctA(core)(Cys-S*t*Bu) (**2.30**)) was synthesized as described above using a Rainin PS3 peptide synthesizer (0.1 mmol). S*t*Bu protected Fmoc-cysteine residues were coupled to the growing peptide manually using HOBt (54 mg, 0.4 mmol, 4 equiv) as coupling reagent and DIC (50.2 mg, 62 μL, 0.4 mmol, 4 equiv) as activating reagent (45 min). The terminal Fmoc group was removed at the end of the synthesis. *See also Notebook IV, Page 73*.

For the synthesis of azidopeptide-LctA(core)(Cys-S*t*Bu) (**2.31**), into a 10 mL round-bottomed flask was placed pre-swelled resin containing peptide **2.30** (0.1 mmol, 1 equiv). To this flask was added photocleavable linker **2.17** (70 mg, 0.2 mmol, 2 equiv) dissolved in DMF (5 mL). DIPEA (64.5 mg, 87 μL, 0.5 mmol, 5 equiv) was added and the solution was stirred at room temperature with a non-ridged silica coated stirbar for 12-16 h. At this time the resin was filtered, washed with DMF (3 × 5 mL), and pipetted into a 20 mL scintillation vial with DMF. After removal of DMF, the peptide was cleaved from resin by adding a solution of TFA (5 mL), thioanisole (200 μL), H_2O (200 μL), and TIPS (100 μL) and stirring for 2 h at room temperature. The solution was concentrated by purging with a nitrogen stream and the peptide was precipitated with cold diethyl ether. The crude peptide was dissolved in 10% MeCN in 0.1% aqueous TFA, lyophilized, and purified by preparative RP-HPLC on a C18 column (solvent A = 0.1% TFA in H_2O; solvent B = 80% acetonitrile in H_2O, 0.086% TFA). Fractions containing product were collected and lyophilized yielding **2.31** (42.5 mg, 12%, 96% yield per step based on resin loading). *See also Notebook V, Page 09*.

N_3—Linker—LctA(core)(Cys-S*t*Bu)—OH (**2.31**). RP-HPLC; Gradient, 10-48% solvent B in 25 min, 48-68% solvent B in 15 min, R_t = 39.4-41.4 min. LRMS (MALDI): calcd $C_{147}H_{225}N_{44}O_{42}S_7[M+H]^+$ 3503.5, observed 3504.0.

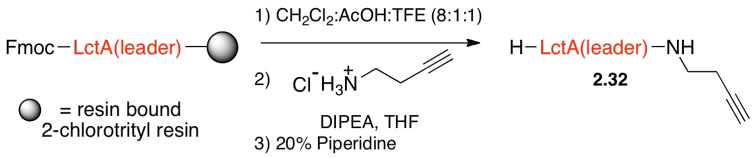

Coupling of C-terminal alkyne to LctA(leader) (2.32).

Fmoc-LctA(leader) peptide was prepared on 2-chlorotrityl chloride resin (0.1 mmol) on a CEM Liberty microwave peptide synthesizer. Preloaded 2-chlorotrityl glycine resin (0.1 mmol) was first swollen in a 1:1 DMF:DCM mixture (10 mL). Fmoc-amino acids (0.2 M in DMF, 2.5 mL) were coupled using HCTU (0.5 M in DMF, 1 mL) as coupling reagent and DIPEA (2.0 M in 1-methyl-2-pyrrolidinone, 0.5 mL) as activating reagent with microwave irradiation (3 min, 20 W, 75 ºC). Fmoc deprotection was performed with piperidine (20% in DMF) with microwave irradiation (3 min, 30 W, 75 ^{o}C). After completion of the coupling of the final amino acid, the Fmoc group was not removed. *See also Notebook, Page 98*.

Peptide cleavage from resin was achieved by stirring the resin in a mixture of methylene chloride (8 mL), acetic acid (1 mL), and trifluoroethanol (1 mL) at room temperature for 1 h. (Note: peptide cleavage from 2-chlorotrityl chloride resin in 10% acetic acid does not remove the amino acid protecting groups). At this time, the solid resin was removed by filtration, the methylene chloride and TFE in the filtrate were removed by rotary evaporation, and the remaining solution was concentrated by azeotropic removal of AcOH with hexanes (3 × 8 mL). The peptide was then dissolved in THF (10 mL) and DMF (10 mL).

In a separate 50 mL round-bottomed flask was added but-3-yn-1-amine hydrochloride (52.5 mg, 0.5 mmol, 5 equiv) and DIPEA (64.6 mg, 87.1 µL, 0.5 mmol, 5 equiv) in THF (5 mL). To this solution was added a premixed solution of HOBt (67.6 mg, 0.5 mmol, 5 equiv) and DIC (63.1 mg, 77.1 µL, 0.5 mmol, 5 equiv) in THF (5 mL) and DMF (5 mL). This mixture was then added to the flask containing the purified leader peptide and the reaction mixture was stirred for

12 h at room temperature. At this time, the solution was concentrated by rotary evaporation and a 20% piperidine/DMF solution (15 mL) was added to remove the terminal Fmoc group. The solution was stirred for 30 min followed by the removal of the piperidine and DMF under reduced pressure. The protecting groups were then removed from the amino acid side chains by adding a solution of TFA (7 mL), EDT (100 μL), TIPS (100 μL) and H_2O (200 μL) and stirring the solution for 2 h at room temperature. The solution was concentrated by purging with a nitrogen stream and was precipitated with cold diethyl ether. The peptide was dissolved in a 1:1 solution of MeCN and H_2O, lyophilized, and purified by preparative RP-HPLC on a Phenomenex C18 column (1.0 cm × 25.0 cm) employing a water-acetonitrile solvent system. The gradient used was from 2-80% solvent B in 45 min (solvent A = 0.1% TFA in H_2O; solvent B = 80% acetonitrile in H_2O, 0.086% TFA). Peptides were monitored by their absorbance at 220 nm. Fractions containing product as analyzed by MALDI-TOF MS were collected and lyophilized yielding **2.32** as a white powder. *See also Notebook VI, Page 10.*

H—LctA(leader)—Alkyne (**2.32**). Preparative RP-HPLC; R_t = 38.6-39.4 min. LRMS (MALDI): calcd $C_{116}H_{187}N_{29}O_{40}$, $[M+H]^+$ 2627.4, observed 2623.2

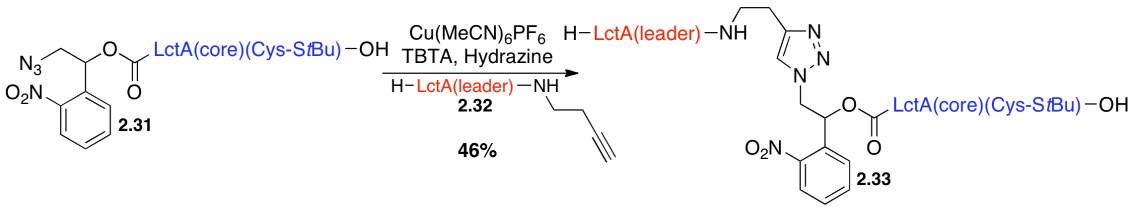

Preparation of triazole-linked substrate (2.33).

Peptides **2.31** (2.0 mg, 0.76 μmol, 1 equiv) and **2.32** (1.5 mg, 0.76 μmol, 1 equiv) were placed in a 3 mL pear-shaped flask equipped with a septum and the flask was sparged with a nitrogen stream for 3 min. The peptides were then dissolved in a degassed solution of 1:1 Tris

buffer (5 mM, pH 7.0):dioxane (1 mL), and DMSO (100 μL). In a separate 5 mL round-bottomed flask was placed TBTA (0.1 mg, 0.19 μmol, 0.25 equiv). This flask was sparged with a nitrogen stream for 3 min followed by the addition of 500 μL of a 1:1 mixture of Tris buffer (5 mM, pH 7.0) and dioxane. To this solution was added tetrakis(MeCN)copper(I)hexafluorophosphate (40 μL of a 1.25 mg/mL aqueous solution). After brief stirring, a hydrazine solution (20 μL of a 1% hydrazine solution in 1:1 Tris (5 mM, pH 7.0): dioxane) was added to the cupric solution followed by the addition of the peptide solution. The reaction solution turned cloudy either after the addition of hydrazine or after addition of the peptide solution. The solution was stirred under an inert nitrogen atmosphere for 1.5 h and analyzed by MALDI-TOF MS after diluting with 50% MeCN. The lyophilized crude peptide was purified by preparative RP-HPLC on a Phenomenex C18 column employing a water-acetonitrile solvent system. A linear gradient was used from 2% to 80% solvent B over 45 min (solvent A = 0.1% TFA in H_2O; solvent B = 80% acetonitrile in H_2O, 0.086% TFA). Fractions containing product (as analyzed by MALDI-TOF MS) were lyophilized yielding **2.33** (1.6 mg, 46%) as a white powder. *See also Notebook VI, Page 85*.

Triazole-linked LctA(leader)-LctA(core)(Cys-S*t*Bu) (**2.33**). R_t = 34.4-35.4 min LRMS (ESI): calcd $C_{262}H_{415}N_{71}O_{79}S_{07}$ $[M+H]^+$ 6131.85, observed 6131.6.

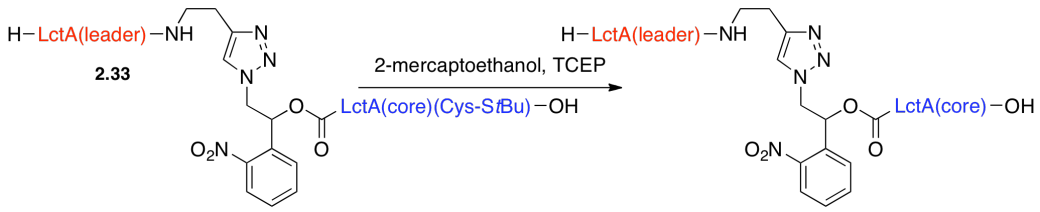

Deprotection of S*t*Bu protected triazole-linked substrate.

Into a 10 mL microwave flask was added RP-HPLC purified triazole-linked LctA substrate (**2.33**; 3.0 mg, 0.49 μmol, 1 equiv) dissolved in 40% MeCN, 60% Tris (37.5 mM, pH 8.3) (1.3 mL). To this flask was added β-mercaptoethanol (167 mg, 150 μL, 2.13 mmol, 4300 equiv) and TCEP (6 mg, 0.24 mmol, 490 equiv). The reaction was heated to 60 ºC for 30 min using a CEM Discover microwave reactor (100 W, 250 psi). The crude product was acidified (pH 1-2) with 1 M HCl and the lyophilized crude product was purified by preparative RP-HPLC on a C18 column employing a water-acetonitrile solvent system. The gradient used was from 2% to 80% solvent B in 45 min (solvent A = 0.1% TFA in H_2O; solvent B = 80% acetonitrile in H_2O, 0.086% TFA). Peptides were monitored by their absorbance at 220 nm. Fractions containing product (as analyzed by ESI-MS) were collected and lyophilized yielding S*t*Bu deprotected triazole-linked LctA(leader)-LctA(core) substrate as a white powder. *See also Notebook VI, Page 87.*

Triazole-linked LctA(Leader)-LctA(core) R_t = 35.0-36.5 min. LRMS (ESI): calcd $C_{254}H_{391}N_{70}O_{82}S_4$ $[M+H]^+$ 5867.75, observed 5867.3.

General procedure for LctM assays.

His_6-LctM was overexpressed and purified as previously reported.[30] To a 1.6 mL Eppendorf tube was added Tris-HCl (100 μL, 500 mM, pH 7.5), $MgCl_2$ (100 μL, 100 mM), ATP (40 μL, 50 mM), BSA (12.5 μL, 2 mg/mL), and sterile deionized H_2O (665.9 μL). Triazole-

linked LctA(leader)-LctA(core) substrate (40 μL, 500 μM in H_2O) was then added followed by LctM (41.5 μL, 34.1 μM) and the solution was incubated for 12 h. At this time the solution was acidified to pH 1-2 with 5% TFA and the crude product was purified by analytical RP-HPLC on a C4 column employing a water-acetonitrile solvent system. The gradient used was from 2% to 80% solvent B in 45 min (solvent A = 0.1% TFA in H_2O; solvent B = 80% acetonitrile in H_2O, 0.086% TFA). Peptides were monitored by their absorbance at 220 nm. Fractions containing product (as analyzed by ESI-MS were collected and lyophilized yielding LctM-modified triazole-linked LctA(leader)-LctA(core) substrate as a white powder. *See also Notebook VI, Page 89.*

LctM-modified triazole-linked LctA(leader)-LctA(core) R_t = 34.4-35.2 min. LRMS (ESI): calcd $C_{254}H_{383}N_{70}O_{78}S_4$ $[M+H]^+$ 5795.67 g/mol, observed 5795.0 g/mol.

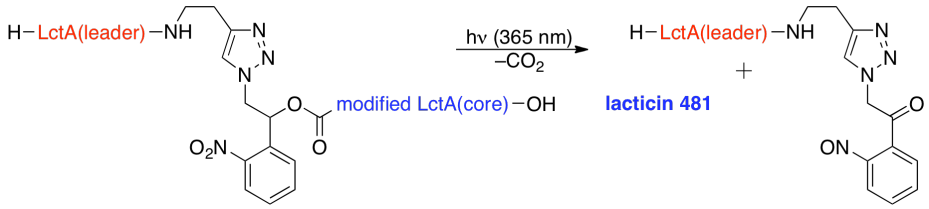

Photolysis of LctM-modified, triazole-linked LctA(leader)-LctA(core).

Purified LctM modified peptide in RP-HPLC solvent was irradiated at 365 nm for 20 min. The product was analyzed by MALDI-TOF MS and ESI-MS. *See also Notebook VI, Page 90.*

Lacticin 481. LRMS (MALDI): calcd $C_{126}H_{186}N_{40}O_{34}S_4$ $[M+H]^+$ 2934.3, observed 2936.1

Bioactivity assay of photocleaved lacticin 481.

M17 agar media (4 g M17 media, 1.5 g agar per 100 mL H_2O) was liquefied in the microwave and 20 mL were dispensed into a 50 mL conical vial. The vial was incubated at 42 ºC for 5 min at which time 20% glucose (500 μL) and *L. lactis* HP cells (200 μL; OD = 1.0) were added. The solution was poured into a sterile Nunc dish and allowed to solidify near a flame for 30 min. To a second 50 mL conical vial was added liquefied M17 agar media (30 mL), which was again incubated at 42 ^{o}C for 5 min. To this vial was added 20% glucose (750 μL) and *L. lactis* HP cells (300 μL; OD = 1.0) and the contents were poured on top of the solidified first layer of M17 media. A sterile 96 well PCR rack was immediately added to the upper layer and the media was allowed to solidify for 45 min near a flame. At this time the PCR rack was removed and the surface was air-dried near a flame for 3-4 h. Finally, 15 μL aliquots of lacticin 481, non-photocleaved product and photocleaved product were added to separate wells. The bioassay plate was then incubated at 30 ^{o}C for 16-24 h. *See also Notebook VII, Page 15*.

2.5. REFERENCES

(1) Bindman, N.; Merkx, R.; Koehler, R.; Herrman, N.; van der Donk, W. A., Photochemical cleavage of leader peptides, *Chem. Commun.* **2010**, *46*, 8935.

(2) Szekat, C.; Jack, R. W.; Skutlarek, D.; Farber, H.; Bierbaum, G., Construction of an expression system for site-directed mutagenesis of the lantibiotic mersacidin, *Appl. Environ. Microbiol.* **2003**, *69*, 3777.

(3) Cooper, L. E.; McClerren, A. L.; Chary, A.; van der Donk, W. A., Structure-activity relationship studies of the two-component lantibiotic haloduracin, *Chem. Biol.* **2008**, *15*, 1035.

(4) Islam, M. R.; Shioya, K.; Nagao, J.; Nishie, M.; Jikuya, H.; Zendo, T.; Nakayama, J.; Sonomoto, K., Evaluation of essential and variable residues of nukacin ISK-1 by NNK scanning, *Mol. Microbiol.* **2009**, *72*, 1438.

(5) Deegan, L. H.; Suda, S.; Lawton, E. M.; Draper, L. A.; Hugenholtz, F.; Peschel, A.; Hill, C.; Cotter, P. D.; Ross, R. P., Manipulation of charged residues within the two-peptide lantibiotic lacticin 3147, *Microb. Biotechnol.* **2010**, *3*, 222.

(6) Knerr, P. J.; Oman, T. J.; Garcia De Gonzalo, C. V.; Lupoli, T. J.; Walker, S.; van der Donk, W. A., Non-proteinogenic Amino Acids in Lacticin 481 Analogues Result in More Potent Inhibition of Peptidoglycan Transglycosylation, *ACS Chem. Biol.* **2012**, *7*, 1791.

(7) Bindman, N. A.; van der Donk, W. A., A general method for fluorescent labeling of the N-termini of lanthipeptides and its application to visualize their cellular localization, *J. Am. Chem. Soc.* **2013**, *135*, 10362.

(8) Håvarstein, L. S.; Diep, D. B.; Nes, I. F., A family of bacteriocin ABC transporters carry out proteolytic processing of their substrates concomitant with export, *Mol. Microbiol.* **1995**, *16*, 229.

(9) Furgerson Ihnken, L. A.; Chatterjee, C.; van der Donk, W. A., In vitro reconstitution and substrate specificity of a lantibiotic protease, *Biochemistry* **2008**, *47*, 7352.

(10) Velásquez, J. E.; Zhang, X.; van der Donk, W. A., Biosynthesis of the Antimicrobial Peptide Epilancin 15X and its Unusual N-terminal Lactate Moiety, *Chem. Biol.* **2011**, *18*, 857.

(11) Lin, Y.; Teng, K.; Huan, L.; Zhong, J., Dissection of the bridging pattern of bovicin HJ50, a lantibiotic containing a characteristic disulfide bridge, *Microbiol. Res.* **2011**, *166*, 146.

(12) Caetano, T.; Krawczyk, J. M.; Mosker, E.; Süssmuth, R. D.; Mendo, S., Heterologous expression, biosynthesis, and mutagenesis of type II lantibiotics from *Bacillus licheniformis* in *Escherichia coli*, *Chem. Biol.* **2011**, *18*, 90.

(13) Oldach, F.; Al Toma, R.; Kuthning, A.; Caetano, T.; Mendo, S.; Budisa, N.; Süssmuth, R. D., Congeneric lantibiotics from ribosomal in vivo peptide synthesis with noncanonical amino acids, *Angew. Chem. Int. Ed.* **2012**, *51*, 415.

(14) Shi, Y.; Yang, X.; Garg, N.; van der Donk, W. A., Production of lantipeptides in *Escherichia coli*, *J. Am. Chem. Soc.* **2011**, *133*, 2338.

(15) Ökesli, A.; Cooper, L. E.; Fogle, E. J.; van der Donk, W. A., Nine post-translational modifications during the biosynthesis of cinnamycin, *J. Am. Chem. Soc.* **2011**, *133*, 13753.

(16) Goto, Y.; Li, B.; Claesen, J.; Shi, Y.; Bibb, M. J.; van der Donk, W. A., Discovery of unique lanthionine synthetases reveals new mechanistic and evolutionary insights, *PLoS Biol.* **2010**, *8*, e1000339.

(17) Plat, A.; Kluskens, L. D.; Kuipers, A.; Rink, R.; Moll, G. N., Requirements of the engineered leader peptide of nisin for inducing modification, export, and cleavage, *Appl. Environ. Microbiol.* **2011**, *77*, 604.

(18) Tang, W.; van der Donk, W. A., Structural characterization of four prochlorosins: a novel class of lantipeptides produced by planktonic marine cyanobacteria, *Biochemistry* **2012**, *51*, 4271.

(19) Garg, N.; Tang, W.; Goto, Y.; van der Donk, W. A., Geobacillins: lantibiotics from *Geobacillus thermodenitrificans*, *Proc. Natl. Acad. Sci. U. S. A.* **2012**, *109*, 5241.

(20) England, P. M.; Lester, H. A.; Davidson, N.; Dougherty, D. A., Site-specific, photochemical proteolysis applied to ion channels in vivo, *Proc. Natl. Acad. Sci. U. S. A.* **1997**, *94*, 11025.

(21) Lee, H. M.; Priestman, M. A.; Lawrence, D. S., Light-mediated spatial control via photolabile fluorescently quenched peptide cassettes, *J. Am. Chem. Soc.* **2010**, *132*, 1446.

(22) Chan, T. R.; Hilgraf, R.; Sharpless, K. B.; Fokin, V. V., Polytriazoles as copper(I)-stabilizing ligands in catalysis, *Org. Lett.* **2004**, *6*, 2853.

(23) Levengood, M. R.; Knerr, P. J.; Oman, T. J.; van der Donk, W. A., In vitro mutasynthesis of lantibiotic analogues containing nonproteinogenic amino acids, *J. Am. Chem. Soc.* **2009**, *131*, 12024.

(24) Maurel, D.; Banala, S.; Laroche, T.; Johnsson, K., Photoactivatable and photoconvertible fluorescent probes for protein labeling, *ACS Chem. Biol.* **2010**, *5*, 507.

(25) Shimadzu; News, A., www.shimadzu.com.br/analitica/aplicacoes/analisadores/ta/t97.pdf.

(26) Marinzi, C.; Offer, J.; Longhi, R.; Dawson, P. E., An o-nitrobenzyl scaffold for peptide ligation: synthesis and applications, *Biorg. Med. Chem.* **2004**, *12*, 2749.

(27) Olejnik, J.; Sonar, S.; Krzymanska-Olejnik, E.; Rothschild, K. J., Photocleavable biotin derivatives: a versatile approach for the isolation of biomolecules, *Proc. Natl. Acad. Sci. U. S. A.* **1995**, *92*, 7590.

(28) Walker, J. W.; Reid, G. P.; McCray, J. A.; Trentham, D. R., Photolabile 1-(2-nitrophenyl)ethyl phosphate esters of adenine nucleotide analogs. Synthesis and mechanism of photolysis, *J. Am. Chem. Soc.* **1988**, *110*, 7170.

(29) You, Y. O.; van der Donk, W. A., Mechanistic investigations of the dehydration reaction of lacticin 481 synthetase using site-directed mutagenesis, *Biochemistry* **2007**, *46*, 5991.

(30) Xie, L.; Miller, L. M.; Chatterjee, C.; Averin, O.; Kelleher, N. L.; van der Donk, W. A., Lacticin 481: In vitro reconstitution of lantibiotic synthetase activity, *Science* **2004**, *303*, 679.

Chapter 3: Facile Removal of Leader Peptides from Lanthipeptides by Incorporation of a Hydroxy Acid

3.1. INTRODUCTION

As discussed in Chapter 1, the ability to produce lanthipeptides by the in vitro reconstitution of their biosynthetic enzymes has allowed researchers to generate lanthipeptide analogues with increased solubility and activity, thus improving their therapeutic potential.[1,2] The in vitro methodology is also attractive because it allows a facile way to introduce non-proteinogenic amino acids into lanthipeptides during solid phase peptide synthesis (SPPS) of the precursor peptide.[2,3] Unfortunately, several drawbacks still exist that challenge the construction of lanthipeptides in vitro. For instance, the solubilities of the unmodified precursor peptides are often quite low, which depresses the yield of the in vitro reaction. Also, because of the complexity of the cellular milieu, the cofactors necessary to achieve full lanthipeptide modification in vitro are not always known. Alternatively, our laboratory, along with Sonomoto and coworkers, has pioneered the in vivo coexpression of LanA precursor peptides with their cognate biosynthetic enzymes (LanM or LanB/LanC) in *Escherichia coli*.[4,5] After cell lysis, the modified precursor peptides, which generally can be obtained in higher yields when compared to the in vitro lanthipeptide production method, are purified from the cellular lysate by immobilized metal affinity chromatography (IMAC) via an N-terminal hexahistidine tag. Removal of the leader peptide from the core region results in the mature lanthipeptide. However, as discussed in Chapter 2, no general solutions exist for the removal of the leader peptide in lanthipeptides because the native proteases have rarely been reconstituted in vivo or in vitro. Moreover, the use of commercial proteases to remove the leader peptide is only productive if the core peptide does

not contain the proteolytic cleavage site, which is often a Lys, Glu, or Arg. The photocleavable linker discussed in Chapter 2 is a general solution for leader peptide removal in that it can be inserted into any lanthipeptide and its photoactivation does not cleave any other regions of the biomolecule. However, the linker can only be introduced by SPPS and is not amenable to lanthipeptide biosynthesis in vivo.

For a leader peptide removal strategy to be general for lanthipeptides modified in vivo, two criteria have to be met. First, a labile linkage needs to be incorporated into the peptide backbone between the leader and core peptides during ribosomal synthesis of the peptide. Second, the chemistry required to cleave this linkage must be orthogonal to the rest of the peptide and yield the core region without any adornments. To the best of our knowledge, no photolabile compounds exist that meet both of these criteria. The 2-nitrophenyl glycine derivative **2.1** discussed in Chapter 2 can be genetically incorporated into the peptide backbone,[6] but yields a nitrosoaryl-containing N-terminus on the C-terminal fragment of the precursor peptide (which would constitute the core region of lanthipeptides) upon irradiation. Other labile linkages have cleavage reactivities orthogonal to the functionalities present in peptides and proteins, but their incorporation into the peptide backbone during ribosomal synthesis has not yet been achieved.

Interestingly, the biosynthetic machinery of *E. coli* can recognize hydroxy acids and incorporate them into the backbone of proteins or peptides[7] and the subsequent ester bonds can be site-specifically cleaved by alkaline hydrolysis,[8,9] fulfilling both criteria as outlined above. Unfortunately, the incorporation of hydroxy acids into proteins has usually been accomplished via cell-free translation systems,[8,10-12] which are more complicated and suffer from lower yields when compared to site-specific genetic incorporation strategies involving orthogonal aminoacyl-

tRNA synthetase (aaRS)-amber suppressor tRNA pairs in *E. coli*. Recently, a novel aaRS-tRNA pair from *Methanosarcina mazei*, pyrrolysyl-tRNA synthetase (PylRS)- $tRNA_{CUA}^{Pyl}$ (PylT),[13] which naturally incorporates pyrrolysine (Pyl) in response to the amber stop codon (UAG), was shown to incorporate several non-proteinogenic lysine derivatives into proteins, including the hydroxy acid of Boc$^{\varepsilon}$-L-lysine.[14] In the case of the incorporation of the hydroxy acid, the new ester linkage was then site-specifically fragmented by an alkaline-catalyzed hydrolysis reaction. We envisioned that a similar strategy could be used to cleave off the leader peptide after in vivo lanthipeptide production. Replacing the first residue of the core peptide with a hydroxy acid via the genetic incorporation of the residue at an amber stop codon with PylRS-PylT would install an ester linkage directly between the leader and core regions of the modified lanthipeptide (Scheme 3.1). Site-specific hydrolysis of the ester bond would produce the core peptide with an N-terminal hydroxyl group. We demonstrate herein that this methodology is successful for the in vivo production and leader peptide removal of the lantibiotic lacticin 481, two analogues of lacticin 481 with N-terminal mutations, and nukacin ISK-1. The methodology was also attempted with the prochlorosins 1.1 and 1.6, however in this system the PylRS-PylT pair did not suppress the amber stop codon to a large extent and truncated ProcA analogues were produced.

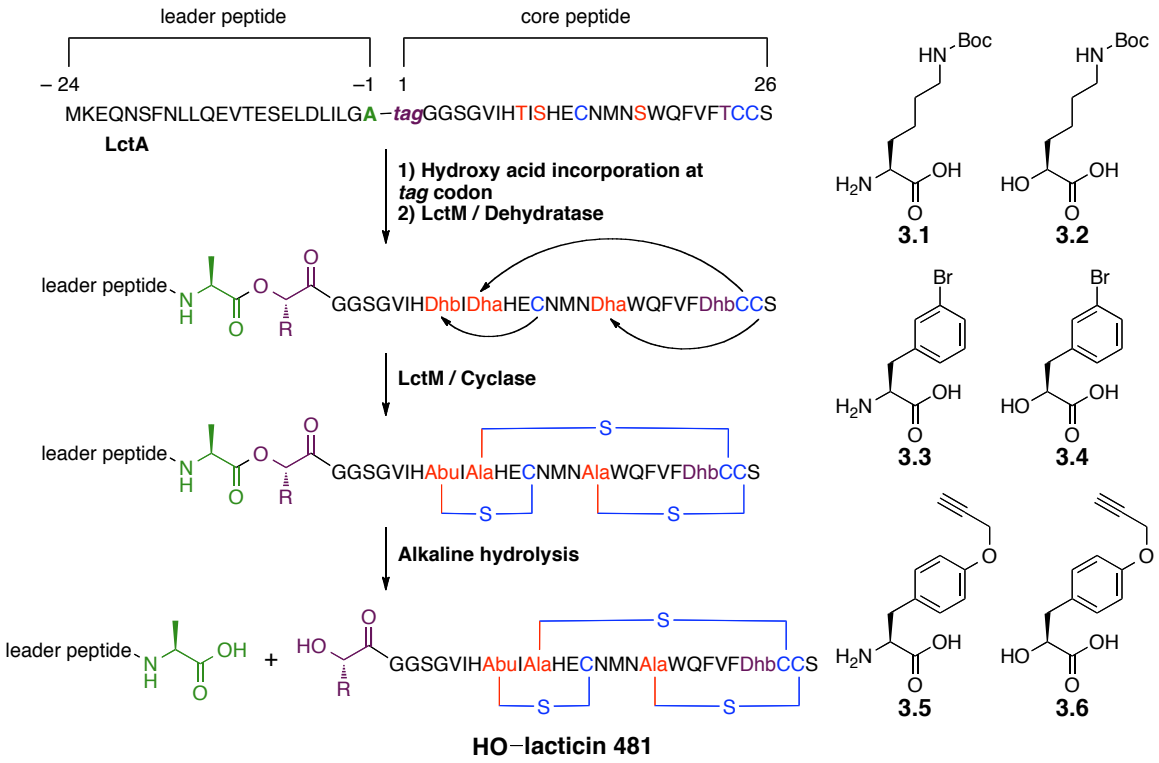

Scheme 3.1. Biosynthesis of lacticin 481 with an N-terminal hydroxyl group by incorporation of a hydroxy acid between leader and core peptides. Left, biosynthesis of lacticin 481 incorporating a hydroxy acid at the amber stop codon (*tag*). After modification of the LctA precursor peptide by LctM, alkaline hydrolysis of the ester bond yields lacticin 481 with an N-terminal hydroxyl group. Wild type (wt) lacticin 481 contains a lysine at its N-terminus. Right, structures of non-proteinogenic amino and hydroxy acids (**3.1-3.6**) introduced into lanthipeptides in this chapter.

3.2. RESULTS AND DISCUSSION

3.2.1. Production of modified Δ1-lacticin 481 in vivo.

We first sought to test the incorporation of an ester bond between the leader and core regions of the class II lantibiotic lacticin 481. As discussed in Chapter 1, nukacin-ISK1, several prochlorosins, and the lantibiotics haloduracin and nisin, among others, have been biosynthesized in *E. coli* by coexpressing the lanthipeptide precursor peptides with their

biosynthetic enzyme(s).[4,5] Previous work on the biosynthesis of lacticin 481 has focused on the in vitro modification of the lacticin 481 precursor peptide, LctA, by its cognate biosynthetic enzyme, LctM.[15] However, for the current methodology to be successful, the activity of the biosynthetic enzyme must be reconstituted in vivo. To test the production of lacticin 481 in *E. coli* BL21 (DE3) cells, the gene sequence encoding His_6-LctA was cloned into MCS1 of a pRSFDuet vector containing *lctM* in MCS2. After induction of coexpression by the addition of IPTG, the culture was incubated for 4 h at 37 ºC, at which point the cells were harvested and lysed. Purification of the lanthipeptide by IMAC and removal of the leader peptide and the first residue of the core peptide with LysC yielded a small amount of Δ1-lacticin 481 that had been completely processed (four dehydrations and three cyclizations) and a large amount of unprocessed product (no dehydrations) (Figure 3.1, left). To increase the production of fully processed Δ1-lacticin 481, the coexpression was repeated except the culture was incubated at 18 ºC overnight after induction with IPTG. We anticipated that the lower temperature would slow the production of LctA, decreasing the opportunity for aggregates of the unmodified LctA precursor peptide to form inclusion bodies, which are not modified. Analysis of the LysC-cleaved product by MALDI-TOF MS showed production of Δ1-lacticin 481 in greater amounts (Figure 3.1, right).[16]

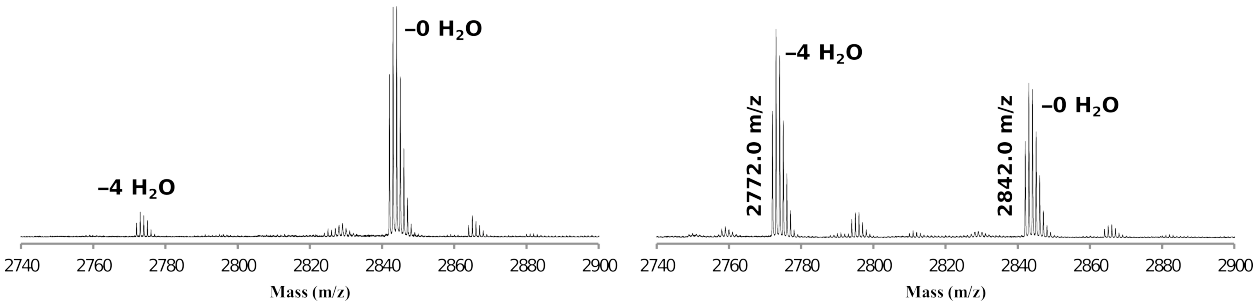

Figure 3.1. Biosynthesis of Δ1-lacticin 481 produced in *E. coli*. MALDI-TOF MS spectra of LysC-cleaved His_6-LctA modified by LctM in *E. coli* grown at 37 ºC (left) and 18 ºC (right). LysC-cleaved His_6-LctA –4 H_2O $[M+H]^+$ calc'd = 2772.2 Da.; LysC-cleaved His_6-LctA –0 H_2O with disulfide $[M+H]^+$ = 2842.2 Da.

3.2.2. Incorporation of H-Lys(Boc)-OH (3.1) into LctA.

We next investigated the incorporation of a non-canonical amino acid into a modified lanthipeptide using PylRS in *E. coli*. This strategy requires first the suppression of the amber codon by the PylRS-PylT pair and then the successful modification of the lanthipeptide analogue by its cognate synthetase. To this end, plasmids were designed to incorporate *lctA*, *lctM*, *pylRS*, and *pylT* into a coexpression system in *E. coli*. A pEVOL plasmid[17] incorporating the latter two genes was donated by Professor Wenshe Liu (Texas A&M). PylRS production from the plasmid is induced by the addition of arabinose and PylT expression is under the control of a strong *proK* promoter. A pRSFDuet plasmid was then constructed integrating genes encoding His_6-LctA(K1*tag*) and LctM into MCS1 and MCS2, respectively. The first amino acid of the core region in the LctA analogue, Lys, was replaced with a *tag* codon so that the non-canonical amino acid H-Lys(Boc)-OH (**3.1**, Scheme 3.1) (for synthesis see section 3.4.2), which has previously been used as a substrate for PylRS-PylT,[18] could be incorporated at that position. Finally, an additional copy of *pylT* was inserted into the pRSFDuet plasmid to increase the efficiency of

incorporation of the non-canonical amino acid into the lanthipeptide (personal communication with Professor Wenshe Liu). Coexpression of His_6-LctA(K1*tag*), LctM, PylRS, and PylT was achieved by the addition of IPTG and arabinose to the cells and 2 mM **3.1** to the growth medium. The coexpression culture was then incubated at 37 ºC for 4 h. After purification of the His_6-tagged peptide by IMAC, analysis by MALDI-TOF MS showed that H-Lys(Boc)-OH had been successfully incorporated into His_6-LctA(K1*tag*) (**3.1**-LctA) (Figure 3.2A). The extent of modification of the LctA analogue by LctM was determined by MALDI-TOF MS after GluC cleavage and Boc removal and LctA was found to be dehydrated four times (wt lacticin 481 has four dehydrations) (Figure 3.2B). Although this result was unexpected as a large portion of wt LctA was not fully processed at 37 ºC, the introduction of a second plasmid to the coexpression system may have the same effect on slowing the expression of LctA and disrupting its ability to form inclusion bodies as lowering the temperature after IPTG induction. Importantly, a leader peptide truncation peak at 4531 Da, corresponding to the translation of LctA halting at the amber stop codon, was not observed. When the coexpression was repeated in the absence of **3.1**, the full-length LctA analogue was not detected. Several peaks were seen in the 7300-7600 Da region (Figure 3.2C solid line), however these masses were frequently observed in our coexpression reactions and likely represent *E. coli* proteins purified during IMAC (see also Figure 3.12A). These results indicate that the PylRS-PylT pair readily introduces **3.1** into lacticin 481 but does not incorporate any of the twenty canonical amino acids native to *E. coli* cells.[19]

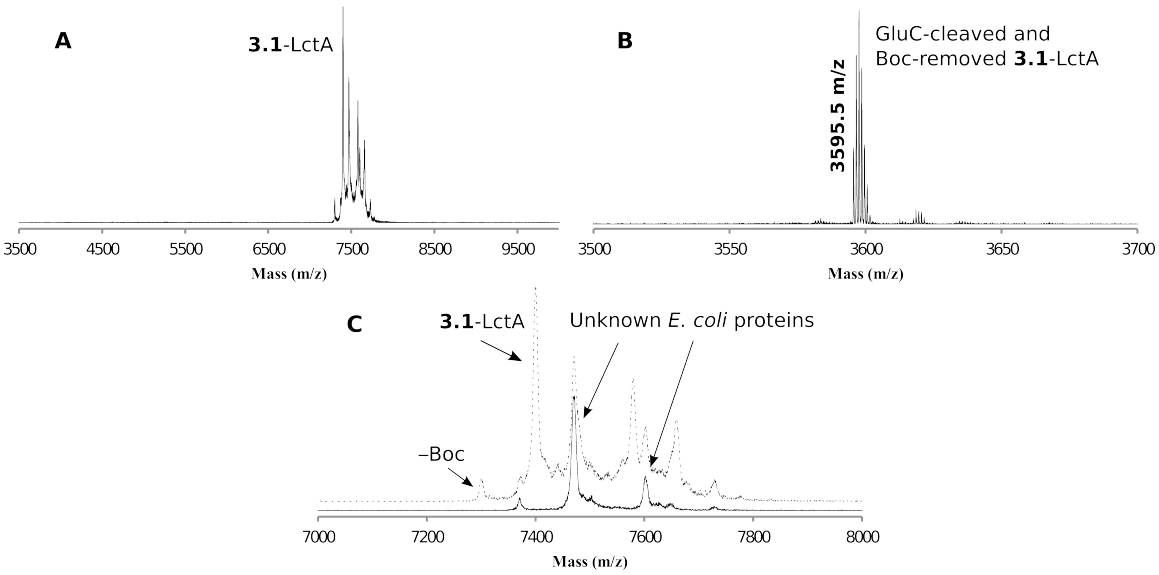

Figure 3.2. MALDI-TOF MS spectra of LctM-modified LctA(K1*tag*) in the presence or absence of **3.1**. **3.1**-LctA before (A) and after (B) GluC cleavage and Boc removal. C) MALDI-TOF MS spectra of LctM-modified His_6-LctA(K1*tag*) in the presence (dashed line) and absence (solid line) of **3.1**. Mass ions seen in the absence of **3.1** are likely *E. coli* proteins. –Boc represents loss of the Boc group from **3.1**-LctA during analysis by MALDI-TOF MS. LctM-modified **3.1**-LctA $[M+H]^+$ calc'd = 7389 Da.; GluC-cleaved, Boc-removed, and LctM-modified **3.1**-LctA $[M+H]^+$ calc'd = 3595.7 Da.

3.2.3. Incorporation of HO-Lys(Boc)-OH (3.2) into LctA.

PylRS recognizes the α-amino group of its substrate loosely because the amine is stabilized in the active site of PylRS by a single hydrogen bond to a water molecule.[20] By contrast, in phenylalanyl-tRNA synthetase, a close structural analogue of PylRS, the side chains of three active site residues form hydrogen bonds with the α-amino group of L-phenylalanine and non-α-amino substrates are not recognized.[21] Based on these studies, and as mentioned in the introduction of this chapter, Yokoyama and coworkers used the PylRS-PylT pair to incorporate

several non-α-amino Boc-Lys derivatives, including the hydroxy acid HO-Lys(Boc)-OH (**3.2**) (Scheme 3.1), into a protein of interest.[14] They were then able to site-specifically cleave the resulting ester bond by mild alkaline hydrolysis.

With the ability of PylRS/PylT to incorporate hydroxy acid **3.2** into proteins and the initial success of LctM modification of **3.1**-LctA, the incorporation of hydroxy acid **3.2** into His_6-LctA(K1*tag*) was tested using the coexpression system outlined above. Unfortunately, after IMAC purification, very little full-length LctA analogue (**3.2**-LctA) was observed by MALDI-TOF MS (Figure 3.3, left). Instead, the major mass ion corresponded to the leader peptide truncation product. This result could have come about in two different ways; 1) the amber stop codon was not suppressed by the PylRS-PylT pair, halting translation at the UAG codon or 2) hydroxy acid **3.2** was successfully incorporated into His_6-LctA(K1*tag*) but the subsequent ester bond was hydrolyzed before or during IMAC purification, allowing the core region, without a His_6-tag, to pass through the nickel column without binding. To probe the latter possibility, the last amino acid of the leader peptide (i.e. the residue immediately preceding the ester bond in His_6-LctA(K1*tag*)) was mutated from Ala to Ile (His_6-LctA(A–1I/K1*tag*)). The rationale for this substitution was that cleavage of an ester bond in the peptide backbone at near-neutral pH is strongly prevented when the ester is directly preceded by a large hydrophobic residue, such as Ile.[9] His_6-LctA(A–1I/K1*tag*) was coexpressed with LctM, PylRS, and PylT in the presence of 2 mM **3.2**, purified by IMAC, and analyzed by MALDI-TOF MS. Gratifyingly, the hydroxy acid was incorporated into the LctA analogue, which was fully modified by LctM (**3.2**-LctA(A–1I)) (Figure 3.3, right). Further analysis of **3.2**-LctA(A–1I) by RP-HPLC showed only one peak, which corresponded to the full-length LctA analogue and not the leader peptide truncation

product (Figure 3.4, right). As before, when the coexpression was repeated in the absence of **3.2** full-length LctA analogue was not observed.

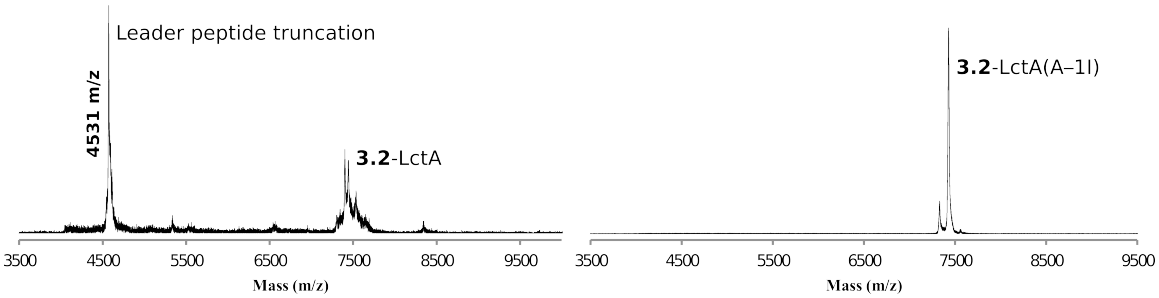

Figure 3.3. Incorporation of **3.2** into LctA(*tag*) and LctA(A–1I/K1*tag*). MALDI-TOF MS spectra of (left) LctM-modified His_6-LctA(K1*tag*) incorporating hydroxy acid **3.2** and (right) LctM-modified His_6-LctA(A–1I/K1*tag*) incorporating hydroxy acid **3.2**. His_6-LctA(K1*tag*) leader peptide truncation $[M+H]^+$ calc'd = 4533 Da.; LctM-modified **3.2**-LctA $[M+H]^+$ calc'd = 7390 Da.; LctM-modified **3.2**-LctA(A–1I) $[M+H]^+$ calc'd = 7427 Da.

To produce lacticin 481 with an N-terminal hydroxyl group (HO-lacticin 481), the Boc group in **3.2**-LctA(A–1I) was removed by incubating the fully modified peptide in 5% TFA at 50 ºC. The pH of the peptidic solution was then increased to 10.5, catalyzing the site-specific release of the leader peptide via ester hydrolysis. Analysis of these reactions by MALDI-TOF MS and analytical RP-HPLC showed depletion of the full-length LctA analogue and a buildup of peaks corresponding to the leader peptide and HO-lacticin 481 (Figure 3.4), which was obtained in a typical yield of 0.1 mg/L culture. The bioactivity of HO-lacticin 481 against *Lactococcus lactis* HP was tested and will be discussed in section 3.2.5.

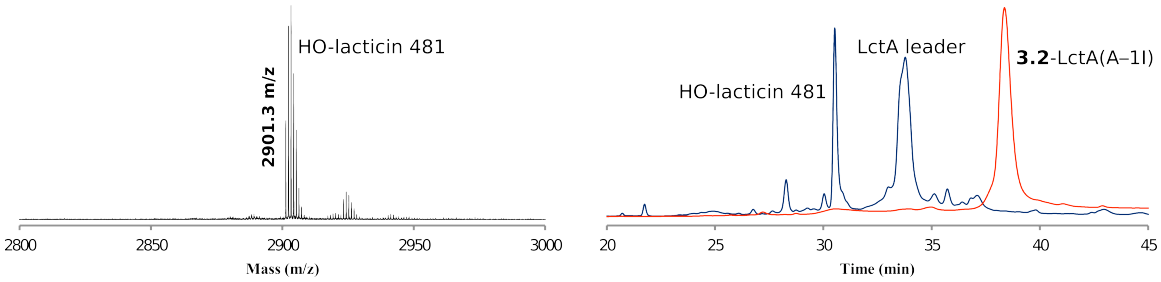

Figure 3.4. Production of HO-lacticin 481. Left, MALDI-TOF MS spectrum of LctM-modified **3.2**-LctA(A–1I) after Boc removal and alkaline hydrolysis yielding HO-lacticin 481. Right, analytical RP-HPLC trace of LctM-modified **3.2**-LctA(A–1I) before (red) and after (blue) Boc removal and alkaline hydrolysis. HO-lacticin 481 $[M+H]^+$ calc'd = 2901.3 Da.

3.2.4. Incorporation of HO-Phe(3Br)-OH (3.4) and HO-Tyr(propargyl)-OH (3.6) into LctA.

A previous study incorporating non-proteinogenic amino acids into lacticin 481 found several positions where a point mutation increased the bioactivity against *L. lactis* HP cells.[2] However, the effect of point mutations to the N-terminal lysine of lacticin 481 on bioactivity has not been tested because, in the methodology used, this residue is removed during cleavage of the leader peptide by the endoprotease LysC, yielding Δ1-lacticin 481. We anticipated that the proposed methodology could enable us to study the bioactivities of lacticin 481 analogues with N-terminal Lys mutations because removal of the leader peptide by alkaline hydrolysis (rather than LysC) would yield the entire core peptide.

Lacticin 481 fortuitously contains a Lys as its N-terminal residue. To investigate whether this strategy might also work for other amino acids, we investigated a mutation at residue 1. Recently, Liu and coworkers developed a PylRS mutant (mut-PylRS; N346A/C348A) that successfully loads Phe analogues with small meta substituents and Tyr analogues with larger para substituents onto $tRNA^{Pyl}_{CUA}$.[22,23] For our studies we chose 3-bromo-L-phenylalanine (H-

Phe(3-Br)-OH), *O*-propargyl-L-tyrosine (H-Tyr(propargyl)-OH), and their corresponding hydroxy acid analogues (Scheme 3.1) as substrates for incorporation into LctA.

To ensure mut-PylRS could suppress the amber stop codon in lanthipeptides produced in vivo, we first sought to incorporate the amino acids **3.3** and **3.5** (Scheme 3.1) into His_6-LctA(A–1I/K1*tag*). Coexpression of the LctA precursor with LctM, mut-PylRS, and pylT in enriched LB media (for composition see section 3.4.4) supplemented with **3.3** or **3.5** resulted in full-length LctA analogues without discernible detection of leader peptide truncation products (**3.3**-LctA(A–1I) and **3.5**-LctA(A–1I)) (Figure 3.5A,C). After GluC cleavage, the major ions observed corresponded to the 4-fold dehydrated products (Figure 3.5B,D). Interestingly, when **3.3** or **3.5** were not added to the media, a very small peak corresponding to full-length LctA was sometimes observed, indicating suppression of the stop codon. Analysis of this GluC-cleaved substrate by MALDI-TOF MS demonstrated that Phe had been incorporated into LctA at the amber codon, a result that was not surprising as mut-PylRS weakly recognizes L-Phe.[23] However, the incorporation of L-Phe into His_6-LctA(A–1I/K1*tag*) was negligible in the presence of 2 mM **3.3** or **3.5** (Figure 3.5B,D), even in rich media, suggesting the non-proteinogenic amino acid outcompetes L-Phe in vivo.

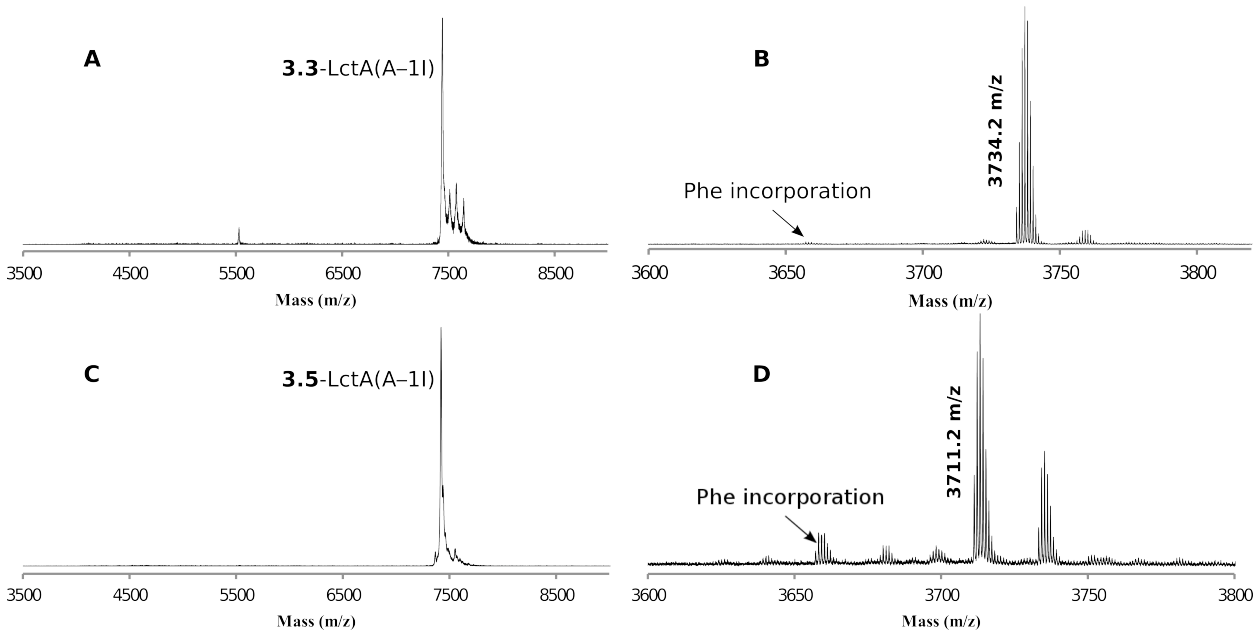

Figure 3.5. MALDI-TOF MS spectra of full-length and GluC-cleaved LctM-modified His_6-LctA(A–1I/K1*tag*) incorporating **3.3** or **3.5**. A) LctM-modified **3.3**-LctA(A–1I) ($[M+H]^+$ calc'd = 7428 Da.). B) LctM-modified and GluC-cleaved **3.3**-LctA(A–1I) ($[M+H]^+$ calc'd = 3734.7 Da.). C) LctM-modified **3.5**-LctA(A–1I) ($[M+H]^+$ calc'd = 7403 Da). D) LctM-modified and GluC-cleaved **3.5**-LctA(A–1I) ($[M+H]^+$ calc'd = 3710.7 Da.).

The incorporation of HO-Phe(3Br)-OH (**3.4**) or HO-Tyr(propargyl)-OH (**3.6**) into His_6-LctA(A–1I/K1*tag*) was then attempted. Coexpression of the LctA precursor peptide with LctM, mut-PylRS, and PylT in enriched LB containing **3.4** or **3.6** was followed by IMAC and RP-HPLC purification. The products displayed major mass ions corresponding to fully modified LctA analogues (**3.4**-LctA(A–1I) and **3.6**-LctA(A–1I)) (Figure 3.6A,C). Alkaline hydrolysis of the full-length peptides produced lacticin 481 analogues with the desired N-terminal mutations (**3.4**-HO-lacticin 481, **3.6**-HO-lacticin 481) in typical yields of 0.04 mg/L and 0.05 mg/L culture, respectively (Figure 3.6B,D).

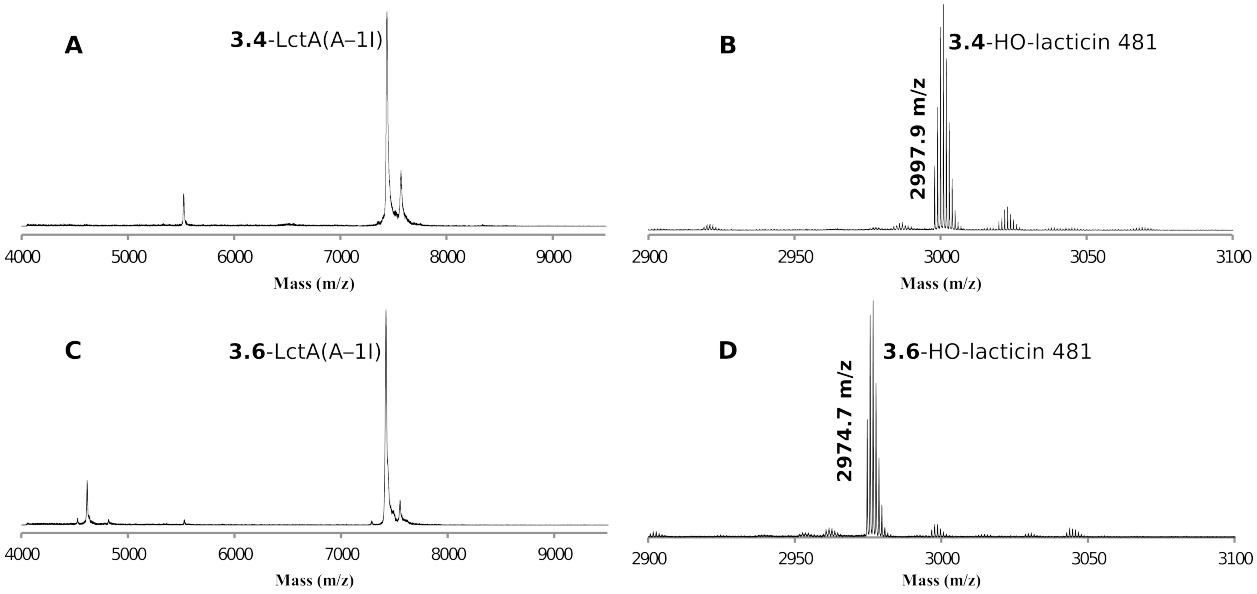

Figure 3.6. MALDI-TOF MS spectra of full-length and base-hydrolyzed LctM-modified His_6-LctA(A–1I/K1*tag*) incorporating **3.4** or **3.6**. A) LctM-modified **3.4**-LctA(A–1I) ($[M+H]^+$ calc'd = 7429 Da.). B) LctM-modified and base-hydrolyzed **3.4**-LctA(A–1I) ($[M+H]^+$ calc'd = 2998.1 Da.). C) LctM-modified **3.6**-LctA(A–1I) ($[M+H]^+$ calc'd = 7404 Da). D) LctM-modified and base-hydrolyzed **3.6**-LctA(A–1I) ($[M+H]^+$ calc'd = 2974.2 Da.).

3.2.5. Antimicrobial activities of wt lacticin 481, Δ1-lacticin 481, HO-lacticin 481, 3.4-HO-lacticin 481, and 3.6-HO-lacticin 481.

We first compared the bioactivity of wt lacticin 481, isolated from *L. lactis* subsp. *lactis* CNRZ 481, with Δ1-lacticin 481 by agar diffusion antimicrobial assays and liquid growth media assays against *L. lactis* HP (Figure 3.7, left). Originally, it appeared that Δ1-lacticin 481 (IC_{50} = 105 nM ± 16 nM) was approximately 4-fold more active than wt lacticin 481 (IC_{50} = 444 nM ± 51 nM). This result was surprising as lacticin 481-N15R/F21H was previously found to be 5-fold more active than its corresponding analogue lacking an N-terminal lysine.[2,16] To ensure the amounts of wt lacticin 481 and Δ1-lacticin 481 used for the liquid growth assay were equivalent,

equal amounts of both compound stocks were injected into an analytical RP-HPLC instrument and the corresponding absorbances at 220 nm were compared (Figure 3.7, right). Interestingly, the amount of wt lacticin 481 observed was much less than that of Δ1-lacticin 481 suggesting that the wt lacticin 481 used in the bioactivity studies was not pure and that the stock concentration was overestimated; the wt lacticin 481 was presumably contaminated by ammonium acetate, which was used to buffer the mobile phase in the final step of purification. To remove the ammonium acetate, the impure stock of wt lacticin 481 was desalted by RP-HPLC and eluted with an MeCN mobile phase lacking ammonium acetate and lyophilized (Figure 3.7, right). The new stock of wt lacticin 481 was tested against *L. lactis* HP in a liquid media growth assay and its antimicrobial activity (IC_{50} = 120 nM ±15 nM) was 4-fold greater than the impure wt lacticin 481 and similar to Δ1-lacticin 481. Thus, wt lacticin 481 isolated from the native producer has an IC_{50} at least 4-fold greater against *L. lactis* HP than originally reported by our laboratory.[16]

The bioactivities of wt lacticin 481 and Δ1-lacticin 481 were then compared with HO-lacticin 481, **3.4**-HO-lacticin 481, and **3.6**-HO-lacticin 481 by agar diffusion antimicrobial assays and liquid media growth assays (Figure 3.7, left). HO-lacticin 481 (IC_{50} = 224 nM ± 65 nM) showed similar activity to that of wt lacticin 481 and Δ1-lacticin 481 suggesting the introduction of a hydroxyl group at the N-terminus of lacticin 481 has just a small effect on bioactivity. However, the bioactivity of HO-lacticin 481 was decidedly higher than that of **3.4**-HO-lacticin 481 (IC_{50} = 3,870 nM ± 55 nM) and **3.6**-HO-lacticin 481 (IC_{50} = 720 nM ± 170 nM). This result supports previous findings that the N-terminal lysine of lacticin 481 is important, but not essential, for bioactivity.[2]

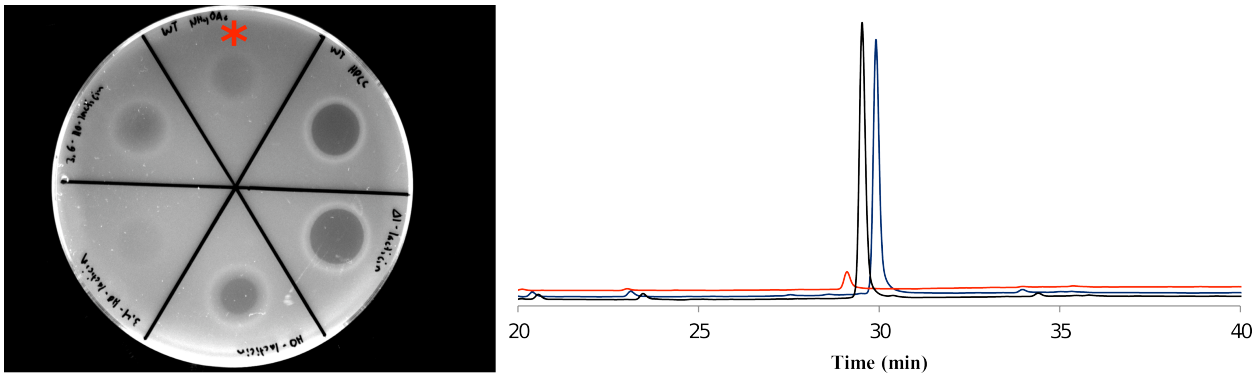

Figure 3.7. Zones-of-growth-inhibition displayed by and purification of lacticin 481 and analogues. Left, zones-of-growth-inhibition displayed by (clockwise from red star) impure-wt lacticin 481, wt-lacticin 481, Δ1-lacticin 481, HO-lacticin 481, **3.4**-HO-lacticin 481, and **3.6**-HO-lacticin 481 against *L. lactis* HP. A total of 10 µL of 12.5 µM compound solution was added to each spot. Right, analytical RP-HPLC trace of impure-wt lacticin 481 (red), lacticin 481 after HPLC purification in mobile phase lacking ammonium acetate (black), and Δ1-lacticin 481 (blue) to determine purities and relative concentrations of compounds used in the antimicrobial assays. A total of 100 µL of 34 µM substrate was injected.

3.2.6. Incorporation of non-proteinogenic amino and hydroxy acids between the leader and core regions of nukacin ISK-1.

Given the success of incorporation of non-proteinogenic amino and hydroxy acids into lacticin 481, we sought to show the leader peptide removal strategy by ester hydrolysis was general for other lanthipeptides. We chose nukacin ISK-1 (precursor peptide is NukA; Figure 3.8) because it is a close structural analogue of lacticin 481 and, like lacticin 481, has an N-terminal lysine. Moreover, in all previous attempts to biosynthesize nukacin ISK-1 in *E. coli* the removal of the leader peptide was achieved by incubating the modified precursor peptide with the endoprotease LysC, which also removed the first three residues of the core peptide

(LysLysLys) yielding Δ1-3-nukacin ISK-1.[4,24] Using our hydroxy acid incorporation strategy, we sought to produce nukacin ISK-1 without an N-terminal truncation.

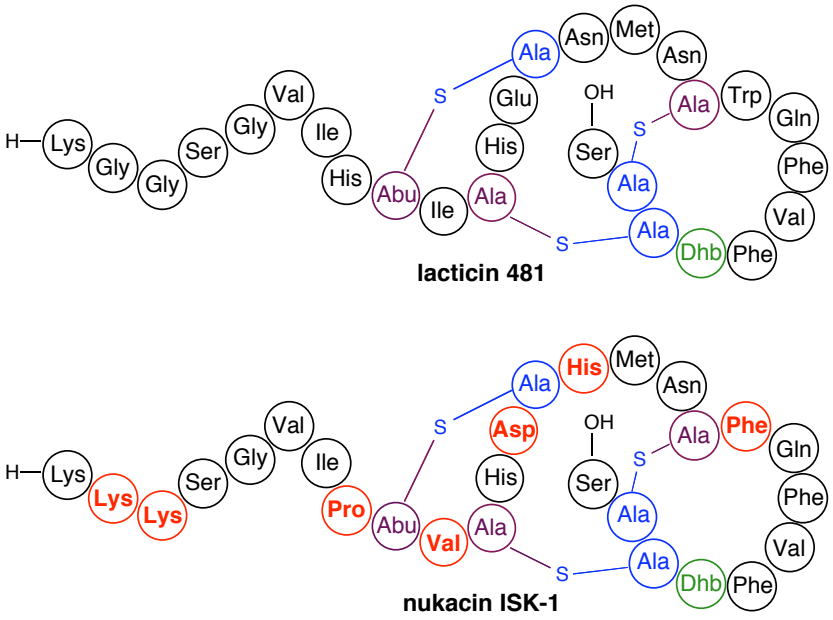

Figure 3.8. Structures of lanthipeptides lacticin 481 and nukacin ISK-1. Residues in nukacin ISK-1 that differ from lacticin 481 are highlighted in red.

3.2.6.1. Production of modified Δ1-3 nukacin ISK-1 in vivo.

Previous attempts to biosynthesize nukacin ISK-1 in our lab have focused on the in vitro modification of an LctA leader/NukA core chimeric peptide (LctNukA) with LctM.[24] Although NukA is not the native substrate for LctM, the core region of the chimeric peptide was successfully dehydrated and cyclized.[24] For our ester incorporation strategy to be successful, nukacin ISK-1 must be produced in vivo in *E. coli* so the gene sequence encoding LctNukA was introduced into MCS1 of a pRSFDuet vector incorporating the gene for LctM in MCS2. After induction of coexpression by the addition of IPTG, harvesting of the cells, lysis, IMAC, and removal of the leader peptide and the first three residues of the core peptide with LysC yielded a

mixture of fully and partially modified Δ1-3-nukacin ISK-1. Unfortunately, during the LysC cleavage step a large amount of Δ1-3-nukacin ISK-1 was oxidized (Figure 3.9, left). The LctNukA expression was then repeated and all solutions were sparged with nitrogen before addition to the peptide. After LysC cleavage, the major mass ion corresponded to Δ1-3-nukacin ISK-1 with no oxidation product (Figure 3.9, right).

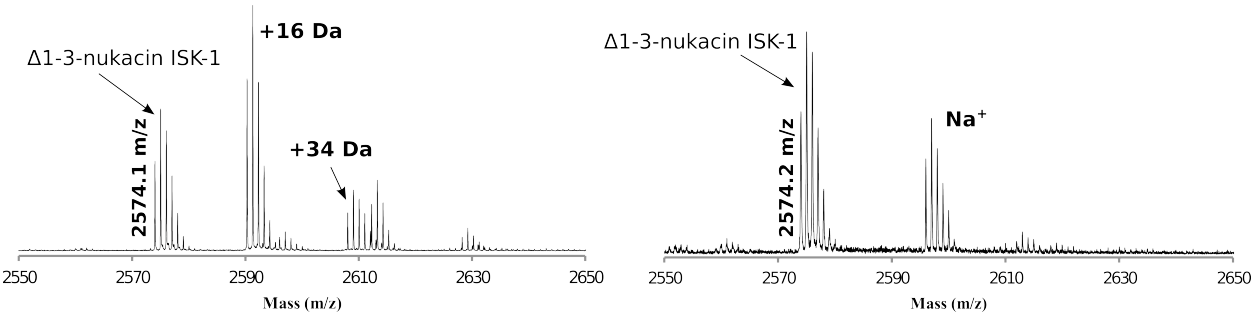

Figure 3.9. Biosynthesis of Δ1-3-nukacin ISK-1 in *E. coli*. Coexpression cultures containing a pRSFDuet plasmid encoding LctNukA and LctM were incubated at 18 ºC after IPTG induction. Left, LysC assay solution was not sparged with nitrogen. Right, LysC assay solution was sparged with nitrogen. The peak at +16 Da likely represents oxidized Δ1-3-nukacin ISK-1, however incomplete dehydration of one Ser/Thr residue and the formation of one disulfide bond cannot be ruled out. The peak at +34 Da represents the incomplete dehydration of two Ser/Thr residues (+36 Da) and the formation of one disulfide bond (–2 Da). The peak at Na^+ represents a sodium adduct. Δ1-3-nukacin ISK-1 $[M+H]^+$ calc'd = 2574.1 Da.

3.2.6.2. Incorporation of 3.1 and 3.2 into nukacin ISK-1.

To produce nukacin ISK-1 with a non-proteinogenic amino or hydroxy acid inserted between its leader and core peptides, a gene sequence encoding LctNukA(A–1I/K1*tag*) was incorporated into a pRSFDuet vector. As before, a pEVOL plasmid carried genes encoding

PylRS and PylT. Coexpression of LctNukA(A–1I/K1*tag*), LctM, PylRS, and PylT in the presence of **3.1** yielded an LctNukA analogue incorporating **3.1** between its leader and core regions (**3.1**-LctNukA(A–1I); Figure 3.10A). Removal of a portion of the leader peptide of **3.1**-LctNukA(A–1I) by GluC showed that the core peptide was dehydrated four times (Figure 3.10B) (the same number of dehydrations as in wt nukacin ISK-1). Interestingly, as seen in our studies with lacticin 481, no partially modified LctNukA core peptide was observed when LctNukA was coexpressed with LctM, PylRS, and PylT (Figure 3.10B).

The incorporation of hydroxy acid **3.2** into LctNukA(A–1I/K1*tag*) was then attempted. Analysis by MALDI-TOF MS of the coexpression of the LctNukA mutant with LctM, PylRS, and PylT in the presence of **3.2** showed a large peak corresponding to full-length LctNukA without detection of leader peptide truncation product (**3.2**-LctNukA(A–1I); Figure 3.10C). The Boc-group of **3.2**-LctNukA(A–1I) was then removed with acid followed by alkaline-catalyzed hydrolysis of the leader peptide from the core peptide yielding nukacin ISK-1 with an N-terminal hydroxyl group (HO-nukacin ISK-1; Figure 3.10D).

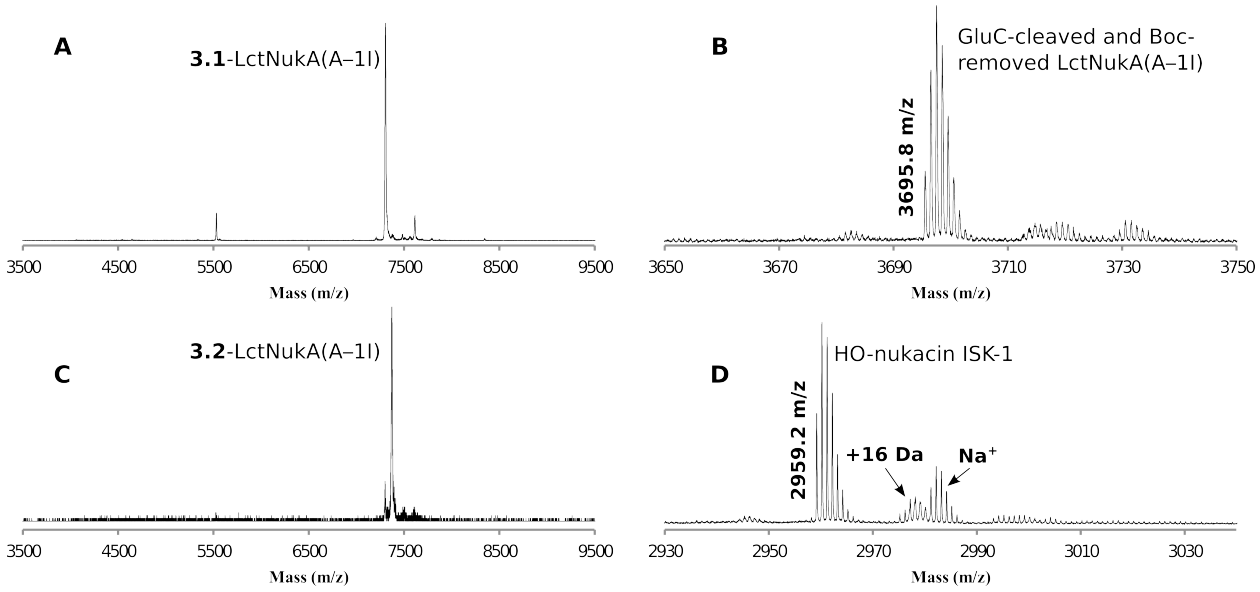

Figure 3.10. Incorporation of **3.1** and **3.2** into LctNukA(A–1I/K1*tag*). MALDI-TOF MS spectra of A) LctM-modified **3.1**-LctNukA(A–1I/K1*tag*) ($[M+H]^+$ calc'd = 7484 Da.), B) Boc-deprotected GluC-cleaved **3.1**-LctNukA(A–1I/K1*tag*) that was modified by LctM ($[M+H]^+$ calc'd = 3695.8 Da.), C) LctM-modified **3.2**-LctNukA(A–1I/K1*tag*) ($[M+H]^+$ calc'd = 7485 Da.), D) Boc-deprotected and alkaline hydrolyzed **3.2**-LctNukA(A–1I/K1*tag*) that was modified by LctM producing HO-nukacin ISK-1 ($[M+H]^+$ calc'd = 2959.3 Da. Peak at +16 Da represents oxidation of **3.2**-nukacin ISK-1. Na^+ represents sodium adduct.

3.2.6.3. Antimicrobial activities of Δ1-3 nukacin ISK-1 and HO-nukacin ISK-1.

The bioactivities of Δ1-3-nukacin ISK-1 and HO-nukacin ISK-1 were first tested by agar diffusion antimicrobial assays against *L. lactis* HP and *Bacillus coagulans*. Unfortunately, no bioactivity was observed even at concentrations up to 250 μM for each peptide. The antimicrobial activities of the nukacin analogues were then tested against *L. lactis* HP in liquid media growth assays. At concentrations of 12.5 and 25 μM HO-nukacin ISK-1 retarded cell growth whereas normal cell growth was observed when the same concentrations of Δ1-3-nukacin

ISK-1 were added (Figure 3.11). These results are in agreement with a previous study showing the removal of the N-terminal LysLysLys of nukacin ISK-1 reduced the bioactivity of the compound.[25]

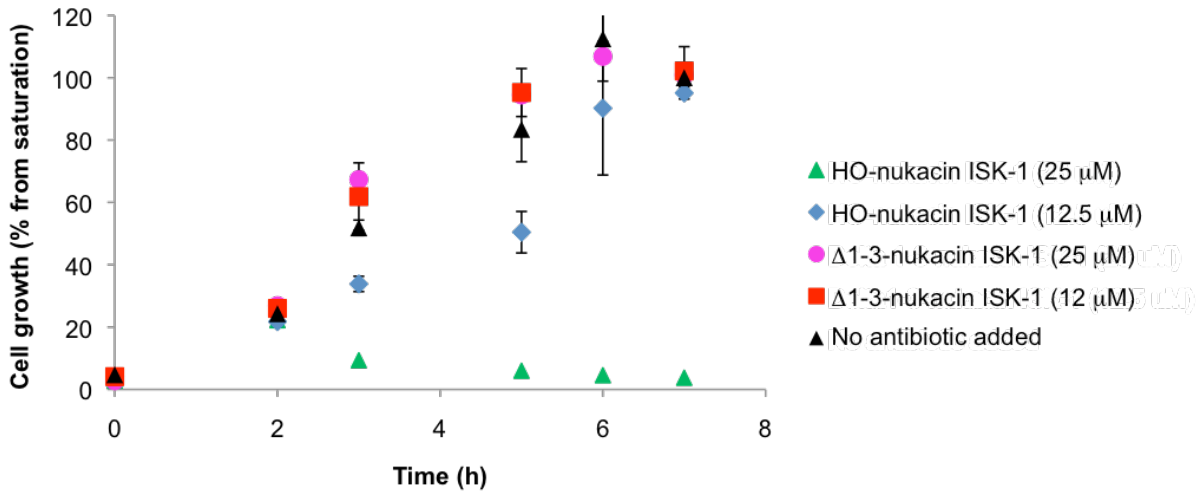

Figure 3.11. Growth of *L. lactis* HP cells in liquid media in the presence of HO-nukacin ISK-1 and Δ1-3-nukacin ISK-1. For all compounds tested n = 3 except HO-nukacin ISK-1 and Δ1-nukacin ISK-1 at 25 μM (n = 1).

3.2.7. Incorporation of non-proteinogenic amino and hydroxy acids between the leader and core regions of prochlorosins.

We then attempted our ester bond incorporation strategy on the prochlorosin (Pcn) group of lanthipeptides.[26] We chose the prochlorosins as substrates because they are unrelated to lacticin 481 and nukacin ISK-1 and the native protease responsible for leader peptide removal has not been identified. Hence, a hydrolytic removal of the leader peptide would be valuable. The prochlorosin precursor peptides ProcA1.1 and ProcA1.6 (corresponding to Pcn1.1 and Pcn1.6 after leader peptide removal) are ideally suited for this methodology because their core

peptides begin with Phe and Lys, respectively. Therefore, the incorporation of **3.2** or **3.4** into ProcA1.1 or ProcA1.6, respectively, followed by alkaline hydrolysis, would yield Pcn1.1 and Pcn1.6 with N-terminal hydroxyl groups.

3.2.7.1. Incorporation of 3.1 and 3.3 into ProcA1.1.

The prochlorosins are members of the class II lanthipeptides and, like lacticin 481 and nukacin ISK-1, are modified by a single bifunctional enzyme (ProcM). To produce a ProcA1.1 analogue incorporating non-proteinogenic amino or hydroxy acids between its leader and core regions, a gene encoding ProcA1.1(G–1I/F1*tag*) was inserted into MCS1 of a pRSFDuet vector with ProcM in MCS2. Analysis of the coexpression of ProcA1.1(G–1I/F1*tag*) with ProcM, mut-PylRS, and PylT in enriched LB containing **3.3** by MALDI-TOF MS and analytical RP-HPLC showed two distinct peaks: a very small peak corresponding to full-length ProcA1.1 incorporating **3.3** (**3.3**-ProcA1.1(A–1I)) and a much larger peak corresponding to translation halting at the amber stop codon (Figure 3.12). Several potential causes for the low level of amber codon suppression by mut-PylRS-PylT in ProcA1.1 were investigated and will be discussed below.

We hypothesized that the amount of mut-PylRS being produced in the coexpression was too low to efficiently suppress the amber stop codon in ProcA1.1. Indeed, in this work and other studies, ProcA was expressed in much greater yields than lacticin 481[27,28] so higher concentrations of mut-PylRS, or lower concentrations of the ProcA1.1 transcript, might be necessary to achieve the same level of amber suppression as seen for lacticin 481. We first sought to decrease the amount of ProcA1.1 produced during coexpression by modifying the composition of the media from enriched LB to minimal media (for composition of minimal

media see section 3.4.4). The decrease in nutrients in minimal media should slow the biosynthesis of ProcA1.1, giving mut-PylRS more time to incorporate **3.3**. Gratifyingly, the amount of leader peptide truncation product, after coexpression of His_6-ProcA1.1(G–1I/F1*tag*) with ProcM, mut-PylRS, and PylT in minimal media, was dramatically reduced; the yield of full-length ProcA1.1 incorporating **3.3** after coexpression was also reduced, but by much less (Figure 3.12). This result gave credibility to our hypothesis that influencing the concentration of the ProcA1.1 transcript, or mut-PylRS, during coexpression could increase the amount of full-length ProcA1.1 produced.

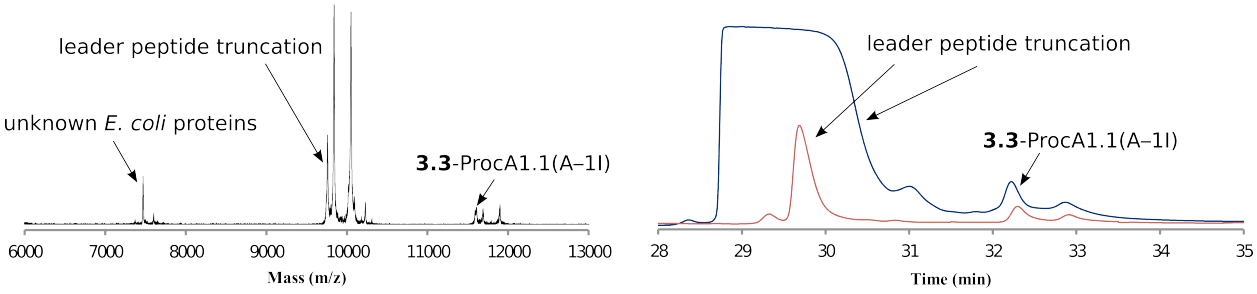

Figure 3.12. Comparison of enriched LB and minimal media for the incorporation of **3.3** into His_6-ProcA1.1(G–1I/F1*tag*). Left, MALDI-TOF MS spectrum of ProcM-modified His_6-ProcA1.1(G–1I/F1*tag*) incorporating **3.3** in enriched LB (**3.3**-ProcA1.1(A–1I) $[M+H]^+$ calc'd = 11753 Da.; His_6-ProcA1.1(G–1I/F1*tag*) leader peptide truncation $[M+H]^+$ calc'd = 9744 Da.). Right, analytical RP-HPLC trace of ProcM-modified His_6-ProcA1.1(G–1I/F1*tag*) incorporating **3.3** in enriched LB (blue) or minimal media (red). MALDI-TOF MS analysis of the analytical RP-HPLC purification of His_6-ProcA1.1(G–1I/F1*tag*) in enriched media confirmed the elution of the leader peptide truncation product began at 28.6 min and ended around 31.0 min.

The expression of ProcA1.1 and mut-PylRS is dependent on two different small molecules, IPTG and arabinose respectively, and hence the level of expression of either gene product can be independently manipulated. We hoped that either an increase in arabinose concentration (from 0.2%), and consequently an increase in the expression of mut-PylRS, or a decrease in the amount of IPTG (from 250 μM), leading to lower levels of ProcA1.1 production, would increase the amber codon suppression ability in the coexpression system. We first increased the concentration of arabinose to 0.5% and 1.0% during coexpression of His_6-ProcA1.1(G–1I/F1*tag*) with ProcM, PylRS, and PylT, in minimal media in the presence of **3.3**. Each coexpression product was purified by IMAC and analyzed by MALDI-TOF MS and analytical RP-HPLC (Figure 3.13, left). Unfortunately, the concentration of arabinose had no effect on the incorporation of **3.3**, a result that was not unexpected because induction with 0.2% arabinose is already considered saturating for plasmids containing the *araBAD* promoter.[29] Next, we decreased the concentration of IPTG during coexpression to 250 μM, 50 μM, and 25 μM while keeping the concentration of arabinose constant (0.2%). We hoped slowing down the expression of ProcA1.1 would allow the ribosome more time to incorporate the non-proteinogenic amino acid at the *tag* codon. For these experiments we attempted the introduction of the Lys analogue **3.1** into His_6-ProcA1.1(G–1I/F1*tag*) using wt PylRS as this system gave higher yields with lacticin 481. Analysis of the coexpression experiments by analytical RP-HPLC showed that a decrease in the concentration of IPTG did reduce the amount of ProcA1.1 produced during coexpression, however the ratio of full-length ProcA1.1 to leader peptide truncation product remained largely unchanged (Figure 3.13, right). Hence, varying the concentration of IPTG in the coexpression had no beneficial effect on the efficiency of stop codon suppression.

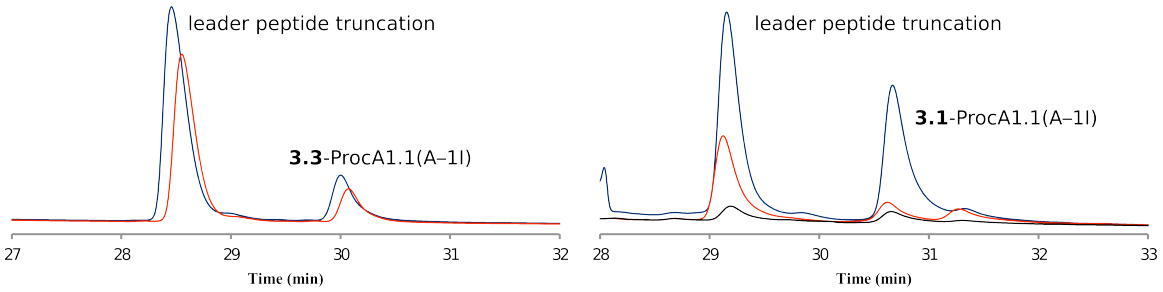

Figure 3.13. Comparison of different concentrations of arabinose or IPTG on incorporation of **3.1** or **3.3** into His_6-ProcA1.1(G–1I/F1*tag*). Left, analytical RP-HPLC traces of His_6-ProcA1.1(G–1I/F1*tag*) incorporating **3.3** with 1.0% (blue) and 0.5% (red) arabinose in the coexpression culture. Right, analytical RP-HPLC traces of His_6-ProcA1.1(G–1I/F1*tag*) incorporating **3.1** with 250 μM (blue), 25 μM (red), and 5 μM (black) IPTG in the coexpression culture.

3.2.7.2. Incorporation of 3.1 into ProcA1.6.

After our unsuccessful attempts at efficiently incorporating **3.1** or **3.3** into ProcA1.1, we sought instead to incorporate **3.1** into ProcA1.6 using wt PylRS. A gene encoding His_6-ProcA1.6(G–1I/K1*tag*) was introduced into MCS1 of a pRSFDuet vector with ProcM integrated into MCS2. Coexpression of the ProcA1.6 mutant with ProcM, PylRS, and PylT in the presence of **3.1** in minimal media again yielded mostly leader peptide truncation product with a small amount of full-length ProcA1.6 (**3.1**-ProcA1.6(A–1I)) (Figure 3.14, left). To assess if the incorporation of **3.1** into His_6-ProcA1.6(G–1I/K1*tag*) was affected by the bulky residue at the –1 position, the Ile was mutated to Gly (ProcA1.6(K1*tag*)) and the coexpression was repeated. Unfortunately, the mutation at the –1 position had no effect on amber codon suppression as the major peak still corresponded to the leader peptide truncation product (Figure 3.14, right).

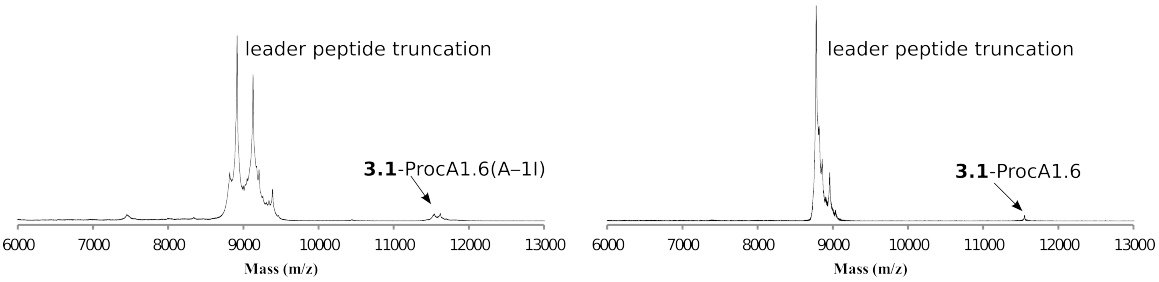

Figure 3.14. MALDI-TOF MS spectra of the incorporation of **3.1** into ProcA1.6 mutants. Left, MALDI-TOF MS spectrum of ProcM-modified His_6-ProcA1.6(G–1I/K1*tag*) incorporating **3.1**. Right, MALDI-TOF MS spectrum of His_6-ProcA1.6(K1*tag*) incorporating **3.1** after modification by ProcM**.** Leader peptide truncation product for His_6-ProcA1.6(A–1I/K1*tag*) $[M+H]^+$ calc'd = 8820 Da.; ProcM-modified **3.1**-ProcA1.6(A–1I) $[M+H]^+$ calc'd = 11482 Da.; Leader peptide truncation product for His_6-ProcA(K1*tag*) $[M+H]^+$ calc'd = 8764 Da.; ProcM-modified **3.1**-ProcA1.6 $[M+H]^+$ calc'd = 11426 Da.

3.3. SUMMARY AND OUTLOOK.

When compared with lanthipeptide biosynthesis in vitro, the coexpression of lanthipeptides with their biosynthetic enzymes in *E. coli* produces the biomolecules in higher yields and purities, allowing many studies that were previously not possible. Indeed, the in vivo route to lanthipeptide production facilitated recent work on the mode of action,[28] ring topology,[30,31] and stereochemistry[27] of lanthipeptides, as well as the characterization of important biosynthetic proteins[32,33] and new lanthipeptide gene clusters.[30,34] In these studies, the removal of the leader peptide to produce the mature lanthipeptide/lantibiotic was achieved by engineering a proteolytic cleavage site at the –1 position followed by leader peptide removal using a commercial protease. However, in several cases the protease could not cleave at the desired location, hindering further studies on the peptides.[27,28] Thus, the ability to more easily control the

release of the leader region from the core region after lanthipeptide production in vivo would be beneficial.

My studies described in this chapter show the incorporation of six non-proteinogenic amino or hydroxy acids directly between the leader and core regions of the lantibiotic lacticin 481 using amber suppression technology with PylRS and mut-PylRS. In nearly every case, the suppression of the amber codon was excellent as substantial amounts of leader truncation product were not detected. The observation of truncated product when hydroxy acid **3.2** was incorporated into LctA(K1*tag*) was likely the result of premature ester bond cleavage and not the translation of LctA halting at the amber codon. Indeed, when the residue immediately preceding the ester bond in LctA was mutated to Ile, truncation product was not detected, presumably because the bulky amino acid prevented hydrolysis at neutral pH. Mild alkaline conditions promoted full cleavage of the ester linkages allowing the production of lacticin 481, and analogues, with an N-terminal hydroxyl group. Although lanthipeptides normally contain N-terminal amines, incorporation of lactate is a posttranslational modification at the N-terminus of some lanthipeptides and is thought to protect those compounds from aminopeptidases.[35,36]

The incorporation of amino and hydroxy acids **3.1** and **3.2** into nukacin ISK-1 was also successful. Ester hydrolysis of **3.2**-LctNukA(A–1I) yielded fully modified nukacin ISK-1 with an N-terminal hydroxyl group. The formation of oxidized nukacin ISK-1 lowered the total yield of nukacin ISK-1 produced in *E. coli*, however sparging the LysC and base hydrolysis assay solutions largely prevented oxidation. This biosynthesis marked the first time that nukacin ISK-1, and not Δ1-3-nukacin ISK-1, had been produced after expression of its modified precursor peptide in *E. coli*.

The incorporation of the non-proteinogenic amino acids **3.1** and **3.3** into prochlorosins 1.1 and 1.6 was unsuccessful. In every case, the leader peptide truncation peak, corresponding to translation halting at the amber stop codon, was dominant over full-length ProcA. Reducing the amount of ProcA synthesized during coexpression by replacing rich with minimal media seemed to increase the ratio of full-length ProcA to truncation product, likely because the expression of ProcA was slowed. However, decreasing the concentration of IPTG to further reduce the amount of ProcA produced was not beneficial, and the amber codon suppression product was never obtained as major product.

The amber codon suppression of PylRS-PylT in *E. coli* has to compete with innate release factors (RFs) that recognize stop codons and terminate translation. Prokaryotes have two RFs that recognize stop codons; RF1 recognizes UAA and UAG while RF2 recognizes UAA and UGA.[37] Thus, knocking out RF1 should slow, and possibly even eliminate, the ability of *E. coli* to terminate gene expression at a UAG codon. Indeed, when RF1 was suppressed or knocked out in *E. coli* cells, incorporation efficiency of non-proteinogenic amino acids into proteins using PylRS or tyrosyl-tRNA synthetase was increased, even when multiple UAG codons were introduced into the gene being expressed.[38,39] This technology could aid incorporating non-proteinogenic amino or hydroxy acids into prochlorosins or other lanthipeptides.

In conclusion, we have successfully produced lacticin 481, nukacin ISK-1, and analogues incorporating N-terminal mutations, with N-terminal hydroxyl groups in vivo. Given the ease of site-directed mutagenesis, this methodology could be extended to lantibiotic analogues with improved activity or solubility. Importantly, unlike peptide cleavage using commercial proteases, the ester bond hydrolysis reaction is not sequence dependent and is completely site-selective. After optimization of the incorporation of the non-proteinogenic amino and hydroxy acids, we

anticipate that, like the photocleavable linker in Chapter 2, this general methodology may find use for other lanthipeptides and other classes of ribosomally synthesized and posttranslationally modified peptides.

3.4. EXPERIMENTAL

3.4.1 Materials

All compounds used in the synthetic schemes were purchased from Sigma Aldrich with the exception of L-lysine monohydrochloride (Eastman Chemical Company), 8-quinolinol (Fisher Scientific), di-tert-butyl dicarbonate (Boc_2O, Fluka Analytical), propargyl bromide (TCI America), and 3-bromo-L-phenylalanine (H-Phe(3Br)-OH, Chem Impex Int.). Solvents commonly used in peptide purification, including trifluoroacetic acid (TFA) and acetonitrile (MeCN), were obtained in RP-HPLC grade or better and used directly without further purification. Oligonucleotide primers used for molecular cloning were purchased from Integrated DNA Technologies. Phusion High-Fidelity DNA polymerase, T4 DNA ligase, Gibson Assembly master mix, and all restriction endonucleases were purchased from New England Biolabs. Gel extraction, plasmid miniprep, and PCR purification kits were purchased from QIAGEN. Endoproteinases LysC and GluC were purchased from Roche Applied Science and 3-(cyclohexylamino)-1-propanesulfonic acid (CAPS) was purchased from Sigma Aldrich. Other items procured for cell culture and peptide work included isopropyl β-D-1-thiogalactopyranoside (IPTG) (Gold Biotechnology), kanamycin monosulfate (IBI Scientific), chloramphenicol (IBI Scientific), and L(+)-arabinose (Fisher Scientific). MALDI-TOF MS analyses were conducted at the Mass Spectrometry Facility (UIUC) using an UltrafleXtreme TOF/TOF (Bruker Daltonics).

3.4.2. Synthesis of amino and hydroxy acids 3.1-3.6.

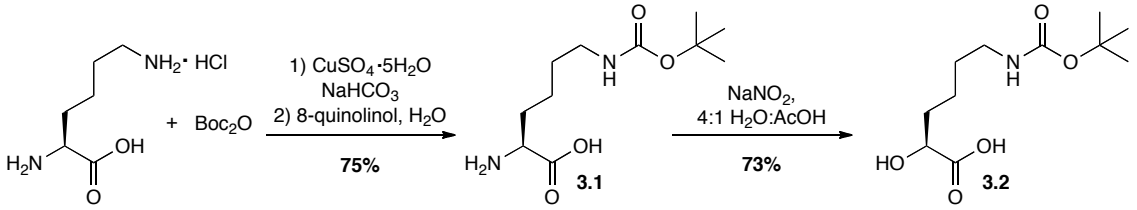

Synthetic design of HO-Lys(Boc)-OH (3.2)

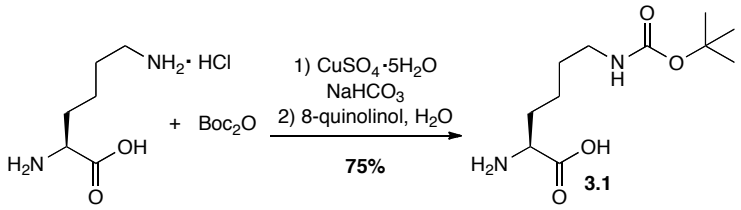

H-Lys(Boc)-OH (3.1).

Into a 250 mL round-bottomed flask was added L-lysine monohydrochloride (3.74 g, 20.5 mmol, 1 equiv) in 1 M aqueous $NaHCO_3$ (41 mL). To this mixture was slowly added $CuSO_4 \cdot 5$ H_2O (2.56 g, 10.25 mmol, 0.5 equiv) followed by solid $NaHCO_3$ (1.72 g, 20.5 mmol). Finally, Boc_2O (5.82 g, 26.7 mmol, 1.3 equiv) in acetone (24.6 mL) was added and the reaction was stirred overnight (ON) at room temperature. The reaction was then quenched with MeOH (6.0 mL) and was stirred for 2 h followed by the addition of H_2O (20 mL) and EtOAc (20 mL). The blue solid was then filtered, washed with H_2O, dried and used immediately in the subsequent reaction.

To a vigorously stirred solution of the intermediate just generated dissolved in H_2O (200 mL) was added 8-quinolinol (3.88 g, 26.7 mmol). The reaction was stirred ON at which time the green suspension was filtered and the solid was washed with H_2O (100 mL) and discarded. The filtrate was washed with DCM (2 × 100 mL), concentrated to a smaller volume by rotary

evaporation, and lyophilized yielding compound **3.1** (3.74 g, 75%) as a fluffy white solid. *See also Notebook XIII, page 38*.[40]

^{1}H NMR: (499.695 MHz, 1:1 D_2O:CD_3OD) δ=1.40 (m, 11H), 1.49 (m, 2H, CH_2) 1.76 (m, 2H, CH_2), 3.04 (t, J = 7 Hz, 2H, CH_2) 3.52 (t, J = J Hz, 1H, CH).

^{13}C NMR: (499.434 MHz, 1:1 D_2O:CD_3OD) δ = 22.4, 27.9, 29.3, 31.8, 40.0, 55.4, 80.1, 158.1, 176.8.

HRMS $[M+Na]^+$ $C_{11}H_{23}N_2O_4^+$ calc'd = 266.9632, found = 266.9642.

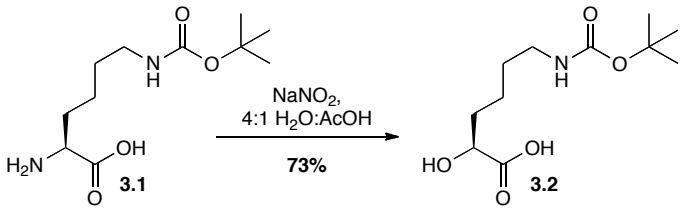

HO-Lys(Boc)-OH (3.2).

Into a 250 mL round-bottomed flask was placed **3.1** (1.4 g, 5.69 mmol) dissolved in 57 mL of 4:1 H_2O:AcOH and the vial was added to a 0 ºC icebath. To this mixture was slowly added sodium nitrite (12 mL, 1 M) via a syringe pump over 30 min. The reaction was stirred for 4 h at room temperature at which point methylamine (40% in H_2O, 0.9 mL) was added and the reaction was stirred for 10 min. The reaction was then acidified with 1 M HCl (until the pH reached 2.5) and product was extracted with EtOAc (3 × 50 mL). The organic layer was dried with $MgSO_4$, filtered, and the filtrate was concentrated via rotary evaporation. To the yellow liquid was added 60% aqueous MeCN/0.1% TFA (2 mL) and this solution was lyophilized to yield **3.2** (1.02 g, 73% yield) as a yellow oil.[41] *See also Notebook XIII, Page 48*. Characterization data matched that previously reported.[42]

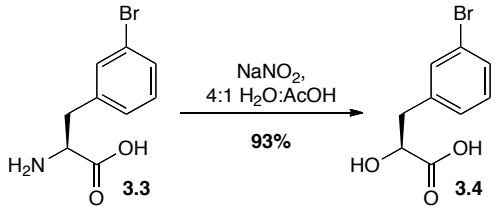

Synthetic design of HO-Phe(3Br)-OH (3.4)

HO-Phe(3Br)-OH (3.4).

Into a 250 mL round-bottomed flask was placed **3.3** (0.8 g, 3.4 mmol) dissolved in 32 mL of 4:1 H_2O:AcOH and the flask was added to a 0 ºC icebath. To this mixture was slowly added sodium nitrite (6.6 mL, 1 M) via a syringe pump over 30 min. The reaction was stirred for 4 h at room temperature at which point methylamine (40% in H_2O, 0.5 mL) was added and the reaction was stirred for 10 min. The reaction was then acidified with 1 M HCl (until the pH reached 2.5) and product was extracted with EtOAc (3 × 50 mL). The organic layer was dried with $MgSO_4$, filtered, and the filtrate was concentrated via rotary evaporation. To the orange liquid was added 60% aqueous MeCN/0.1% TFA (2 mL), which was lyophilized to yield **3.4** (750 mg, 93% yield) as an orange oil. *See also Notebook XIII, Page 47*.[41]

^{1}H NMR: (499.434 MHz, CD_3OD) δ=2.90 (dd, J = 14.0, 8.0 Hz, 1H, CH_2), 3.09 (dd, J = 14.0, 4.0 Hz, 1H, CH_2) 4.35 (m, 1H, CH), 7.16 (m, 1H, CH_{phenyl}) 7.22 (m, 1H, CH_{phenyl}), 7.33 (dt, J = 10.0, 1.8 Hz, 1H, CH_{phenyl}), 7.43 (t, J = 2.5 Hz, 1H, CH_{phenyl}).

^{13}C NMR: (499.434 MHz, CD_3OD) δ = 39.9, 71.2, 122.0, 128.3, 129.5, 129.8, 132.5, 140.4, 175.7.

HRMS $[M+Na]^+$ $C_9H_9BrNaO_3^+$ calc'd = 266.9632, found = 266.9642.

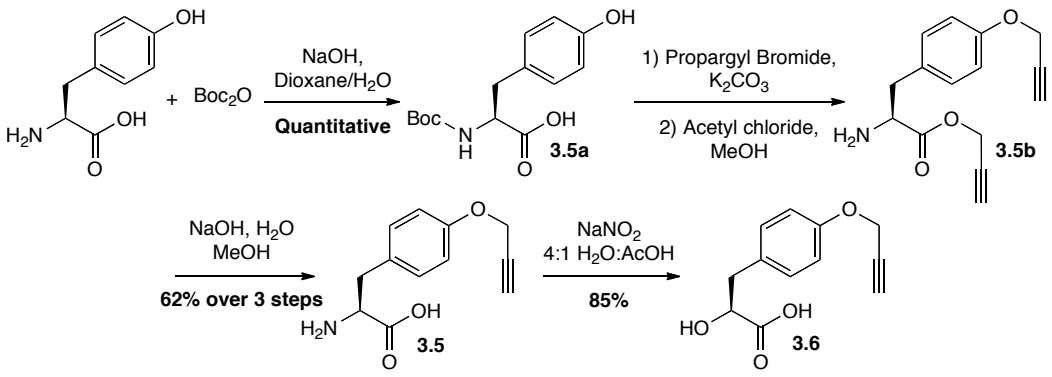

Synthetic design of HO-Tyr(propargyl)-OH (3.6)

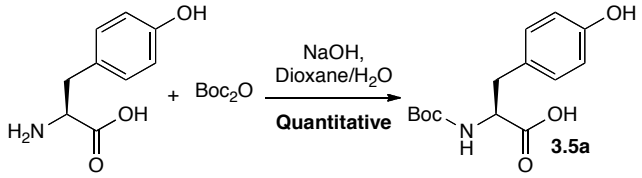

Boc-Tyr-OH (3.5a).

Into a 500 mL round-bottomed flask was placed L-tyrosine (4.0 g, 22.0 mmol, 1 equiv) dissolved in dioxane:H_2O (2:1, 150 mL). To this solution was added aqueous NaOH (1 M, 50 mL) and Boc_2O (5.28 g, 24.2 mmol, 1.1 equiv) sequentially. The reaction was stirred at room temperature for 3 h, acidified to pH 2.3 with 5 M HCl, and product was extracted with EtOAc (3 × 50 mL). The organic layer was washed with sat. aqueous NaCl (50 mL), dried with $MgSO_4$, and concentrated via rotary evaporation yielding **3.5a** (6.18 g, quantitative) as a crystalline white solid. Characterization data matched that previously reported.[43] *See also Notebook XIII, Page 22*.

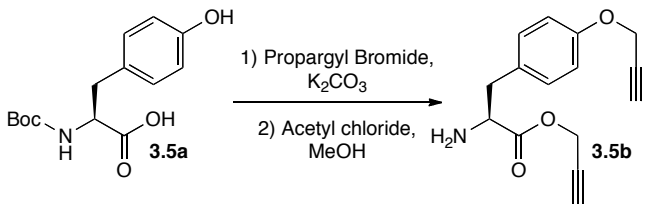

H-Tyr(propargyl)-O-propargyl (3.5b).

Into a 250 mL round-bottomed flask was placed **3.5a** (6.2 g, 22.1 mmol, 1 equiv) and K_2CO_3 (9.16 g, 66.3 mmol, 3.0 equiv) suspended in anhydrous DMF (37 mL). The flask was cooled in a 0 ºC ice bath and propargyl bromide (7.89 g, 5.03 mL, 66.3 mmol, 3 equiv) was added dropwise. The reaction was warmed to room temperature and stirred for 20 h. At this time, H_2O (150 mL) was added and the aqueous layer was extracted with Et_2O (3 × 100 mL). The organic layer was washed with H_2O (100 mL) and sat. aqueous NaCl (2 × 100 mL), dried with $MgSO_4$, and concentrated by rotary evaporation yielding a yellow-orange oil. Characterization data matched that previously reported.[44]

Into a separate 250 mL round-bottomed flask containing anhydrous MeOH (74.6 mL) at 0 ºC was slowly added acetyl chloride (9.54 g, 8.64 mL, 121.6 mmol). This solution was added to the oil isolated above, warmed to room temperature, and stirred for 16 h. All volatile components were removed on a vacuum line yielding **3.5b**, which was immediately used in the subsequent step. *See also Notebook XIII, Page 72.*

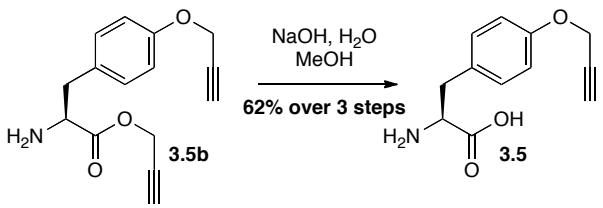

H-Tyr(propargyl)-OH (3.5).

Into a 250 mL round-bottomed was placed intermediate **3.5b** dissolved in MeOH (22 mL) followed by aqueous NaOH (2 M, 32 mL). The reaction was stirred at room temperature for 20 h, acidified to pH 3.0 with concentrated HCl, and cooled at 4 ºC overnight. The following morning a tan precipitate had formed, which was filtered, washed with acidified cold H_2O (pH 3.0), and dried yielding **3.5** (3.0 g, 62% over 3 steps) as a tan solid. Characterization data matched that previously reported.[44] *See also Notebook XII, page 73*.

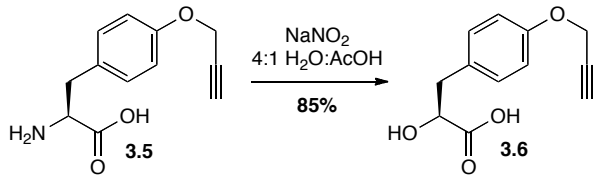

HO-Tyr(propargyl)-OH (3.6).

Into a 250 mL round-bottomed flask was placed **3.5** (2.55 g, 10 mmol) dissolved in 100 mL of 4:1 H_2O:AcOH and the flask was added to a 0 ºC icebath. To this mixture was slowly added sodium nitrite (20 mL, 1 M) via a syringe pump over 30 min. The reaction was stirred for 4 h at room temperature at which point methylamine (40% in H_2O, 1.56 mL) was added and the reaction was stirred for 10 min. The reaction was then acidified with 1 M HCl (until the pH reached 2.5) and product was extracted with EtOAc (3 × 50 mL). The organic layer was dried with $MgSO_4$, filtered, and the filtrate was concentrated via rotary evaporation. To the orange liquid was added 60% aqueous MeCN/0.1% TFA (2 mL), which was lyophilized to yield **3.6**

(2.2 g, 85% yield) as an orange oil. Characterization data matched that previously reported.[44] *See also Notebook XIII, Page 77*.

3.4.3. Construction of plasmids for coexpression.

DNA constructs were assembled by overlap extension PCR, followed either by digestion and ligation or Gibson Assembly of the PCR product into the appropriate plasmid.

Overlap extension PCR.

A 5' gene fragment was amplified by PCR using Phusion High-Fidelity DNA polymerase from a template containing the sequence of interest using a forward primer with the desired restriction site and a reverse primer either incorporating the internal mutation or insertion or beginning at the first nucleotide immediately after the internal mutation or insertion. An overlapping 3' gene fragment was amplified by PCR from the same template using a reverse primer with the desired restriction site and a forward primer incorporating the internal mutation. For primers used, see Table 3.1. Then, a PCR with the overlapping gene fragments and the primers with the desired restriction sites, was used to generate the full-length mutants; the overlapping gene fragments were first added to the PCR mixture and after 8 rounds of amplification the primers with the desired restriction sites were added. After digestion of the mutant gene fragment and the appropriate vector with the desired restriction enzymes, the PCR products containing point mutations, insertions, or deletions were ligated into the plasmid using T4 DNA ligase. Incorporation of the correct mutation into the plasmid DNA was confirmed by sequencing at ACGT, Inc.

General protocol for PCR.

To a 0.2 mL PCR tube was added H_2O (34 μL), buffer HF (10 μL, 5X stock solution, provided with Phusion High-Fidelity DNA polymerase), template (0.5 μL, 100 ng/μL), primers (1 μL each, 100 μM), DMSO (1 μL), dNTPs (1 μL, 10 mM), and Phusion High-Fidelity DNA polymerase (0.5 μL, 2,000 U/mL, NEB). The DNA template was amplified using the following protocol. The reaction was 1) heated to 95 ºC for 2 min; 2) heated at 95 ºC for 30 s; 3) heated at annealing temperature (see individual cases below) for 30 s; 4) heated at 72 ºC for the elongation time (see below); 5) steps 2-4 were repeated for 29 cycles; 6) heated at 72 ºC for 10 min.

Construction of inserts for plasmids pRSFDuet*(lctA(K1tag)/lctM/pylT*) and pRSFDuet*(lctA(A–1I/K1tag)/lctM/pylT*).

The *lctA* mutants were generated in MCS1 of a pRSFDuet vector with *lctM* in MCS2 using pRSFDuet(*lctAwt/lctM*)[16] as template by overlap extension PCR. The primers *lctA EcoRI FMP 5'* and *lctA(K1tag) FMP* (or *A–1I FMP*) *3'* were used to make the 5' overlapping fragment and the primers *lctA(K1tag) RMP* (or *A–1I RMP*) *5'* and *lctA NotI RMP 3'* were used to make the 3' overlapping fragment. The restriction sites were EcoRI and NotI. The annealing temperature was 60 ^{o}C with an elongation time of 20 s. After overlap extension PCR, the inserts were ligated into MCS1 of a pRSFDuet vector as described below.

pylT was amplified by PCR from pEVOL*(pylRS/pylT)* using *pylT AgeI 5'* and *pylT DrdI 3'* as primers and the product was digested using AgeI and DrdI. The gene fragment was then ligated into the *lctA* plasmids from above that had been treated with the same restriction enzymes generating pRSFDuet*(lctA(K1tag)/lctM/pylT)* and pRSFDuet*(lctA(A–1I/K1tag)/lctM/pylT)*.

Construction of inserts for plasmids pRSFDuet*(procA1.1(F1tag)/procM/pylT*) and pRSFDuet*(procA1.1(G–1I/F1tag)/procM/pylT*).

The *procA1.1* mutants were generated in MCS1 of a pRSFDuet vector with *procM* in MCS2. The *procA1.1* inserts were obtained by PCR overlap extension PCR using pET15b(*procA1.1(G–1E))*[26] as template. The primers *procA1.1 EcoRI FMP 5'* and *procA1.1(F1tag) FMP* (or *G–1I FMP*) *3'* were used to make the 5' overlapping fragment and the primers *procA1.1(F1tag) RMP* (or *G–1I RMP*) *5'* and *procA1.1 NotI RMP 3'* were used to make the 3' overlapping fragment. The restriction sites were EcoRI and NotI. The annealing temperature was 60 ^{o}C with an elongation time of 20 s. After overlap extension PCR, the inserts were ligated into MCS1 of a pRSFDuet vector as described below.

pylT was inserted into the pRSFDuet vectors exactly as described for the *lctA* mutants.

Construction of insert for plasmid pRSFDuet*(procA1.6(G–1I/K1tag)/procM/pylT)*.

The *procA1.6* mutant was generated in MCS1 of a pRSFDuet vector with *procM* in MCS2. The *procA1.6* insert was obtained by overlap extension PCR using pET15b(*procA1.6(G–1R)*) (unpublished work from our laboratory) as template. The primers *procA1.6 EcoRI FMP 5'* and *procA1.6(G–1I/K1tag) FMP 3'* were used to make the 5' overlapping fragment and the primers *procA1.6(G–1I/K1tag) RMP 5'* and *procA1.6 NotI RMP 3'* were used to make the 3' overlapping fragment. The restriction sites were EcoRI and NotI. The annealing temperature was 60 ^{o}C with an elongation time of 20 s. After overlap extension PCR, the insert was ligated into MCS1 of a pRSFDuet vector as described below.

Construction of inserts for plasmids pRSFDuet*(lctNukA)/lctM/pylT)* and pRSFDuet*(lctNukA(A–1I/K1tag)/lctM/pylT).*

lctNukA was amplified by PCR from pET15b*(lctNukA)*[24] using *lctNukA Gibson 5'* and *lctNukA Gibson 3'* as primers. The gene fragment was then ligated by Gibson Assembly into MCSI of pRSFDuet*(lctA(K1tag)/lctM/pylT)*, which had been treated with EcoRI and NotI, producing pRSFDuet*(lctNukA)/lctM/pylT)*. The annealing temperature was 58 ^{o}C with an elongation time of 20 s.

The *lctNukA(A–1I/K1tag)* mutant was generated using pET15b*(lctNukA)* as template by overlap extension PCR and ligated into MCS1 of pRSFDuet*(lctA(K1tag)/lctM/pylT)* by Gibson Assembly. The primers *lctNukA Gibson 5'* and *lctNukA(A–1I/K1tag) FMP 3'* were used to make the 5' overlapping fragment and the primers *lctNukA(A–1I/K1tag) RMP 5'* and *lctNukA Gibson 3'* were used to make the 3' overlapping fragment. The parent plasmid was treated with EcoRI and NotI. The annealing temperature was 58 ^{o}C with an elongation time of 20 s.

Table 3.1. Primers used in molecular cloning.

lctA EcoRI FMP 5':	CCT CTG GCG GAT CCG AAT TCG ATG AAA TGA AAG AAC AAA AC
lctA(K1tag) FMP 3':	CTT ATT TTA GGT GCA TAG GGC GGC AGT GGA GTT
lctA(K1tag) RMP 5':	AAC TCC ACT GCC GCC CTA TGC ACC TAA AAT AAG
lctA(A–1I/K1tag FMP 3':	TCC ACT GCC GCC CTA AAT ACC TAA AAT AAG G
lctA(A–1I/K1tag RMP 5':	CCT TAT TTT AGG TAT TTA GGG CGG CAG TGG A
lctA NotI RMP 3':	CGG TTA AAG CGG CCG CTT AAG AGC AGC AAG TAA ATA C
procA1.1 EcoRI FMP 5':	GGT GAG TGG AAT TCG ATG AAA AAG CGA CTC AAC
procA1.1(G–1I/F1tag) FMP 3':	CTG CAC ACA GAA CTA AAT CCC AGC CAC ACC T
procA1.1(G–1I/F1tag) RMP 5':	AGG TGT GGC TGG GAT TTA GTT CTG TGT GCA G
procA1.1 NotI RMP 3':	AAT AAA TAT GCG GCC GCT CAG CAC ACA TTG ATA GT
procA1.6 EcoRI FMP 5':	GGT GAG TGG AAT TCG ATG ATG TCA GAA GAA CAA CTC
procA1.6(K1tag) FMP 3':	CAT CCA TTA GTA GAC TAA CCG CCA GCT ACA CCT TC
procA1.6(K1tag) RMP 5':	GAA GGT GTA GCT GGC GGT TAG TCT ACT AAT GGA TG
procA1.6(G–1I/K1tag) FMP 3':	CAT CCA TTA GTA GAC TAA ATG CCA GCT ACA CCT TC
procA1.6(G–1I/K1tag) RMP 5':	GAA GGT GTA GCT GGC ATT TAG TCT ACT AAT GGA TG
procA1.6 NotI RMP 3':	AAT AAA TAT GCG GCC GCT CAC AGC CAA CAC TCT AG
pylT AgeI 5':	GAG TAT GAA CCG GTT GTG CTT CTC AAA TGC CTG A
pylT DrdI 3':	GTA CTG AGA GAC AGT CTA GTC CAT GCA AAA AAG CCT GCT C
lctNukA Gibson 5'	CAC AGC CAC AGC CAG GAT CCG ATG AAA GAA CAA AAC TCT TTT AAT C
lctNukA Gibson 3'	CGA CTT AAG CAT TAT GCT TAT GAA CAA CAA GTA AAT ACA AAT TG
lctNukA(A–1I/K1tag) FMP 3'	GAT TAC TCC TGA CTT TTT CTA AAT ACC TAA AAT AAG GTC C
lctNukA(A–1I/K1tag) RMP 5'	GGA CCT TAT TTT AGG TAT TTA GAA AAA GTC AGG AGT AAT C

Digestion of plasmids and DNA inserts.

To a 1.7 mL Eppendorf tube with insert or plasmid DNA (40 μL, 100-250 ng/μL) was added digestion buffer (5 μL; NEB, provided with the restriction enzymes), digestion enzyme(s) (1.5 μL, concentrations are below), BSA (if necessary, 0.5 μL, 100X, provided with digestion enzyme), and H_2O (to 50 μL). The components were incubated at 37 ^oC for 2-4 h. At this time calf intestine phosphatase (CIP) (1 μL) was added to plasmid DNA only and the sample was incubated for an additional 1 h. The samples were then analyzed by DNA gel electrophoresis and the desired band was purified by a QIAGEN Gel Extraction kit eluting in buffer EB (30 μL).

Note: Both digestion enzymes were added in one single digest if the buffer was compatible. If buffer was not compatible, two successive digests were performed.

NotI = 10,000 U/mL, EcoRI = 20,000 U/mL, AgeI = 5000 U/mL, DrdI = 5000 U/mL, CIP = 10,000 U/mL.

Ligation of digested plasmid and DNA insert.

To three 0.6 mL Eppendorf tubes was added plasmid DNA (1 μL, 100 ng/μL). Insert DNA (1 μL of a solution of different concentrations to give a ratio of plasmid to insert of 1:1, 1:10 and 1:100) was then added as well as T4 DNA ligase reaction buffer (0.7 μL, provided with the ligation enzyme), T4 DNA ligase (0.8 μL, 400,000 cohesive end U/mL), and H_2O (to 5 μL). The samples were incubated at 18 ^oC for 16-20 h at which time the entire reactions were used to transform *E. coli* DH5α cells.

Gibson Assembly.

To a 0.6 mL Eppendorf tube was added plasmid DNA (1 μL, 25 ng/μL), insert DNA (equal mol amount), Gibson Assembly Mastermix (2.5 μL, NEB), and H_2O (to 5 μL). The samples were incubated at 18 ºC for 1 h at which time the entire reaction was used to transform *E. coli* DH5α cells.

3.4.4. Heterologous production, purification, and characterization of LanA analogues.

The lanthipeptides were expressed using *E. coli* BL21 (DE3) cells transformed with a pRSFDuet plasmid containing the *lanA*, *lanM,* and *pylT* genes and a pEVOL plasmid containing the *pylRS* (2 copies of either wt or N346A/C348A mutant) and *pylT* genes. For production of Δ1-

lacticin 481 and Δ1-3-nukacin ISK1 only the pRSFDuet plasmid was used because non-canonical amino or hydroxy acid was not incorporated. All coexpression cultures were incubated at 18 ºC ON after induction with IPTG except for the coexpression cultures in which **3.1**-**3.6** were incorporated into LctA, which were incubated at 37 ºC for 4 h after induction. Composition of 1 L enriched LB: 35 g tryptone, 20 g yeast extract, 5 g NaCl. Composition of 25 mL minimal media with supplements: 5X minimal media (5 mL), glycerol (20%, 1.25 mL, 1% final concentration), $MgSO_4$ (1 M, 50 μL), $CaCl_2$ (1 M, 2.5 μL), NaCl (20%, 250 μL), all amino acid solution except Phe, Tyr, and Cys (5 mg/mL, 1 mL), and H_2O (to 25 mL).

Overexpression and purification of His_6-tagged modified peptide mutants.

An overnight culture of *E. coli* BL21 (DE3) cells was added to a culture flask containing either enriched LB (35 g tryptone, 20 g yeast extract, 5 g NaCl), LB broth, or minimal media (1:100; volume overnight culture: volume overexpression culture for rich media; 1:20 for minimal media) and appropriate antibiotics depending on the plasmids used (1:1000 v:v; kanamycin (50 mg/mL), chloramphenicol (25 mg/mL)). The culture was then incubated in a 37 ºC shaker (220 rpm) until the optical density reached 1.0 (enriched LB), 0.6 (LB) or 0.3 (minimal media). For LctA and LctNukA, overexpression was immediately induced with arabinose (0.2% final concentration) and isopropyl β-D-1-thiogalactopyranoside (IPTG, 0.25 mM final concentration) in the presence of non-proteinogenic amino or hydroxy acid (2 mM final concentration) and the flask was incubated for 4 h in a shaker at 37 ºC and 220 rpm. Conversely, for ProcA1.1 and ProcA1.6, the culture was first placed on ice (5 min) to cool to around 30 ºC. Overexpression was then induced by the addition of arabinose and IPTG in the presence of non-proteinogenic amino or hydroxy acid and the flask was incubated overnight in a shaker at 30 ºC

and 220 rpm. The following morning the cells were harvested by centrifugation (11,867 ×*g*, 4 ºC, 20 min), the supernatant was discarded and the cells were lysed using a cell homogenizer (Avestin Emulsiflex-C3; 5,000 PSI) in LanA start buffer (2 mL per 100 mL culture; 20 mM NaH_2PO_4, 500 mM NaCl, 0.5 mM imidazole, 20% glycerol, pH 7.5). The soluble and insoluble layers were then separated by centrifugation (22,789 ×*g*, 4 ^oC, 20 min) and the soluble layer was saved for purification. The insoluble layer was suspended in LanA lysis buffer (1 mL per 100 mL culture; 6 M guanidine HCl, 20 mM NaH_2PO_4, pH 7.5, 500 mM NaCl, 0.5 mM imidazole) and the suspension was sonicated. The soluble and insoluble layers were again separated by centrifugation (22,789 ×*g*, 4 ^oC, 20 min) and the modified His_6-LanA peptide was purified from the combined soluble layers using a Ni HisTrap HP column (5 mL, GE Healthcare). The column was washed with LanA wash buffer (4 M guanidine-HCl, 20 mM NaH_2PO_4, pH 7.5, 500 mM NaCl, 30 mM imidazole) to remove non-specific binding proteins. The His_6-LanA peptide was eluted with LanA elute buffer (3 × 5 mL, 20 mM NaH_2PO_4, 100 mM NaCl, 500 mM imidazole, pH 7.5). Finally, the peptide was further purified by preparative reversed phase high-performance liquid chromatography (RP-HPLC) and lyophilized.

GluC cleavage of LctA(K1*tag*) and LctA(A–1/K1*tag*) incorporating 3.1, 3.3, or 3.5.

To lyophilized peptide was added HEPES buffer (500 µL, pH 7.5, 50 mM final concentration) and GluC (1 µL, 2 mg/mL). The reaction was incubated for 2 h at 37 ºC. The reaction was analyzed by MALDI-TOF MS.

Boc removal of LctA(A–1I) and nukacin ISK-1 incorporating 3.2.

To RP-HPLC purified and lyophilized peptide was added aqueous 5% TFA (2 mL). The reaction was incubated for 4 h at 50 ºC. The peptidic solution was then concentrated by purging with a nitrogen stream and used in the alkaline hydrolysis reaction without further purification.

Alkaline hydrolysis of 3.2-, 3.4-, and 3.6-LctA(A–1I) and 3.2-nukacin ISK-1.

To the concentrated peptide solution from the Boc-removal reaction or RP-HPLC purified and lyophilized peptide, was added CAPS buffer (4 mL, 250 mM, pH 10.5) and 1 M NaOH (until pH reached 10.5). The reaction was incubated for 2 h at 37 ºC and purified by preparative RP-HPLC on a C18 column (solvent A = 0.1% TFA in H_2O; solvent B = 80% acetonitrile in H_2O, 0.086% TFA). Fractions containing product were collected and lyophilized.

Isolation of authentic lacticin 481.

Lactococcus lactis subsp. *lactis* CNRZ 481 was grown for 9 h at 30 ºC in EG'P media (1.74 L, Elliker broth medium without gelatin) supplemented with sodium β-glycerophosphate (26.1 g, (15 g/L)) maintaining the culture pH at 5.5 by adding aliquots of 3 M ammonium hydroxide every hour. After 9 h the pH was again adjusted to 5.5 and cells were removed by centrifugation (11,900 × g, 20 min). The culture supernatant was heat-treated (80 ºC, 1 h) to deactivate proteases, cooled to 4 ºC, and the lantibiotic was concentrated with an ammonium sulfate precipitation step, saturating the solution at 60% at 4 ^{o}C (649.4 g of ammonium sulfate into 1.74 L culture supernatant). The sample was vigorously stirred for 4 h and then centrifuged (17,100 × g, 45 min, 4 ºC). After resuspension of the pellet in Sorensen buffer (20 mL, 176 mM NaH_2PO_4, 24 mM Na_2HPO_4, pH 6.0), lacticin 481 was further purified by solid phase extraction

using a Vydac 214SPE3000 C4 column, with 20 mM ammonium acetate and MeCN as eluting solvents. After addition of the lantibiotic solution, the column was washed with 20 mM ammonium acetate and 20 mM ammonium acetate with 30% MeCN. Peptide was then eluted with 20 mM ammonium acetate with 40% MeCN. The fraction containing product was concentrated by lyophilization and further purified by analytical RP-HPLC (Grace Vydac C18 column (214TP54)) using a gradient from 30-40% MeCN in 20 mM ammonium acetate, pH 5.5, over 30 min. The combined fractions were lyophilized yielding 6 mg of impure lacticin 481.

RP-HPLC purification of lacticin 481 isolated from *L. lactis* subsp. *lactis* 481.

To the lyophilized impure lacticin 481 (2 mg) from above was added H_2O (4 mL) and the peptide was purified by preparative RP-HPLC on a C18 column (solvent A = 0.1% TFA in H_2O; solvent B = 80% acetonitrile in H_2O, 0.086% TFA). Product eluted from 26.5-27.0 min yielding 300 μg of pure lacticin 481. This peptide was then used for MIC studies.

Purification and yield of LanA analogues produced in large scale.

His_6-LctA. RP-HPLC: R_t = 29.0-34.0 min (C4, Waters Delta-pak™).

3.2-LctA(A–1I). RP-HPLC: R_t = 32.7-35.7 min (C4, Waters Delta-pak™).

3.4-LctA(A–1I). RP-HPLC: R_t = 34.0-37.0 min (C4, Waters Delta-pak™).

3.6-LctA(A–1I). RP-HPLC: R_t = 31.0-36.0 min (C4, Waters Delta-pak™).

His_6-LctNukA. RP-HPLC: R_t = 28.0-33.0 min (C4, Waters Delta-pak™).

3.2-NukLctA (A–1I). RP-HPLC: R_t = 28.0-35.0 min (C4, Waters Delta-pak™).

Δ1-lacticin 481. Yield: 0.16 mg/L culture; RP-HPLC: R_t = 27.9-28.3 min (C18, Phenomenex).

HO-lacticin 481. Yield: 0.10 mg/L culture; RP-HPLC: R_t = 27.2-28.2 min (C18, Phenomenex).

3.4-HO-lacticin 481. Yield: 0.04 mg/L culture; RP-HPLC: R_t = 31.8-32.3 min (C18, Phenomenex).

3.6-HO-lacticin 481. Yield: 0.045 mg/L culture; RP-HPLC: R_t = 30.4-31.0 min (C18, Phenomenex).

Δ1-3-nukacin ISK-1. Yield: 0.07 mg/L culture; RP-HPLC: R_t = 24.9-25.4 min (C18, Phenomenex)

HO-nukacin ISK-1. Yield: 0.05 mg/L culture; RP-HPLC: R_t = 22.8-23.4 min (C18, Phenomenex)

Minimum inhibitory concentration determination.

Ninety six-well microtiter plates (Corning Costar) were utilized for anaerobic cultures. Each well contained 90 μL of an overnight culture containing *L. lactis* HP (approximately 1×10^8 CFU mL^{-1}) and a 10x stock of peptide (10 μL) of the desired concentration. The plates were incubated at 30 ºC overnight with no agitation. In addition, each plate contained several blank (growth media with no bacteria) and control (SDW in place of peptide) wells. The optical density at 600 nm (OD_{600}) was recorded at hourly intervals from 0-8 h for nukacin ISK-1 analogues and after 16 h for lacticin 481 analogues. The MIC was determined as the lowest concentration at which no cell growth was observed after 16-18 h.

3.5. REFERENCES

(1) You, Y. O.; van der Donk, W. A., Mechanistic investigations of the dehydration reaction of lacticin 481 synthetase using site-directed mutagenesis, *Biochemistry* **2007**, *46*, 5991.

(2) Levengood, M. R.; Knerr, P. J.; Oman, T. J.; van der Donk, W. A., In vitro mutasynthesis of lantibiotic analogues containing nonproteinogenic amino acids, *J. Am. Chem. Soc.* **2009**, *131*, 12024.

(3) Bindman, N.; Merkx, R.; Koehler, R.; Herrman, N.; van der Donk, W. A., Photochemical cleavage of leader peptides, *Chem. Commun.* **2010**, *46*, 8935.

(4) Nagao, J.; Harada, Y.; Shioya, K.; Aso, Y.; Zendo, T.; Nakayama, J.; Sonomoto, K., Lanthionine introduction into nukacin ISK-1 prepeptide by co-expression with modification enzyme NukM in *Escherichia coli*, *Biochem. Biophys. Res. Commun.* **2005**, *336*, 507.

(5) Shi, Y.; Yang, X.; Garg, N.; van der Donk, W. A., Production of lantipeptides in *Escherichia coli*, *J. Am. Chem. Soc.* **2011**, *133*, 2338.

(6) England, P. M.; Lester, H. A.; Davidson, N.; Dougherty, D. A., Site-specific, photochemical proteolysis applied to ion channels in vivo, *Proc. Natl. Acad. Sci. U. S. A.* **1997**, *94*, 11025.

(7) Fahnestock, S.; Rich, A., Ribosome-catalyzed polyester formation, *Science* **1971**, *173*, 340.

(8) England, P. M.; Lester, H. A.; Dougherty, D. A., Mapping disulfide connectivity using backbone ester hydrolysis, *Biochemistry* **1999**, *38*, 14409.

(9) Watanabe, T.; Miyata, Y.; Abe, R.; Muranaka, N.; Hohsaka, T., N-terminal specific fluorescence labeling of proteins through incorporation of fluorescent hydroxy acid and subsequent ester cleavage, *ChemBioChem* **2008**, *9*, 1235.

(10) Koh, J. T.; Cornish, V. W.; Schultz, P. G., An experimental approach to evaluating the role of backbone interactions in proteins using unnatural amino acid mutagenesis, *Biochemistry* **1997**, *36*, 11314.

(11) Tan, Z.; Forster, A. C.; Blacklow, S. C.; Cornish, V. W., Amino acid backbone specificity of the *Escherichia coli* translation machinery, *J. Am. Chem. Soc.* **2004**, *126*, 12752.

(12) Ellman, J. A.; Mendel, D.; Schultz, P. G., Site-specific incorporation of novel backbone structures into proteins, *Science* **1992**, *255*, 197.

(13) Srinivasan, G.; James, C. M.; Krzycki, J. A., Pyrrolysine encoded by UAG in Archaea: charging of a UAG-decoding specialized tRNA, *Science* **2002**, *296*, 1459.

(14) Kobayashi, T.; Yanagisawa, T.; Sakamoto, K.; Yokoyama, S., Recognition of non-alpha-amino substrates by pyrrolysyl-tRNA synthetase, *J. Mol. Biol.* **2009**, *385*, 1352.

(15) Xie, L.; Miller, L. M.; Chatterjee, C.; Averin, O.; Kelleher, N. L.; van der Donk, W. A., Lacticin 481: In vitro reconstitution of lantibiotic synthetase activity, *Science* **2004**, *303*, 679.

(16) Oman, T. J.; Knerr, P. J.; Bindman, N. A.; Velasquez, J. E.; van der Donk, W. A., An engineered lantibiotic synthetase that does not require a leader peptide on its substrate, *J. Am. Chem. Soc.* **2012**, *134*, 6952.

(17) Young, T. S.; Ahmad, I.; Yin, J. A.; Schultz, P. G., An enhanced system for unnatural amino acid mutagenesis in *E. coli*, *J. Mol. Biol.* **2010**, *395*, 361.

(18) Yanagisawa, T.; Ishii, R.; Fukunaga, R.; Kobayashi, T.; Sakamoto, K.; Yokoyama, S., Multistep engineering of pyrrolysyl-tRNA synthetase to genetically encode N(epsilon)-(o-azidobenzyloxycarbonyl) lysine for site-specific protein modification, *Chem. Biol.* **2008**, *15*, 1187.

(19) Blight, S. K.; Larue, R. C.; Mahapatra, A.; Longstaff, D. G.; Chang, E.; Zhao, G.; Kang, P. T.; Green-Church, K. B.; Chan, M. K.; Krzycki, J. A., Direct charging of tRNA(CUA) with pyrrolysine in vitro and in vivo, *Nature* **2004**, *431*, 333.

(20) Yanagisawa, T.; Ishii, R.; Fukunaga, R.; Kobayashi, T.; Sakamoto, K.; Yokoyama, S., Crystallographic studies on multiple conformational states of active-site loops in pyrrolysyl-tRNA synthetase, *J. Mol. Biol.* **2008**, *378*, 634.

(21) Reshetnikova, L.; Moor, N.; Lavrik, O.; Vassylyev, D. G., Crystal structures of phenylalanyl-tRNA synthetase complexed with phenylalanine and a phenylalanyl-adenylate analogue, *J. Mol. Biol.* **1999**, *287*, 555.

(22) Wang, Y. S.; Fang, X.; Chen, H. Y.; Wu, B.; Wang, Z. U.; Hilty, C.; Liu, W. R., Genetic incorporation of twelve meta-substituted phenylalanine derivatives using a single pyrrolysyl-tRNA synthetase mutant, *ACS Chem. Biol.* **2013**, *8*, 405.

(23) Wang, Y. S.; Fang, X.; Wallace, A. L.; Wu, B.; Liu, W. R., A rationally designed pyrrolysyl-tRNA synthetase mutant with a broad substrate spectrum, *J. Am. Chem. Soc.* **2012**, *134*, 2950.

(24) Patton, G. C.; Paul, M.; Cooper, L. E.; Chatterjee, C.; van der Donk, W. A., The importance of the leader sequence for directing lanthionine formation in lacticin 481, *Biochemistry* **2008**, *47*, 7342.

(25) Asaduzzaman, S. M.; Nagao, J.; Aso, Y.; Nakayama, J.; Sonomoto, K., Lysine-oriented charges trigger the membrane binding and activity of nukacin ISK-1, *Appl. Environ. Microbiol.* **2006**, *72*, 6012.

(26) Li, B.; Sher, D.; Kelly, L.; Shi, Y.; Huang, K.; Knerr, P. J.; Joewono, I.; Rusch, D.; Chisholm, S. W.; van der Donk, W. A., Catalytic promiscuity in the biosynthesis of cyclic peptide secondary metabolites in planktonic marine cyanobacteria, *Proc. Natl. Acad. Sci. U.S.A.* **2010**, *107*, 10430.

(27) Tang, W.; van der Donk, W. A., Structural characterization of four prochlorosins: a novel class of lantipeptides produced by planktonic marine cyanobacteria, *Biochemistry* **2012**, *51*, 4271.

(28) Bindman, N. A.; van der Donk, W. A., A general method for fluorescent labeling of the N-termini of lanthipeptides and its application to visualize their cellular localization, *J. Am. Chem. Soc.* **2013**, *135*, 10362.

(29) Siegele, D. A.; Hu, J. C., Gene expression from plasmids containing the araBAD promoter at subsaturating inducer concentrations represents mixed populations, *Proc. Natl. Acad. Sci. U. S. A.* **1997**, *94*, 8168.

(30) Garg, N.; Tang, W.; Goto, Y.; van der Donk, W. A., Geobacillins: lantibiotics from *Geobacillus thermodenitrificans*, *Proc. Natl. Acad. Sci. U. S. A.* **2012**, *109*, 5241.

(31) Lin, Y.; Teng, K.; Huan, L.; Zhong, J., Dissection of the bridging pattern of bovicin HJ50, a lantibiotic containing a characteristic disulfide bridge, *Microbiol. Res.* **2011**, *166*, 146.

(32) Shi, Y.; Bueno, A.; van der Donk, W. A., Heterologous production of the lantibiotic Ala(0)actagardine in *Escherichia coli*, *Chem. Commun.* **2012**, *48*, 10966.

(33) Ökesli, A.; Cooper, L. E.; Fogle, E. J.; van der Donk, W. A., Nine post-translational modifications during the biosynthesis of cinnamycin, *J. Am. Chem. Soc.* **2011**, *133*, 13753.

(34) Wang, J.; Gao, Y.; Teng, K.; Zhang, J.; Sun, S.; Zhong, J., Restoration of a bioactive lantibiotic suicin from a remnant lan locus of pathogenic Streptococcus suis serotype 2, *Appl. Environ. Microbiol.* **2013**.

(35) Velásquez, J. E.; Zhang, X.; van der Donk, W. A., Biosynthesis of the antimicrobial peptide epilancin 15X and its unusual N-terminal lactate moiety, *Chem. Biol.* **2011**, *18*, 857.

(36) van de Kamp, M.; van den Hooven, H. W.; Konings, R. N.; Bierbaum, G.; Sahl, H. G.; Kuipers, O. P.; Siezen, R. J.; de Vos, W. M.; Hilbers, C. W.; van de Ven, F. J., Elucidation of the primary structure of the lantibiotic epilancin K7 from *Staphylococcus epidermidis* K7. Cloning and characterisation of the epilancin-K7-encoding gene and NMR analysis of mature epilancin K7, *Eur. J. Biochem.* **1995**, *230*, 587.

(37) Scolnick, E.; Tompkins, R.; Caskey, T.; Nirenberg, M., Release factors differing in specificity for terminator codons, *Proc. Natl. Acad. Sci. U. S. A.* **1968**, *61*, 768.

(38) Huang, Y.; Russell, W. K.; Wan, W.; Pai, P. J.; Russell, D. H.; Liu, W., A convenient method for genetic incorporation of multiple noncanonical amino acids into one protein in *Escherichia coli*, *Mol. BioSyst.* **2010**, *6*, 683.

(39) Johnson, D. B.; Xu, J.; Shen, Z.; Takimoto, J. K.; Schultz, M. D.; Schmitz, R. J.; Xiang, Z.; Ecker, J. R.; Briggs, S. P.; Wang, L., RF1 knockout allows ribosomal incorporation of unnatural amino acids at multiple sites, *Nat. Chem. Biol.* **2011**, *7*, 779.

(40) Weijak, S.; Masiukiewicz, E.; Rzeszotarska, B., Large scale synthesis of mono- and di-urethane derivatives of lysine, *Chem. Pharm. Bull.* **1999**, *47*, 1489.

(41) Deechongkit, S.; You, S. L.; Kelly, J. W., Synthesis of all nineteen appropriately protected chiral alpha-hydroxy acid equivalents of the alpha-amino acids for Boc solid-phase depsi-peptide synthesis, *Org. Lett.* **2004**, *6*, 497.

(42) Li, Y. M.; Yang, M. Y.; Huang, Y. C.; Li, Y. T.; Chen, P. R.; Liu, L., Ligation of expressed protein alpha-hydrazides via genetic incorporation of an alpha-hydroxy acid, *ACS Chem. Biol.* **2012**, *7*, 1015.

(43) Zakharova, V. M.; Serpi, M.; Krylov, I. S.; Peterson, L. W.; Breitenbach, J. M.; Borysko, K. Z.; Drach, J. C.; Collins, M.; Hilfinger, J. M.; Kashemirov, B. A.; McKenna, C. E., Tyrosine-based 1-(S)-[3-hydroxy-2-(phosphonomethoxy)propyl]cytosine and -adenine ((S)-

HPMPC and (S)-HPMPA) prodrugs: synthesis, stability, antiviral activity, and in vivo transport studies, *J. Med. Chem.* **2011**, *54*, 5680.

(44) Zhang, Z.; Yin, L.; Xu, Y.; Tong, R.; Lu, Y.; Ren, J.; Cheng, J., Facile functionalization of polyesters through thiol-yne chemistry for the design of degradable, cell-penetrating and gene delivery dual-functional agents, *Biomacromolecules* **2012**, *13*, 3456.

Chapter 4: A General Method for Fluorescent Labeling of the N-termini of Lanthipeptides and Its Application to Visualize their Cellular Localization

Reprinted (adapted) with permission from Bindman and van der Donk, *J. Am. Chem. Soc.*, **2013**, 135 (28), 10362-10371. [1]

4.1. INTRODUCTION

Currently, the mode(s) of action of only a small subset of lantibiotics has been deduced, including the best studied family member nisin. Labeling of natural products with biophysical probes has aided investigations of their modes of action and has provided tools for visualization of their targets. For instance, fluorescent microscopy studies with fluorescently labeled nisin has greatly contributed to understanding its mechanism of action.[2] Site-specific labeling of nisin was possible because it contains only a single carboxylate (the C-terminus). However, for most lantibiotics/lanthipeptides, no such chemoselective handle for convenient modification is available because they contain multiple reactive groups, and hence to date, biophysical labeling studies of lanthipeptides have been limited. For instance, labeling of the lanthipeptides duramycin and nukacin ISK-1 with amine-reactive probes resulted in labeling of at least two positions.[3,4] Similarly, most lanthipeptides contain multiple dehydroamino acids, and therefore the use of Michael-type additions to introduce biophysical probes[5] would also result in multiple sites of labeling. In recent years, complete chemical synthesis of lantibiotics on a solid support has been reported[6-8] and could potentially be a viable route to lanthipeptides carrying biophysical probes, but such an application has not been reported to date and would not be a source of renewable materials. Therefore, development of a general means to label lantibiotics while only

minimally affecting their bioactivities would aid the investigation of this large and promising class of compounds.[9,10]

One approach that might allow site specific labeling of either the N- or C-termini of lanthipeptides involves removal of any Lys, or Asp and Glu residues. Indeed, because of their ribosomal origin, site directed mutagenesis has been applied extensively to lanthipeptides and generally (but not always) does not affect the posttranslational modification process.[11-14] Unfortunately, Lys and Asp/Glu residues have been shown to be very important for the activities of many lantibiotics,[15-23] rendering this approach ineffective for most applications.

Many site-specific peptide- and protein-labeling techniques have emerged in recent years that use either chemical or enzymatic methods to introduce chemical handles for derivatization.[24] For most enzymatic approaches, a peptide tag is incorporated into a protein or peptide of interest at the gene level.[25-29] Through site-specific enzymatic modification of the tag, a reactive chemical functionality is introduced that may be used for a 'bioorthogonal' conjugation with a reporter molecule carrying a suitable complementary functionality. The termini of peptides and proteins have been particularly attractive for the incorporation of chemical probes because it generally minimizes undesired effects of the probe on function.[30-34] Many of these labeling strategies have incorporated a ketone or aldehyde into a peptide or protein of interest followed by bioconjugation with an aminooxy-, hydrazine-, or alkoxyamine-containing biophysical probe.[25,35-37] These reactions are chemoselective with respect to most peptides and proteins because the twenty canonical amino acids do not contain reactive carbonyl groups. However, introduction of a peptide tag at the N- or C-terminus of a lanthipeptide is still a considerable perturbation in structure because lanthipeptides are typically only 20-25 amino acids in length. Interestingly, an N-terminal ketone (2-oxobutyryl or pyruvyl) is a naturally occurring post-

translational modification in some lanthipeptides, including Pep5,[38] plantaracin-W β,[39] and prochlorosin 1.7 (Pcn1.7; Figure 4.1).[40] The N-terminal ketone arises from a dehydrated Ser/Thr at position 1 of the core peptide. After proteolytic removal of the leader peptide, the N-terminal dehydro amino acid hydrolyzes to an α-ketoamide (Scheme 4.1). We hypothesized that such a ketone handle could be used to site-specifically label this subset of lanthipeptides with minimal perturbation, and that a similar approach might be used for the installation of a 2-oxobutyryl group onto the N-termini of lanthipeptides that naturally lack this functionality. We demonstrate here that this methodology is successful for prochlorosins 1.7 and 2.8, nisin, lacticin 481, haloduracin α, and haloduracin β (for structures, see Figures 4.1 & 4.2). The resulting ketones of the latter three compounds were conjugated to a fluorescent probe, and the distribution of the fluorescent lantibiotic analogues in bacteria was visualized by confocal fluorescence microscopy.

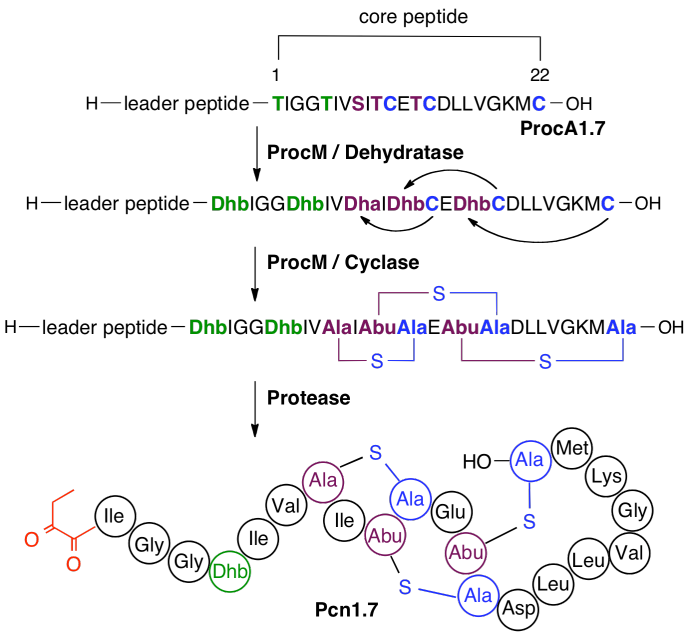

Figure 4.1. Biosynthesis of Pcn1.7 with its naturally occurring N-terminal 2-oxobutyryl group (red). For the sequence of the leader peptide, see Figure 4.4. Scheme adapted from Bindman and van der Donk.[1]

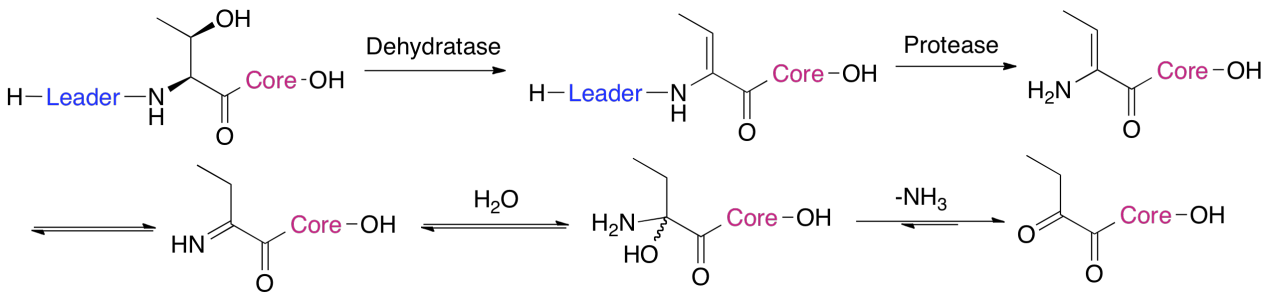

Scheme 4.1. Proposed installation of an N-terminal 2-oxobutyryl group. Dehydration of a Thr at the N-terminus of the core peptide followed by proteolysis yields the core peptide with an N-terminal enamine. In aqueous conditions the enamine spontaneously converts to a 2-oxobutyryl group. Scheme adapted from Bindman and van der Donk.[1]

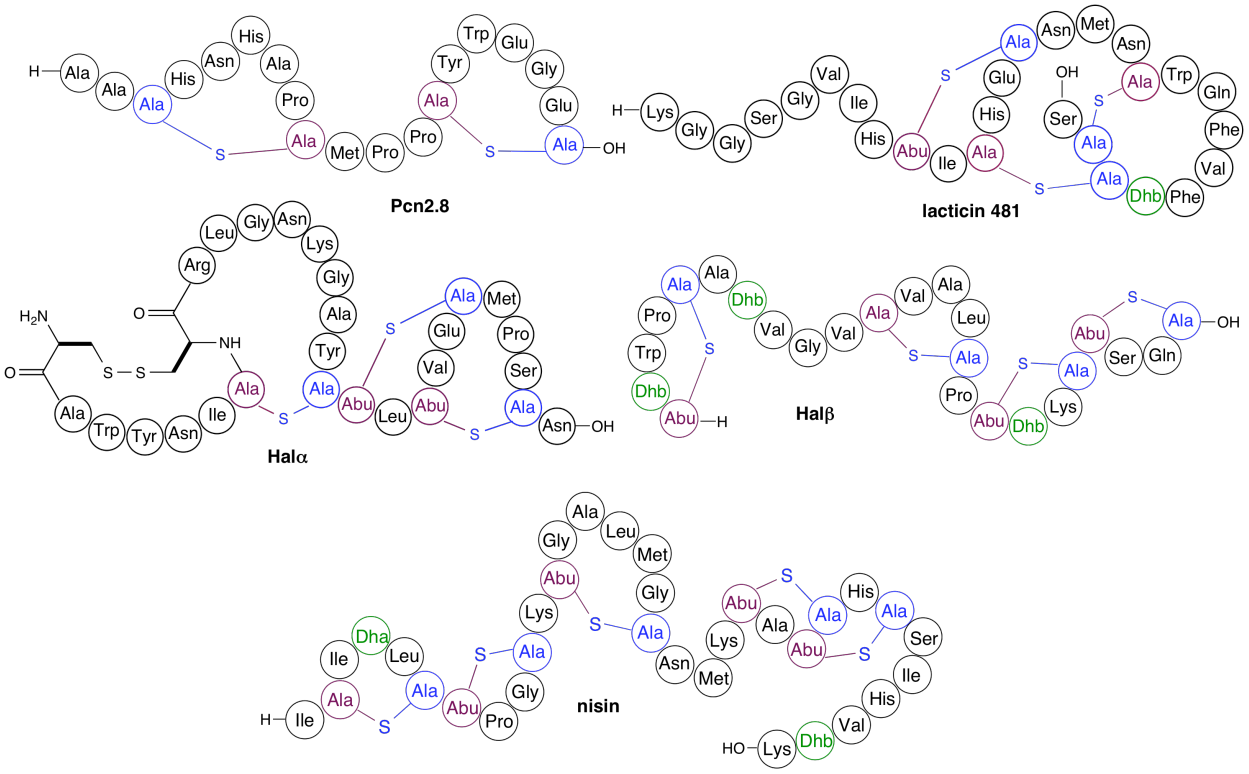

Figure 4.2. Structures of the lanthipeptides Pcn2.8, lacticin 481, Halα, Halβ, and nisin. Scheme adapted from Bindman and van der Donk.[1]

4.2 RESULTS

4.2.1. Installation of a ketone on the N-terminus of Pcn1.7.

The proposed methodology requires solutions to two hurdles. The first is to successfully install a dehydroamino acid at the first amino acid of the core peptide, and the second is to site specifically remove the leader peptide through proteolysis after residue –1. We first investigated the site-specific labeling of a lanthipeptide with a naturally occurring N-terminal 2-oxobutyryl group for which the first hurdle is already solved in nature. We chose Pcn1.7 (Figure 4.1) because it has been produced by coexpression of the precursor peptide ProcA1.7 with the lanthionine synthetase ProcM in *Escherichia coli*,[41] and because biophysical labeling of prochlorosins may help in elucidating their biological functions, which at present are unknown.[40] The second hurdle, site-specific removal of the leader peptide in vitro, is challenging for Pcn1.7. As mentioned in Chapter 2, the cognate proteases that remove the leader peptides in lanthipeptide-producing bacteria are not a general solution for in vitro removal of leader peptides. Instead, incorporation of Lys or Glu at the –1 position, followed by treatment with endoproteases trypsin, LysC, or GluC, has been often used.[42-45]

For Pcn1.7, leader peptide removal by inserting a Lys at position –1 and treatment of the ProcM-modified ProcA1.7 mutant with LysC was unsuccessful in previous work as cleavage at a Lys in the core peptide was observed.[41] An alternative approach was therefore used in this study, involving mutation of the last residue of the ProcA1.7 leader peptide from Gly to Glu.[40] The gene encoding His_6-ProcA1.7(G–1E) was inserted into multiple cloning site 1 (MCS1) of a pRSFDuet plasmid in which the gene encoding the modification enzyme ProcM was inserted in MCS2. Coexpression in *E. coli* resulted in the desired five-fold dehydrated His_6-ProcA1.7(G–1E). After GluC cleavage, the major ion observed by matrix-assisted laser desorption ionization

time-of-flight mass spectrometry (MALDI-TOF MS) corresponded to a peptide that still showed the loss of five water molecules, indicating no proteolysis occurred following Glu12, likely because the residue was deactivated by the overlapping ring system in Pcn1.7. Unfortunately, the GluC-cleaved peptide had been proteolyzed after Glu–6 in the leader peptide, rather than after Glu–1, resulting in Pcn1.7 with a five amino acid overhang (Figure 4.3, left). We next mutated Thr1 to Ser in an attempt to decrease the steric bulk around the cleavage site. The mutant peptide His_6-ProcA1.7(G–1E/T1S) was coexpressed with the modification enzyme ProcM, and the resulting product, as analyzed by MALDI-TOF MS, was dehydrated 5 times. However, proteolysis with GluC still resulted in cleavage after Glu–6 with very little cleavage after Glu–1 (Figure 4.3, right). This reluctance of a protease to cleave next to a posttranslationally modified amino acid (Dhb1 for Pcn1.7), and therefore prefer alternative cleavage sites in the leader peptide, is a common observation[41,45,46] that hampers the generality of the proposed methodology. Similar difficulties were also observed with use of a larger recognition sequence such as the IleGluGlyArg motif that is recognized by Factor Xa.[45]

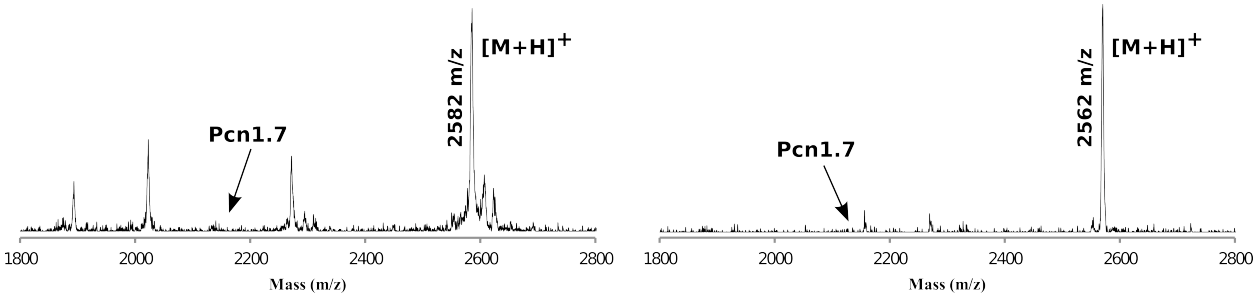

Figure 4.3. MALDI-TOF mass spectra of GluC-cleaved ProcA1.7 mutants failing to yield Pcn1.7. Left, GluC-cleaved and ProcM-modified His_6-ProcA1.7(G–1E). Right, GluC-cleaved and ProcM-modified His_6-ProcA1.7(G–1E/T1S). $[M+H]^+$ corresponds to proteolysis after Glu–6. GluC-cleaved (G–1E) $[M+H]^+$ calc'd = 2579.3 Da.; GluC-cleaved (G–1E/T1S) $[M+H]^+$ calc'd = 2565.3 Da.

To overcome these obstacles, we envisioned a two-stage leader peptide removal strategy in which most of the leader peptide is initially removed by trypsin, GluC, or LysC, and an aminopeptidase is used subsequently to remove the remaining amino acids of the leader peptide. Aminopeptidase activity was expected to self-terminate after reaching the first dehydrated amino acid (Dha1 or Dhb1) assuming that the conversion of the N-terminal enamine to an α-ketoamide (Scheme 4.1) occurs faster than aminopeptidase-catalyzed hydrolysis. The use of an aminopeptidase in lanthipeptide cleavage reactions has been employed previously to remove the NisA leader peptide from various core peptides and to study how the N-terminal lactate in epilancin 15X protects the peptide from degradation.[47,48] The last two amino acids of the leader peptide of many lanthipeptides consist of the "double-glycine" motif,[49] which poses a problem because commercial Leu-selective aminopeptidase from *Aeromonas proteolytica* is not very effective at removing this sequence.[48] Thus, two new mutants, His_6-ProcA1.7(G–2A/G–1A) and His_6-ProcA1.7(G–2L/G–1L) (Figure 4.4), were generated. Coexpression of these double mutants with ProcM resulted in five-fold dehydrated ProcA peptides, demonstrating that neither the two Ala nor Leu residues interfered with posttranslational processing. The peptides were purified by immobilized metal affinity chromatography (IMAC) and RP-HPLC resulting in a typical yield of about 8 mg/L of purified product. The double Ala mutant peptide was then treated with GluC first (cleaves after Glu –6) and then aminopeptidase (Figure 4.5, left). The product was analyzed by MALDI-TOF MS and the aminopeptidase was found to remove residues GVAA but did not hydrolyze Ala–1, generating Pcn1.7 with an Ala overhang (Ala-Pcn1.7). The double Leu mutant was then successively treated with GluC and aminopeptidase and analyzed by MALDI-TOF MS. The product mass was found to be identical to the anticipated mass of Pcn1.7 without a leader peptide overhang signifying the removal of GVALL by the aminopeptidase (Figure 4.5, right).

ProcA1.7$_{(-68)-(-20)}$QANSQKNLSDAELEGVALLTIGGTIVSITCETCDLLVGKMC

ProcA2.8$_{(-64)-(-20)}$LNSHRQNLSDDELEGVAGKTACHNHAPSMPPSYWEGEC

LctA$_{(-24)-(-15)}$QEVTESELDLILGAKAAALLKTAGSGVIHTISHECNMNSWQFVFTCCS

HalA1$_{(-41)-(-20)}$GDIFQELEDQDILAGVNGETCAWYNISCRLGNKGAYCTLTVECMPSCN

HalA2$_{(-41)-(-20)}$EVNEKELSSLAGSGDVHAETATTWPCATVGVSVALCPTTKCTSQC

NisA$_{(-23)-(-15)}$LVSVSKKDSGASPRLTSISLCTPGCKTGALMGCNMKTATCHCSIHVSK

Figure 4.4. Optimized peptide sequences that yield lanthipeptides with an N-terminal 2-oxobutyryl group. Native core peptides are underlined. Red, inserted Thr; blue, protease cleavage site; green, aminopeptidase cleavage sequence; brown, other amino acid insertions or mutations (see text). The Thr at the N-terminus of the core peptides ProcA1.7 and nisin are naturally occurring. The leader peptide segments that are not shown in the figure are: ProcA1.7$_{(-68)}$MSEEQLKAFIAKVQADTSLQEQLKVEGADVVAIAKASGFAITTEDLKAH$_{(-20)}$, ProcA2.8$_{(-64)}$MSEEQLKAFLTKVQADTSLQEQLKIEGADVVAIAKAAGFSITTED$_{(-20)}$, LctA$_{(-24)}$MKEQNSFNLL$_{(-15)}$, HalA1$_{(-41)}$MTNLLKEWKMPLERTHNNSNPA$_{(-20)}$, HalA2$_{(-41)}$MVNSKDLRNPEFRKAQGLQFVD$_{(-20)}$, and NisA$_{(-23)}$MSTKDFNLD$_{(-15)}$. Figure adapted from Bindman and van der Donk.[1]

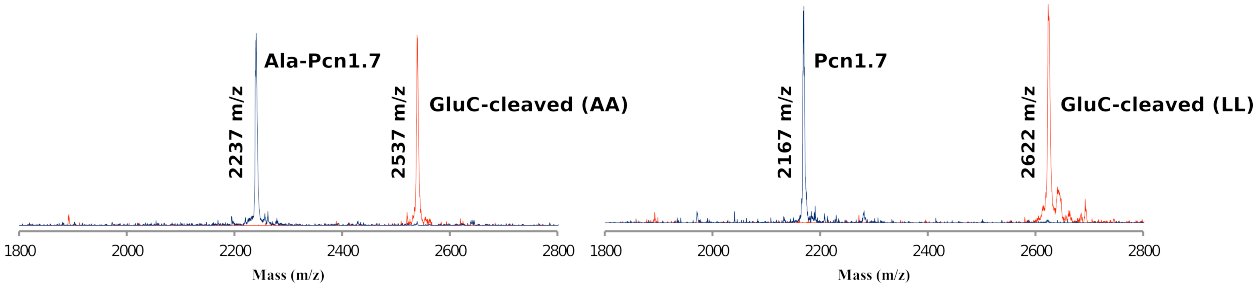

Figure 4.5. MALDI-TOF mass spectra of GluC-cleaved ProcA1.7 analogues yielding Ala-Pcn1.7 and Pcn1.7. Left, GluC-cleaved and ProcM-modified His_6-ProcA1.7(G–2A/G–1A) before (red) ($[M+H]^+$ calc'd = 2536.3 Da) and after (blue) ($[M+H]^+$ calc'd = 2238.1 Da.) treatment with aminopeptidase. Right, GluC-cleaved His_6-ProcA1.7(G–2L/G–1L) before (red) ($[M+H]^+$ calc'd = 2620.3 Da.) and after (blue) ($[M+H]^+$ calc'd = 2168.1 Da) treatment with aminopeptidase.

The successful conversion of the N-terminal dehydro amino acid to an α-ketoamide was demonstrated in two ways. In the first method the orthogonal reactivity of the ketone was exploited by reacting GluC- and aminopeptidase-cleaved ProcA1.7(G–2L/G–1L) with 1,2-phenylenediamine followed by analysis by MALDI-TOF MS (Figure 4.6). Although this reaction should produce Δ1-Pcn1.7 as the sole product, peaks corresponding to Δ1-2- and Δ1-3-Pcn1.7 were also present because the aminopeptidase was not removed prior to addition of 1,2-phenylenediamine and, after reaction with 1,2-phenylenediamine, the N-terminal ketone was no longer present to stall aminopeptidase activity. The phenylenediamine assay was necessary because detection of the mass difference between an N-terminal ketone and dehydrated amino acid (ketone is 1 Da larger) was not possible using the available MALDI-TOF instrument. However, a more sensitive MALDI-TOF instrument (Bruker Ultraflex) recently became available. Using this new instrument, the exact mass (0.1 Da error) of the GluC- and

aminopeptidase-cleaved His_6-ProcA1.7(G–2L/G–1L) peptide was determined. This product mass was found to be identical to the anticipated mass of Pcn1.7 with an N-terminal ketone (Figure 4.7, red).

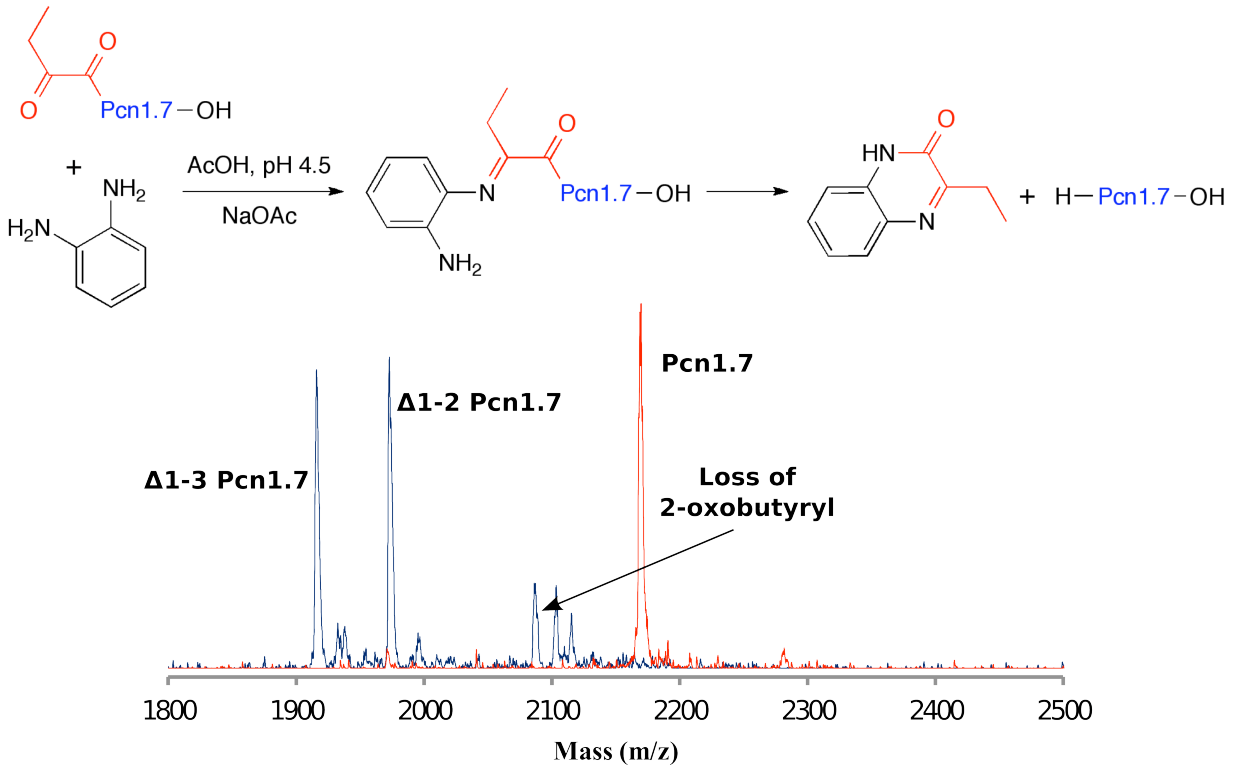

Figure 4.6. Reaction between Pcn1.7 and 1,2-phenylenediamine promotes loss of 2-oxobutyryl group. Top, Schematic representation of the reaction between 1,2-phenylenediamine and Pcn1.7. Bottom, MALDI-TOF mass spectra of Pcn1.7 before (red) and after (blue) the addition of 1,2-phenylenediamine in the presence of aminopeptidase.

4.2.2. Synthesis of aminooxy-alkyne (4.1) and its use in a site-specific oxime bioconjugation with Pcn1.7.

As a way to take advantage of the minimal cross-reactivity between the ketone functionality and the side chains of the proteinogenic amino acids, a bioconjugation reaction

specific for the N-terminal ketone of Pcn1.7 was attempted. Pcn1.7 was reacted with aminooxy-linked alkyne (**4.1**), rather than a hydrazine-linked alkyne, because of the increased hydrolytic stability of the oxime compared to the hydrazone.[50] Aminooxy-alkyne tag **4.1** was synthesized by first reacting propargyl bromide with N-hydroxyphthalimide in an S_N2 displacement reaction, followed by removal of the phthalimide by methylhydrazine (Scheme 4.2). Acidification produced the HCl salt **4.1**. The synthetic aminooxy alkyne was then reacted with RP-HPLC-purified Pcn1.7 (Scheme 4.3). Analysis of the product by MALDI-TOF MS indicated that the alkyne-functionalized Pcn1.7 (alk-Pcn1.7) was indeed generated (Figure 4.7). Addition of aniline (100 mM) to the buffered solution of peptide and **4.1** dramatically increased the product yield (Figure 4.7).[51] When the bioconjugation was attempted with GluC-cleaved ProcA1.7(G–1E), an analogue lacking the N-terminal ketone, no reaction occurred demonstrating that oxime formation was specific for the N-terminus of Pcn1.7 (Figure 4.8).

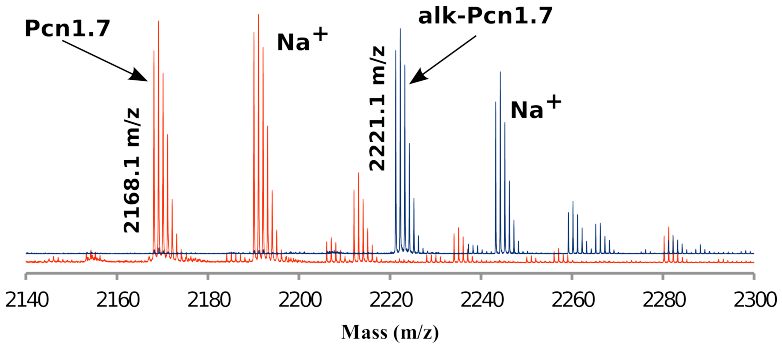

Figure 4.7. MALDI-TOF mass spectra of the products of the reaction between Pcn1.7 and aminooxy alkyne (**4.1**). Reaction was attempted with (blue) and without (red) the addition of aniline (100 mM). Pcn1.7 $[M+H]^+$ calc'd = 2168.1 Da.; Alk-Pcn1.7 $[M+H]^+$ calc'd = 2221.1 Da.

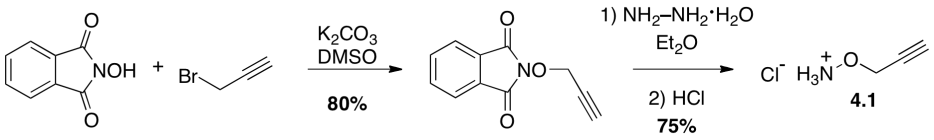

Scheme 4.2. Synthetic scheme towards aminooxy alkyne **4.1**.

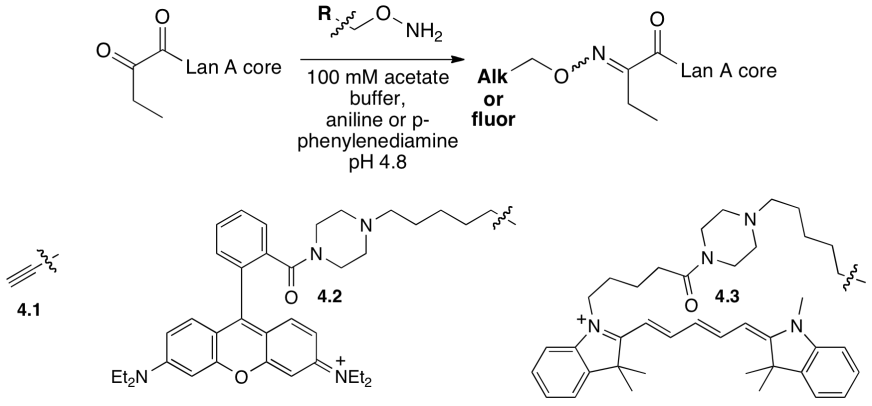

Scheme 4.3. Production of alkyne and fluorescently labeled lanthipeptides by oxime bioconjugation. Aniline- or p-phenylenediamine-catalyzed oxime bioconjugation between keto-LanA core and an aminooxy moiety functionalized with either an alkyne (alk, **4.1**) or the fluorophores (fluor) rhodamine B (**4.2**) or Cy5 (**4.3**). Scheme adapted from Bindman and van der Donk.[1]

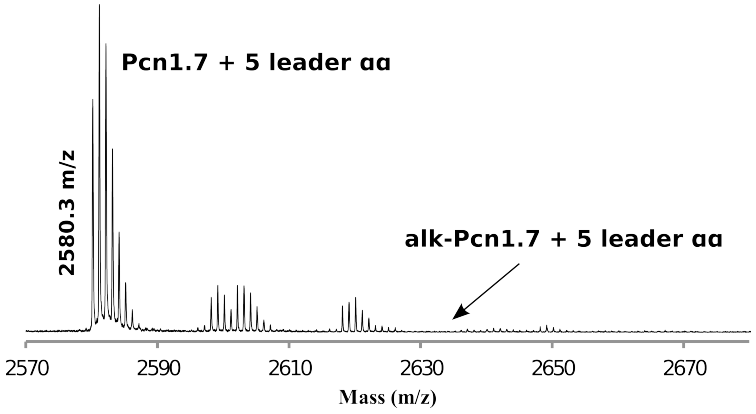

Figure 4.8. MALDI-TOF mass spectrum of the reaction between GluC-cleaved and ProcM-modified His_6-ProcA1.7(G–1E) and **4.1**. ($[M+H]^+$ calc'd = 2580.3 Da.)

4.2.3. Installation of a non-native N-terminal 2-oxobutyryl group in lanthipeptides.

Unlike Pcn1.7, most lanthipeptides do not contain an N-terminal 2-oxobutyryl group. Therefore, to make the labeling strategy general for other lanthipeptides, a ketone needs to be appended to their N-termini. Harnessing the well-established promiscuity of the lanthipeptide synthetases,[12] we hypothesized that installation of a Ser or Thr between the leader and core peptides or replacing the first residue of the core peptide with a Ser or Thr might result in dehydration by the cognate dehydratase. Proteolytic removal of the leader peptide would then afford the modified core peptide with an N-terminal ketone. We chose to install a Thr rather than Ser because an analysis of almost 40 lanthipeptides found that Ser escaped dehydration more than twice as often as Thr.[52]

4.2.3.1. Installation of a ketone on the N-terminus of prochlorosin 2.8 and its bioconjugation with aminooxy-alkyne 4.1.

We tested the methodology with prochlorosin 2.8 (Pcn2.8) (Figure 4.2). Because the core peptide of Pcn2.8 does not contain a Lys, a G–1K mutation was introduced in addition to replacement of Ala1 with Thr (Figure 4.4). The His_6-ProcA2.8(G–1K/A1T) mutant peptide was coexpressed with the modification enzyme ProcM in *E. coli* cells. After purification by IMAC and cleavage of the leader peptide from the modified core peptide with trypsin, analysis by MALDI-TOF MS demonstrated a major ion corresponding to the core peptide with three dehydrations and a minor, although significant, ion with only two dehydrations (Figure 4.9, left); the core peptide of wild-type (wt) Pcn2.8 contains two dehydrations (Figure 4.2). The mass of the product peak with three dehydrations was 1 Da larger than the calculated peptide mass containing an N-terminal enamine, demonstrating the formation of a 2-oxobutyryl group on the

N-terminus of Pcn2.8 (keto-Pcn2.8) (Figure 4.9, left). Keto-Pcn2.8 was obtained in a typical yield of 3 mg/L after RP-HPLC purification, and was site-specifically labeled with **4.1** in an aniline-catalyzed conjugation (Figure 4.9, right). As with Pcn1.7, the alkyne added only once to keto-Pcn2.8.

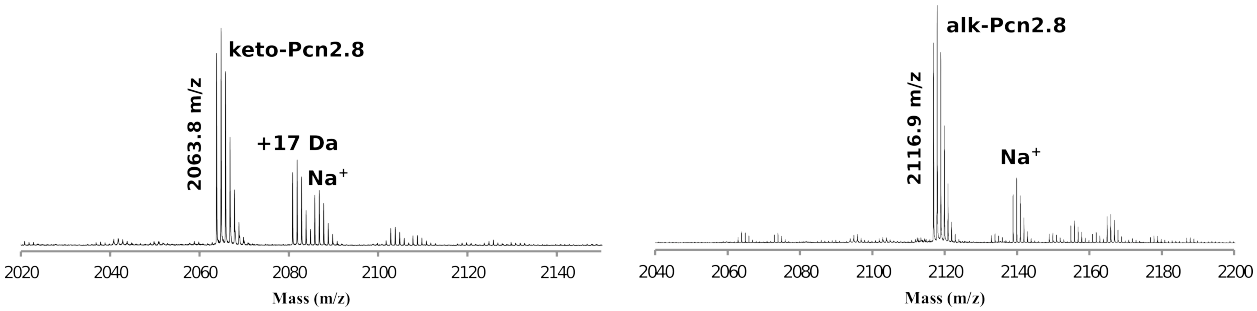

Figure 4.9. MALDI-TOF mass spectra of alk- and keto-Pcn2.8. Left, keto-Pcn2.8 ($[M+H]^+$ calc'd = 2063.8 Da.). Right, alk-Pcn2.8 ($[M+H]^+$ calc'd = 2116.8 Da.). The peak at +17 Da represents incomplete dehydration of the inserted Thr based on MS/MS analysis (the incomplete dehydration also prevents the hydrolysis to the ketone, hence a difference of 17 Da and not 18 Da). Na^+ represents a sodium adduct. The MALDI MS spectrometer used (Bruker UltraFlex) has sufficient resolution to distinguish peptides differing by 1 Da if calibrated, such as peptides with an N-terminal 2-aminobutyric acid and an N-terminal 2-oxobutyric acid group.

As discussed above, a significant portion of the ProcA2.8 core region, after modification by ProcM, contained two dehydrations. We hypothesized that modifying the residues flanking the inserted Thr might increase the efficiency of its dehydration. Indeed, dehydration of Ser or Thr residues in lanthipeptides occurs more often when the dehydratable residue is flanked by hydrophobic amino acids.[52] Unfortunately, most commercial proteases hydrolyze the amide bond immediately C-terminal to a charged amino acid side chain. Thus, in the current methodology, the insertion of Thr immediately after the protease cleavage site may decrease the efficiency of

dehydration of that residue. However, if a hydrophobic amino acid were inserted between the proteolytic cleavage site and the Thr, the residue was expected to be dehydrated to a greater extent. Proteolysis would then afford the modified core region with a hydrophobic residue overhang, which could be removed with an aminopeptidase. When the mutant peptide His_6-ProcA2.8(G–1K-A1T ins LL), with two Leu residues inserted between Lys and Thr, was coexpressed with ProcM, MALDI-TOF MS analysis of the trypsin-cleaved product showed almost complete modification of the N-terminal Thr (three dehydrations compared with two for wt ProcA2.8; Figure 4.10). Subsequent aminopeptidase cleavage of the Leu-Leu overhang afforded keto-Pcn2.8. Although the increase in dehydration efficiency of His_6-ProcA2.8(G–1K-A1T ins LL) was advantageous, when the extra time required and the expense of the aminopeptidase and purification steps were taken into consideration the original method, trypsin cleavage of His_6-ProcA2.8(G–1K/A1T), was deemed superior with regard to synthesizing keto-Pcn2.8.

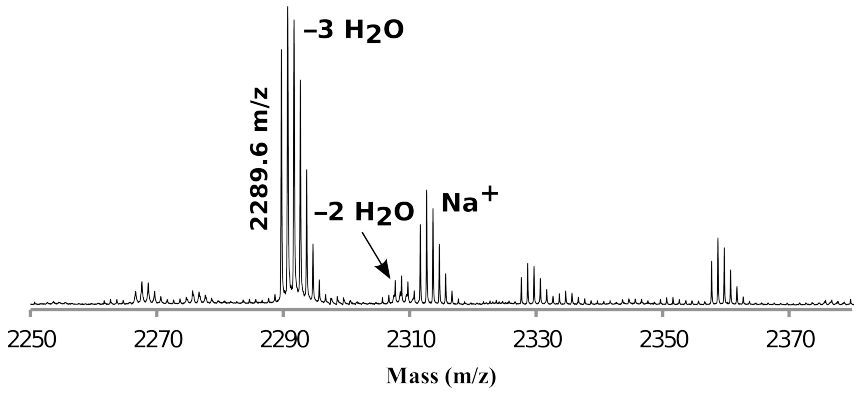

Figure 4.10. MALDI-TOF mass spectrum of trypsin-cleaved His_6-ProcA2.8(G–1K-A1T ins LL). $[M+H]^+$ of –3 H_2O calc'd = 2289.0 Da. Instrument was not calibrated prior to analysis.

4.2.3.2. Installation of a ketone on the N-terminus of haloduracin α and its bioconjugation with aminooxy-alkyne 4.1.

The experiments with the two prochlorosins established the feasibility of the site-specific labeling approach, but because their bioactivities are unknown, we could not assess whether N-terminal labeling interfered with activity. The two-peptide systems are an interesting subclass of lantibiotics, which achieve maximum antimicrobial activity from the synergistic activity of two disparate peptides that are produced by the same organism. One example is haloduracin (Figure 4.2), consisting of Halα, produced from the HalA1 precursor peptide by the lanthionine synthetase HalM1, and Halβ, generated from the HalA2 precursor peptide by the synthetase HalM2.[53,54]

To synthesize keto-Halα, a gene encoding His_6-HalA1(A–1-C1 ins IEGRT) was generated by site-directed mutagenesis in which the Factor Xa recognition sequence (Ile-Glu-Gly-Arg) and a Thr were inserted between the last residue of the leader peptide (Ala) and the first residue of the core peptide (Cys). The gene was inserted into MCS1 of a pRSFDuet plasmid and the gene encoding HalM1 was inserted in MCS2. Coexpression of the mutant HalA1 peptide with HalM1, followed by exposure to Factor Xa, resulted in no discernable formation of keto-Halα, as assessed by MALDI-TOF MS. However, the successful dehydration of the inserted Thr in HalM1-modified His_6-HalA1(A–1-C1 ins IEGRT) was determined by MALDI-TOF MS analysis after cleavage of the peptide by the endoprotease GluC. The major mass ion corresponded to four-fold dehydrated Halα with a Gly-Arg overhang (Figure 4.11) (wt Halα contains three dehydrations; Figure 4.2). No cleavage was observed after Glu22 in the HalA1 core region as the residue was likely deactivated to proteolysis by the proximal methyllanthionine ring. Removal of the Gly-Arg overhang with aminopeptidase was attempted,

however aminopeptidase activity halted after hydrolysis of Gly–2, and keto-Halα was not produced.

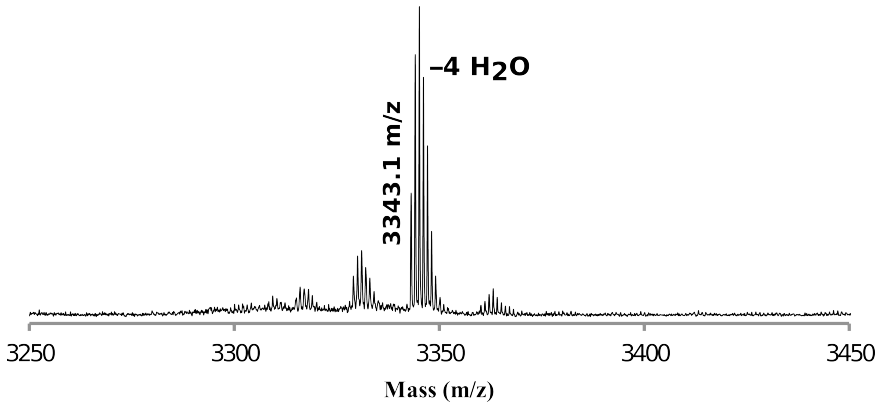

Figure 4.11. MALDI-TOF mass spectrum of GluC-cleaved His_6-HalA1(A–1-C1 ins IEGRT). $[M+H]^+$ calc'd = 3342.6 Da. Instrument was not calibrated prior to analysis.

The experiments with His_6-HalA1(A–1-C1 ins IEGRT) illustrated that the synthetase HalM1 could modify a Thr inserted at the N-terminus of the HalA1 core peptide and that GluC could cleave off most of the HalA1 leader peptide without disruption of the core region. However, the leader peptide could never be fully removed. To achieve this goal, a gene encoding His_6-HalA1(A–1E-C1 ins T) (Figure 4.4), where Ala–1 was mutated to Glu for leader peptide removal and a Thr was incorporated between this Glu and the first residue of the core peptide (Cys1), was inserted into MCS1 of a pRSFDuet vector with *halM1* in MCS2. Because of the relatively low yield of haloduracin production in *E. coli* in this and a previous study,[42] a second copy of the *halA1* mutant was inserted into a pET15b plasmid in an attempt to increase the peptide yield. Coexpression of the HalA1 peptide with HalM1, and purification by IMAC and RP-HPLC, resulted in a fully modified peptide with a yield of about 8 mg/L. Subsequent cleavage of its leader peptide with the endoprotease GluC yielded a Halα analogue containing an

N-terminal 2-oxobutyryl moiety (keto-Halα) (Figure 4.12, left). The keto analogue was reacted with **4.1** in an aniline-catalyzed conjugation to yield alkyne-labeled alk-Halα (Figure 4.12, right).

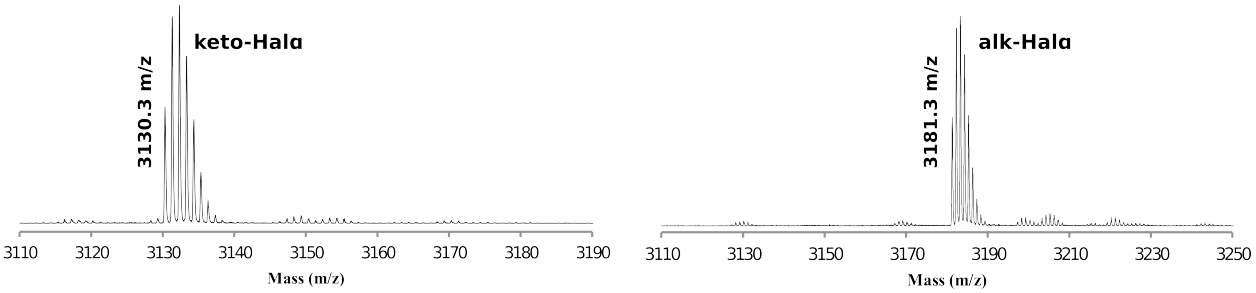

Figure 4.12. MALDI-TOF mass spectra of keto- and alk-Halα. Left, keto-Halα ($[M+H]^+$ calc'd = 3130.3 Da.). Right, alk-Halα ($[M+H]^+$ calc'd = 3181.3 Da).

4.2.3.3. Installation of a ketone on the N-terminus of haloduracin β and its bioconjugation with aminooxy-alkyne 4.1.

To obtain keto-Halβ, a gene encoding His_6-HalA2(Q–1E-T1 ins T) was generated by site-directed mutagenesis. In this mutant peptide, the last residue of the leader peptide of HalA2 (Gln–1) was mutated to Glu and a Thr was inserted between the Glu and the first residue of the core peptide (Thr1). The *halA2* mutant gene was inserted into MCS1 of a pRSFDuet plasmid containing the *halM2* gene in MCS2. Coexpression of the HalA2 mutant peptide with HalM2, and purification by IMAC and RP-HPLC was followed by leader peptide cleavage with endoprotease GluC. MALDI-TOF MS analysis of the ensuing product demonstrated successful modification of the inserted Thr. Unfortunately, only partial proteolytic leader peptide removal was observed; a large mass peak corresponding to peptide cleavage after Glu–14, but not after Glu–1, was detected (Figure 4.13A). We hypothesized that the lack of cleavage after Glu–1 was because the D-stereocenter of the N-terminal lanthionine ring interfered with protease activity.

This problem was overcome by coexpressing HalM2 with His_6-HalA2(Q–1E-T1 ins TA) (Figure 4.4), a mutant incorporating a ThrAla sequence between Glu–1 and Thr1 to separate the cleavage site from the N-terminal methyllanthionine ring. The peptide was purified as described above resulting in a fully modified peptide with a yield of about 10 mg/L. Subsequent cleavage of the HalA2 leader peptide with GluC yielded a Halβ analogue containing an N-terminal 2-oxobutyryl moiety (keto-Halβ) as the only observed product (Figure 4.13B). The keto analogue was reacted with **4.1** in an aniline-catalyzed conjugation to yield alk-Halβ (Figure 4.13C).

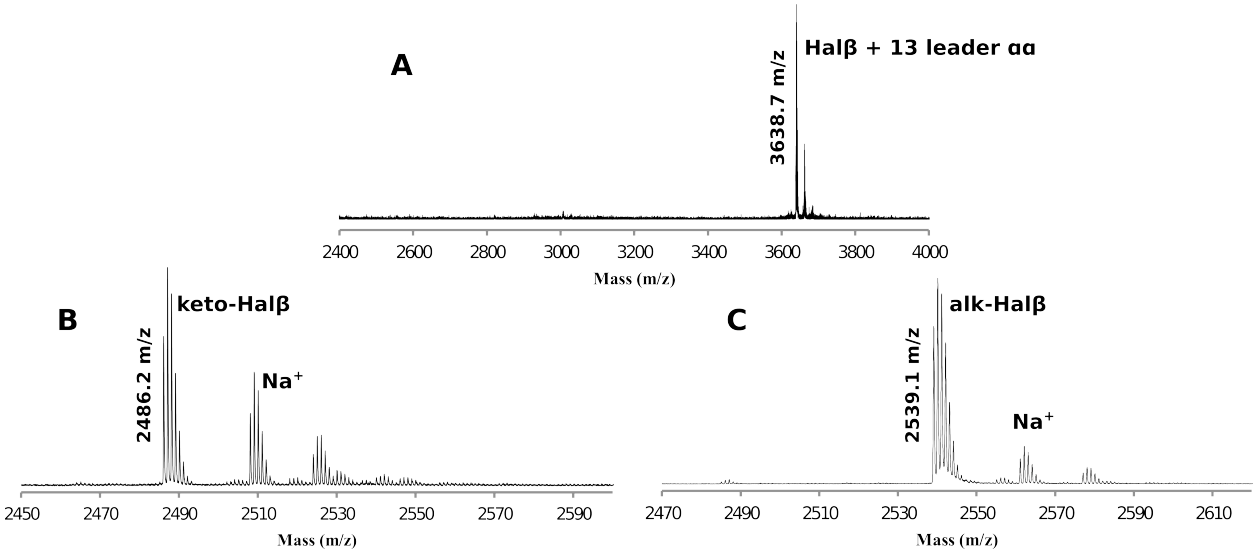

Figure 4.13. MALDI-TOF mass spectra of Halβ analogues. A) GluC-cleaved His_6-HalA2(Q–1E-T1 ins T) (the peak at 3638 Da corresponds to cleavage after Glu–14) ($[M+H]^+$ calc'd = 3637.7 Da.), B) keto-Halβ ($[M+H]^+$ calc'd = 2486.2 Da.), and C) alk-Halβ ($[M+H]^+$ calc'd = 2539.1 Da). Instrument was not calibrated before analysis of spectrum A.

4.2.3.4. Installation of a ketone on the N-terminus of lacticin 481 and its bioconjugation with aminooxy-alkyne 4.1.

Previous work determined that Ser4 is not modified in wt lacticin 481 (Figure 4.2) because it is both too close to the leader peptide and because it is flanked by two Gly residues.[55] This Ser was only dehydrated by the synthetase LctM when three Ala residues were inserted between the leader and core peptides and Gly3 and Gly5 were mutated to Ile and His, respectively.[55] We therefore anticipated that a Thr inserted directly between the leader and core peptides in lacticin 481 would not be dehydrated based on its close proximity to the leader peptide and its flanking amino acids. Taking these previous studies as a guideline, a gene encoding the peptide His_6-LctA(K1-G2 ins AAAKT), was prepared. In this peptide, the sequence AAAKT was inserted between residues 1 and 2 of the core peptide to place the inserted Thr at a longer distance from the end of the leader peptide. Furthermore, a Lys was placed before the inserted Thr such that the leader peptide could be removed with LysC or trypsin. The mutant LctA peptide and its cognate synthetase LctM were coexpressed from a pRSFDuet plasmid in *E. coli* cells.[56] After LysC cleavage of LctM-modified His_6-LctA(K1-G2 ins AAAKT), MALDI-TOF MS analysis of the resulting peptide showed the majority of product contained four dehydrations, the number of dehydrations in wt lacticin 481, with a very small peak corresponding to the desired five dehydrations (Figure 4.14A). It was likely that the amino acid escaping dehydration was the inserted Thr between the core and the leader peptide.

In a second attempt to synthesize keto-lacticin 481, a gene encoding the peptide mutant His_6-LctA(K1-G2 ins AAAKLLT) was generated. This mutant further separated the inserted Thr from the leader peptide by the introduction of two Leu residues and introduced a hydrophobic Leu immediately before Thr1, which helped increase the dehydration efficiency of Thr1 in

ProcA2.8. Removal of the leader peptide could be achieved by a combination of the protease LysC and aminopeptidase. After LysC cleavage of the peptide coexpressed with LctM, MALDI-TOF MS analysis demonstrated the majority of the product still corresponded to four dehydrations, however a larger portion had the desired five dehydrations (Figure 4.14B).

To confirm the amino acid escaping dehydration in four-fold dehydrated His_6-LctA(K1-G2 ins AAAKLLT) was Thr1, the LysC-cleaved peptide was incubated with an aminopeptidase. If Thr1 had been dehydrated successfully by LctM, aminopeptidase hydrolysis would stop after the removal of the two N-terminal Leu residues (Leu–2 and Leu–1) because an N-terminal α-ketoamide would have formed. However, if Thr1 was not dehydrated the aminopeptidase would likely remove that residue as well as the residues immediately succeeding it. MALDI-TOF MS analysis of the aminopeptidase reaction on LysC-cleaved His_6-LctA(K1-G2 ins AAAKLLT) demonstrated that the aminopeptidase removed the LeuLeuThr sequence as well as several subsequent amino acids, finally halting at Ile7 and His8, just before the methyllanthionine ring (Figure 4.14C). Thus, the amino acid escaping dehydration in four-fold dehydrated His_6-LctA(K1-G2 ins AAAKLLT) was Thr1.

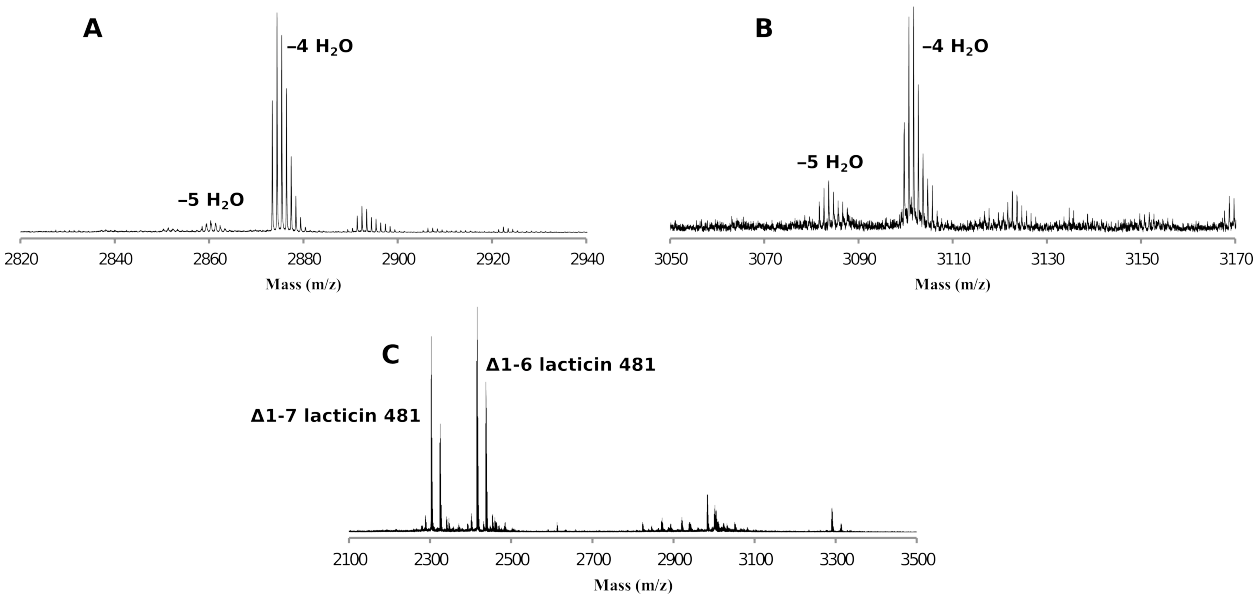

Figure 4.14. MALDI-TOF mass spectra of LysC- and/or aminopeptidase-cleaved and LctM-modified LctA analogues in an attempt to produce keto-lacticin 481. A) LysC-cleaved and LctM-modified His_6-LctA(K1-G2 ins AAAKT), B) LysC-cleaved and LctM-modified His_6-LctA(K1-G2 ins AAAKLLT), and C) LysC- and aminopeptidase-cleaved and LctM-modified His_6-LctA(K1-G2 ins AAALLKT).

We suspected that the modest increase in dehydration efficiency between His_6-LctA(K1-G2 ins AAAKT) and His_6-LctA(K1-G2 ins AAAKLLT) was due to the increased distance between the leader and core regions and the insertion of a hydrophobic amino acid immediately preceding the inserted Thr. To further enhance dehydration of the inserted Thr, we hypothesized that mutating the Gly immediately succeeding the inserted Thr to a hydrophobic residue might further increase the dehydration efficiency. Therefore, the peptides His_6-LctA(K1-G2A ins AAAKLLT) and His_6-LctA(K1-G2L ins AAAKLLT), with Gly2 mutated to Ala and Leu respectively, were coexpressed with LctM and modified precursor peptides were cleaved by LysC and analyzed by MALDI-TOF MS. The G2L mutation had no distinguishable impact on

the dehydration of Thr1 (Figure 4.15, red), however when Gly2 was mutated to Ala, Thr1 was dehydrated to a larger extent (Figure 4.15, blue). Purification of the LysC cleaved G2A mutant yielded LctA core with a Leu–2/Leu–1 overhang. The peptide was then subjected to aminopeptidase cleavage to remove the remaining two amino acids of the leader peptide. Unfortunately, even at high aminopeptidase concentrations Leu–1 was not successfully removed in the 5-fold dehydrated species.

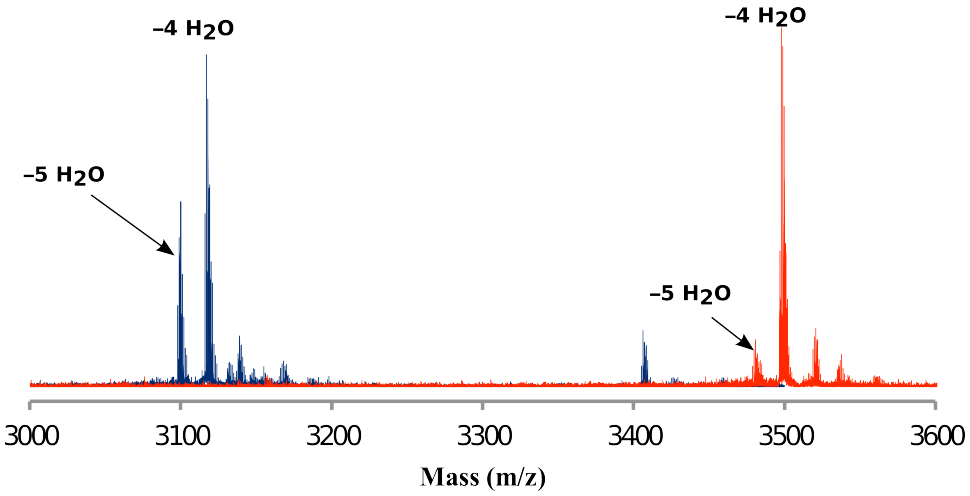

Figure 4.15. MALDI-TOF mass spectra of LysC-cleaved LctA(K1-G2X ins AAAKLLT) in an attempt to produce keto-lacticin 481. Red, X = L. Blue, X = A); the G2L mutant is cleaved after Lys–7 rather than Lys–3.

As a final attempt to synthesize keto-lacticin 481, the construct His_6-LctA(K1-G2A ins AAALLKT) (Figure 4.4) was inserted into MCS1 of a pRSFDuet vector with LctM in MCS2. Compared to the previous construct, the inserted Thr was of equal distance to the end of the leader peptide, however the order of the Leu and Lys residues were switched so LysC cleavage of the modified peptide would directly form keto-lacticin 481. The mutant LctA peptide was

coexpressed with LctM in *E. coli* cells and the leader peptide was removed with LysC. Analysis of the product by MALDI-TOF MS showed that a small portion was successfully dehydrated five times (Figure 4.16A, red), indicating that the amount of Thr1 dehydrated had decreased compared to His_6-LctA(K1-G2A ins AAAKLLT), a result likely due to the removal of the hydrophobic Leu directly preceding Thr1. Further analysis of the five-fold dehydrated species showed that an N-terminal 2-oxobutyryl had been introduced onto lacticin 481 (keto-lacticin 481 is the product).

We hypothesized that an increase in the concentration of LctM in the coexpression system would lead to an enhancement in dehydration efficiency of the inserted Thr. We increased the concentration of LctM by adding copies of *lctM* to pCDFDuet and pACYCDuet vectors. Coexpression of the *his_6-lctA*(*K1-G2A ins AAALLKT*) construct with 3 copies of *lctM* afforded the posttranslationally modified LctA in a typical yield of 3 mg/L, and with the five-fold dehydrated peptide as the major product (Figure 4.16A, blue). Treatment of the five-fold dehydrated product with LysC followed by aniline-catalyzed conjugation with **4.1** resulted in the desired alkyne-conjugated-lacticin 481 (alk-lacticin 481; Figure 4.16B). We note that this analogue lacks the N-terminal Lys that is found in wt lacticin 481. However, my studies in Chapter 3 have shown the Δ1K analogue to be as active as the wt compound. Using an analogous strategy, we also generated keto-lacticin 481-E13A from the corresponding LctA mutant (4.16C). This analogue was important for mode of action studies as discussed in section 4.2.7.

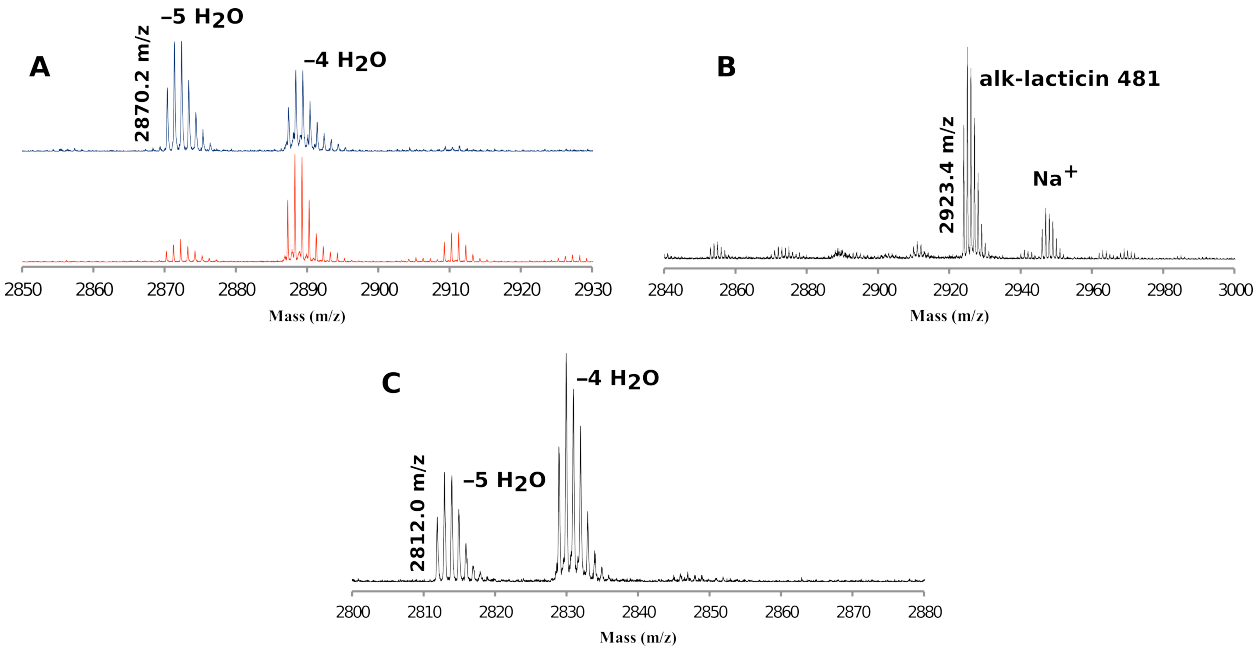

Figure 4.16. MALDI-TOF mass spectra of keto- and alk-lacticin 481 and keto-lacticin 481-E13A. A) LysC-cleaved His_6-LctA(K1-G2A ins AAALLKT) overexpressed in *E. coli* with 3 copies (blue) and 1 copy (red) of the *lctM* gene ($[M+H]^+$ of –5 H_2O calc'd = 2870.2 Da.), B) alk-lacticin 481 ($[M+H]^+$ calc'd = 2923.2 Da.), and C) keto-lacticin 481-E13A ($[M+H]^+$ of –5 H_2O calc'd = 2812.2 Da.) Figure adapted from Bindman and van der Donk.[1]

4.2.3.5. Installation of a ketone on the N-terminus of nisin and its bioconjugation with aminooxy-alkyne 4.1.

Posttranslational modification of NisA, the precursor peptide for the class I lantibiotic nisin, relies on two enzymes, the dehydratase NisB and the cyclase NisC, compared to class II lanthipeptides whose modification depends on one bifunctional enzyme (e.g. LctM). Previously, the coexpression of nisin in *E. coli* was successful by employing a two-vector system in which *nisA* and *nisB* were introduced into MCS1 and MCS2, respectively, of a pRSFDuet vector and *nisC* was incorporated into MCS2 of a pACYCDuet vector.[42] In an attempt to synthesize keto-

nisin, the gene sequence encoding the peptide NisA(R–1-I1 ins IT) was incorporated into MCS1 of a pRSFDuet vector with NisB in MCS2. In this peptide, an IleThr sequence was inserted between the NisA leader and core regions. This insertion mimics Ile1 and Dhb2 of wt nisin and we anticipated that the inserted Thr, flanked by two hydrophobic Ile residues, would be dehydrated. No artificial cleavage site was introduced into the NisA mutant because the entire leader sequence could be cleaved off after Arg–1 by the endoprotease trypsin. After coexpression of the NisA mutant peptide with NisB and NisC, IMAC purification, and trypsin cleavage, analysis of the product by MALDI-TOF MS displayed a major mass ion corresponding to dehydration of seven of the desired nine amino acids with smaller peaks accounting for six and eight dehydrations (Figure 4.17, black). We anticipated that along with Thr1, Ser33 escaped dehydration as this residue is not always dehydrated in the native producer.[57]

Due to the positive affect the additional copies of *lctM* had in obtaining the maximum number of dehydrations in the biosynthesis of keto-lacticin 481, we conjectured that increasing the concentration of NisB would boost the number of dehydrations during coexpression with the NisA mutant. Indeed, in previous work certain nisin analogues were dehydrated to a greater extent when the concentration of NisB was increased in vivo.[57] Thus, a copy of the gene encoding the protein NisB was incorporated into MCS1 of the pACYCDuet vector with NisC in MCS2. NisA(R–1-I1 ins IT) was then coexpressed with NisC and two copies of NisB. When compared to the overexpression with one copy of NisB, the dehydration efficiency of the NisA peptide was increased; the major peak, again, consisted of seven dehydrations but larger peaks were seen corresponding to eight and nine dehydrations (Figure 4.17, red). When NisA(R–1-I1 ins IT) was coexpressed with NisC and three copies of NisB (the additional copy of *nisB* was incorporated into MCS2 of a pCDFDuet vector), MALDI-TOF MS analysis exhibited a major

ion corresponding to the NisA mutant peptide with nine dehydrations (Figure 4.17, blue). IMAC purification, followed by removal of the leader peptide by trypsin and then aminopeptidase yielded keto-nisin-1. Unfortunately, this nisin mutant was not bioactive against *Lactococcus lactis* HP, a result that was somewhat expected as modification of the N-terminus of nisin has been shown previously to abolish bioactivity.[58]

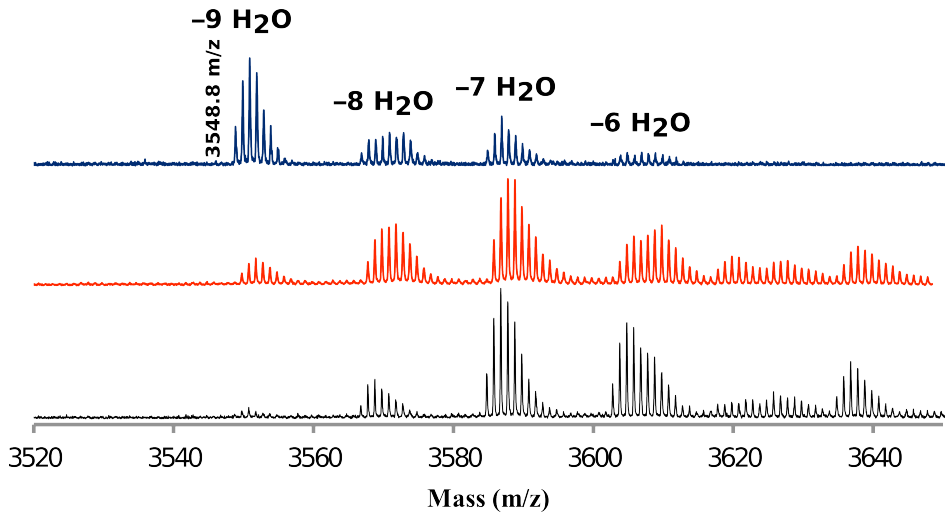

Figure 4.17. Modification of His_6-NisA(R–1-I1 ins IT) with multiple copies of NisB. MALDI-TOF mass spectra of trypsin-cleaved His_6-NisA(R–1-I1 ins IT) overexpressed in *E. coli* with 1 (black), 2 (red), or 3 (blue) copies of the *nisB* gene. $[M+H]^+$ of –9 H_2O calc'd = 3548.8 Da.

To increase the probability of bioactivity of nisin with an N-terminal ketone, the biosynthesis of NisA(I1L) was attempted. The second amino acid in the core peptide of wt nisin is a Dhb, so aminopeptidase cleavage of the first amino acid (Leu) would yield Δ1 nisin with an N-terminal 2-oxobutyryl group. Unlike keto-nisin-1, this peptide would not be elongated at the N-terminus and therefore might still be bioactive. NisA(I1L) was coexpressed with only one copy of NisB due to its similarity with wt nisin. After IMAC purification and trypsin cleavage of

the leader peptide, the main product, as shown by MALDI-TOF MS, had the desired eight dehydrations. Aminopeptidase cleavage of the N-terminal Leu and RP-HPLC purification yielded keto-nisin-2 (Figure 4.18, left), which was bioactive (Figure 4.19A). keto-Nisin-2 was then reacted with **4.1** in an aniline catalyzed oxime bioconjugation to yield alk-nisin (Figure 4.18, right).

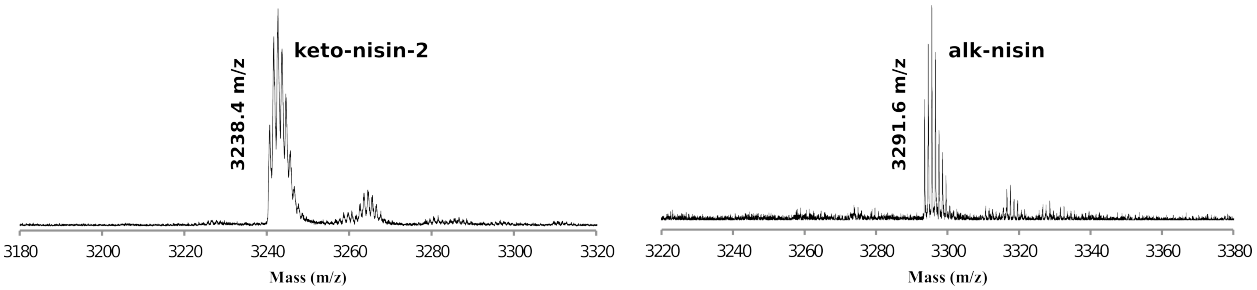

Figure 4.18. MALDI-TOF mass spectra of keto-nisin-2 and alk-nisin. Left, keto-nisin-2 ($[M+H]^+$ calc'd = 3238.5 Da) Right, alk-nisin ($[M+H]^+$ calc'd = 3291.5 Da).

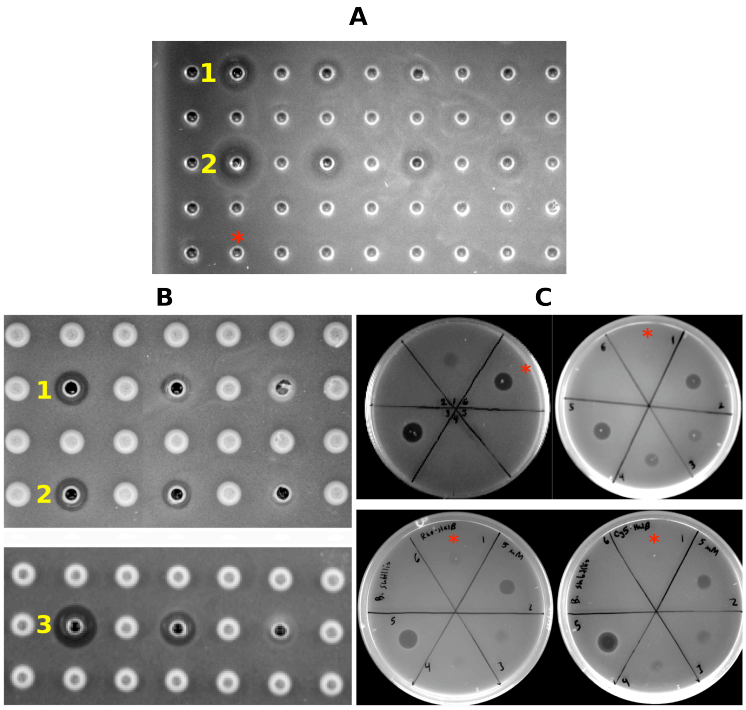

Figure 4.19. Bioactivities of nisin, lacticin 481 and haloduracin analogues against *L. lactis* HP or *B. subtilis*. A) Zones of growth inhibition displayed by wt nisin (row 1; concentrations from left to right: 4 μM, 2 μM, 1 μM, 0.5 μM), keto-nisin-2 (row 2; concentrations from left to right: 200 μM, 100 μM, 50 μM, 25 μM), and alk-nisin (red star; concentration was greater than 100 μM) against *L. lactis* HP. A total of 10 μL of compound was added to each well. B) Zones of growth inhibition displayed by wt lacticin 481 (row 1), alk-lacticin 481 (row 2) and rho-lacticin 481 (row 3) against *B. subtilis* 168. Concentrations from left to right: 50, 25 and 12.5 μM. A total of 20 μL was added to each well. C) Zones of growth inhibition displayed by haloduracin analogues against *B. subtilis* 168. Top left, zones-of-growth inhibition of alk-haloduracin. Clockwise from red star: alk-Halα + alk-Halβ (12.5 μM each), alk-Halβ (12.5 μM), alk-Halα (12.5 μM), alk-Halα + alk-Halβ (25 μM each), alk-Halβ (25 μM), alk-Halα (25 μM). Top right, zones-of-growth inhibition of rho-Halα. Each peptide was added at a concentration of 5 μM. Clockwise from red star: rho-Halα, rho-Halα + wt Halβ, rho-Halα + rho-Halβ, rho-Halα + Cy5-Halβ, wt Halα + wt Halβ. Bottom left, zones-of-growth inhibition of rho-Halβ. Each peptide was added at a concentration of 5 μM. Clockwise from red star: rho-Halβ, rho-Halβ + wt Halα, wt Halα, wt Halβ, wt Halα + wt Halβ. Spot 6 was not used. Bottom right, zones-of-growth inhibition of Cy5-Halβ. Each component was added at a concentration of 5 μM. Clockwise from red star: Cy5-Halβ, Cy5-Halβ + wt Halα, wt Halα, wt Halβ, wt Halα + wt Halβ. Spot 6 was not used. A total of 10 μL was added to each spot.

4.2.4. Bioactivities of alkyne-labeled lacticin 481, haloduracin α, haloduracin β, and nisin.

alk-Lacticin 481, alk-Halα, alk-Halβ, and alk-nisin were used for agar well-diffusion antimicrobial assays against *Bacillus subtilis* 168. The zones of growth inhibition compared with those obtained with the wt standard showed that alk-lacticin 481 retained its activity (Figure 4.19B). Because haloduracin is a two-component lantibiotic, both components, alk-Halα and alk-Halβ, were administered individually and in tandem to *B. subtilis* 168. Like wt haloduracin, alk-Halα and alk-Halβ alone displayed little bioactivity. However, the alk-Halα and alk-Halβ peptides exhibited potent antibacterial activity when combined (Figure 4.19C). In contrast, alk-nisin exhibited no bioactivity against *L. lactis* HP (Figure 4.19A), demonstrating that the labeling methodology to insert an N-terminal 2-oxobutyryl group may not be suitable for lantibiotics whose N-termini are important for bioactivity.

4.2.5. Fluorescent labeling of lacticin 481, lacticin 481-E13A, haloduracin α, and haloduracin β.

Aminooxy-rhodamine (**4.2**) and aminooxy-Cy5 (**4.3**) were synthesized using published procedures with minor changes (Schemes 4.4 and 4.5).[59-61] Briefly, Boc-protected linker **4.5** was synthesized from 1,6-dibromohexane via successive nucleophilic substitution reactions first with *N*-Boc-hydroxylamine and then with piperazine. Next, the secondary amine of **4.5** was coupled to the free carboxylate of either rhodamine B or Cy5 followed by Boc removal to yield the fluorescent aminooxy derivatives **4.2** and **4.3**. Very recently, *p*-phenylenediamine was reported to be an improved catalyst over aniline for oxime bioconjugations, in part because of its increased water solubility.[62] Therefore, keto-lacticin 481 and keto–Halα were labeled with **4.2** via *p*-phenylenediamine-catalyzed oxime bioconjugations, providing rho-lacticin 481 and rho-

Halα in modestly improved yields compared to using aniline as catalyst (Scheme 4.3). Similarly, keto-Halβ was ligated with **4.2** or **4.3** yielding rho- or Cy5-Halβ. The purity of each peptide was assessed by analytical RP-HPLC (Figure 4.20) and analysis by MALDI-TOF MS showed that the aminooxy-fluorophore added only once (Figure 4.21). Reaction of Δ1-lacticin 481, which lacked the N-terminal ketone, with **4.2** did not yield an addition product, indicating the fluorophore was incorporated at the N-terminus of the lantibiotic analogue. Reaction of the analogue keto-lacticin 481-E13A with **4.2** also resulted in the desired rho-lacticin 481-E13A (Figure 4.21).

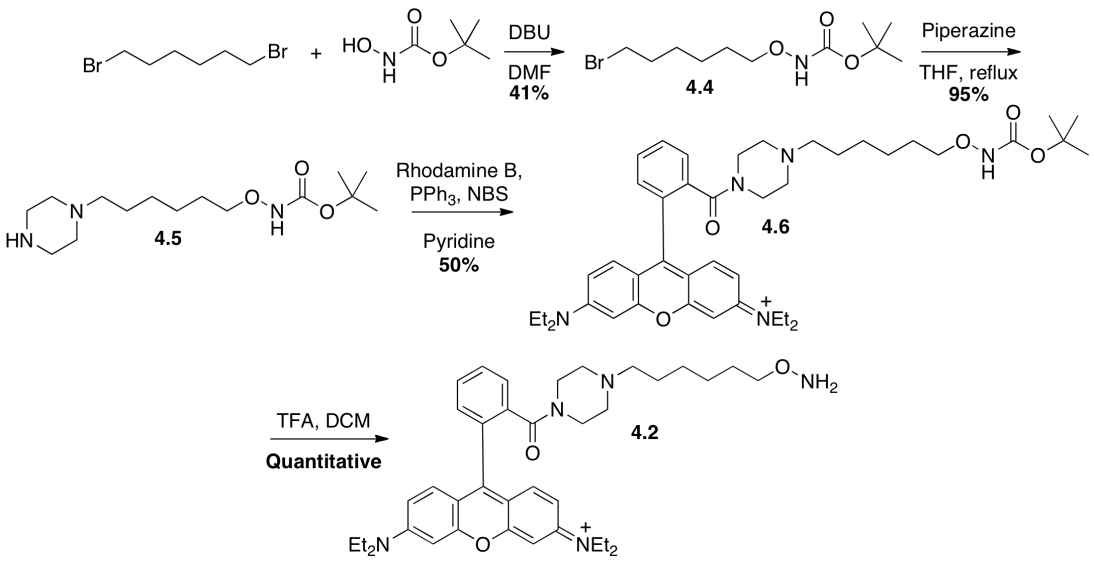

Scheme 4.4. Synthetic scheme towards aminooxy-rhodamine (**4.2**).

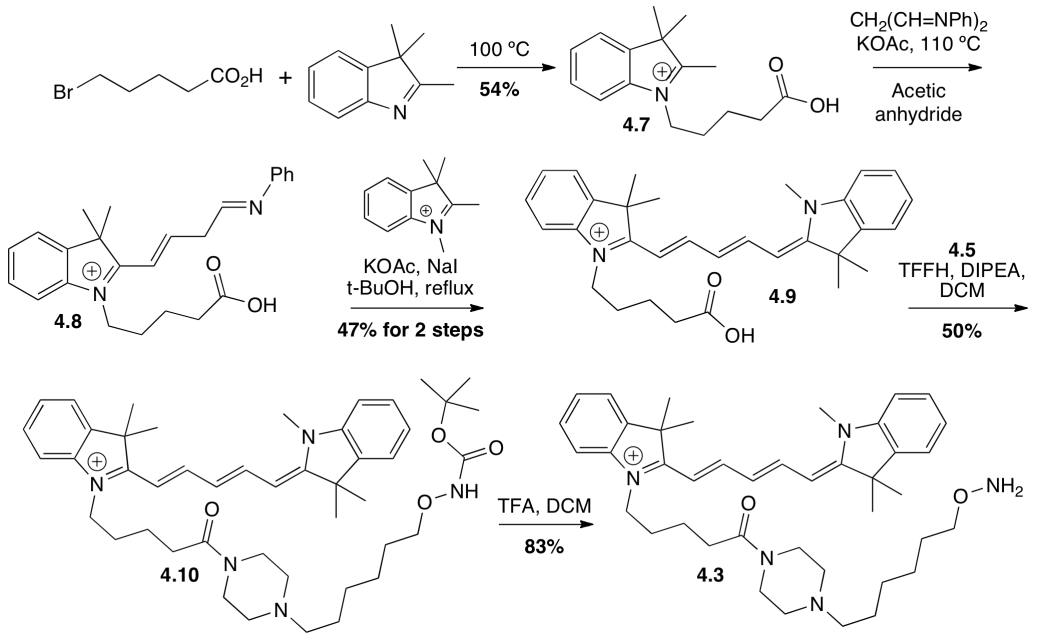

Scheme 4.5. Synthetic scheme towards aminooxy-Cy5 (**4.3**).

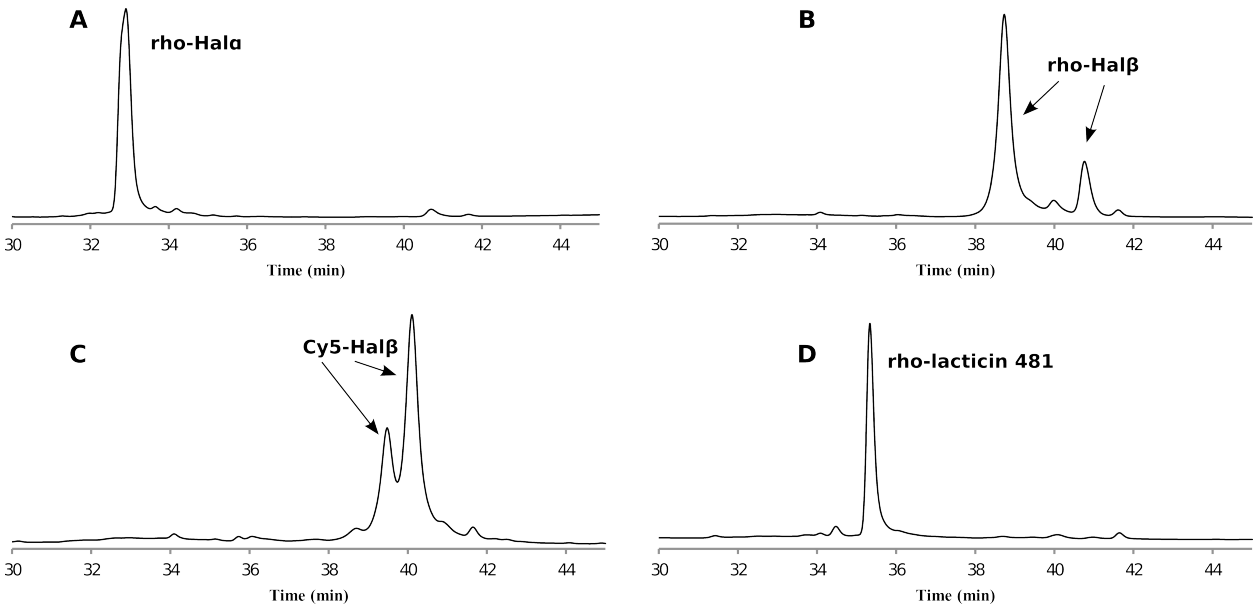

Figure 4.20. Analytical RP-HPLC traces of fluorescent lantibiotics. A) rho-Halα, B) rho-Halβ, C) Cy5-Halβ, and D) rho-lacticin 481. The two isobaric products observed for rho- and Cy5-Halβ presumably represent the two diastereomers formed during oxime bioconjugation. We did not attempt to separate these two products.

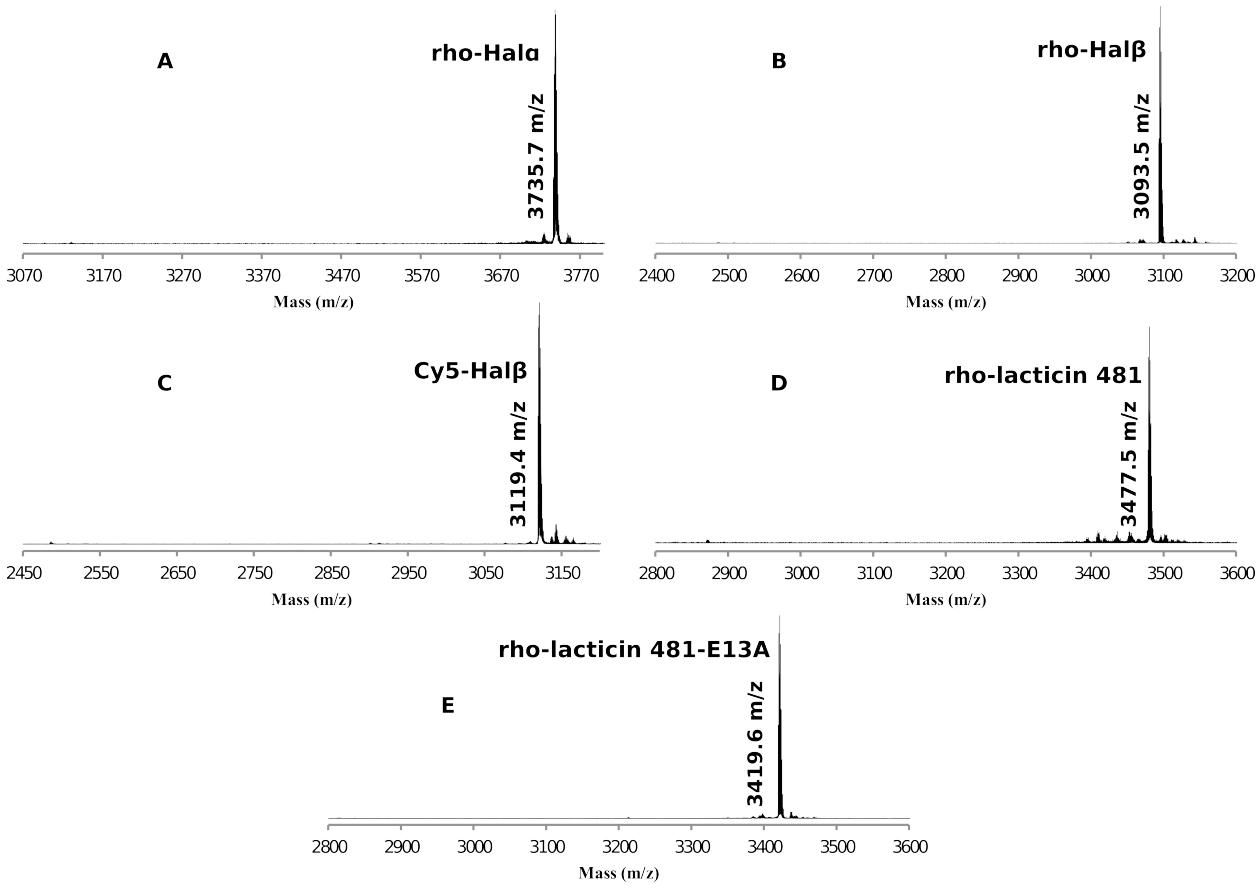

Figure 4.21. MALDI-TOF mass spectra of fluorescent lantibiotics. A) rho-Halα ($[M+H]^+$ calc'd = 3735.7 Da.), B) rho-Halβ ($[M+H]^+$ calc'd = 3093.5 Da.), C) Cy5-Halβ ($[M+H]^+$ calc'd = 3119.5 Da.), D) rho-lacticin 481 ($[M+H]^+$ calc'd = 3477.6 Da.), and E) rho-lacticin 481-E13A ($[M+H]^+$ calc'd = 3419.6 Da.).

The bioactivities of the fluorescently labeled peptides were tested by agar diffusion and liquid media growth assays and compared to their respective wt peptides. Rho-lacticin 481 was active at micromolar concentrations against *B. subtilis* 168 (Figure 4.19B) and *L. lactis* HP but with a minimum inhibitory concentration (MIC) that was increased 6-fold compared to wt lacticin 481 (Table 4.1). Rho-Halα and rho/Cy5-Halβ displayed antimicrobial activity against *B. subtilis* 168 when added together with their unlabeled partner (Halβ and Halα, respectively), but

exhibited only low level bioactivity when administered alone, as is also observed for the wt peptides (Figure 4.19C). The MICs of rho-Halα when coincubated with wt Halβ and of rho- or Cy5-Halβ when coincubated with wt Halα were increased about 8 to 15-fold compared to the wt peptides (Table 4.1). Although, not surprisingly, the bioactivities of the analogues were decreased, a similar mode of action of the fluorescently labeled peptides compared to the wt lantibiotics is suggested by additional experiments discussed later.

Peptide (indicator strain)	**MIC (μM)**
lacticin 481 (*L. lactis* HP)	2.50
rho-lacticin 481 (*L. lactis* HP)	15.0
wt Halα w/ 2.5 μM wt Halβ (*B. subtilis* 168)	0.16
wt Halβ w/ 2.5 μM wt Halα (*B. subtilis* 168)	0.16
rho-Halα w/ 2.5 μM wt Halβ (*B. subtilis* 168)	1.25
rho-Halβ w/ 2.5 μM wt Halα (*B. subtilis* 168)	1.25
Cy5-Halβ w/ 2.5 μM wt Halα (*B. subtilis* 168)	2.50

Table 4.1. Minimum inhibitory concentrations of wt and fluorescently labeled lantibiotics against *B. subtilis* 168 or *L. lactis* HP. When determining the MIC of Halα or Halβ and analogues, the concentration of one peptide was held constant at 2.5 μM while the other was varied. Neither wt Halα nor wt Halβ were active by themselves against *B. subtilis* 168 cells at a concentration of 2.5 μM.

4.2.6. Lacticin 481 binds to lipid II on cell surfaces.

Lacticin 481 was recently shown to inhibit the transglycosylation step of peptidoglycan biosynthesis, most likely by binding to the cell wall precursor lipid II.[22] This hypothesis is also supported by a recent study that showed using ITC that nukacin ISK-1, a close structural analogue of lacticin 481, binds to lipid II.[63] Therefore, analysis of the interaction of rho-lacticin

481 with sensitive bacteria by confocal fluorescence microscopy was anticipated to show preferential staining of lipid II.

Previous studies of the peptidoglycan architecture in *B. subtilis* using fluorescently labeled vancomycin and ramoplanin, two lipid II-binding antibiotics, demonstrated intense staining at the midcell, corresponding to new division sites, and at the poles, corresponding to old division sites.[64,65] In addition, staining of the bacterial sidewalls was observed as peripheral dots connected by weak transverse bands, suggesting a ring-type structure. More recently, two research groups used the cellular biosynthetic machinery to incorporate alkyne, azide, and fluorescently functionalized D-alanine analogues into the lipid II of several bacteria, including *B. subtilis*.[66,67] The alkyne and azide analogues were then visualized in living cells with azide- or alkyne-linked fluorophores via click chemistry. Analysis of these bacteria by fluorescence microscopy also showed a punctate distribution of the lipid II analogues with intense bands at the midcell of the bacteria. Thus, these metabolic labeling studies provide an independent and complementary determination of lipid II localization. In the current work, rho-lacticin 481 was incubated with *B. subtilis* 168 at sublethal concentrations and the staining pattern was examined by confocal fluorescence microscopy (Figure 4.22A). In most bacteria, the fluorescence intensity was greatest at midcell (Figure 4.22A, green arrows). We also observed peripheral dots with weak transverse bands along the longitudinal axis of the rod-shaped bacilli. These results are very similar to the patterns seen with the lipid II-binding antibiotics and fluorescent lipid II analogues in *B. subtilis*, strongly suggesting that lacticin 481 binds lipid II in living cells.

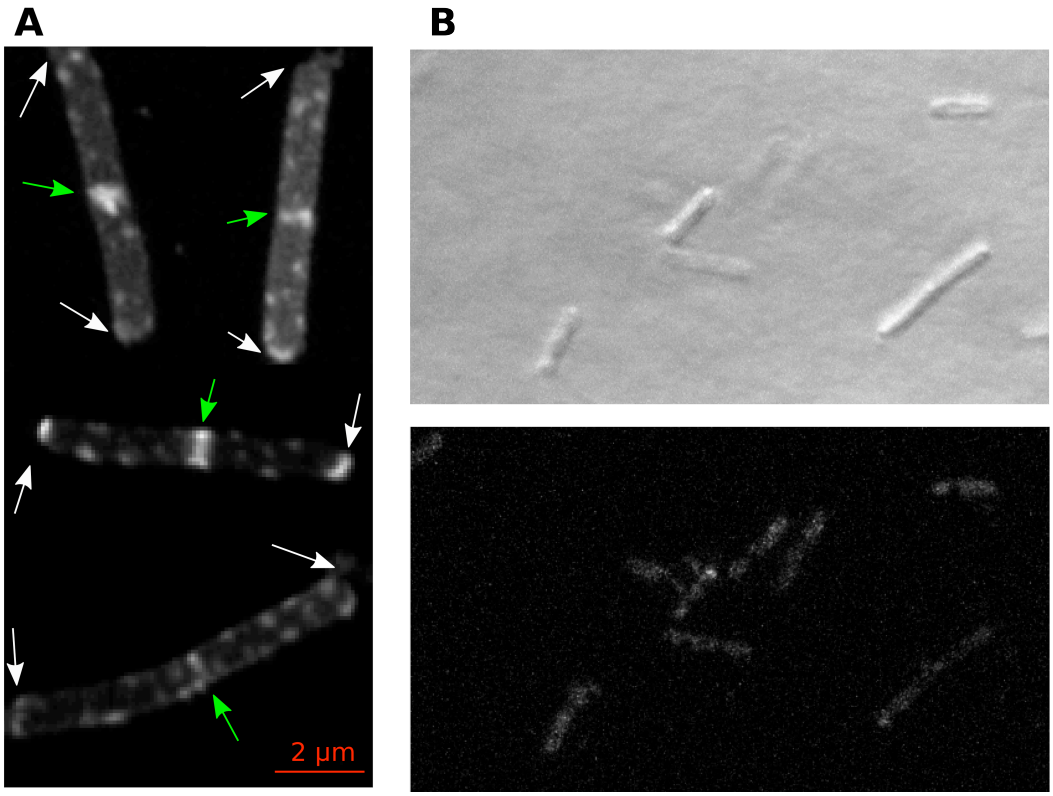

Figure 4.22. Cellular distribution of fluorescent lacticin 481 analogues. A) Staining of *B. subtilis* 168 with rho-lacticin 481 (1 µM). B) Staining of *B. subtilis* 168 with rho-lacticin 481-E13A (top, brightfield; bottom, rhodamine channel). New and old cellular division sites are represented by green and white arrows, respectively. Figure adapted from Bindman and van der Donk.[1]

4.2.7. Lacticin 481-E13A does not localize in a specific pattern on cell surfaces.

A conserved Glu/Asp is found in several class II lantibiotics and is integral to their bioactivities.[15,17,18,21,22] In lacticin 481, this residue is Glu13 and a Glu13Ala mutant abolished antimicrobial activity.[22] Thus, a fluorescent analogue of this mutant was used to confirm that the observed localization of rho-lacticin 481 is mediated by the peptide and not the fluorophore. rho-Lacticin 481-E13A was incubated with *B. subtilis* 168, and the staining pattern was examined by confocal fluorescence microscopy. Very little staining was observed (Figure 4.22B), even at

concentrations 20 times larger than that used to stain *B. subtilis* 168 with rho-lacticin 481, demonstrating that Glu13 is essential for the localization of lacticin 481 and that the rhodamine in rho-lacticin 481 is not responsible for the observed localization pattern.

4.2.8. Haloduracin β colocalizes with haloduracin α.

The two components of haloduracin act synergistically to achieve their bioactivity. Halα binds to lipid II with high affinity to inhibit peptidoglycan biosynthesis.[21] Halβ either does not bind to lipid II or has a much reduced affinity, but it is required for optimal bioactivity. These and other observations[68-70] have led to a model that Halα binds lipid II and that this complex is recognized by Halβ, but experimental evidence of the binding interactions of Halβ are lacking.

To probe Halα localization on bacterial cells, we added rho-Halα at sublethal concentrations to *B. subtilis* 168 cells and analyzed the cells, fixed to a cover slip by 1% agarose, by confocal fluorescence microscopy. Similar to the results seen with rho-lacticin 481, the most intense fluorescent signal was at midcell (Figure 4.23A). In addition, a staining pattern of peripheral dots with weak transverse bands was seen on the bacterial sidewall, consistent with binding of Halα to lipid II. However, when the experiment was repeated in the presence of 50 equivalents of wt Halα, no fluorescent staining was observed, suggesting that the unlabeled peptide competes for the same binding site on the cell surface (Figure 4.24A). When rho-Halα was preincubated with 50 equivalents of wt Halβ (25 μM), rho-Halα still localized at the midcell and poles (Figure 4.24B), but the transverse bands were less frequently observed. These observations suggest that Halβ does not compete with Halα for its binding target. We next administered Cy5-Halβ to *B. subtilis* cells. Consistent with the model, no specific fluorescent pattern was observed (Figure 4.23B). Some non-specific labeling was seen, likely because of a

hydrophobic interaction between the lantibiotic and bacterial membrane. This interaction is expected to increase upon addition of the hydrophobic Cy5 functionality. Interestingly, when Cy5-Halβ and unlabeled Halα were added in concert, the Halβ analogue did localize in a specific pattern (Figure 4.23C). Preferential staining was observed at midcell and poles. Furthermore, coincubation of rho-Halα and Cy5-Halβ with *B. subtilis* cells showed colocalization of Halα and Halβ (Figure 4.23D). To rule out a role for the cyanine group of Cy5-Halβ, the microscopy experiments were also conducted with rho-Halβ. As anticipated, rho-Halβ localized in a site-specific pattern on *B. subtilis* cells only in the presence of Halα (Figure 4.25A). The localization of rho-Halβ in the presence of wt Halα was not altered in the presence of 50 equivalents of unlabeled Halβ (25 μM) (Figure 4.25B); higher concentrations could not be used because of toxicity to the cells, which is already starting to be visible at 25 μM Halβ. Although this result was not anticipated, it may be due to an increased binding affinity to the bacterial membrane of rho-Halβ compared to wt Halβ. Thus, the addition of 50 equivalents of wt Halβ may not be enough to outcompete the fluorescently labeled analogue.

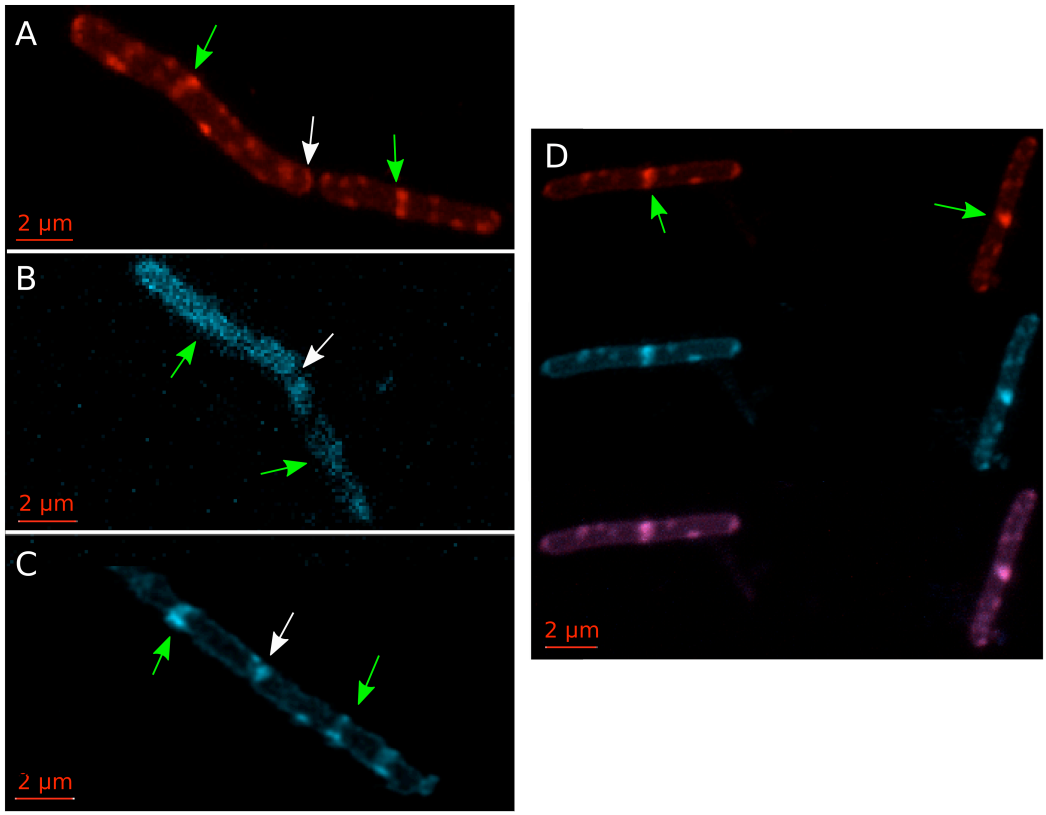

Figure 4.23. Cellular distribution of haloduracin analogues. A) Staining of *B. subtilis* 168 with 0.25 µM rho-Halα (red). B) Staining of *B. subtilis* 168 with 4 µM Cy5-Halβ (blue). C) Staining of *B. subtilis* 168 with 1 µM each of wt Halα + Cy5-Halβ (blue). D) Staining of *B. subtilis* 168 with 1 µM each of rho-Halα (red) + Cy5-Halβ (blue). Top, rhodamine channel (red); center, Cy5 channel (blue); bottom, merge of rhodamine and Cy5 (purple). New and old cellular division sites are represented by green and white arrows, respectively. Figure adapted from Bindman and van der Donk.[1]

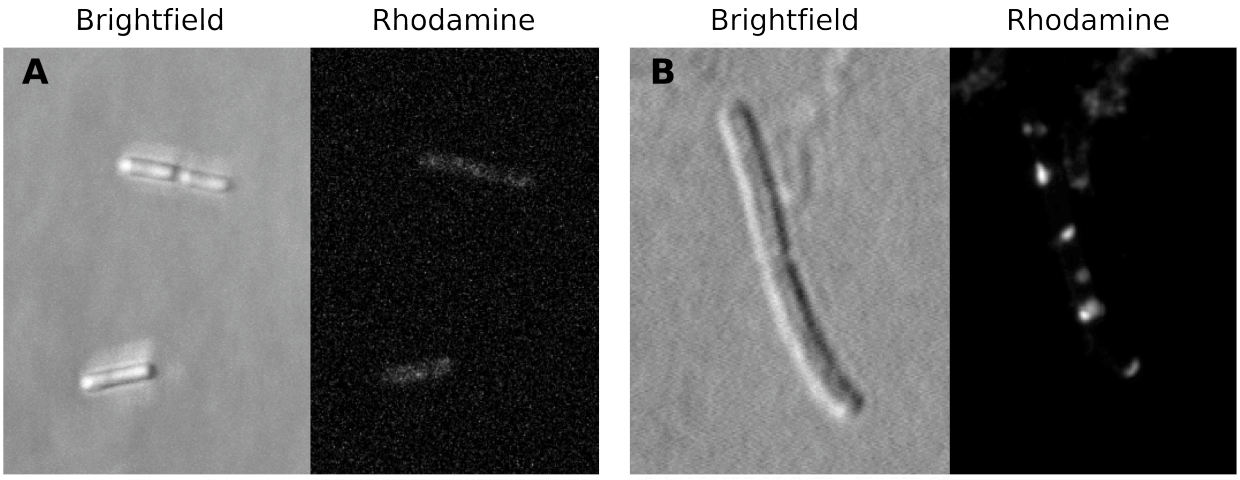

Figure 4.24. Cellular distribution of rho-Halα. A) Confocal fluorescence microscopy of *B. subtilis* 168 stained with 0.5 μM rho-Halα (white) preincubated with wt Halα (25 μM). B) Confocal fluorescence microscopy of *B. subtilis* 168 stained with 0.5 μM rho-Halα (white) preincubated with wt Halβ (25 μM).

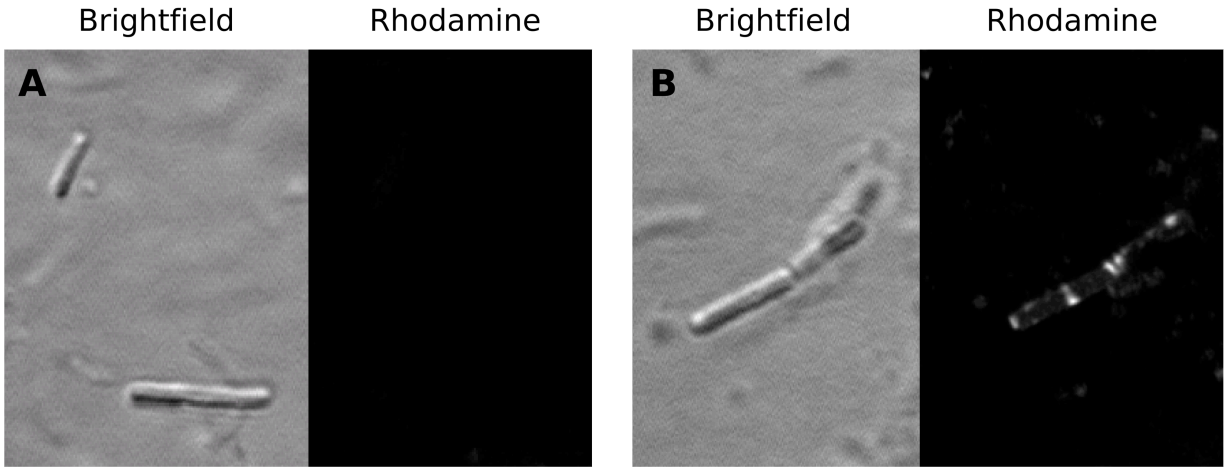

Figure 4.25. Cellular distribution of rho-Halβ. A) Confocal fluorescence microscopy of *B. subtilis* 168 stained with 0.5 μM rho-Halβ. B) Confocal fluorescence microscopy of *B. subtilis* 168 stained with 0.5 μM rho-Halβ (white) preincubated with wt Halα (0.5 μM).

4.3. SUMMARY AND OUTLOOK

This study demonstrates the successful use of the biosynthetic machinery of six different lanthipeptides to introduce a ketone group at their N-termini, and illustrates the utility of the method for site-specific labeling of this class of compounds. This strategy has a distinct advantage over other lanthipeptide-specific labeling techniques, such as introduction of non-proteinogenic amino acids,[42,71] because of its generality, scalability, and relatively high yields. Several structurally unique N-termini were successfully modified including lanthipeptides containing an N-terminal disulfide bond (Halα) and an N-terminal lanthionine crosslink (Halβ). To produce keto-Pcn2.8 and keto-Halα, the only perturbation compared to our previously developed lanthipeptide coexpression system was the insertion of a Thr directly after the proteolytic cleavage site. In these peptides the modification enzyme successfully dehydrated the inserted Thr, and proteolytic removal of the leader peptide yielded the lanthipeptide with an N-terminal ketone. In the biosynthesis of Pcn1.7, keto-Halβ, and nisin, the inserted Thr was successfully dehydrated but the cleavage of the leader peptide from the core peptide occurred at an undesired location, giving the modified core peptide with an N-terminal amino acid overhang originating from the leader peptide. This problem was overcome in Halβ by inserting an Ala directly after the N-terminal Thr, which distanced the proteolytic cleavage site from the lanthionine ring at the N-terminus of Halβ (Figure 4.2). The protease, GluC, could then cleave the leader peptide at the desired site, presumably because the D-stereocenter of the lanthionine ring no longer interfered with protease binding. Conversely, in ProcA1.7 the two amino acids immediately preceding the inserted Thr were mutated to Leu and the leader peptide was removed in a two-step procedure of treatment with GluC and aminopeptidase. This two-step procedure was also utilized in the biosynthesis of keto-nisin-2, where most of the leader peptide was

removed with trypsin followed by hydrolysis of the N-terminal Leu by aminopeptidase. The biosynthesis of keto-lacticin 481 proved to be the most challenging and required distancing the inserted Thr from the leader peptide and introduction of two extra copies of the *lctM* gene into the coexpression system.

Using the fluorescent labeling strategy, we were able to visualize the distribution of lacticin 481 and haloduracin on *B. subtilis* 168 cells. The most intense labeling with rho-lacticin 481 was at the new cell division sites at the bacterial midcell, which we believe represents the relatively large amounts of lipid II present during cell division. In most cases, rho-lacticin 481 also stained the sidewall of *B. subtilis* as peripheral dots, which in some images could be seen to be linked by transverse bands. In contrast, incubation of *B. subtilis* with the Glu13Ala mutant of lacticin 481 did not result in a specific pattern, consistent with the previous proposals that this conserved residue is critical to mediate interactions with lipid II in a variety of lantibiotics.[15,17,18,21,22] The results with the fluorescently labeled lacticin 481 mutant also strongly suggest that the observed specific localization pattern is a consequence of the activity of lacticin 481 and not the fluorophore.

We also gained a deeper understanding of the mode of action of the two-component lantibiotic haloduracin using the fluorescently labeled analogues. Incubation of sublethal concentrations of rho-Halα with *B. subtilis* cells showed a staining pattern similar to that seen with rho-lacticin 481, consistent with binding to lipid II. This conclusion is also supported by the observation that unlabeled wt Halα abolished the specific labeling pattern of rho-Halα. Rho- and Cy5-Halβ did not exhibit a specific localization pattern unless wt Halα was also present. In the presence of Halα, the fluorescently labeled Halβ analogues localized at the poles and midcell, suggesting co-localization. Localization in transverse bands was also observed but less

frequently for unknown reasons. Simultaneous use of rho-Halα and Cy5-Halβ showed co-localization at the midcell and poles. Fluorescently labeled Halβ in the presence of Halα could not be displaced from these sites by unlabeled Halβ at the maximum non-toxic concentrations achievable, possibly because of the higher affinity of the fluorescently labeled analogues for the membrane. Collectively, these results support the previously proposed model of synergistic activity, in which Halα binds to lipid II, followed by the binding of Halβ to the Halα-lipid II complex (Figure 4.26), although the resolution of confocal microscopy is such that co-localization in these experiments does not necessarily mean complex formation. Further experiments will be needed to confirm or refute a direct molecular interaction between Halβ and the Halα-lipid II complex.

In summary, we report a general labeling strategy for lanthipeptides, which may be used for studies on family members for which the mode(s) of action and targets are currently unknown, such as the prochlorosins and the Pep5/epilancin class of lantibiotics. Potential applications also include use of ^{99m}Tc-labeled lanthipeptides for imaging purposes[3] and introduction of photoaffinity probes.

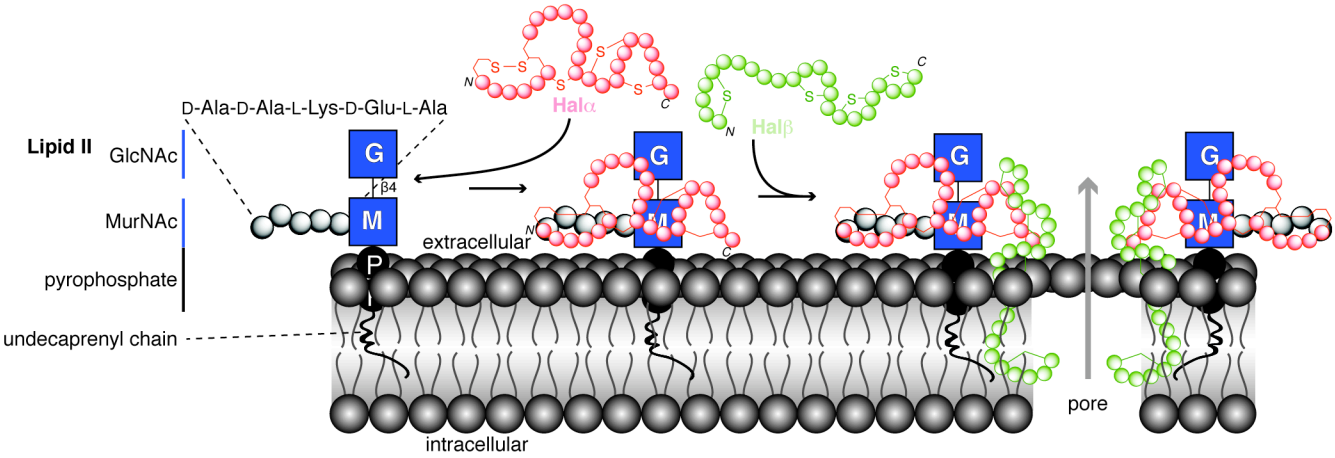

Figure 4.26. Proposed mode of action of the two-component lantibiotic haloduracin. First, Halα associates with the cell wall precursor lipid II. Then, Halβ binds to the Halα-lipid II complex causing pore formation. GlcNAc, *N*-acetylglucosamine (blue squares labeled G); MurNAc, *N*-acetylmuramic acid (blue squares labeled M). The molecular details of the binding interaction of Halα and lipid II are not known. Figure adapted from Bindman and van der Donk.[1]

4.4. EXPERIMENTAL

4.4.1. Materials.

All compounds used in the synthetic schemes were purchased from Sigma Aldrich with the exception of propargyl bromide (TCI America), *p*-phenylenediamine (TCI America), *N*-Boc-hydroxylamine (Alpha Aesar), sodium iodide (J.T. Baker Chemical Company), tetramethylfluoroformamidinium hexafluorophosphate (TFFH) (Chem Impex) and 4-(2-hydroxyethyl)-1-piperazineethanesulfonic acid (HEPES) (Fisher Scientific). Solvents commonly used in peptide purification, including trifluoroacetic acid (TFA) and acetonitrile (MeCN), were obtained in HPLC grade or better and used directly without further purification. Oligonucleotide primers used for molecular cloning were purchased from Integrated DNA Technologies. Phusion High-Fidelity DNA polymerase, T4 DNA ligase, DpnI, and all restriction endonucleases were

purchased from New England Biolabs. Gel extraction, plasmid miniprep, and PCR purification kits were purchased from QIAGEN. Terrific broth (TB) and LB broth were purchased from Fisher Scientific. Endoproteases LysC, GluC, and trypsin were purchased from Roche Applied Science and aminopeptidase from *Aeromonas proteolytica* was purchased from Sigma Aldrich (A8200). Other items procured for cell culture and peptide work included isopropyl β-D-1-thiogalactopyranoside (IPTG) (Gold Biotechnology), kanamycin monosulfate (IBI Scientific), chloramphenicol (IBI Scientific), spectinomycin dihydrochloride pentahydrate (Sigma Aldrich), ampicillin sodium salt (Fisher Scientific) and tris-(2-carboxyethyl)phosphine·HCl (TCEP·HCl) (Molecular Probes). Agarose with low gelling temperature used in bacterial imaging was purchased from Sigma Aldrich. MALDI-TOF MS analyses were conducted at the Mass Spectrometry Facility (UIUC) using an UltrafleXtreme TOF/TOF (Bruker Daltonics) or Voyager-DE STR. Fluorescence confocal microscopy analyses were conducted at the core facility at the Institute of Genomic Biology (UIUC) using a Zeiss LSM 700 Confocal Microscope. Rhodamine B analogues were excited using a 555 nm laser and emission was detected at wavelengths between 560 and 625 nm. Cy5 analogues were excited using a 639 nm laser and emission was detected at wavelengths between 640 and 735 nm. Images were deconvoluted using the program AutoQuant X3 (Media Cybernetics).

4.4.2. Synthesis of aminooxy derivatives 4.1, 4.2, and 4.3.

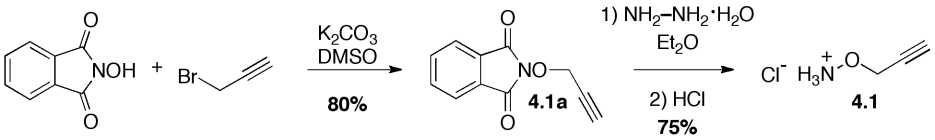

Synthetic design of aminooxy-alkyne (4.1).

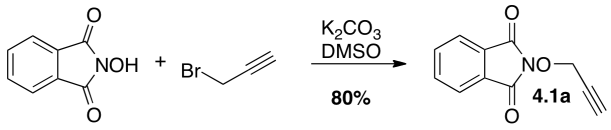

2-(Prop-2-yn-1-yloxy)isoindoline-1,3-dione (4.1a).

Into a 50 mL round-bottomed flask was added *N*-hydroxyphthalimide (2.78 g, 17.1 mmol, 1 equiv) followed by DMSO (30 mL). To this solution was added K_2CO_3 (1.52 g, 11.0 mmol, 0.64 equiv) and the reaction immediately turned dark red. Finally, propargyl bromide (4.0 g, 3.0 mL, 33.6 mmol, 1.92 equiv) was added dropwise and the solution was stirred overnight at room temperature. The solid residue was then removed by filtration followed by the addition of ice water (200 mL) to the filtrate. The resulting solid was filtered and recrystallized from hot ethanol yielding compound **4.1a** as a light brown solid (2.7 g, 80%). Characterization data matched that previously reported.[72] *See also Notebook VIII, Page 53.*

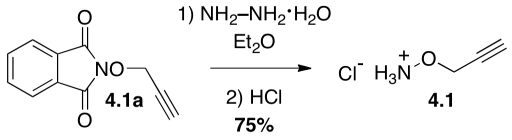

***O*-(Prop-2-yn-1-yl)hydroxylamine (4.1).**

Into a 25 mL round-bottomed flask was added **4.1a** (500 mg, 2.5 mmol, 1 equiv) followed by hydrazine monohydrate (64-65%, 0.135 mL, 139.3 mg, 2.78 mmol, 1.11 equiv). To

this mixture was added diethyl ether (2.5 mL), the large clumps were broken with a spatula, and the reaction mixture was stirred for 2 h at room temperature. The solid residue was then removed by filtration, and HCl in ether (2 M, 1.8 mL) was added to the filtrate with continuous stirring. After a few moments a solid precipitated from the ethereal solution. The reaction was stirred for an additional 2 h and the resulting solid was filtered and dried yielding **4.1** (200 mg, 75%) as a light yellow solid. Characterization data matched that previously reported.[73] *See also Notebook XII, Page 07*.

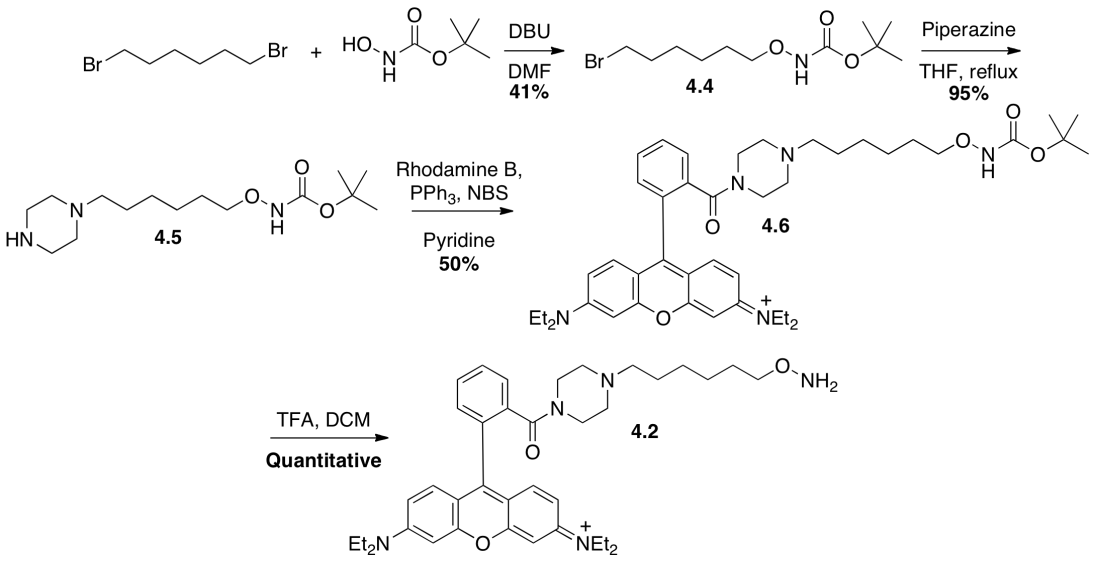

Synthetic design of aminooxy-rhodamine B (4.2).

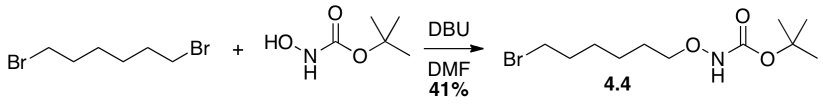

***tert*-Butyl-(6-bromohexyl)oxycarbamate (4.4).**

Into a 50 mL round-bottomed flask was added *N*-Boc-hydroxylamine (0.67 g, 5 mmol, 1 equiv) in DMF (5 mL). To this solution was added 1,8-diazabicyclo[5.4.0]undec-7-ene (DBU)

(0.91 g, 0.90 mL, 6.0 mmol, 1.2 equiv). The mixture was then slowly added to a solution of 1,6-dibromohexane (2.44 g, 1.54 mL, 10 mmol, 2 equiv) in DMF (5 mL) via cannula. The reaction was stirred overnight at room temperature. The following morning more 1,6-dibromohexane (200 μL) and DBU (200 μL) were added and the reaction was again stirred overnight. The DMF was then concentrated to 5 mL under reduced pressure, the solution was combined with 9:1 EtOAc:MeOH (50 mL), and was washed with H_2O (3 × 30 mL). The organic layer was dried with $MgSO_4$ and concentrated. The product was purified by SiO_2 gel column chromatography. The column was washed with 100% hexanes (200 mL), and 5% EtOAc in hexanes (100 mL) and product eluted in 10% EtOAc in hexanes (100 mL) (R_f = 0.5, 3:1 EtOAc:Hex) yielding **4.4** (600 mg, 41%) as a clear oil. Characterization data matched that previously reported.[59] *See also Notebook XII, Page 13*

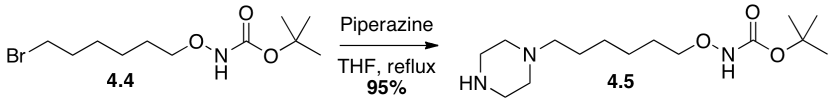

***tert*-Butyl (6-(piperazin-1-yl)hexyl)oxycarbamate (4.5).**

Into a 50 mL round-bottomed flask equipped with a reflux condenser was added piperazine (585.6 mg, 6.8 mmol, 10 equiv) in THF (5 mL) and the solution was heated to reflux. To the heated solution was added **4.4** (200 mg, 0.68 mmol, 1 equiv) in THF (5 mL) via a syringe pump over 30 min. The reaction was stirred at reflux overnight. The solid residue was filtered and the supernatant was concentrated and partitioned between Et_2O (30 mL) and sat. aqueous NaCl (30 mL). The aqueous layer was extracted with Et_2O (3 × 30 mL) and the combined organic layers were dried with $MgSO_4$ and concentrated under reduced pressure yielding **4.5** (195 mg, 95%, R_f = 0.5 (4:1 EtOAc:Hex with 0.5% NEt_3)) as a yellow oil. *See also Notebook XII, Page 16.*

^{1}H NMR: (500 MHz, $CDCl_3$) δ = 3.81-3.78 (t, J = 6.5 Hz, 2H); 2.87-2.85 (t, J = 5 Hz, 4H); 2.37 (bs, 4H); 2.28-2.25 (m, 2H); 1.62-1.56 (p, J = 6.9 Hz, 2H); 1.49-1.43 (m, 11H); 1.37-1.25 (m, 5H); 1.22 (s, 1H).

^{13}C NMR: (500 MHz, $CDCl_3$) δ = 157.2, 81.5, 76.9, 59.5, 54.7, 46.1, 28.5, 28.2, 27.6, 26.7, 26.1.

HRMS $[M+H]^+$ $C_{15}H_{32}N_3O_3$ calc'd = 302.2444, found = 302.2451.

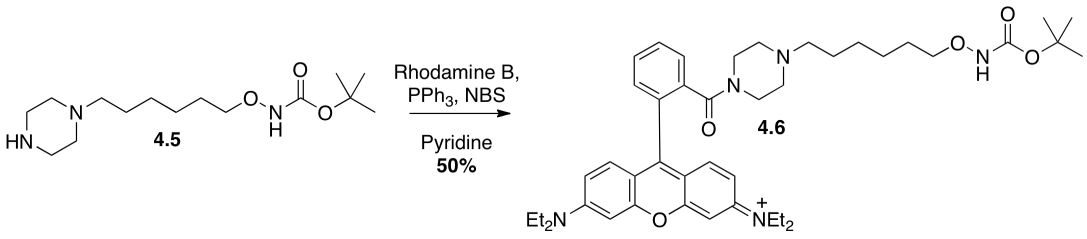

Boc-protected aminooxy-rhodamine B (4.6).

Into a 50 mL round-bottomed flask was added rhodamine B (312 mg, 0.704 mmol, 2 equiv), triphenylphosphine (277 mg, 1.056 mmol, 3 equiv) and dry dichloromethane (DCM) (7 mL, from a solvent dispensing system (SDS)). This solution was cooled to 0 ^{o}C, *N*-bromosuccinimide (220 mg, 1.232 mmol, 3.5 equiv, recrystallized) was added, and the solution was stirred for 15 min. At this time, **4.5** (107 mg, 0.352 mmol, 1 equiv) and pyridine (97.5 mg, 0.1 mL, 1.232 mmol, 35 equiv) in dry DCM (5 mL) were added and the reaction was allowed to warm to room temperature and stirred overnight. The solvent was then removed under reduced pressure, and the residue partitioned between EtOAc (50 mL) and saturated aqueous $NaHCO_3$ (50 mL). The aqueous layer was extracted with EtOAc (6 × 30 mL), and the combined organic layers were dried with $MgSO_4$ and concentrated under reduced pressure. The product was purified by SiO_2 gel column chromatography by dissolving in 5% dry methanol (from SDS) in dry DCM (5 mL). The column was washed with 5% dry methanol in DCM (200 mL) and

product was eluted with 10% dry methanol in DCM (200 mL). The fractions containing product were concentrated under reduced pressure yielding **4.6 (**128 mg, 50% yield) as a metallic red solid. Characterization data matched that previously reported.[59] *See also Notebook X, Page 43.*

Note: Dry MeOH was necessary because propionaldehyde and formaldehyde impurities in technical grade MeOH react with **4.2**.

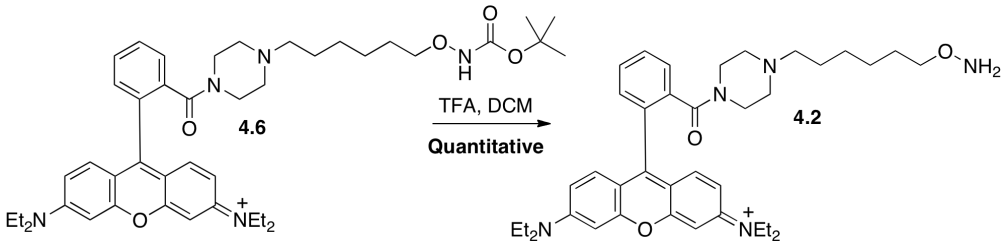

Aminooxy-rhodamine B (4.2).

Into a 20 mL scintillation vial was added **4.6** (10 mg) in dry DCM (2 mL). To this solution was added TFA (2 mL) and the solution was left unperturbed for 5 min, at which time the solvent was removed under reduced pressure. DCM (5 mL) was then added, and the solvent was again removed under reduced pressure. The addition of DCM and concentration to dryness was repeated three times, at which point the metallic red solid was dried at a vacuum line (8.5 mg, quantitative). Characterization data matched that previously reported.[59] *See also Notebook X, Page 44.*

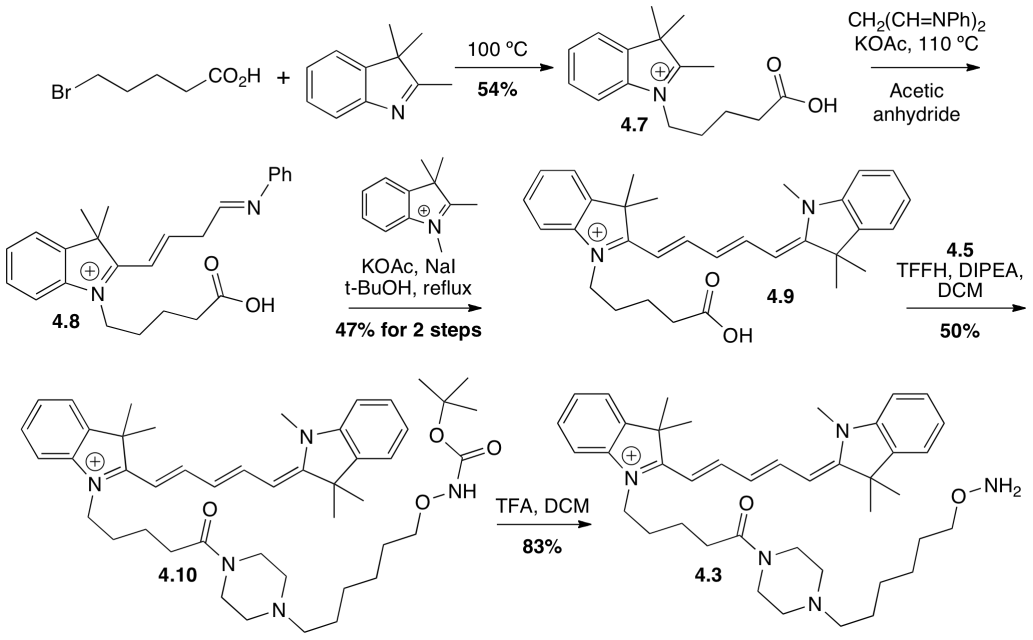

Synthetic design of aminooxy-Cy5 (4.3).

Aminooxy-Cy5 was synthesized following published procedures with some variations.[61]

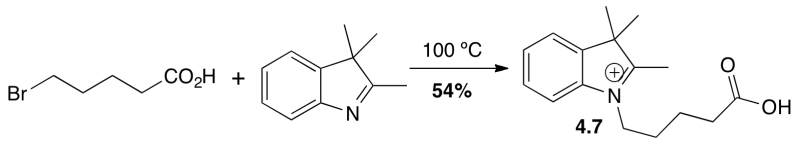

1-(4-Carboxybutyl)-2,3,3-trimethyl-3H-indol-1-ium (4.7).

Into a 15 mL round-bottomed flask was added 5-bromovaleric acid (1.58 g, 1.59 mL 9.94 mmol, 1.2 equiv) and 2,3,3-trimethylindolenine (1.5 g, 8.29 mmol, 1.0 equiv). The reaction was heated to 100 ºC with stirring for 3 h. The red solid was treated with 6 mL of EtOAc, heated at reflux for 2 min, and cooled allowing the solid product to settle at the bottom of the reaction vessel. The red supernatant was then removed from the solid and discarded. This solvent treatment and removal was repeated once more with EtOAc and six times with acetone. After the final wash, the light pink solid was filtered and dried yielding **4.7** (1.17 g, 54%). Characterization data matched that previously reported.[61] *See also Notebook XII, Page 10.*

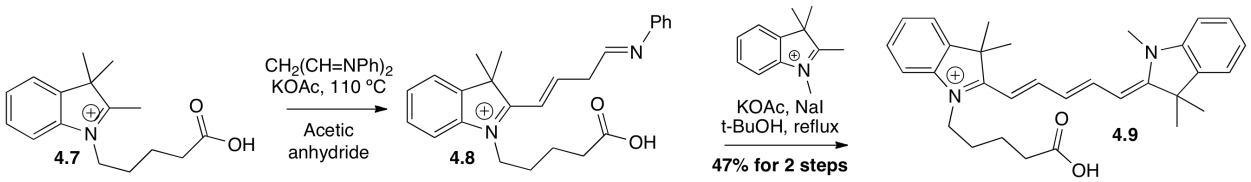

***N*-Valeric acid-Cy5 (4.9).**

Into a 25 mL round-bottomed flask was added malonaldehyde bis(phenylimine) monohydrochloride (466 mg, 1.93 mmol) and KOAc (183 mg, 2.0 mmol). To this solution was then added acetic anhydride (10 mL) and the mixture was heated to 110 ºC for 15 min. Compound **4.7** (100.0 mg, 0.32 mmol) was then added in small aliquots over 30 min until the reaction had a light green color. (*Note:* the color of the solution of the product of a single addition of **4.7** to malonaldehyde bis(phenylimine) monohydrochloride was yellow, whereas the color of the product of addition of a second molecule of **4.7** was blue. Hence, when the solution turned green, the addition of compound **4.7** was terminated.) The reaction was stirred at 110 ºC for 2 h at which point the green solution was concentrated by azeotropic removal of acetic anhydride with heptanes (30 mL aliquots until dryness) on a rotary evaporator. The resulting solid was dissolved in DCM and product was extracted with sat. aqueous $NaHCO_3$ (2 × 50 mL). The aqueous layer was then acidified with 1 M HCl (until the pH reached 2-3) and product was extracted with DCM (2 × 100 mL). The organic layer was concentrated yielding crude intermediate **4.8** (76 mg). To the intermediate was added KOAc (40 mg, 0.41 mmol, 2.0 equiv), NaI (450 mg, 3.0 mmol, 15 equiv), and *tert*-butanol (12 mL). 1,2,3,3-Tetramethyl-3H-indolium iodide (121 mg, 0.4 mmol, 2.0 equiv) was then added and the reaction was stirred under reflux for 1.5 h. The reaction was concentrated to dryness and the metallic blue solid residue was dissolved in DCM (50 mL), washed with saturated aqueous NaCl (2 × 50 mL), dried with $MgSO_4$, and concentrated under reduced pressure. Product was purified by silica gel column chromatography using a gradient from 2-10% methanol in DCM. Product eluted between 5-10%

methanol in DCM and was concentrated yielding **4.9** as a metallic blue solid (70 mg, 47% in two steps; R_f = 0.15 (10% MeOH in DCM)). Characterization data matched that previously reported.[61] *See also Notebook XII, Page 60.*

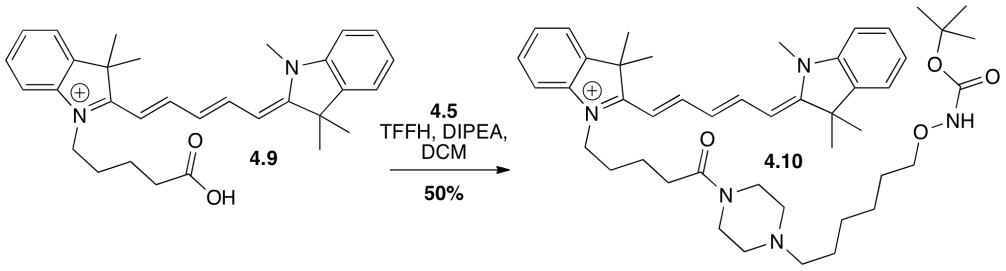

Boc-protected aminooxy-Cy5 (4.10).

Into a 25 mL round-bottomed flask was added **4.9** (20 mg, 0.04 mmol, 1.0 equiv) in DCM (8 mL). To this solution was added tetramethylfluoroformamidinium hexafluorophosphate (TFFH) (13.6 mg, 0.04 mmol, 1.0 equiv) and DIPEA (5.56 mg, 0.04 mmol, 1.0 equiv) and the reaction was stirred for 15 min. At this time, **4.5** (38 mg, 0.12 mmol, 3.0 equiv) was added in DCM (2 mL) and the reaction was stirred for an additional 30 min. The solvent was then removed under reduced pressure, and the crude product purified by silica gel column chromatography using a gradient from 0-7% dry MeOH in DCM. The product fractions were concentrated yielding **4.10** as a dark metallic blue solid (16 mg, 50%; Rf = 0.2 (5% MeOH in DCM)). *See also Notebook XI, Page 15.*

Note: TLC of column-purified **4.10** showed two product spots. These two species may represent different protonation states. Wash of **4.10** with 5% citric acid converted all product to the top spot on TLC. Wash of **4.10** with 5% $NaHCO_3$ converted all product to the bottom spot on TLC.

^{1}H NMR: (500 MHz, Methanol-d_4) δ=8.26-8.21 (t, J = 12.5, Hz, 1H); 7.60-7.57 (t, J = 7.5 Hz, 1H); 7.54-7.51 (d, J = 7.5 Hz, 0.5H); 7.49-7.48 (d, J = 7.5 Hz, 1.5H); 7.43-7.40 (dt, J = 7.5, 3 Hz, 1.5H); 7.31-7.24 (m, 5H); 6.66-6.61 (t, J = 12.5 Hz, 0.5H); 6.32-6.23 (m, 2H); 4.15-4.12 (t, J = 7.0 Hz, 1H); 3.77-3.74 (t, J = 6.5 Hz, 3H); 3.62 (s, 3H); 3.60-3.58 (bt, J = 6 Hz, 2H); 3.56-3.54 (bt, J = 6 Hz, 2H); 2.50-2.41 (m, 6H); 2.39-2.36 (m, 3H); 1.94-1.84 (m, 2.0H); 1.77-1.71 (m, 9.0H); 1.63-1.57 (p, J = 6.5 Hz, 3H); 1.56-1.49 (p, 7.5 Hz, 3H); 1.46 (s, 12H); 1.42-1.32 (m, 4H)
HRMS $[M]^+$ $C_{46}H_{66}N_5O_4^+$ calc'd = 752.5115, found = 752.5115

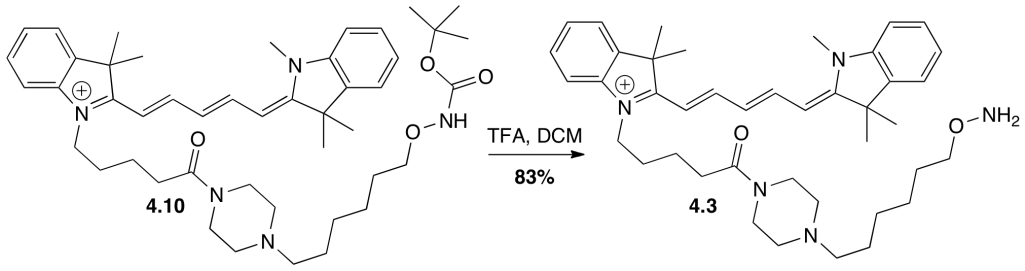

Aminooxy-Cy5 (4.3).

Into a 20 mL scintillation vial was added Boc-protected aminooxy-Cy5 (**4.10**, 10 mg, 0.013 mmol) in dry DCM (2 mL). To this solution was added TFA (2 mL), and the reaction was left unperturbed for 5 min, which turned into a clear and colorless solution. The dark blue color returned upon removing the solvent under reduced pressure. DCM (5 mL) was then added and the solution was concentrated again. The addition of DCM and concentration to dryness was repeated three times, at which point the metallic blue solid was dried on a vacuum line yielding **4.3** (7.0 mg, 83%). *See also Notebook XI, Page 19.*

^{1}H NMR: (500 MHz, Methanol-d$_4$) δ = 8.29-8.22 (dt, J = 12.5, 3 Hz, 1H); 7.61-7.57 (t, J = 7.5 Hz, 1H); 7.55-7.53 (d, J = 7.5 Hz, 0.5H); 7.50-7.48 (d, J = 7.5 Hz, 1.5H); 7.44-7.38 (m, 1.5H);

7.36-7.35 (d, J = 3 Hz, 0.5 H); 7.33-7.25 (m, 4.5H); 6.65-6.59 (t, J = 12.5 Hz, 0.5H); 6.32-6.25 (m, 2H); 4.15-4.11 (t, J = 7.5 Hz, 2H); 4.05-4.01 (dt, J = 6, 1.5 Hz, 3H); 3.70-3.40 (b, 3H); 3.63 (s, 3H); 3.2-2.9 (b, 4H), 3.17-3.11 (m, 2H); 2.55-2.52 (t, J = 7 Hz, 2H); 1.95-1.82 (m, 4.0H); 1.80-1.67 (m, 14.0H); 1.52-1.38 (m, 6H).

HRMS $[M]^+$ $C_{41}H_{58}N_5O_2^+$ calc'd = 652.4590, found = 652.4580 Da.

4.4.3. Construction of plasmids for coexpression.

DNA constructs were assembled by QuikChange site directed mutagenesis using the appropriate primers or by overlap extension PCR, followed by digestion and ligation of the PCR product into the appropriate plasmid.

QuikChange Site Directed Mutagenesis (Stratagene).

The entire template plasmid was amplified by QuikChange site directed mutagenesis using the appropriate mutant forward and reverse primers (see Table 4.2). The DNA was purified using the QIAquick PCR Purification Kit, eluting into a 1.6 mL Eppendorf tube with buffer EB (35 μL, provided by the supplier). To the elution was added DpnI (1 μL; 20,000 U/mL) and digestion buffer (4 μL, provided with DpnI). The reaction was incubated at 37 ^oC for 1-2 h and then at 80 ^oC for 20 min to heat-inactivate the enzyme. Chemically competent *E. coli* DH5α cells were transformed with plasmid DNA, plated on LB-agar with the appropriate antibiotic marker, single colonies were picked, and clones were analyzed by sequencing at ACGT, Inc.

Overlap extension PCR.

A 5' gene fragment was amplified by PCR using Phusion High-Fidelity DNA polymerase from a template containing the sequence of interest using a forward primer with the desired restriction site and a reverse primer either incorporating the internal mutation or insertion or beginning at the first nucleotide immediately after the internal mutation or insertion. An overlapping 3' gene fragment was amplified by PCR from the same template using a reverse primer with the desired restriction site and a forward primer incorporating the internal mutation. For primers used, see Table 4.2. Then, a PCR with the overlapping gene fragments and the primers with the desired restriction sites, was used to generate the full length mutants; the overlapping gene fragments were first added to the PCR mixture and after 8 rounds of amplification the primers with the desired restriction sites were added. After digestion of the mutant gene fragment and the appropriate vector with the desired restriction enzymes, the PCR products containing point mutations, insertions, or deletions were ligated into the plasmid using T4 DNA ligase. Incorporation of the correct mutation into the plasmid DNA was determined by sequencing at ACGT, Inc.

General protocol for PCR:

To a 0.2 mL PCR tube was added H_2O (34 μL), buffer HF (10 μL, 5X stock solution, provided with Phusion High-Fidelity DNA polymerase), template (0.5 μL, 100 ng/μL), primers (1 μL each, 100 μM), DMSO (1 μL), dNTPs (1 μL, 10 mM), and Phusion High-Fidelity DNA polymerase (0.5 μL, 2,000 U/mL, NEB). The DNA template was amplified using the following protocol. The reaction was 1) heated to 95 ºC for 2 min; 2) heated at 95 ºC for 30 s; 3) heated at

annealing temperature (see individual cases below) for 30 s; 4) heated at 72 ºC for the elongation time (see below); 5) steps 2-4 were repeated for 29 cycles; 6) heated at 72 ºC for 10 min.

Construction of plasmids pRSFDuet*(procA1.7(G–1E/T1S)/procM*), pRSFDuet*(procA1.7(G–2A/G–1A)/procM*), pRSFDuet*(procA1.7(G–2L/G–1L)/procM*).

The *procA1.7* mutants were generated in MCSI of a pRSFDuet vector with *procM* in MCS2 using pRSFDuet(*procA1.7(G–1E)/procM*) (unpublished work) as template by Quikchange mutagenesis. The primers used were *procA1.7(mutant) 5'* and *3'* (see primer Table). The PCR conditions were as described above with an annealing temperature of 60 ^{o}C and an elongation time of 2 min.

Construction of inserts for plasmids pRSFDuet*(procA2.8(G–1K/A1T)/procM*) and pRSFDuet*(procA2.8(G–1K/A1T ins LL)/procM*).

The *procA2.8* mutants were generated in MCS1 of a pRSFDuet vector with *procM* in MCS2 using pRSFDuet(*procA2.8(G–1K)/procM*) as template by overlap extension PCR. The primers *procA2.8 EcoRI FMP 5'* and *procA2.8(G–1K/A1T) FMP* (or *LL FMP*) *3′* were used to make the 5' overlapping fragment and the primers *procA2.8(G–1K/A1T) RMP* (or *LL RMP*) *5′* and *procA2.8 NotI RMP 3′* were used to make the 3' overlapping fragment. The restriction sites were EcoRI and NotI. The annealing temperature was 60 ^{o}C with an elongation time of 20 s. After overlap extension PCR, the full-length inserts were ligated into MCS1 of a pRSFDuet vector as described below.

Construction of plasmids pRSFDuet*(lctA(K1-G2 ins AAAKT)/lctM*), pRSFDuet*(lctA(K1-G2 ins AAAKLLT)/lctM*), pRSFDuet*(lctA(K1-G2A ins AAAKLLT)/lctM*), pRSFDuet*(lctA(K1-G2L ins AAAKLLT)/lctM*), pRSFDuet*(lctA(K1-G2A ins AAALLKT)/lctM*).

The *lctA* mutants were cloned into MCSI of a pRSFDuet vector with *lctM* in MCS2 using pRSFDuet(*lctAwt/lctM*)[56] as template by Quikchange mutagenesis. The primers used were *lctA(mutant) 5′* and 3'. The annealing temperature was 58 ^{o}C with an elongation time of 2 min.

Construction of plasmids pACYCDuet*(lctM)* and pCDFDuet*(lctM*).

lctM was cut out of MCSII of pRSFDuet*(lctA(K1-G2A ins AAALLKT)/lctM)* using restriction enzymes BglII and XhoI. The gene fragment was then ligated into either a pACYCDuet or a pCDFDuet vector that had been treated with the same enzymes, producing pACYCDuet*(lctM) and* pCDFDuet*(lctM).*

Construction of plasmid pRSFDuet(*lctA(K1-G2A ins AAALLKT/E13A)/lctM*).

The *lctA* mutant was generated from pRSFDuet(*lctA(K1-G2A ins AAALLKT)/lctM*) as template by Quikchange mutagenesis. The primers used were *lctA(K1-G2A AAALLKT/E13A) 5′* and 3' (Table 4.2). The annealing temperature was 56 ^{o}C with an elongation time of 2 min.

Construction of inserts for plasmids pRSFDuet(*halA1(A–1-C1 ins IEGRT)/halM1*), pRSFDuet(*halA1(A–1E-C1 ins T)/halM1*).

The *halA1* mutants were cloned into MCSI of a pRSFDuet vector that contained *halM1* in MCS2 using pRSFDuet(*halA1-Xa/halM1*)[42] as template by overlap extension PCR. The primers *halA1 SacI FMP* 5' and *halA1(G–1E-C1 ins T) FMP* (or *IEGRT FMP*) *3'* were used to make the

5’ overlapping fragment and the primers *halA1(G–1E-C1 ins T) RMP* (or *IEGRT RMP*) *5’* and *halA1 SbfI RMP 3’* were used to make the 3’ overlapping fragment. The restriction sites used were SacI and SbfI. The annealing temperature was 64 ^{o}C with an elongation time of 20 s. The gene fragments were then ligated into MCS1 of a pRSFDuet vector as described below.

Construction of plasmid pET15b(*halA1(A–1E-C1 ins T)/halM1*):

The *halA1* mutant DNA was constructed with a 5’ NdeI and 3’ XhoI restriction site by PCR with pRSFDuet(*halA1(G–1E-C1 ins T)/halM1*) as template. The PCR product and pET15b vector were separately digested and then ligated together.

Construction of inserts for plasmids pRSFDuet*(halA2(Q–1E-T1 ins T)/halM2*) and pRSFDuet*(halA2(Q–1E-T1 ins TA)/halM2*).

The *halA2* mutants were cloned into MCS1 of a pRSFDuet vector that already contained *halM2* in MCS2 using pRSFDuet(*halA2-Xa/halM2*)[42] as template by overlap extension PCR. The primers *halA2 BamHI FMP 5’* and *halA2(Q–1E-T1 ins T(A)) FMP 5’* were used to make the 5’ overlapping fragment and the primers *halA2(Q–1E-T1 ins T(A)) RMP 3’* and *halA2 SbfI RMP 3’* were used to make the 3’ overlapping fragment. The restriction sites used were BamHI and SbfI. The annealing temperature was 60 ^{o}C with an elongation time of 20 s. After overlap extension PCR, the full length inserts were ligated into MCS1 of a pRSFDuet vector as described below.

Construction of plasmids pRSFDuet*(nisA(R–1-I1 ins IT)/nisB*) and pRSFDuet*(nisA(I1L)/nisB*).

The *nisA* mutants were cloned into MCS1 of a pRSFDuet vector that already contained *nisB* in MCS2 using pRSFDuet(*nisA/nisB*)[42] as template by Quikchange mutagenesis. The primers used were *nisA(R–1-I1 ins IT) 5′* and *3*' and *nisA(I1L) 5'* and *3'*. The annealing temperature was 60 ^{o}C with an elongation time of 2 min.

Table 4.2. Primers used in molecular cloning.

procA1.7(G–1E/T1S) 5':	CTG GAA GGT GTG GCT GGG GAA AGC ATT GGG GGA ACC AT
procA1.7(G–1E/T1S)3':	CCC AGC CAC ACC TTC CAG CTC AGC ATC AGA
procA1.7(G–2A/G–1A)5':	CTG GAA GGT GTG GCT GCG GCG ACC ATT GGG GGA ACC AT
procA1.7(G–2A/G–1A)3':	AGC CAC ACC TTC CAG CTC AGC ATC AGA
procA1.7(G–2L/G–1L) 5':	CTG GAA GGT GTG GCT CTG CTG ACC ATT GGG GGA ACC AT
procA1.7(G–2L/G–1L) 3':	AGC CAC ACC TTC CAG CTC AGC ATC AGA
procA2.8 EcoRI FMP 5':	GCA ACC TAG AAT TCG ATG TCA GAA GAG CAA CTG AAG G
procA2.8(G–1K/A1T) FMP 3':	GGT TAT GAC AGG CGG TTT TCC CAG CCA CAC CTT C
procA2.8(G–1K/A1T) RMP 5':	GAA GGT GTG GCT GGG AAA ACC GCC TGT CAT AAC C
procA2.8(G–1K/A1T ins LL) FMP 3':	GGT TAT GAC AGG CGG TCA GCA GTT TCC CAG CCA CAC C
procA2.8(G–1K/A1T ins LL) RMP 5':	GGT GTG GCT GGG AAA CTG CTG ACC GCC TGT CAT AAC C
procA2.8 NotI RMP 3':	ATA TAA TGC GGC CGC TTA GCA CTC ACC CTC
lctA(K1-G2 ins AAAKT) 5':	TTA GGT GCA AAA GCA GCA GCA AAA ACC GGC GGC AGT GGA GTT
lctA(K1-G2 ins AAAKT)3':	TTT TGC ACC TAA AAT AAG GTC CAA TTC ACT
lctA(K1-G2 ins AAAKLLT) 5':	GGT GCA AAA GCA GCA GCA AAA CTG CTG ACC GGC GGC AGT
lctA(K1-G2 ins AAAKLLT 3':	TGC TGC TGC TTT TGC ACC TAA AAT AAG GTC
lctA(K1-G2A ins AAAKLLT) 5':	GGT GCA AAA GCA GCA GCA AAA CTG CTG ACC GCG GGC AGT
lctA(K1-G2A ins AAAKLLT) 3':	TGC TGC TGC TTT TGC ACC TAA AAT AAG GTC
lctA(K1-G2L ins AAAKLLT) 5':	GGT GCA AAA GCA GCA GCA AAA CTG CTG ACC CTG GGC AGT
lctA(K1-G2L ins AAAKLLT) 3':	TGC TGC TGC TTT TGC ACC TAA AAT AAG GTC
lctA(K1-G2A ins AAALLKT) 5':	GGT GCA AAA GCA GCA GCA CTG CTG AAA ACC GCG GGC AGT
lctA(K1-G2A ins AAALLKT) 3':	TGC TGC TGC TTT TGC ACC TAA AAT AAG GTC
lctA(K1-G2A ins AAALLKT/E13A) 5':	CAT ACA ATT TCT CAT GCG TGT AAT ATG AAT AGC
lctA(K1-G2A ins AAALLKT/E13A) 3':	ATG AGA AAT TGT ATG AAT AAC TCC ACT GCC
halA1 SacI FMP 5':	CGC CAC TCG GAG CTC GAT GAC AAA TCT TTT AAA AG
halA1(G–1E-C1 ins T) FMP 3':	GAT ATT CTA GCT GGG GTG AAC GGT GAA ACC TGC GCA TGG TAC
halA1(G–1E-C1 ins T) RMP 5':	CCC AGC TAG AAT ATC TTG GTC TTC TAA CTC
halA1(G–1E-C1 ins IEGRT) FMP 3':	GAT ATT CTA GCT GGG ATT GAA GGT CGT ACC TGC GCA TGG TAC AAC
halA1(G–1E-C1 ins IEGRT) RMP 5':	GTT GTA CCA TGC GCA GGT ACG ACC TTC AAT CCC AGC TAG AAT ATC
halA1 SbfI RMP 3':	ATA GTG ATC CTG CAG GTT AGT TGC AAG AAG GCA TG
halA2 BamHI FMP 5':	GGA TCC GAT GGT AAA TTC AAA AGA TTT GCG TAA TCC
halA2(Q–1E-T1 ins TA) FMP 3':	ATC TCC TGA ACC AGC TAG AGA CGA AAG TTC CTT CTC
halA2(Q–1E-T1 ins TA) RMP 5':	TTC AGG AGA TGT GCA TGC GGA AAC CGC GAC AAC TTG G
halA2(Q–1E-T1 ins T) FMP 3':	TTC AGG AGA TGT GCA TGC GGA AAC CAC AAC TTG G
halA2(Q–1E-T1 ins T) RMP 5':	ATC TCC TGA ACC AGC TAG AGA CGA AAG TTC CTT CTC
halA2 SbfI RMP 3':	ATA ATG ATC CTG CAG GTT AGC ACT GGC TTG TAC
nisA(R–1-I1 ins IT 5':	CA GGT GCA TCA CCA CGC ATT ACC ATT ACA AGT ATT TCG CTA
nisA(R–1-I1 ins IT 3':	TAG CGA AAT ACT TGT AAT GGT AAT GCG TGG TGA TGC ACC TG
nisA(I1L) 5':	CA GGT GCA TCA CCA CGC CTG ACA AGT ATT TCG CTA
nisA(I1L)3':	TAG CGA AAT ACT TGT CAG GCG TGG TGA TGC ACC TG

Digestion of plasmids and DNA inserts.

To a 1.7 mL Eppendorf tube with insert or plasmid DNA (40 μL, 100-250 ng/μL) was added digestion buffer (5 μL; NEB, provided with the restriction enzymes), digestion enzyme(s) (1.5 μL, concentrations are below), BSA (if necessary, 0.5 μL, 100X, provided with digestion enzyme), and H_2O (to 50 μL). The components were incubated at 37 ^oC for 2-4 h. At this time calf intestine phosphatase (CIP) (1 μL) was added to plasmid DNA only and the sample was incubated for an additional 1 h. The samples were then analyzed by DNA gel electrophoresis and the desired band was purified by a QIAGEN Gel Extraction kit eluting in buffer EB (30 μL).

Note: Both digestion enzymes were added in one single digest if the buffer was compatible. If buffer was not compatible, two successive digests were performed.

BamHI = 20,000 U/mL, NotI = 10,000 U/mL, XhoI = 20,000 U/mL, BglII = 10,000 U/mL, EcoRI = 20,000 U/mL, SacI = 20,000 U/mL, SbfI = 10,000 U/mL, CIP = 10,000 U/mL.

Ligation of digested plasmid and DNA insert.

To three 0.6 mL Eppendorf tubes was added plasmid DNA (1 μL, 100 ng/μL). Insert DNA (1 mL of a solution of different concentrations to give a ratio of plasmid to insert of 1:1, 1:10 and 1:100) was then added as well as T4 DNA ligase reaction buffer (0.7 mL, provided with the ligation enzyme), T4 DNA ligase (0.8 mL, 400,000 cohesive end U/mL), and H_2O (to 5 μL). The samples were incubated at 18 ^oC for 16-20 h at which time the entire reactions were used to transform *E. coli* DH5a cells.

4.4.4. Heterologous production, purification, and characterization of LanA analogues.

The lanthipeptides were expressed using *E. coli* BL21 cells transformed with a single pRSFDuet plasmid containing the *lanA* and *lanM* genes. For keto-Halα, two plasmids were used to increase the yield of production (pRSFDuet(*halA1(G–1E-C1 ins T)*/*halM1* and pET15b(*halA1)G–1E-C1 ins T*)) and for keto-lacticin 481 and keto-nisin-1 three plasmids were used (pRSFDuet(*lctA(K1-G2A ins AAALLKT)*/*lctM*, pACYCDuet(*lctM*), and pCDFDuet(*lctM*); pRSFDuet(*nisA(R–1-I1 ins IT)/lctM*, pACYCDuet(*nisB/nisC*), and pCDFDuet(*nisB*)).

Overexpression and purification of His_6-tagged modified peptide mutants.

An overnight culture of *E. coli* BL21 (DE3) cells carrying the desired plasmids was added to an overexpression culture flask containing either terrific broth (TB) or LB broth (1:100; volume overnight culture: volume overexpression culture) and appropriate antibiotics depending on the plasmids used (1:1000 v:v; kanamycin (50 mg/mL), chloramphenicol (25 mg/mL), spectinomycin (25 mg/mL, ampicillin (100 mg/mL)). The culture was then incubated in a 37 ºC shaker (220 rpm) until the optical density reached 0.6 (LB) or 1.0 (TB). For HalA1 and HalA2, overexpression was immediately induced with isopropyl β-D-1-thiogalactopyranoside (IPTG, 0.25 mM final concentration) and the flask was incubated for 4 h in a shaker at 37 ºC and 220 rpm. Conversely, for ProcA1.7, ProcA2.8, and LctA, the culture was first placed on ice (15 min). Overexpression was then induced by the addition of IPTG and the flask was incubated overnight in a shaker at 18 ºC and 220 rpm. The following morning the cells were harvested by centrifugation (11,867 ×*g*, 4 ºC, 20 min), the supernatant was discarded and the cells were lysed using a cell homogenizer (Avestin Emulsiflex-C3; 5,000 PSI) in LanA start buffer (1 mL per 100 mL culture; 20 mM NaH_2PO_4, 500 mM NaCl, 0.5 mM imidazole, 20% glycerol, pH 7.5). The

soluble and insoluble layers were then separated by centrifugation (22,789 ×*g*, 4 °C, 20 min) and the soluble layer was saved for purification. The insoluble layer was suspended in LanA lysis buffer (1 mL per 100 mL culture; 6 M guanidine HCl, 20 mM NaH_2PO_4, pH 7.5, 500 mM NaCl, 0.5 mM imidazole) and the cells were lysed by sonication. The soluble and insoluble layers were again separated by centrifugation (22,789 ×*g*, 4 °C, 20 min) and the modified His_6-LanA peptide was purified from the filtered soluble layers (0.45 μm) using a Ni HisTrap HP column (5 mL, GE Healthcare). The column was washed with LanA wash buffer (4 M guanidine-HCl, 20 mM NaH_2PO_4, pH 7.5, 500 mM NaCl, 30 mM imidazole) to remove non-specific binding proteins. The His_6-LanA peptide was eluted with LanA elute buffer (3 × 5 mL, 20 mM NaH_2PO_4, 100 mM NaCl, 500 mM imidazole, pH 7.5). Finally, the peptide was further purified by preparative reversed phase high-performance liquid chromatography (RP-HPLC) and lyophilized.

Proteolytic cleavage of LanA mutants.

To lyophilized peptide was added HEPES buffer (1 mL per 5 mg of peptide, pH 7.5, 50 mM final concentration) and the necessary protease (5 μL/L overexpression culture; stock solutions used: LysC = 3 U/100 μL, GluC = 2 mg/mL, trypsin = 40 μM). To the HalA1 mutant reaction was also added TCEP (1 mM final concentration). The reaction was incubated overnight at room temperature (GluC, trypsin) or at 37 ºC (LysC). The following morning the progress of the reaction was analyzed by MALDI-TOF MS and additional enzyme was added in 5 μL aliquots if the reaction was not complete. Once complete, the reaction was purified by preparative RP-HPLC.

Aminopeptidase cleavage of GluC-cleaved ProcA1.7(G–2L/G–1L).

To a reaction vessel was added HPLC-purified GluC-cleaved ProcA1.7(G–2L/G–1L), HEPES buffer (1 mL per 5 mg of peptide, pH 7.5, 100 mM final concentration), and aminopeptidase (A8200, 6 μL/1 mg peptide, 100 U/mL stock solution). The reaction was incubated at 37 ºC for 24 h. The reaction product was used in a bioconjugation reaction with **4.1** without further purification.

Representative bioconjugation of keto-LanA and 4.1.

To a reaction vessel was added keto-LanA (1.45 μmol) and **4.1** (14.5 μmol, 1.54 mg, 10 equiv). Next, a solution of H_2O (2.04 mL), acetate buffer (75 μL, 4 M, pH 4.75, final concentration 100 mM), and aniline (885 μL, 339 mM, final concentration 100 mM) was added. This solution was degassed with N_2 prior to addition to prevent formation of large amounts of oxidized product. The reaction was stirred for 4 h at room temperature. The crude material was then purified by preparative RP-HPLC.

Representative bioconjugation of keto-LanA and 4.2 or 4.3.

To keto-LanA (0.48 μmol) in a 15 mL conical vial was added **4.2** or **4.3** (24.2 μmol, 50 equiv) dissolved in a degassed solution of acetate buffer (100 mM, 2 mL). To this solution was added p-phenylenediamine (86.4 mg, 400 mM final concentration) and the reaction was vortexed to dissolve the catalyst. The reaction was incubated for 3 h and diluted with 60% MeCN, 0.1% TFA (2 mL). The crude material was then purified by preparative RP-HPLC, except rho-Halα, which was purified by several rounds of analytical RP-HPLC to separate the fluorescently-

labeled peptide from a rhodamine impurity. Excess **4.2** or **4.3** were recovered during HPLC purification and used in subsequent reactions.

Purification of LanA analogues by RP-HPLC.

The cleavage and bioconjugation reactions were directly purified by preparative RP-HPLC on a Phenomenex C18 column (1.0 cm × 25.0 cm) (except for the purification of rho-Halα which was purified by analytical RP-HPLC) employing a water-acetonitrile solvent system. The linear gradient used was from 2-80% solvent B in 45 min (solvent A = 0.1% TFA in H_2O; solvent B = 80% acetonitrile in H_2O, 0.086% TFA). Peptides were monitored by their absorbance at 220 nm. Fractions containing product as analyzed by MALDI-TOF MS were collected and lyophilized.

4.4.5. Yield and purification of LanA analogues.

His_6-ProcA1.7. Yield: 8.5 mg/L. RP-HPLC: R_t = 28.0-32.0 min (C4, Waters Delta-pak™).

His_6-ProcA2.8(G–1K-A1T). Substrate was cleaved by protease immediately after Ni^{2+} purification.

His_6-HalA1(G–1E-C1 ins T). Yield: 7.6 mg/L. RP-HPLC: R_t = 29.0-33.0 min (C4, Waters Delta-pak™).

His_6-HalA2(Q–1E-T1 ins TA) Yield: 10 mg/L. RP-HPLC: R_t = 31.8-36.3 min (C4, Waters Delta-pak™).

His_6-LctA(K1-G2A ins AAALLKT). Yield: 3.1 mg/L mixture of product with 4 and 5 dehydrations. RP-HPLC: Rt = 33.0-37.0 min (C4, Waters Delta-pak™).

His_6-LctA(K1-G2A ins AAALLKT/E13A). Yield: 1.2 mg/L mixture of product with 4 and 5 dehydrations. RP-HPLC: R_t = 31.0-35.0 min (C4, Waters Delta-pak™).

Pcn1.7. RP-HPLC: R_t = No HPLC was performed before bioconjugation with ***1***.

keto-Pcn2.8. Yield: 3 mg/L culture. RP-HPLC: R_t = 25.7-27.7 min (C18, Waters Delta-pak™).

keto-Halα. Yield: 0.9 mg/L culture. RP-HPLC: R_t = 24.5-27.0 min (C18, Phenomenex).

keto-Halβ. Yield: 1.55 mg/L culture. RP-HPLC: R_t = 38.6-41.6 min (C18, Waters Delta-pak™).

keto-lacticin 481. Yield: 0.1 mg/L culture. RP-HPLC: R_t = 30.0-30.8 min (C18, Phenomenex).

keto-lacticin 481/E13A. RP-HPLC: R_t = 30.1-30.7 min (C18, Phenomenex).

alk-Pcn1.7. RP-HPLC: R_t = 37.5-38.2 and 39.0-39.8 min (C18, Phenomenex). Two diastereomers are formed during the oxime bioconjugation (*E* and *Z*). Only in alk-Pcn1.7 and alk-Halβ were the isomers distinguishable by preparative HPLC.

alk-Pcn2.8. RP-HPLC: R_t = 28.0-29.0 min (C18, Phenomenex).

alk-Halα. Bioconjugation yield after HPLC: 5%. RP-HPLC: R_t = 32.0-32.8 min (C18, Phenomenex).

alk-Halβ. Bioconjugation yield after HPLC: 10%. RP-HPLC: R_t = 41.0-42.3 min (C18, Phenomenex).

alk-lacticin 481. Bioconjugation yield after HPLC: 30%. RP-HPLC: R_t = 31.2-31.6 min (C18, Phenomenex).

rho-Halα. Bioconjugation yield after HPLC: 12.5%. RP-HPLC: R_t = 32.6-33.2 min (C18, Phenomenex, analytical).

rho-Halβ. Bioconjugation yield after HPLC: 28%. RP-HPLC: R_t = 38.2-39.0 and 40.6-40.9 min (C18, Phenomenex, analytical).

Cy5-Halβ. Bioconjugation yield after HPLC: 16%. RP-HPLC: R_t = 39.0-39.8 and 39.8-40.4 min (C18, Phenomenex, analytical).

rho-lacticin 481. Bioconjugation yield after HPLC: 47%. RP-HPLC: R_t = 35.2-35.6 min (C18, Phenomenex, analytical).

rho-lacticin481/E13A. RP-HPLC: R_t = 35.0-35.3 min (C18, Phenomenex).

4.4.6. Confocal fluorescence microscopy with *B. subtilis*.

A 150 µL aliquot from an overnight culture of *B. subtilis* 168 was used to inoculate LB (5 mL) and the culture was grown to an OD of 0.5. This culture was transferred into 2.0 mL Eppendorf tubes (1.5 mL) and centrifuged at 1,431 ×*g* for 2 min in a microfuge. Into the tubes with cells were added cold solutions of fluorescently-labeled lantibiotic at the desired concentration in 1X Dulbecco's Phosphate-Buffered Saline (D-PBS) (1 mL, Fisher Scientific). The reactions were kept on ice for 30 min. At this time the reactions were centrifuged at 4 ºC (1 min, 1,431 ×*g*). The supernatant was carefully removed and the cells were carefully suspended in 1 mL of 1X D-PBS. The solution was again centrifuged, the supernatant was removed and cells were carefully suspended in 1 mL of 1X D-PBS. Finally, the suspension was centrifuged and D-PBS was removed to give a suspension of around 200 µL. Aliquots of the suspension (10 µL) and liquified low gelling temperature agarose (10 µL, 1.5%) were added to a microscopy plate and the localization of the lantibiotic was analyzed by confocal fluorescence microscopy using a Zeiss LSM 700 Confocal Microscope. Rhodamine B analogues were excited using a 555 nm laser and emission was detected at wavelengths between 560 and 625 nm. Cy5 analogues were excited using a 639 nm laser and emission was detected at wavelengths between 640 and 735 nm. Images were deconvoluted using the program AutoQuant X3 (Media Cybernetics).

4.4.7. Minimum inhibitory concentration determination.

Ninety six-well and forty eight-well microtiter plates (Corning Costar) were utilized for anaerobic and aerobic cultures, respectively. For ninety six-well plates, each well contained 90 μL of an overnight culture containing *L. lactis* HP (approximately 1×10^8 CFU mL^{-1}) and a 10x stock of peptide (10 μL) of the desired concentration. The plates were incubated at 30 ºC overnight with no agitation. For forty eight-well plates, each well contained 180 μL of an overnight culture containing *B. subtilis* 168 (approximately 1×10^8 CFU mL^{-1}) and a 10x stock of peptide (20 μL) of the desired concentration. The plates were incubated at 30 ºC overnight with moderate shaking. In addition, each ninety six and forty eight-well plate contained several blank (growth media with no bacteria) and control (SDW in place of peptide) wells. The optical density at 630 nm (OD_{630}) was recorded at hourly intervals from 0-6 h and a final recording at 22-24 h. For experiments with Cy5-Halβ, the optical density was read at 570 nm (OD_{570}) to minimize the undesired excitation of Cy5. The MIC was determined as the lowest concentration at which no cell growth was observed after 22-24 h.

4.5 REFERENCES

(1) Bindman, N. A.; van der Donk, W. A., A general method for fluorescent labeling of the N-termini of lanthipeptides and its application to visualize their cellular localization, *J. Am. Chem. Soc.* **2013**, *135*, 10362.

(2) Hasper, H. E.; Kramer, N. E.; Smith, J. L.; Hillman, J. D.; Zachariah, C.; Kuipers, O. P.; de Kruijff, B.; Breukink, E., An alternative bactericidal mechanism of action for lantibiotic peptides that target lipid II, *Science* **2006**, *313*, 1636.

(3) Zhao, M.; Li, Z.; Bugenhagen, S., 99mTc-labeled duramycin as a novel phosphatidylethanolamine-binding molecular probe, *J. Nucl. Med.* **2008**, *49*, 1345.

(4) Okuda, K.; Aso, Y.; Nakayama, J.; Sonomoto, K., Cooperative transport between NukFEG and NukH in immunity against the lantibiotic nukacin ISK-1 produced by Staphylococcus warneri ISK-1, *J. Bacteriol.* **2008**, *190*, 356.

(5) Schoof, S.; Baumann, S.; Ellinger, B.; Arndt, H. D., A fluorescent probe for the 70 S-ribosomal GTPase-associated center, *ChemBioChem* **2009**, *10*, 242.

(6) Ross, A. C.; Liu, H.; Pattabiraman, V. R.; Vederas, J. C., Synthesis of the lantibiotic lactocin S using peptide cyclizations on solid phase, *J. Am. Chem. Soc.* **2010**, *132*, 462.

(7) Liu, W.; Chan, A. S.; Liu, H.; Cochrane, S. A.; Vederas, J. C., Solid supported chemical syntheses of both components of the lantibiotic lacticin 3147, *J. Am. Chem. Soc.* **2011**, *133*, 14216.

(8) Knerr, P. J.; van der Donk, W. A., Chemical synthesis of the lantibiotic lacticin 481 reveals the importance of lanthionine stereochemistry, *J. Am. Chem. Soc.* **2013**, *135*, 7094.

(9) Cotter, P. D.; Hill, C.; Ross, R. P., Bacterial lantibiotics: strategies to improve therapeutic potential, *Curr. Protein Pept. Sci.* **2005**, *6*, 61.

(10) van Heel, A. J.; Montalban-Lopez, M.; Kuipers, O. P., Evaluating the feasibility of lantibiotics as an alternative therapy against bacterial infections in humans, *Expert Opin. Drug Metab. Toxicol.* **2011**, *7*, 675.

(11) Kuipers, O. P.; Bierbaum, G.; Ottenwälder, B.; Dodd, H. M.; Horn, N.; Metzger, J.; Kupke, T.; Gnau, V.; Bongers, R.; van den Bogaard, P.; Kosters, H.; Rollema, H. S.; de Vos, W. M.; Siezen, R. J.; Jung, G.; Götz, F.; Sahl, H. G.; Gasson, M. J., Protein engineering of lantibiotics, *Antonie van Leeuwenhoek* **1996**, *69*, 161.

(12) Ross, A. C.; Vederas, J. C., Fundamental functionality: recent developments in understanding the structure-activity relationships of lantibiotic peptides, *J. Antibiot.* **2011**, *64*, 27.

(13) Field, D.; Hill, C.; Cotter, P. D.; Ross, R. P., The dawning of a 'Golden era' in lantibiotic bioengineering, *Mol. Microbiol.* **2011**, *78*, 1077.

(14) Cortés, J.; Appleyard, A. N.; Dawson, M. J., Chapter 22. Whole-cell generation of lantibiotic variants, *Methods Enzymol.* **2009**, *458*, 559.

(15) Szekat, C.; Jack, R. W.; Skutlarek, D.; Farber, H.; Bierbaum, G., Construction of an expression system for site-directed mutagenesis of the lantibiotic mersacidin, *Appl. Environ. Microbiol.* **2003**, *69*, 3777.

(16) Asaduzzaman, S. M.; Nagao, J.; Aso, Y.; Nakayama, J.; Sonomoto, K., Lysine-oriented charges trigger the membrane binding and activity of nukacin ISK-1, *Appl. Environ. Microbiol.* **2006**, *72*, 6012.

(17) Cooper, L. E.; McClerren, A. L.; Chary, A.; van der Donk, W. A., Structure-activity relationship studies of the two-component lantibiotic haloduracin, *Chem. Biol.* **2008**, *15*, 1035.

(18) Islam, M. R.; Shioya, K.; Nagao, J.; Nishie, M.; Jikuya, H.; Zendo, T.; Nakayama, J.; Sonomoto, K., Evaluation of essential and variable residues of nukacin ISK-1 by NNK scanning, *Mol. Microbiol.* **2009**, *72*, 1438.

(19) Levengood, M. R.; Knerr, P. J.; Oman, T. J.; van der Donk, W. A., In vitro mutasynthesis of lantibiotic analogues containing nonproteinogenic amino acids, *J. Am. Chem. Soc.* **2009**, *131*, 12024.

(20) Deegan, L. H.; Suda, S.; Lawton, E. M.; Draper, L. A.; Hugenholtz, F.; Peschel, A.; Hill, C.; Cotter, P. D.; Ross, R. P., Manipulation of charged residues within the two-peptide lantibiotic lacticin 3147, *Microb. Biotechnol.* **2010**, *3*, 222.

(21) Oman, T. J.; Lupoli, T. J.; Wang, T. S.; Kahne, D.; Walker, S.; van der Donk, W. A., Haloduracin alpha binds the peptidoglycan precursor lipid II with 2:1 stoichiometry, *J. Am. Chem. Soc.* **2011**, *133*, 17544.

(22) Knerr, P. J.; Oman, T. J.; Garcia De Gonzalo, C. V.; Lupoli, T. J.; Walker, S.; van der Donk, W. A., Non-proteinogenic amino acids in lacticin 481 analogues result in more potent inhibition of peptidoglycan transglycosylation, *ACS Chem. Biol.* **2012**, *7*, 1791.

(23) Suda, S.; Hill, C.; Cotter, P. D.; Ross, R. P., Investigating the importance of charged residues in lantibiotics, *Bioeng. Bugs* **2010**, *1*, 345.

(24) Stephanopoulos, N.; Francis, M. B., Choosing an effective protein bioconjugation strategy, *Nat. Chem. Biol.* **2011**, *7*, 876.

(25) Chen, I.; Howarth, M.; Lin, W.; Ting, A. Y., Site-specific labeling of cell surface proteins with biophysical probes using biotin ligase, *Nat. Methods* **2005**, *2*, 99.

(26) Carrico, I. S.; Carlson, B. L.; Bertozzi, C. R., Introducing genetically encoded aldehydes into proteins, *Nat. Chem. Biol.* **2007**, *3*, 321.

(27) Griffin, B. A.; Adams, S. R.; Tsien, R. Y., Specific covalent labeling of recombinant protein molecules inside live cells, *Science* **1998**, *281*, 269.

(28) Yin, J.; Liu, F.; Li, X.; Walsh, C. T., Labeling proteins with small molecules by site-specific posttranslational modification, *J. Am. Chem. Soc.* **2004**, *126*, 7754.

(29) Gautier, A.; Juillerat, A.; Heinis, C.; Correa, I. R., Jr.; Kindermann, M.; Beaufils, F.; Johnsson, K., An engineered protein tag for multiprotein labeling in living cells, *Chem. Biol.* **2008**, *15*, 128.

(30) Wagner, A. M.; Fegley, M. W.; Warner, J. B.; Grindley, C. L.; Marotta, N. P.; Petersson, E. J., N-terminal protein modification using simple aminoacyl transferase substrates, *J. Am. Chem. Soc.* **2011**, *133*, 15139.

(31) Antos, J. M.; Chew, G. L.; Guimaraes, C. P.; Yoder, N. C.; Grotenbreg, G. M.; Popp, M. W.; Ploegh, H. L., Site-specific N- and C-terminal labeling of a single polypeptide using sortases of different specificity, *J. Am. Chem. Soc.* **2009**, *131*, 10800.

(32) Heal, W. P.; Wright, M. H.; Thinon, E.; Tate, E. W., Multifunctional protein labeling via enzymatic N-terminal tagging and elaboration by click chemistry, *Nat. Protoc.* **2012**, *7*, 105.

(33) Watanabe, T.; Miyata, Y.; Abe, R.; Muranaka, N.; Hohsaka, T., N-terminal specific fluorescence labeling of proteins through incorporation of fluorescent hydroxy acid and subsequent ester cleavage, *ChemBioChem* **2008**, *9*, 1235.

(34) Scheck, R. A.; Francis, M. B., Regioselective labeling of antibodies through N-terminal transamination, *ACS Chem. Biol.* **2007**, *2*, 247.

(35) Rabuka, D.; Rush, J. S.; deHart, G. W.; Wu, P.; Bertozzi, C. R., Site-specific chemical protein conjugation using genetically encoded aldehyde tags, *Nat. Protoc.* **2012**, *7*, 1052.

(36) Cohen, J. D.; Zou, P.; Ting, A. Y., Site-specific protein modification using lipoic acid ligase and bis-aryl hydrazone formation, *ChemBioChem* **2012**, *13*, 888.

(37) Agarwal, P.; van der Weijden, J.; Sletten, E. M.; Rabuka, D.; Bertozzi, C. R., A Pictet-Spengler ligation for protein chemical modification, *Proc. Natl. Acad. Sci. U. S. A.* **2013**, *110*, 46.

(38) Kellner, R.; Jung, G.; Josten, M.; Kaletta, C.; Entian, K. D.; Sahl, H. G., Pep5: structure elucidation of a large lantibiotic, *Angew. Chem.* **1989**, *101*, 618.

(39) Holo, H.; Jeknic, Z.; Daeschel, M.; Stevanovic, S.; Nes, I. F., Plantaricin W from *Lactobacillus plantarum* belongs to a new family of two-peptide lantibiotics, *Microbiology* **2001**, *147*, 643.

(40) Li, B.; Sher, D.; Kelly, L.; Shi, Y.; Huang, K.; Knerr, P. J.; Joewono, I.; Rusch, D.; Chisholm, S. W.; van der Donk, W. A., Catalytic promiscuity in the biosynthesis of cyclic

peptide secondary metabolites in planktonic marine cyanobacteria, *Proc. Natl. Acad. Sci. U.S.A.* **2010**, *107*, 10430.

(41) Tang, W.; van der Donk, W. A., Structural characterization of four prochlorosins: a novel class of lantipeptides produced by planktonic marine cyanobacteria, *Biochemistry* **2012**, *51*, 4271.

(42) Shi, Y.; Yang, X.; Garg, N.; van der Donk, W. A., Production of lantipeptides in *Escherichia coli*, *J. Am. Chem. Soc.* **2011**, *133*, 2338.

(43) Ökesli, A.; Cooper, L. E.; Fogle, E. J.; van der Donk, W. A., Nine post-translational modifications during the biosynthesis of cinnamycin, *J. Am. Chem. Soc.* **2011**, *133*, 13753.

(44) Goto, Y.; Li, B.; Claesen, J.; Shi, Y.; Bibb, M. J.; van der Donk, W. A., Discovery of unique lanthionine synthetases reveals new mechanistic and evolutionary insights, *PLoS Biol.* **2010**, *8*, e1000339.

(45) Plat, A.; Kluskens, L. D.; Kuipers, A.; Rink, R.; Moll, G. N., Requirements of the engineered leader peptide of nisin for inducing modification, export, and cleavage, *Appl. Environ. Microbiol.* **2011**, *77*, 604.

(46) Garg, N.; Tang, W.; Goto, Y.; van der Donk, W. A., Geobacillins: lantibiotics from *Geobacillus thermodenitrificans*, *Proc. Natl. Acad. Sci. U. S. A.* **2012**, *109*, 5241.

(47) Majchrzykiewicz, J. A.; Lubelski, J.; Moll, G. N.; Kuipers, A.; Bijlsma, J. J.; Kuipers, O. P.; Rink, R., Production of a class II two-component lantibiotic of *Streptococcus pneumoniae* using the class I nisin synthetic machinery and leader sequence, *Antimicrob. Agents Chemother.* **2010**, *54*, 1498.

(48) Velásquez, J. E.; Zhang, X.; van der Donk, W. A., Biosynthesis of the antimicrobial peptide epilancin 15X and its unusual N-terminal lactate moiety, *Chem. Biol.* **2011**, *18*, 857.

(49) Dirix, G.; Monsieurs, P.; Marchal, K.; Vanderleyden, J.; Michiels, J., Screening genomes of Gram-positive bacteria for double-glycine-motif-containing peptides, *Microbiology* **2004**, *150*, 1121.

(50) Kalia, J.; Raines, R. T., Hydrolytic stability of hydrazones and oximes, *Angew. Chem. Int. Ed.* **2008**, *47*, 7523.

(51) Dirksen, A.; Hackeng, T. M.; Dawson, P. E., Nucleophilic catalysis of oxime ligation, *Angew. Chem. Int. Ed.* **2006**, *45*, 7581.

(52) Rink, R.; Kuipers, A.; de Boef, E.; Leenhouts, K. J.; Driessen, A. J.; Moll, G. N.; Kuipers, O. P., Lantibiotic structures as guidelines for the design of peptides that can be modified by lantibiotic enzymes, *Biochemistry* **2005**, *44*, 8873.

(53) McClerren, A. L.; Cooper, L. E.; Quan, C.; Thomas, P. M.; Kelleher, N. L.; van der Donk, W. A., Discovery and in vitro biosynthesis of haloduracin, a two-component lantibiotic, *Proc. Natl. Acad. Sci. U. S. A.* **2006**, *103*, 17243.

(54) Lawton, E. M.; Cotter, P. D.; Hill, C.; Ross, R. P., Identification of a novel two-peptide lantibiotic, Haloduracin, produced by the alkaliphile *Bacillus halodurans* C-125, *FEMS Microbiol. Lett.* **2007**, *267*, 64.

(55) Chatterjee, C.; Patton, G. C.; Cooper, L.; Paul, M.; van der Donk, W. A., Engineering dehydro amino acids and thioethers into peptides using lacticin 481 synthetase, *Chem. Biol.* **2006**, *13*, 1109.

(56) Oman, T. J.; Knerr, P. J.; Bindman, N. A.; Velasquez, J. E.; van der Donk, W. A., An engineered lantibiotic synthetase that does not require a leader peptide on its substrate, *J. Am. Chem. Soc.* **2012**, *134*, 6952.

(57) Karakas Sen, A.; Narbad, A.; Horn, N.; Dodd, H. M.; Parr, A. J.; Colquhoun, I.; Gasson, M. J., Post-translational modification of nisin. The involvement of NisB in the dehydration process, *Eur. J. Biochem.* **1999**, *261*, 524.

(58) Bonev, B. B.; Breukink, E.; Swiezewska, E.; De Kruijff, B.; Watts, A., Targeting extracellular pyrophosphates underpins the high selectivity of nisin, *FASEB J.* **2004**, *18*, 1862.

(59) Gilmore, J. M.; Scheck, R. A.; Esser-Kahn, A. P.; Joshi, N. S.; Francis, M. B., N-terminal protein modification through a biomimetic transamination reaction, *Angew. Chem. Int. Ed. Engl.* **2006**, *45*, 5307.

(60) Nguyen, T.; Francis, M. B., Practical synthetic route to functionalized rhodamine dyes, *Org. Lett.* **2003**, *5*, 3245.

(61) Korbel, G. A.; Lalic, G.; Shair, M. D., Reaction microarrays: a method for rapidly determining the enantiomeric excess of thousands of samples, *J. Am. Chem. Soc.* **2001**, *123*, 361.

(62) Rashidian, M.; Mahmoodi, M. M.; Shah, R.; Dozier, J. K.; Wagner, C. R.; Distefano, M. D., A highly efficient catalyst for oxime ligation and hydrazone-oxime exchange suitable for bioconjugation, *Bioconjug. Chem.* **2013**, *24*, 333.

(63) Islam, M. R.; Nishie, M.; Nagao, J.; Zendo, T.; Keller, S.; Nakayama, J.; Kohda, D.; Sahl, H. G.; Sonomoto, K., Ring A of nukacin ISK-1: a lipid II-binding motif for type-A(II) lantibiotic, *J. Am. Chem. Soc.* **2012**, *134*, 3687.

(64) Tiyanont, K.; Doan, T.; Lazarus, M. B.; Fang, X.; Rudner, D. Z.; Walker, S., Imaging peptidoglycan biosynthesis in Bacillus subtilis with fluorescent antibiotics, *Proc. Natl. Acad. Sci. U. S. A.* **2006**, *103*, 11033.

(65) Daniel, R. A.; Errington, J., Control of cell morphogenesis in bacteria: two distinct ways to make a rod-shaped cell, *Cell* **2003**, *113*, 767.

(66) Kuru, E.; Hughes, H. V.; Brown, P. J.; Hall, E.; Tekkam, S.; Cava, F.; de Pedro, M. A.; Brun, Y. V.; Vannieuwenhze, M. S., In Situ Probing of Newly Synthesized Peptidoglycan in Live Bacteria with Fluorescent D-Amino Acids, *Angew. Chem. Int. Ed.* **2012**, *51*, 12519.

(67) Siegrist, M. S.; Whiteside, S.; Jewett, J. C.; Aditham, A.; Cava, F.; Bertozzi, C. R., d-Amino acid chemical reporters reveal peptidoglycan dynamics of an intracellular pathogen, *ACS Chem. Biol.* **2013**, *8*, 500.

(68) Morgan, S. M.; O'Connor P, M.; Cotter, P. D.; Ross, R. P.; Hill, C., Sequential actions of the two component peptides of the lantibiotic lacticin 3147 explain its antimicrobial activity at nanomolar concentrations, *Antimicrob. Agents Chemother.* **2005**, *49*, 2606.

(69) Wiedemann, I.; Bottiger, T.; Bonelli, R. R.; Wiese, A.; Hagge, S. O.; Gutsmann, T.; Seydel, U.; Deegan, L.; Hill, C.; Ross, P.; Sahl, H. G., The mode of action of the lantibiotic lacticin 3147--a complex mechanism involving specific interaction of two peptides and the cell wall precursor lipid II, *Mol. Microbiol.* **2006**, *61*, 285.

(70) Oman, T. J.; van der Donk, W. A., Insights into the mode of action of the two-peptide lantibiotic haloduracin, *ACS Chem. Biol.* **2009**, *4*, 865.

(71) Oldach, F.; Al Toma, R.; Kuthning, A.; Caetano, T.; Mendo, S.; Budisa, N.; Süssmuth, R. D., Congeneric lantibiotics from ribosomal in vivo peptide synthesis with noncanonical amino acids, *Angew. Chem. Int. Ed.* **2012**, *51*, 415.

(72) Kim, J. N.; Kim, K. M.; Ryu, E. K., Improved synthesis of N-alkoxyphthalimdes, *Synth. Commun.* **1992**, *22*, 1427.

(73) Tecle, H.; Barrett, S. D.; Lauffer, D. J.; Augelli-Szafran, C.; Brann, M. R.; Callahan, M. J.; Caprathe, B. W.; Davis, R. E.; Doyle, P. D.; Eubanks, D.; Lipiniski, W.; Mirzadegan, T.; Moos, W. H.; Moreland, D. W.; Nelson, C. B.; Pavia, M. R.; Raby, C.; Schwarz, R. D.; Spencer, C. J.; Thomas, A. J.; Jaen, J. C., Design and synthesis of m1-selective muscarinic agonists: (R)-(-)-(Z)-1-Azabicyclo[2.2.1]heptan-3-one, O-(3-(3'-methoxyphenyl)-2-

propynyl)oxime maleate (CI-1017), a functionally m1-selective muscarinic agonist, *J. Med. Chem.* **1998**, *41*, 2524.